Osaka University

Doctoral Thesis

Exotic heavy meson molecules

Author:
Shunsuke Ohkoda

Supervisor:
Prof. Atsushi Hosaka

A thesis submitted in fulfilment of the requirements
for the degree of Doctor of Phisics

in the

Research Center for Nuclear Physics
Department of Physics

February 2014

Declaration of Authorship

I, Shunsuke Ohkoda, declare that this thesis titled, 'Exotic heavy meson molecules' and the work presented in it are my own. I confirm that:

- This work was done wholly or mainly while in candidature for a research degree at this University.
- Where any part of this thesis has previously been submitted for a degree or any other qualification at this University or any other institution, this has been clearly stated.
- Where I have consulted the published work of others, this is always clearly attributed.
- Where I have quoted from the work of others, the source is always given. With the exception of such quotations, this thesis is entirely my own work.
- I have acknowledged all main sources of help.
- Where the thesis is based on work done by myself jointly with others, I have made clear exactly what was done by others and what I have contributed myself.

Signed: _____

Date: _____

"We dance round in a ring and suppose, But the Secret sits in the middle and knows."

Robert Frost

OSAKA UNIVERSITY

Abstract

Theory group
Department of Physics

Doctor of Phisics

Exotic heavy meson molecules

by Shunsuke OHKODA

Exotic hadrons are of special interest in hadron physics. Exotic heavy meson moleculs are strong candidates of new forms of matter as exotic hadrons. In this thesis, we have studied the properties of these states from various point of view. The properties of twin resonances, $Z_b(10610)$ and $Z_b(10650)$, are well explained by the hadronic molecule picture. We find that heavy quark symmetry plays an important role in the system of heavy meson molecules.

Acknowledgements

I would like to express my special appreciation and thanks to my advisor Professor Atsushi Hosaka, you have been a tremendous mentor for me. I would like to thank you for encouraging my research and for allowing me to grow as a scientist. Your advice on both research as well as on my career have been priceless. I would also like to thank Dr. Shigehiro Yasui and Yasuhiro Yamaguchi who gave me invaluable comments and fruitful discussions. I would like to thank Grant-in-Aid for Scientific Research from JSPS for a grant that made it possible to complete this study.

A special thanks to my family. Words cannot express how grateful I am to my mother, and father for all of the sacrifices that you ' ve made on my behalf. Your prayer for me was what sustained me thus far. I would also like to thank all of my friends who supported me in writing, and incented me to strive towards my goal.

Contents

List of Figures

List of Tables

Chapter 1

Introduction

1.1 Exotic hadrons

Exotic hadrons are of special interest in hadron physics. It is well known that the ordinary hadrons are well described by the quark model, which explains mesons as quark-antiquark states and baryons as three quark states [6, 7, 8, 9]. Exotic hadrons are also composed of quarks and gluons, but which do not fit into the usual scheme of hadrons. Although they will be bound by strong interaction, which is described by quantum chromodynamics (QCD) in principle, they are not predicted by conventional quark model. The study of exotic hadrons is expected to shed light on the understanding of low-energy dynamics in QCD.

There have been many analyses which imply that they are multi-quark systems or hadronic molecules. In strangeness sector, there are several candidates of exotic hadrons, such as $f_0(980)$, $a_0(980)$, $\Lambda(1405)$ and so on. The scalar mesons $f_0(980)$ and $a_0(980)$ may be regarded as tetra-quark systems or $K\bar{K}$ molecules [10, 11]. $\Lambda(1405)$ is considered to be generated dynamically by $\bar{K}N$ and $\pi\Sigma$ [12]. In charm and bottom sectors, recently many candidates of exotic hadrons have been reported in experiments and also actively discussed in theoretical studies [6, 13, 14, 15, 16]. $D_s(2317)$ and $D_s(2460)$ may be tetra-quarks or KD molecules. X(3872), Y(4260), $Z(4050)^{\pm}$, $Z(4250)^{\pm}$, $Z(4430)^{\pm}$ and so on are also candidates of exotics states. Especially $Z(4050)^{\pm}$, $Z(4250)^{\pm}$ and $Z(4430)^{\pm}$ cannot be simple charmonia ($c\bar{c}$) because they are electrically charged. There are also exotic hadrons in bottom flavors. Y_b is the first candidate of exotic bottom

hadrons. More recently, $\mathrm{Z_b}(10610)^{\pm}$ and $\mathrm{Z_b}(10650)^{\pm}$ with isospin one have been reported by Belle [2, 17]. They also cannot be simple bottomonia ($\mathrm{b\bar{b}}$) because they are electrically charged. $Z_c(3900)$ is also not simple charmonia ($c\bar{c}$), which is considered as flavor partner of $Z_b(10610)$ in some studies.

1.2 Heavy meson molecules

As a candidate of a form of the matter, we focus on the heavy meson molecules in this study. Meson molecules are described as bound states of more than two hadrons. The hadrons as constituents of molecules are still retained as colorless objects, hence they can interact each other via inter hadron interactions, for example, meson (mainly light mesons) exchanges. They are expected to loosely bound states compared with ordinary hadrons and can have exotic quantum numbers. In particular, we expect the appearance of hadron molecules in the heavy quark region because of the following two reasons.

One is that kinetic term of Hamiltonian is suppressed. The Hamiltonian for the heavy meson molecule is generally given as

$$H = \frac{P^2}{2\mu} + V(r), \tag{1.1}$$

where P is the momentum and $V(r)$ is the potential and μ is the reduced mass of heavy meson molecules. For reference, we present the reduced masses μ of two body systems as follows

$$\mu_{NN} \sim 470\mathrm{MeV} \tag{1.2}$$

$$\mu_{DD^*} \sim 970\mathrm{MeV} \tag{1.3}$$

$$\mu_{BB^*} \sim 2650\mathrm{MeV}. \tag{1.4}$$

We can see that the μ_{BB^*} is five times as large as the μ_{NN}. Hence, the kinetic terms, which always work as repulsive, are suppressed in the heavy meson molecule systems due to the large reduced mass.

The second reason is that the heavy psudo scalar and vector mesons, $D(B)$ and $D^*(B^*)$, are degenerate thanks to heavy quark symmetry. In fact, the mass splittings of them

are decreasing with increasing the heavy meson masses as follows:

$$m_{K^*} - m_K \sim 400\text{MeV} \tag{1.5}$$

$$m_{D^*} - m_D \sim 140\text{MeV} \tag{1.6}$$

$$m_{B^*} - m_B \sim 45\text{MeV}. \tag{1.7}$$

Therefore, both pseudo scalar and vector mesons are considered as fundamental degree of freedom in the system of heavy meson molecules. As a result, the effects of channel couplings becomes larger in heavy quark regions.

Thus the existing of heavy meson molecules are naturally expected around the heavy meson thresholds. We study the spectrum of heavy meson molecules by using the potential based on heavy quark symmetry in Chapter 4. This study will provide an opportunities to understand the properties of exotic hadrons.

1.3 $Z_b(10610)$ and $Z_b(10650)$

As good candidates of exotic hadrons, Z_b is mainly studied in this thesis. Belle Collaboration observed two charged bottomonium-like resonances, $Z_b(10610)$ and $Z_b(10650)$, under the processes, $\Upsilon(5S) \to Z_b\pi \to \Upsilon(nS)\pi\pi(n = 1, 2, 3)$ and $\Upsilon(5S) \to Z_b\pi \to h_b(mP)\pi\pi(m = 1, 2)$ in 2011 [2, 17]. Z_b's have some remarkable properties, which is discussed in detail in Chapter 3. Their analyzed quantum numbers are $1^+(1^+)$, which clearly indicates that Z_b's are not simple bottomonium but exotic mesons containing at least four quarks as constituents. Their masses and widths are given as $M(\mathrm{Z_b}(10610)) = 10607.2 \pm 2.0$ MeV, $\Gamma(\mathrm{Z_b}(10610)) = 18.4 \pm 2.4$ MeV and $M(\mathrm{Z_b}(10650)) = 10652.2 \pm 1.5$ MeV, $\Gamma(\mathrm{Z_b}(10650)) = 11.5 \pm 2.2$ MeV. Their masses are slightly above the respective thresholds, $B\bar{B}^*$ and $B^*\bar{B}^*$ and widths are relatively narrow compared with the typical excited bottomonia above the open flavor thresholds. Z_b's decays are also exotic. In general, a decay processes $\Upsilon(5S) \to h_b\pi\pi$ should be suppressed in heavy quark mass limit, because these processes require a heavy quark spin flip. Nevertheless, the decay rates of $\Upsilon(5S) \to Z_b\pi \to h_b(mP)\pi\pi$ are comparable to those of $\Upsilon(5S) \to Z_b\pi \to \Upsilon(nS)\pi\pi$. These facts strongly suggest that Z_b's have molecular type of structure [18].

We study the Z_b's with a potential model from the point of view of heavy meson molecule picture.

This thesis is organized as follows. Because heavy quark symmetry and effective heavy hadron theory are effectively important to study the dynamics of heavy meson molecules, we introduce the concept of heavy quark symmetry and how to use the effective heavy hadron theory in the low energy dynamics in Chapter 2. Chapter 3 provide the overview of the experimental results regarding Z_b. In Chapter 4, we mainly study the spectroscopy of heavy meson molecules, $P\bar{P}$ and PP, with the potential model ($P(\bar{P})$ stands for heavy meson). The masses of $Z_b(10610)$ and $Z_b(10650)$ will be explained as $B^{(*)}\bar{B}^{(*)}$ states with $I^G(J^P) = 1^+(1^+)$. In addition to the study of $P\bar{P}$ states, we also analyze the PP states, whose constituents are apparently exotic states such as $|bb\bar{u}\bar{d}\rangle$. In Chapter 5, we study the decay and production properties of Z_b and other $B\bar{B}$ molecules. We will introduce the heavy quark spin selection rules in that chapter, which is germane to the decay and production properties of heavy meson molecules. Chapter 6, considering Z_b as heavy meson molecules, we investigate the decay of $Z_b^{(\prime)\pm} \to \Upsilon(nS)\pi^\pm$ in terms of the heavy meson effective theory. We also predict the decay width of $Z_c^\pm \to J/\Psi\pi^\pm$ and $\Psi(2S)\pi^\pm$, where Z_c is a charmonium-like resonance recently reported in experiments [19, 20]. Finally, we study the spin degeneracy of the heavy meson molecules in Chapter 7. It is known that the suppression of spin-spin interaction in heavy quark limit cause the mass degeneracy of heavy hadrons. The properties of heavy meson molecules in heavy quark limit will even provide the useful information heavy meson molecules with finite heavy quark mass. Chapter 8 is devoted for summary.

Chapter 2

Heavy quark symmetry and effective heavy hadron theory

When masses of heavy quarks are sufficiently heavy compared with the scale of nonperturbative strong dinamics, it is good approximation to take the heavy quark mass limit $m_Q \to \infty$ of QCD. In this limit QCD has spin-flavor heavy quark symmetry (HQS). HQS is a good tool to describe and undestand the properties of hadrons containing heavy quarks. In this chapter, we briefly introduce heavy quark symmetry. We also discuss the heavy hadron effective theory, which reflect on HQS, to describe the interaction of heavy mesons.

2.1 Heavy quark symmetry

The QCD Lagrangian describes the strong interaction of quarks and gluons. Although QCD is simple and elegant in its formulation, the difficulty arises to predict the various phenomena of hadrons with this because of long distance QCD effects that are essentially non perturbative. The employing approximate symmetries is useful tool to understand the low energy hadron physics, which is hard to directly access from the QCD Lagrangian. In particular, chiral symmetry, which appears in the $m_q \to 0$ limit of QCD, has succeessed to predict some properties of hadrons containing light quarks. Here, we consider the dynamimcs of hadrons containing a heavy quark, which is heavy with respect to the hadronic scale of QCD. In the limit of infinite masses, $m_Q \to \infty$, the heavy quark symmetry appears.

Heavy quark symmetry is classified as two charactrized symmetries.

In the heavy quark mass limit $m_Q \to \infty$, the strong interactions of the heavy quark do not change its velocity v_Q. Hence, the heavy quark in the meson can be labeled by a velocity four vector v_Q. The heavy quark in the meson behaves like a static spectator particle which transforms as a color triplet. This fact indicates that the interaction of the heavy meson can be regarded as that of the light degree of freedom with this color sorce. It is clear that the infinite mass of heavy quark plays no role in its interaction with the light sector, so that all heavy quarks interact in the same way within heavy mesons. In other words, the dynamics is unchanged under the exchange of heavy quark flavors, $U(N_f)$ (for N_f heavy flavors). This is first symmetry and called heavy quark flavor symmetry.

The second symmetry is a result to the decoupling of the gluon from the quark spin. A heavy quark can only interact with gluons in QCD, as there are no quark-quark interaction in its Lagrangian. In the $m_Q \to \infty$, the static heavy quark can only interact with gluons via its chromoelectric charge. This interaction is spin independent. It conclude that the dynanmics is unchanged under the arbitrary transformations on the spin of the heavy quark, $SU(2)$. This is heavy quark spin symmetry.

Therefore, the effective Lagrangian to describe the interaction of a heavy quark must involve a $U(N_f)$ flavor and a $SU(2)$ spin symmetries in the $M_Q \to \infty$ limit, which symmetries can be embedded into a larger $SU(2N_f)$ spin-flavor symmetry. We will see in next section that the effective Lagrangian can be written in a way that makes this symmetry manifest. The effective theory to describe the dynamics of hadrons containing a single heavy quark is nowadays known as Heavy Quark Effective Theory (HQET) [21, 22, 23, 24, 25, 26].

2.2 Heavy quark effective thoery

As mentioned in the previous section, the Lagrangian to describe the dynamics of a heavy quark or hadrons containing it has to involve the heavy quark spin-flavor symmetry. The QCD Lagrangian does not have heavy quark spin-flavor symmetry as $m_Q \to \infty$ in the obvious manner. It is convenient to constract the effective theory for QCD in which heavy quark symmetry is manifest in the $m_Q \to \infty$.

To begin with, we consider a heavy quark with the velocity v interacting with the external fields such as gluon fields. On the on-shell quark, the velocity v is defined by $p_Q = m_Q v$, where p_Q is a mometum of the heavy quark. Because the mass of a heavy quark is sufficiently heavy compared with Λ_{QCD}, we can regard an off-shell heavy quark as an almost on-shell heavy quark and its momentum p_Q can be written, introducing a residual momentum k of the order of Λ_{QCD}, as

$$p_Q = m_Q v + k \tag{2.1}$$

The usual dirac propagator of a heavy quark simplifies to

$$i\frac{\not{p} + m_Q}{p^2 - m_Q^2 + i\epsilon} = i\frac{m_Q \not{v} + m_Q + k}{2m_Q v \cdot k + k^2 + i\epsilon} \to i\frac{1 + \not{v}}{2v \cdot k + i\epsilon}, \tag{2.2}$$

in the heavy quark limit. A projection operator which is depend on the velocity,

$$\frac{1 + \not{v}}{2} \tag{2.3}$$

appears in the propagator. In the rest frame of the heavy quark this projection operator becomes $(1 + \gamma^0)/2$, which projects onto the particle components of the Dirac spinor. It is useful to formulate the effective Lagragian with the velocity-dependent fields $Q_v(x)$, Using $Q_v(x)$, we can decompose the original heavy quark field into the positive energy $Q_v(x)$ and the negative energy heavy quark fields $\mathcal{Q}_v(x)$ as

$$Q(x) = e^{-im_Q v \cdot x}[Q_v(x) + \mathcal{Q}_v(x)], \tag{2.4}$$

where

$$Q_v(x) = e^{im_Q v \cdot x}\frac{1 + \not{v}}{2}Q(x), \quad \mathcal{Q}(x) = e^{im_Q v \cdot x}\frac{1 - \not{v}}{2}\mathcal{Q}(x). \tag{2.5}$$

The exponential prefactor subtracts $m_Q v^\mu$ from the heavy quark momentum. At the leading order, The Q_v field only appears in the effective Lagrangian, whereas the $\mathcal{Q}_v$ field is suppressed by powers of $1/m_Q$. Neglecting $\mathcal{Q}_v$ and substituting Eq .2.4 into the part of QCD Lagrangian involving the heavy quark field, $\bar{Q}(i\not{D} - m_Q)Q$, we obtain the effective Lagrangian at lowest order as

$$\mathcal{L} = \bar{Q}_v(iv \cdot D)Q_v, \tag{2.6}$$

where $D_\mu = \partial_\mu + igA^a_\mu T^a$ is the $SU(3)$ color covariant derivative. This is clearly heavy quark flavor and spin independent expression.

The HQET Lagrangian including $1/m_Q$ corrections can be derived from the QCD Lagrangian by substituging Q_v for $Q(x)$ in the original QCD Lagrangain as follows [27]:

$$\mathcal{L} = \bar{Q}_v(iv\cdot D)Q_v - \mathcal{Q}_v(iv\cdot D + 2m_Q)\mathcal{Q}_v + \bar{Q}_v i\not{D}\mathcal{Q}_v + \bar{\mathcal{Q}}_v i\not{D}Q_v, + \mathcal{O}(1/m_Q^2) \quad (2.7)$$

using $\not{v}Q_v = Q_v$ and $\not{v}\mathcal{Q}_v = -\mathcal{Q}_v$. We can eliminate $\mathcal{Q}_v$ with the perpendicular component of D defiened by $D^\mu_\perp \equiv D^\mu - Dv\cdot v^\mu$ and obtain

$$\mathcal{L} = \bar{Q}_v v\cdot iDQ_v + \bar{Q}_v\frac{(iD_\perp)^2}{2m_Q}Q_v - g_s\bar{Q}_v\frac{\sigma_{\mu\nu}G^{\mu\nu}}{4m_Q}Q_v + \mathcal{O}(1/m_Q^2), \quad (2.8)$$

where $G^{\mu\nu} = [D^\mu, D^\nu]/ig_s$. This is the heavy quark effective Lagrangians in the $1/m_Q$ expansion. Thus, the spin-spin interaction between a quark and a gluon is suppressed by $1/m_Q$ order.

2.3 The effective Lagrangians for heavy mesons

HQS, which is approximate symmety of QCD in the infinite heavy quark ($Q = c, b$), and Chiral symmetry, which appears in the chiral limit for the light quarks ($m_q \to 0,\ q = u, d, s$), can be used to together to built and effective Lagrangians for heavy and light meson to describe strong interactions among effective meson fields.

2.3.1 Heavy meson fields

In the following section we consider the couplings of the open flavor heavy mesons P and a light meson such as π and K. Here we consider strong interactions of mesons H_Q containing a single heavy quark Q, which is described in the framework of the HQET. Our whole discussions are valid under the heavy quark mass limit $m_Q \to$ in QCD. Thus the heavy mesons P should be reflected on heavy quark symmetry.

Heavy meson fields implies a degenerate doublet of states, such as B and B^* To consider the strong interactions of heavy mesons and a light mesons, it is convenient to define a heavy meson field which can be treated as a single object that transforms linearly under the heavy quark symmetries.

We represent the ground-state $Q\bar{q}$ mesons with the orbital angular momentum $L = 0$ as a field H_v that annihilates the mesons. This field can be represented by a 4×4 Dirac-type matrix, with one spinor index for the heavy quark and the other for the light degrees of freedom. Such fields transform under a Lorentz transformation Λ as

$$H_v \to D(\Lambda) H_v D(\Lambda)^{-1}, \tag{2.9}$$

where $D(\Lambda)$ is the usual 4×4 representation of the Lorentz group. Under a heavy quark spin transformation S belonging to $SU(2)$ as

$$H_v \to S H_v, \tag{2.10}$$

where S satisfies $[\not{v}, S] = 0$ to preserve the constraint $\not{v} H_v = H$. The field H_v is a linear combination of the pseudoscalar field $P_v(x)$ and the vector field $P^*_{v\mu}$ that the annihilate the $S_l = 1/2$ meson multiplet. Vector particles have a polarization vector ϵ_μ, with $\epsilon \cdot \epsilon = -1$ and $v \cdot \epsilon = 0$. A simpe way to express the two fields into a single field with the desired properties is to define

$$H_v = \frac{1 + \not{v}}{2} \left[P^*_{v\mu} \gamma^\mu - P_v \gamma_5 \right]. \tag{2.11}$$

This equation is consistent with P_v transforming as a pseudoscalar, and P^*_v as a vector. The $(1 + \not{v})/2$ is a projection operator, which retains only the particle components of the heavy quark Q. The conjugate field is defined as

$$\bar{H}_v = \gamma_0 H_v^\dagger \gamma_0 = \left[P^*_{v\mu} \gamma^\mu + P_v \gamma_5 \right] \frac{1 + \not{v}}{2}. \tag{2.12}$$

2.3.2 A chiral Lagrangian for heavy meson

The effective Lagrangian for the strong interactions of heavy mesons and a light pseudo scalar meson must satisfy Lorentz and C, P, T invariance. In addition to them, at the leading order in the $1/M_P$ expansion, and in the massless quark limit, ae require flavor and spin symmetry in the heavy mesons sector, and chiral $SU(3)_L \otimes SU(3)_R$ invariance in the light one. The most general Lagrangian is given as

$$\begin{aligned} \mathcal{L} &= i \mathrm{Tr}[H_b v^\mu D_{\mu ab} \bar{H}_a] + ig \mathrm{Tr}[H_b \gamma_\mu \gamma_5 \mathcal{A}^\mu_{ba} \bar{H}_a] \\ &\quad + \frac{f^2}{8} \partial^\mu \Sigma_{ab} \partial_\mu \Sigma^\dagger_{ba}, \end{aligned} \tag{2.13}$$

where $D_\mu = \partial_\mu + \mathcal{V}_\mu$ and $\mathrm{Tr}[\cdots]$ means trace over the 4×4 matrices. The first term in the Lagrangian contains the kinetic terms for the heavy mesons giving the P and P^* propagators,

$$\frac{i}{2v \cdot k}, \tag{2.14}$$

and

$$-\frac{i(g^{\mu\nu} - v^\mu v^\nu)}{2v \cdot k}, \tag{2.15}$$

respectively. The first term also have the interactions among the heavy mesons $P^{(*)}$ and an even number of pions coming from the expansion of the vector current $\mathcal{V}_\mu$. The second term in the Lagrangian describe the strong interactions between the heavy mesons $P^{(*)}$ and odd number of the light pseudoscalar mesons:

$$\mathcal{L}_I = ig\mathrm{Tr}[H_b\gamma_\mu\gamma_5\mathcal{A}^\mu_{ba}\bar{H}_a], \tag{2.16}$$

where the axial current $\mathcal{A}_\mu$ is

$$\mathcal{A}_\mu = \frac{1}{2}(\xi^\dagger\partial_\mu\xi - \xi\partial_\mu\xi^\dagger). \tag{2.17}$$

$\xi(x)$ is the field of the light pseudoscalar mesons and given as $\xi(x) = \exp(i\mathcal{M}(x)/f)$ with $f = 132$ MeV. $\mathcal{M}$ is a 3×3 hermitian, traceless matrix:

$$\mathcal{M} = \begin{pmatrix} \sqrt{\frac{1}{2}}\pi^0 + \sqrt{\frac{1}{6}}\eta & \pi^+ & K^+ \\ \pi^- & -\sqrt{\frac{1}{2}} + \sqrt{\frac{1}{6}}\eta & K^0 \\ K^- & \bar{K}^0 & -\sqrt{\frac{2}{3}}\eta \end{pmatrix}. \tag{2.18}$$

The first term in the expansion of the axial current gives

$$\mathcal{A}_\mu \approx \frac{i}{f}\partial_\mu\mathcal{M} + \cdots, \tag{2.19}$$

which reproduce the three point interactions. Thanks to the heavy quark symmetry, the interactions which the Lagrangian $\mathcal{L}_I$ contains are related only with one parameter g. As an example, this allows to relate the $D^{(*)}D^{(*)}\pi$ couplings, defined thruogh the

matrix elements

$$\langle D^{*+}(p+q,\epsilon)|D^0(p)\pi^+(q)\rangle = g_{DD^*\pi}(\epsilon\cdot q) \quad (2.20)$$

$$\langle D^{*+}(p+q,\epsilon)|D^{*0}(p,\eta)\pi^+(q)\rangle = ig_{D^*D^*\pi}\epsilon^{\alpha\beta\mu\gamma}p_\alpha\epsilon_\beta q_\mu\eta^*_\gamma \quad (2.21)$$

to the coupling g:

$$g_{DD^*\pi} = 2\sqrt{m_D m_{D^*}}\frac{g}{f} \quad (2.22)$$

$$g_{D^*D^*\pi} = -2\frac{g}{f} \quad (2.23)$$

The interaction term $DD\pi$ is forbidden by parity. Here we neglect corrections due to the finite mass of the charm quark. The most common way to determine the coupling g is given from the $D^* \to D\pi$ decay. Using the matrix elements 2.20, we obtain the partial widths:

$$\Gamma(D^{*+}\to D^0\pi^+) = \frac{g^2}{6\pi f^2}|\vec{p}_\pi|^3 \quad (2.24)$$

$$\Gamma(D^{*+}\to D^+\pi^0) = \Gamma(D^{*0}\to D^0\pi^0) = \frac{g^2}{12\pi f^2}|\vec{p}_\pi|^3 \quad (2.25)$$

The decay $D^{*0} \to D^+\pi^-$ is forbidden by the phase space. The direct $B^* \to B\pi$ transition is also not allowed because of lack of phase space. In experiments, the total width of D^{*+} is given as $\Gamma_{tot}(D^{*+}) = 96 \pm 22$ keV [28]. In contrast, there is an exprimental upper bound on the total D^{*0} width: $\Gamma_{tot}(D^{*0}) < 2.1$ MeV. The branching fractions of D^* mesons are summarized in Table. 2.1. By means of the measured branching raitos of D^{*+}, we obtain the coupling $g = 0.59$.

TABLE 2.1: Experimental D^* branching ratio (%)

Decay mode	fraction (Γ_i/Γ)	p(MeV)
$D^{*0} \to D^0\pi^0$	61.9 ± 2.9	43
$D^{*0} \to D^0\gamma$	38.1 ± 2.9	137
$D^{*+} \to D^0\pi^+$	67.7 ± 0.5	39
$D^{*+} \to D^+\pi^0$	30.7 ± 0.5	38
$D^{*+} \to D^+\gamma$	1.6 ± 0.4	136

2.3.3 Couplings of pairs of heavy-light mesons to heavy quarkonium states

Here, we consider the interactions of pairs of heavy-light mesons to heavy quarkonium states in terms of heavy quark effective theory. For heavy quarkonia $Q\bar{Q}$, degeneracy is expected under ratation of the two heavy quark spins. This allows us to build up heavy meson multiplets for each value of the relative angular momentum L For $L = 0$ one has a doublet of a pseudscalar and a vector mesons, η_c and J/ψ in case of charmonium, η_b and Υ in case of bottomonium. The corresponding heavy quarkonium field is defined as [29]

$$R^{Q_1\bar{Q}_2} = \left(\frac{1+\not{v}}{2}\right)\left[L^\mu\gamma_\mu - L\gamma_5\right]\left(\frac{1-\not{v}}{2}\right), \tag{2.26}$$

which is the form of 4×4 matrix with the annihilation operator for pseudoscala meson L and vector meson Λ^μ, $L^\mu = \Upsilon$ and $\Lambda = \eta_b$ in the case of $b\bar{b}$. The annhilation operators L and L^μ are normalized as follows:

$$\langle 0|L|Q\bar{Q}(0^-)\rangle = \sqrt{M_{Q\bar{Q}}} \tag{2.27}$$

$$\langle 0|L^\mu|Q\bar{Q}(1^-)\rangle = \epsilon^\mu\sqrt{M_{Q\bar{Q}}}. \tag{2.28}$$

For $L = 1$, four states can be built which are degenerate in the heavy quark limit. The corresponding spin multiplet reads

$$M^{(Q_1\bar{Q}_2)\mu} = \left(\frac{1+\not{v}}{2}\right)\left[\xi_2^{\mu\alpha}\gamma_\alpha + \frac{1}{\sqrt{2}}\epsilon^{\mu\alpha\beta\gamma}v_\alpha\gamma_\beta\chi_{1\gamma} + \frac{1}{\sqrt{3}}(\gamma^\mu - v^\mu)\chi_0 + h_1^\mu\gamma_5\right]\left(\frac{1-\not{v}}{2}\right) \tag{2.29}$$

where $\xi_2 = \xi_{b2}$, $\xi_1 = \xi_{b1}$ and $\xi_0 = \xi_{b0}$ coresond the spin triplet whereas the spin singlet is $h_1 = h_b$ in the case of $b\bar{b}$. These fields also contain a factor $\sqrt{m}$ with m the meson mass. We again write the field of heavy-light mesons as follows

$$H_{1a} = \left(\frac{1+\not{v}}{2}\right)\left[P^*_{a\mu}\gamma^\mu - P_a\gamma_5\right] \tag{2.30}$$

$$H_{2a} = \left[P'^*_{a\mu}\gamma^\mu - P'_a\gamma_5\right]\left(\frac{1-\not{v}}{2}\right), \tag{2.31}$$

where the quark content of H_{1a} is $Q_1\bar{q}_1$ and H_{2a} is $q_a\bar{Q}$. The meson multipltes transforms under the independent heavy quark spin rotations $S_1 \in SU(2)_{Q_1}$ and $S_2 \in SU(2)_{Q_2}$ as

follows:

$$H_{1a} \to S_1 H_{1a} \qquad \bar{H}_{1a} \to \bar{H}_{1a} S_1^\dagger \tag{2.32}$$

$$H_{2a} \to H_{2a} S_2^\dagger \qquad \bar{H}_{2a} \to S_2 \bar{H}_{2a} \tag{2.33}$$

$$M^{(Q_1\bar{Q}_2)\mu} \to S_1 M^{(Q_1\bar{Q}_2\mu)} \qquad M^{(Q_1\bar{Q}_2\mu)} \to M^{(Q_1\bar{Q}_2\mu)} S_2^\dagger \tag{2.34}$$

$$R^{(Q_1\bar{Q}_2)} \to S_1 R^{(Q_1\bar{Q}_2)} \qquad R^{(Q_1\bar{Q}_2)} S_2^\dagger \tag{2.35}$$

To require the invariance under the independent heavy quark spin rotations, the interactions with the heavy-light vector and pserudoscalar mesons proceed in P-wave and can be desicribed by a Lagrangian containing a derivative term:

$$\mathcal{L}_1 = \frac{g_1}{2} \mathrm{Tr}\left[R^{(Q_1\bar{Q}_2)} \bar{H}_{2a} \overleftrightarrow{\partial} \bar{H}_{1a} \right] + \mathrm{H.c.} + (Q_1 \leftrightarrow Z_2). \tag{2.36}$$

The action of the derivative produces a factor of the residual momentum k. This quantity is defined as the difference of the hadron and heavy quark momentum, $M_H v_\mu = m_Q v_\mu + k_\mu$, and k is finite in the heavy quarak limit. As an example, we derive the couplings of $B^{(*)}$ mesons to Υ from Eq. 2.36:

$$\begin{aligned}
\langle B(p_1)\bar{B}(p_2)|\Upsilon(P,\epsilon)\rangle &= g_{BB\Upsilon}(\epsilon\cdot q) \\
\langle B^*(p_1,\epsilon_1)\bar{B}(p_2)|\Upsilon(P,\epsilon)\rangle &= g_{BB^*\Upsilon} i\epsilon_{\alpha\beta\mu\nu} v^\alpha \epsilon^\beta \epsilon_1^{*\mu} q^\nu \\
\langle B^*(p_1,\epsilon_1)\bar{B}^*(p_2,\epsilon_2)|\Upsilon(P,\epsilon)\rangle &= g_{B^*B^*\Upsilon}[(\epsilon\cdot\epsilon_2^*)(\epsilon_1^*\cdot q) - (\epsilon\cdot q)(\epsilon_1^*\cdot\epsilon_2^*) + (\epsilon\cdot\epsilon_1^*)(\epsilon_2^*\cdot q)],
\end{aligned} \tag{2.37}$$

where q is the diffrence in the residual momenta of the two $B^{(*)}$ mesons, $q = k_1 - k_2$. Since $p_1 = m_Q v + k_1$ and $p_2 = m_Q v + k_2$, q is equivalent to the difference of the two B^* mesons, $q = p_1 - p_2$. The three couplings in Eq. 2.37 are related to the single parameter g_2:

$$\begin{aligned}
g_{BB\Upsilon} &= 2g_1\sqrt{m_\Upsilon} m_B \\
g_{BB^*\Upsilon} &= 2g_1\sqrt{m_\Upsilon m_B m_{B^*}} \\
g_{B^*B^*\Upsilon} &= -2g_1\sqrt{m_\Upsilon} m_{B^*}.
\end{aligned} \tag{2.38}$$

The Lagrangian describing the coupling to two heavy-light mesons $Q_1\bar{q}_a$ and $q_a\bar{Q}_2$ and heavy quarkonium $Q_1\bar{Q}_2$ with $L = 1$ can be written as follows:

$$\mathcal{L}_2 = i\frac{g_2}{2}\mathrm{Tr}[M^{(Q_1\bar{Q}_2)\mu}\bar{H}_{2a}\gamma_\mu\bar{H}_{1a}] + \mathrm{H.C.} + (Q_1 \leftrightarrow Q_2), \tag{2.39}$$

This Lagrangian satisfies chiral and heavy quark spin symmetries. From Eq. 2.39, we can obtain the matrix elements describing the couplings of $B^{(*)}$ mesons and h_b:

$$\langle B^*(p_1,\epsilon_1)\bar{B}(p_2)|h_b(p,\epsilon)\rangle = g_{BB^*h_b}(\epsilon_1^*\cdot\epsilon) \tag{2.40}$$

$$\langle B^*(p_1,\epsilon_1)B^*(p_2,\epsilon_2)|h_b(p,\epsilon)\rangle = ig_{B^*B^*h_b}\epsilon_{\alpha\beta\mu\nu}p^\alpha\epsilon^\beta\epsilon_1^{*\mu}\epsilon_2^{*\nu}, \tag{2.41}$$

where the couplings are given as

$$g_{BB^*h_b} = -2g_2\sqrt{m_{h_b}m_Bm_{B^*}} \tag{2.42}$$

$$g_{B^*B^*h_b} = 2g_2\sqrt{\frac{m_{B^*}^2}{m_{h_b}}}. \tag{2.43}$$

In the same way, we obtain the couplings of $B^{(*)}$ mesons and ξ_{b0} as follows:

$$\langle B(p_1)B(p_2)|\chi_{b0}(p)\rangle = -g_{BB\chi_{b0}} \tag{2.44}$$

$$\langle B^*(p_1,\epsilon_1)B^*(p_2,\epsilon_2)|\chi_{b0}(p)\rangle = -g_{B^*B^*\chi_{b0}}(\epsilon_1^*\cdot\epsilon_2^*), \tag{2.45}$$

with

$$g_{BB\chi_{b0}} = -2\sqrt{3}g_2\sqrt{m_{\xi_{b0}}}m_B \tag{2.46}$$

$$g_{B^*B^*\chi_{b0}} = -\frac{2}{\sqrt{3}}g_2\sqrt{m_{\chi_{b0}}}m_{B^*}. \tag{2.47}$$

It is hard to determine the couplings g_1 and g_2 directly from the experiments. Here we estimate them invoking vector meson dominance (VMD) argumnents. By this, we can obtain g_1 in terms of the Υ leptonic constant f_Υ, defined by $\langle 0|\bar{b}\gamma_\mu b|\Upsilon(p,\epsilon)\rangle = f_\Upsilon m_\Upsilon\epsilon^\mu$. From the VMD result

$$g_{BB\Upsilon} = \frac{m_\Upsilon}{f_\Upsilon}, \tag{2.48}$$

one gets

$$g_1 = \frac{\sqrt{m_\Upsilon}}{2m_Bf_\Upsilon}. \tag{2.49}$$

The constant f_Υ is determined by the leptonic decay of Υ. The hadronic electromagnetic current is given in terms of the vector currents of c and b quarks as follows:

$$J_\mu^{em} = \frac{2}{3}\bar{c}\gamma_\mu c - \frac{1}{3}\bar{b}\gamma_\mu b, \tag{2.50}$$

where $c(x)$ and $b(x)$ refer to the quark fields. This current can be rewritten identically as

$$J_\mu^{em} = \frac{2}{3} J_\mu^{(J/\psi)} - \frac{1}{3} J_\mu^{\Upsilon}, \tag{2.51}$$

where we have introduced combination directly reflect the quark compositions corresponding vector mesons:

$$J_\mu^{(J/\Psi)} = \bar{c}\gamma_\mu c \tag{2.52}$$

$$J_\mu^{\Upsilon} = \bar{b}\gamma_\mu b \tag{2.53}$$

The decay of a given heavy quarkonia $V = J/\Psi, \Upsilon$ into an e^+e^- pair described by the matrix element $\langle 0|J_\mu^{em}|V\rangle$ connecting a vector meson with the QCD vacuum. Thus the leptonic decay constant f_Υ are determined by the e^+e^- decay widths

$$\Gamma(\Upsilon(nS) \to e^+e^-) = \frac{4\pi\alpha_{\rm EM}}{27} \frac{f^2_{\Upsilon(nS)}}{m_{\Upsilon(nS)}}, \tag{2.54}$$

where $\alpha_{\rm EM} = 137.036$ is the fine-structure constant. The experimental results for the leptonic decay widths of the $\Upsilon(nS)$ states are [28]

$$\Gamma(\Upsilon(1S) \to e^+e^-) = 1.340 \pm 0.018 \text{keV} \tag{2.55}$$

$$\Gamma(\Upsilon(2S) \to e^+e^-) = 0.612 \pm 0.011 \text{keV} \tag{2.56}$$

$$\Gamma(\Upsilon(3S) \to e^+e^-) = 0.443 \pm 0.008 \text{keV}. \tag{2.57}$$

Then the decay constants are $f_{\Upsilon(1S)} = 715$ MeV, $\Upsilon(2S) = 497.5$ MeV and $\Upsilon(3S) = 430.2$ MeV. Finally, we obtain the couplings g_1 as $g_{1\Upsilon(1S)} = 1.3 \times 10^{-5}$, $g_{1\Upsilon(2S)} = 1.9 \times 10^{-5}$ and $g_{1\Upsilon(3S)} = 2.2 \times 10^{-5}$. In the same way, we can obtain the couplings g_1 for $Q\bar{Q} = c\bar{c}$. Adopting the same argument, we can also obtain g_2 in terms of the constant $f_{\xi_{b0}}$ that parametrizes the matrix element

$$\langle 0|\bar{b}b|\chi_{b0}(q)\rangle = f_{\chi_{b0}} m_{\chi_{b0}}, \tag{2.58}$$

which implies the relation

$$g_{BB\chi_{b0}} = 2\frac{m_B m_{\xi_{b0}}}{f_{\chi_{b0}}}, \tag{2.59}$$

a relation which determines g_2 once $f_{\chi_{b0}}$ is known:

$$g_2 = -\sqrt{\frac{m_{\chi_{b0}}}{3}}\frac{1}{f_{\chi_{b0}}}. \tag{2.60}$$

Chapter 3

Overview of Z_b

In 2011, Belle Collaboration at KEK B factory observed two charged bottomonium-like resonances, $Z_b(10610)$ and $Z_b(10650)$, that are produced in the $\Upsilon(5S) \to Z_b^{\pm}\pi^{\mp}$ transitions and that decay to $\Upsilon(nS)\pi^{\pm}(n = 1, 2, 3)$ and $h_b(mP)\pi^{\pm}(m = 1, 2)$ channels. The masses of Z_b states are very close to the respective thresholds, $B\bar{B}^*$ and $B^*\bar{B}^*$. Their favored quantum numbers are $I^G(J^P) = 1^+(1^+)$. Hence, these states are charged, which indicate that their quark content is explicit exotic such as $|b\bar{b}u\bar{d}\rangle$. We review status and interpretations on the Z_b states.

3.1 Historical background

First signal to discover Z_b appeared in the processes, $\Upsilon(5S) \to \Upsilon(nS)\pi\pi(n = 1, 2, 3)$. The Belle Collaboration reported the observation of anomalously high rates for $\Upsilon(5S) \to \Upsilon(nS)\pi^+\pi^-(n = 1, 2, 3)$ [30]. The results are based on a data sample of 21.7 fb^{-1} collected with the Belle detector at the KEKB e^+e^- collider. Attributing the signals to the $\Upsilon(5S)$ resonance, the partial widths are obtained as

$$\Gamma(\Upsilon(5S) \to \Upsilon(1S)\pi^+\pi^-) = 0.59 \pm 0.04(\text{stat}) \pm 0.09(\text{syst}) \text{ MeV}, \quad (3.1)$$

$$\Gamma(\Upsilon(5S) \to \Upsilon(2S)\pi^+\pi^-) = 0.85 \pm 0.07 \pm 0.16\text{MeV}, \quad (3.2)$$

$$\Gamma(\Upsilon(5S) \to \Upsilon(3S)\pi^+\pi^-) = 0.52^{0.20}_{0.17} \pm 0.10\text{MeV}, \quad (3.3)$$

from the observed cross sections. The decay widths and branching fractions from $\Upsilon(5S)$ are summarized in Table. 3.1. The branching fraction ratios of these channels are unexpected high probabilities. The measured partial widths, of order $0.6-0.8$ MeV, are more than 2 orders of magnitude lager compared to all other known transitions among $\Upsilon(nS)$ states. The partial widths for $\Upsilon(2S)$, $\Upsilon(3S)$ and $\Upsilon(4S) \to \Upsilon(1S)\pi^+\pi^-$ transitions are all at the keV level (see Table 3.2).

Belle also reported the observation of anomalously high rates for $\Upsilon(5S) \to h_b(mP)\pi^+\pi^-(m = 1,2)$ [1]. In general, the processes $\Upsilon(5S) \to h_b(mP)\pi^+\pi^-$ will be suppressed by the heavy quark spin selection rule because these processes require a heavy quark spin-flip. Nevertheless, these processes are found to have rates that are comparable to those for the heavy quark spin conserving transitions $\Upsilon(5S) \to \Upsilon(nS)\pi^+\pi^-$. The $h_b(1P)$ and $h_b(2P)$ are produced via $e^+e^- \to h_b(mP)\pi^+\pi^-$ in the $\Upsilon(5S)$ region. A 121.4 fb^{-1} data sample is collected near the peak of $\Upsilon(5S)$ resonance ($\sqrt{s} \sim 10.865$ GeV). Belle observe the $h_b(nP)$ states in the $\pi^+\pi^-$ missing masses spectrum of hadronic events. The $\pi^+\pi^-$ missing mass is defined as $M^2_{miss} \equiv (P_{\Upsilon(5S)-P_{\pi^+\pi^-}})^2$, where $P_{\Upsilon(5S)}$ is the 4-momentum of the $\Upsilon(5S)$ determined from beam momenta and $P_{\pi^+\pi^-}$ is the 4-momentum of the $\pi^+\pi^-$ system. The measured masses of $h_b(1P)$ and $h_b(2P)$ are $M = (9898.2^{+1.1}_{-1.0}\ ^{+1.0}_{-1.1})$ MeV/c^2 and $M = (10259.8 \pm 0.6^{+1.4}_{-1.0})$ MeV/c^2, respectively. The M_{miss} spectrum after subtraction of the background contributions is shown with the fitted signal functions in Fig .3.1 [1]. The ratio of cross section for $e^+e^- \to \Upsilon(5S) \to h_b(mP)\pi^+\pi^-$ to that for $e^+e^- \to \Upsilon(5S) \to \Upsilon(2S)\pi^+\pi^-$ are also measured. The ratio of cross section are

$$R \equiv \frac{\sigma(h_b(1P)\pi^+\pi^-)}{\sigma(\Upsilon(2S)\pi^+\pi^-)} = 0.45 \pm 0.08^{+0.07}_{-0.12}, \tag{3.4}$$

$$R \equiv \frac{\sigma(h_b(2P)\pi^+\pi^-)}{\sigma(\Upsilon(2S)\pi^+\pi^-)} = 0.77 \pm 0.08^{+0.22}_{-0.17}. \tag{3.5}$$

Hence, $\Upsilon(5S) \to h_b(mP)\pi^+\pi^-$ and $\Upsilon(5S) \to \Upsilon(2S)\pi^+\pi^-$ proceed at similar rates, despite the fact that the production of $h_b(mP)$ requires a spin flip of a b quark.

These observations differ from naive theoretical expectations and strongly suggest that exotic mechanism are contributing to $\Upsilon(5S)$ decays.

TABLE 3.1: The first uncertainty is statistical and the second is systematic. This data is from [30].

Process	$\mathcal{B}$ (%)	Γ (MeV)
$\Upsilon(1S)\pi^+\pi^-$	$0.53 \pm 0.03 \pm 0.05$	$0.59 \pm 0.04 \pm 0.09$
$\Upsilon(2S)\pi^+\pi^-$	$0.78 \pm 0.06 \pm 0.11$	$0.85 \pm 0.07 \pm 0.16$
$\Upsilon(3S)\pi^+\pi^-$	$0.48^{+0.18}_{-0.15} \pm 0.07$	$0.52^{+0.20}_{-0..17} \pm 0.10$

TABLE 3.2: Most values are from [28, 30].

Process	Γ_{tot}	$\Gamma_{e^+e^-}$	$\Gamma_{\Upsilon(1S)\pi^+\pi^-}$
$\Upsilon(2S) \to \Upsilon(1S)\pi^+\pi^-$	0.032 MeV	0.612 keV	0.0060 MeV
$\Upsilon(3S) \to \Upsilon(1S)\pi^+\pi^-$	0.020 MeV	0.443 keV	0.0009 MeV
$\Upsilon(4S) \to \Upsilon(1S)\pi^+\pi^-$	20.5 MeV	0.272 keV	0.0019 MeV
$\Upsilon(5S) \to \Upsilon(1S)\pi^+\pi^-$	110 MeV	0.31 keV	0.59 MeV

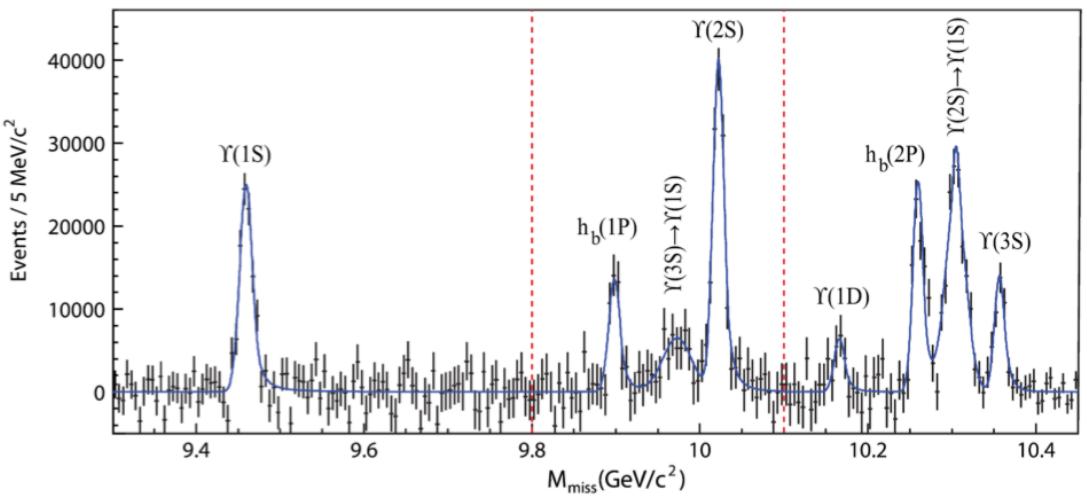

FIGURE 3.1: The inclusive M_{miss} spectrum with the combinatoric background and K^0_S contribution subtracted and signal component of the fit function overlaid [1].

3.2 Observation of Z_b states in the $\Upsilon(nS)\pi^+\pi^-$ and $h_b(mP)\pi^+\pi^-$ states

Belle observed the resonant structure in the $\Upsilon(5S) \to \Upsilon(nS)\pi^+\pi^-$ and $h_b(mP)\pi^+\pi^-$ decays $n = 1, 2, 3; m = 1, 2$ in 2011 [17] and reported with more higher statistics in 2012 [2]. The $\Upsilon(nS)$ states are reconstructed in the $\mu^+\mu^-$ channel and the $h_b(mP)$ states are observed inclusively using missing mass of the $\pi^+\pi^-$ pairs. Invariant mass spectra of the $\Upsilon(nS)\pi^\pm$ and $h_b(mP)\pi^\pm$ combinations are shown in Fig 3.2. Each distribution shows two peaks. The results of the angular analysis indicate that the both states have the same spin-parity $J^P = 1^+$ [17]. Since they are charged states, these states should be isovector states, $I = 1$.

Table 3.3 shows the masses and widths of the two peaks determined from each channels, which are consistent with different channels. The parameters averaged over the five decay channels are

$$M_1 = (10607.4 \pm 2.0)\mathrm{MeV/c^2}, \qquad M_2 = (10652.2 \pm 1.5)\mathrm{MeV/c^2}, \tag{3.6}$$

$$\Gamma_1 = (18.4 \pm 2.4)\mathrm{MeV/c^2}, \qquad \Gamma_2 = (11.5 \pm 2.2)\mathrm{MeV}. \tag{3.7}$$

The peaks are identified as signals of two new states, named $Z_b(10610)$ and $Z_b(10650)$. Thus these decays occur via Z_b resonances, namely $\Upsilon(5S) \to Z_b^\pm\pi^\mp \to \Upsilon(nS)\pi^\pm\pi^\mp$ and $\Upsilon(5S) \to Z_b^\pm\pi^\mp \to h_b(mP)\pi^\pm\pi^\mp$. The results of the amplitude analyses is that the phase between the $Z_b(10610)$ and $Z_b(10650)$ amplitudes is zero for the $\Upsilon(nS)\pi^+\pi^-$ channels, and 180° for the $h_b(mP)\pi^+\pi^-$ channels.

Z_b resonances have remarkable properties. The masses of the $Z_b(10610)$ and $Z_b(10650)$ states are very close to the $B\bar{B}^*$ and $B^*\bar{B}^*$ thresholds, respectively. This fact naturally suggest that Z_b states have a molecular type structure. As stated in the previous section, the decay to the $h_b(mP)\pi^\pm$ is not suppressed relative to the $\Upsilon(nS)\pi^\pm$. This behavior is also explained by molecular interpretation. Considering the heavy-quark spin structure of the $B^{(*)}\bar{B}^*$ molecular states with $I^G(J^P) = 1^+(1^+)$, we can see that Z_b states contain heavy quark singlet and triplet components [18, 31]. The weight of these components would be equal, and therefore the $h_b(mP)\pi^\pm$ decays are not suppressed (See also Section 5.). The $Z_b(10610)$ and $Z_b(10650)$ differ by the sign between heavy quark singlet and triplet components, this explains what the $Z_b(10610)$ and $Z_b(10650)$ amplitudes appear with the sign plus for $\Upsilon(nS)\pi^+\pi^-$ channels and with negative sign

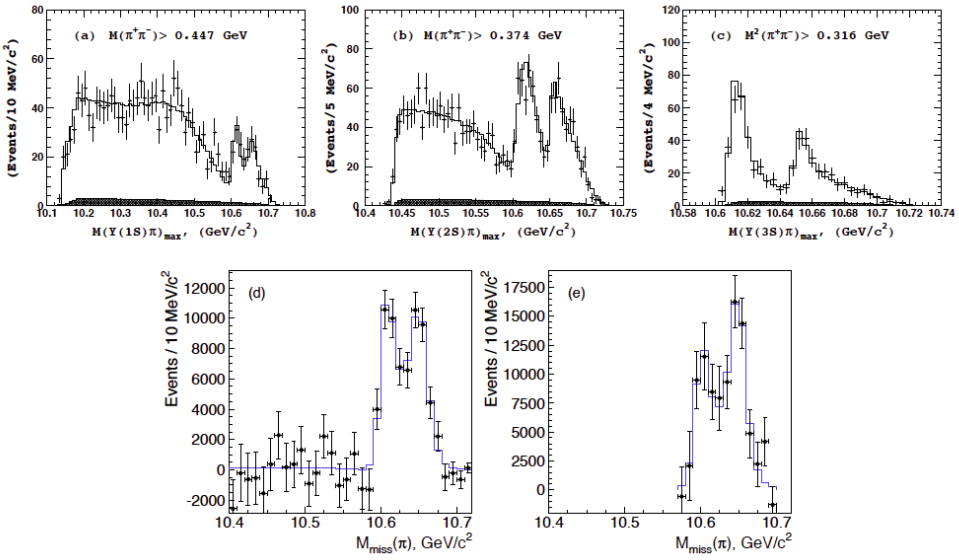

FIGURE 3.2: Invariant mass spectra of the (a) $\Upsilon(1S)\pi^{\pm}$, (b)$\Upsilon(2S)\pi^{\pm}$, (c) $\Upsilon(3S)\pi^{\pm}$, (d)$h_b(1P)\pi^{\pm}$, (e)$h_b(2P)\pi^{\pm}$ combinations [2].

for $h_b(mP)\pi^+\pi^-$ channels. The widths of Z_b states are about $10-20$ MeV, which is narrower compared with the usual expectations of a typical excited bottomonium.

3.3 Observation of the $Z_b(10610) \to B\bar{B}^*$ and $Z_b(10650) \to B^*\bar{B}^*$ decays and branching fractions of Z_b states.

Since Z_b states are slightly above the corresponding thresholds, it is natural to expect that the rate of decays $Z_b(10610) \to B\bar{B}^*$ and $Z_b(10650) \to B^*\bar{B}^*$ are dominant in Z_b decays from the point of view of molecular picture. To search these transitions, Belle studied the $\Upsilon(5S) \to [B^{(*)}\bar{B}^*]^{\pm}\pi^{\mp}$ decays including an observation of the $\Upsilon(5S) \to Z_b^{\pm}(10610)\pi^{\mp} \to [B\bar{B}^* + \text{c.c.}]^{\pm}\pi^{\mp}$ and $\Upsilon(5S) \to Z_b^{\pm}(10650)\pi^{\mp} \to [B^*\bar{B}^*]^{\pm}\pi^{\mp}$ decays as intermediate channels [3]. The distribution of the missing mass of the $B\pi^{\pm}$ pairs shows clear signals of the $\Upsilon(5S) \to [B\bar{B}^* + \text{c.c.}]^{\pm}\pi^{\mp}$ and $\Upsilon(5S) \to [B^*\bar{B}^*]^{\pm}\pi^{\mp}$ as shown in Fig. 3.4 (a). These branching ratios are $(2.83 \pm 0.29 \pm 0.46)$ % and $1.41 \pm 0.19 \pm$

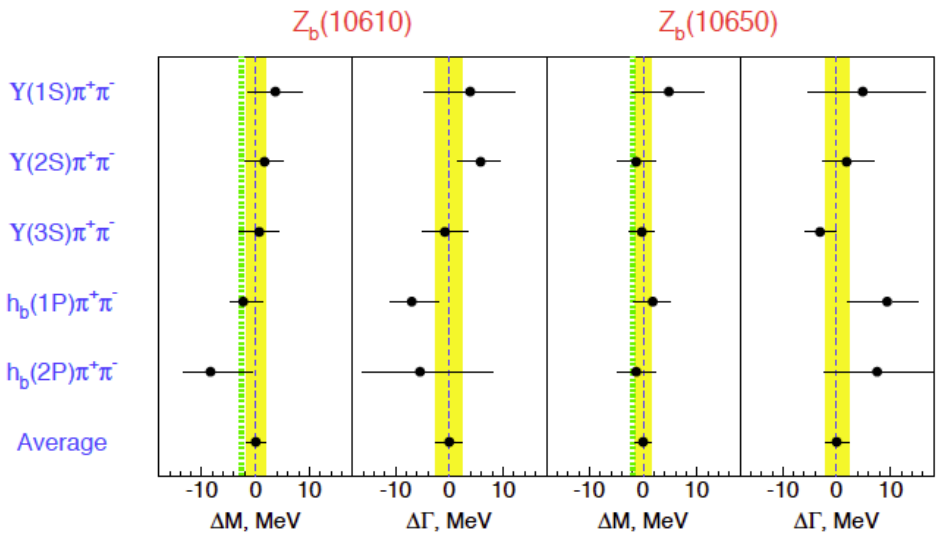

FIGURE 3.3: Green vertical lines indicate the $B\bar{B}^*$ and $B^*\bar{B}^*$ thresholds [2].

0.24 %, respectively. The distributions in the $B\bar{B}^*$ and $B^*\bar{B}^*$ invariant mass for the $\Upsilon(5S) \to [B\bar{B}^* + \text{c.c.}]^{\pm}\pi^{\mp}$ and $\Upsilon(5S) \to [B^*\bar{B}^*]^{\pm}\pi^{\mp}$ regions, which is estimated by the missing mass analysis with the charged pions in Fig. 3.4 (b) and (c), indicate the sharp peak slightly above the respective threshold. These peaks around the thresholds can be interpreted as the signals for the $Z_b(10610) \to B\bar{B}^*$ and $Z_b(10650) \to B^*\bar{B}^*$ decays, with significance of 8σ and 6.8σ, respectively. The significant signal of the $Z_b(10650) \to B\bar{B}^*$ decay is not found. It may implies that the main component of $Z_b(10650)$ is $B^*\bar{B}^*$.

Assuming that the Z_b decays are saturated by the channels so far observed, Belle calculated relative branching fractions of Z_b states (See Table 3.3.). The $B^{(*)}\bar{B}^*$ channel is dominant and accounts for about 80 % in total decay widths, which seems consistent with the expectations of the molecular picture. The $Z_b(10650) \to B\bar{B}^*$ channel is not included in the table because its significance will be marginal, although this decay channel should exist based on potential model (See chapter **??**). We can see that $Z_b \to h_b(mP)\pi^{\pm}$ decays are not suppressed compared with the $Z_b \to \Upsilon(nS)\pi^{\pm}$ decays, as already discussed. This fact is related to the spin structure of Z_b, and discussed in detail in Chapter 5. Another unique feature is that the decay ratios are not simply

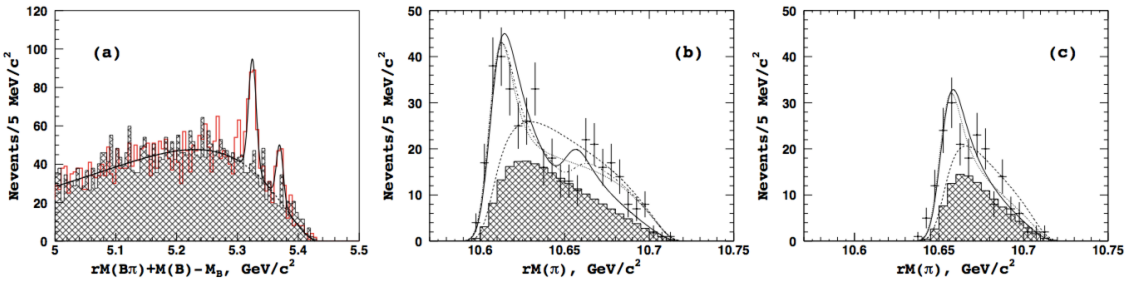

FIGURE 3.4: Missing mass of the pairs formed from the reconstructed B candidate and charged pion (a) and missing mass of the charged pion for the $B\pi$ combinations for (b) $\Upsilon(5S) \to B\bar{B}^*\pi$ and (c) $\Upsilon(5S) \to B^*\bar{B}^*\pi$ candidate events [3].

TABLE 3.3: Branching ratios (Br) of various decay channels from $Z_b(10610)$ and $Z_b'(10650)$.

channel	Br of Z_b	Br of Z_b',
$\Upsilon(1S)\pi^+$	0.32 ± 0.09	0.24 ± 0.07
$\Upsilon(2S)\pi^+$	4.38 ± 1.21	2.40 ± 0.63
$\Upsilon(3S)\pi^+$	2.15 ± 0.56	1.64 ± 0.40
$h_b(1P)\pi^+$	2.81 ± 1.10	7.43 ± 2.70
$h_b(2P)\pi^+$	2.15 ± 0.56	14.8 ± 6.22
$B^+\bar{B}^{*0} + B^{*+}\bar{B}^0$	86.0 ± 3.6	–
$B^{*+}\bar{B}^{*0}$	–	73.4 ± 7.0

proportional to the magnitudes of the phase space. Chapter 6 focuses on the mechanism of the $Z_b \to \Upsilon(nS)\pi^\pm$ decays and this exotic behaviors will be explained.

3.4 Evidence for neutral isotriplet partner $Z_b^0(10610)$

Both $Z_b(10610)$ and $Z_b(10650)$ are isotriplets and only observed the charged components originally. Belle searched for their neutral components using the $\Upsilon(5S) \to \Upsilon(1,2S)\pi^0\pi^0$ decays [4]. The decays are observed and the measured branching fractions, $\mathcal{B}[\Upsilon(5S) \to \Upsilon(1S)\pi^0\pi^0] = (2.25 \pm 0.11 \pm 0.22) \times 10^{-3}$ and $\mathcal{B}[\Upsilon(5S) \to \Upsilon(2S)\pi^0\pi^0] = (3.66 \pm 0.22 \pm 0.48) \times 10^{-3}$, are approximately half size of that for $\Upsilon(5S) \to \Upsilon(1S,2S)\pi^+\pi^-$, which is consistent with isospin relations.

Belle performed the Dalitz plot analyses of the $\Upsilon(5S) \to \Upsilon(1S,2S)\pi^0\pi^0$ transitions and results are summarized in Fig. 3.5. The $Z_b(10610)$ signal is found in the $\Upsilon(2S)\pi^0$ with

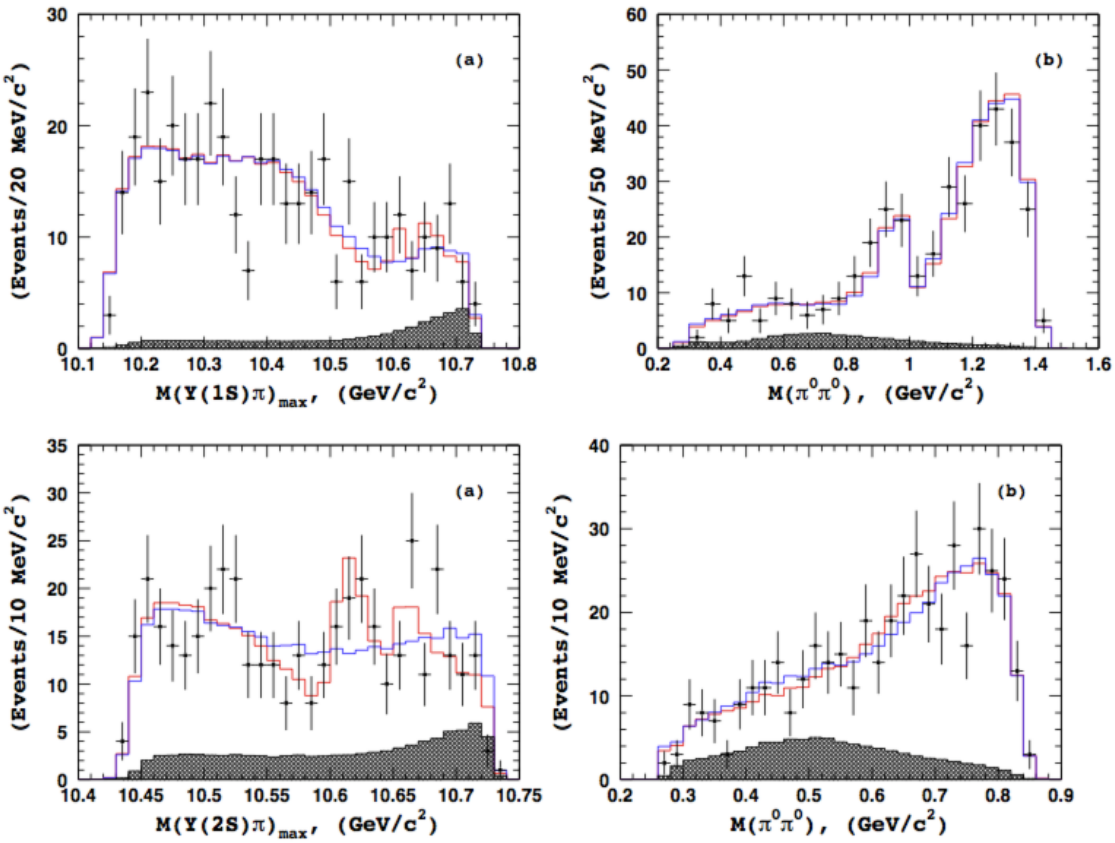

FIGURE 3.5: The projections of the Dalitz plot fit for the $\Upsilon(1S)\pi^0\pi^0$ (top row) and $\Upsilon(2S)\pi^0\pi^0$ (bottom row) channels on the $\Upsilon(nS)\pi^0$ (left column) and $\pi^0\pi^0$ invariant mass [4].

the significance of 4.9σ including systematics. The mass of $Z_b^0(10610)$ are measured as $(10609^{+8}_{-6} \pm 6)\text{MeV}/c^2$, which is consistent with the mass of charged $Z_b^{\pm}(10610)$ states. At this stage, the $Z_b^0(10650)$ signal is not significant in either $\Upsilon(1S)\pi^0\pi^0$ or $\Upsilon(2S)\pi^0\pi^0$ and $Z_b^0(10610)$ in the $\Upsilon(1S)\pi^0$ channel is also insignificant. It should be noted that the Belle data do not contradict the presence of the $Z_b^0(10610) \to \Upsilon(1S)\pi^0$ and the $Z_b^0(10650)$. The available statistics are not enough for the observation of these states.

Chapter 4

Heavy meson molecules with the potential model

We study heavy hadron spectroscopy near open bottom thresholds. We employ B and B^* mesons as effective degrees of freedom near the thresholds, and consider meson exchange potentials between them. All possible composite states which can be constructed from the B and B^* mesons are studied up to the total angular momentum $J \leq 2$. We consider, as exotic states, isosinglet states with exotic J^{PC} quantum numbers and isotriplet states. We solve numerically the Schrödinger equation with channel-couplings for each state. The masses of twin resonances $Z_b(10610)$ and $Z_b(10650)$ found by Belle are reproduced. We predict several possible bound and/or resonant states in other channels, which will be observable in the future experiments.

4.1 $P\bar{P}$ molecules

4.1.1 Introduction for $P\bar{P}$ molecules

As discussed before, $Z_b(10610)^{\pm}$ and $Z_b(10650)^{\pm}$ are strong candidates of exotic heavy meson molecular states. The reported masses and widths of the two resonances are $M(Z_b(10610)) = 10607.2 \pm 2.0$ MeV, $\Gamma(Z_b(10610)) = 18.4 \pm 2.4$ MeV and $M(Z_b(10650)) = 10652.2 \pm 1.5$ MeV, $\Gamma(Z_b(10650)) = (11.5 \pm 2.2)$ MeV [2, 17]. They cannot be simple bottomonia ($b\bar{b}$) because they are electrically charged. Hence, it is useful to study the spectrum of exotic heavy meson molecules.

Well below the thresholds in the heavy quark systems, quarkonia are described by heavy quark degrees of freedom, Q and $\bar{\mathrm{Q}}$ (Q = b, c). Above the thresholds, however, it is a non-trivial problem whether the resonant states are still explained by the quarkonium picture. Clearly, a pair of heavy quark and anti-quark ($\mathrm{Q}\bar{\mathrm{Q}}$) are not sufficient effective degrees of freedom to form the resonances, because they are affected by the scattering states of the two open heavy mesons. Indeed, many resonant states are found around the thresholds in experiments. However they do not fit into the ordinary classification scheme of hadrons, such as the quark model calculation. Properties for masses, decay widths, branching ratios, and so forth, are not predicted by the simple quarkonium picture [16]. Therefore it is necessary to introduce components other than $\mathrm{Q}\bar{\mathrm{Q}}$ as effective degrees of freedom around the thresholds.

Instead of the dynamics of $\mathrm{Q}\bar{\mathrm{Q}}$, in the present discussion, we study the dynamics described by a pair of a pseudoscalar meson $\mathrm{P} \sim (\bar{\mathrm{Q}}\mathrm{q})_{\mathrm{spin}\,0}$ or a vector meson $\mathrm{P}^* \sim (\bar{\mathrm{Q}}\mathrm{q})_{\mathrm{spin}\,1}$ (q = u, d) and their anti-mesons $\bar{\mathrm{P}}$ or $\bar{\mathrm{P}}^*$, which are relevant hadronic degrees of freedom around the thresholds. In the following, we introduce the notation $\mathrm{P}^{(*)}$ for P or P^* for simplicity. We discuss the possible existence of the $\mathrm{P}^{(*)}\bar{\mathrm{P}}^{(*)}$ bound and/or resonant states near the thresholds. An interesting feature is that the pseudoscalar P meson and the vector P^* meson become degenerate in mass in the heavy quark limit ($M_{\mathrm{Q}} \to \infty$). The mass degeneracy originates from the suppression of the Pauli term in the magnetic gluon sector in QCD, which is the quantity of order $\mathcal{O}(1/M_{\mathrm{Q}})$ with heavy quark mass M_{Q} [27, 32]. Therefore, the effective degrees of freedom at the threshold are given, not only by $\mathrm{P}\bar{\mathrm{P}}$, but also by combinations, such as $\mathrm{P}^*\bar{\mathrm{P}}$, $\mathrm{P}\bar{\mathrm{P}}^*$ and $\mathrm{P}^*\bar{\mathrm{P}}^*$. Because $\mathrm{P}^{(*)}$ includes a heavy anti-quark $\bar{\mathrm{Q}}$ and a light quark q, the Lagrangian of P and P^* meson systems is given with respecting the heavy quark symmetry (spin symmetry) and chiral symmetry [27, 33, 34, 35, 36, 37, 38, 39, 40].

A new degree of freedom which does not exist in the $\mathrm{Q}\bar{\mathrm{Q}}$ systems but does only in the $\mathrm{P}^{(*)}\bar{\mathrm{P}}^{(*)}$ systems is an isospin. Then, there appears one pion exchange potential (OPEP) between $\mathrm{P}^{(*)}$ and $\bar{\mathrm{P}}^{(*)}$ mesons at long distances of order $1/m_\pi$ with pion mass m_π. What is interesting in the OPEP between $\mathrm{P}^{(*)}$ and $\bar{\mathrm{P}}^{(*)}$ is that it causes a mixing between states of different angular momentum, such as L and $L \pm 2$, through its tensor component. Therefore, it is expected that the $\mathrm{P}^{(*)}\bar{\mathrm{P}}^{(*)}$ systems behave differently from the quarkonium systems. In reality in addition to the one pion exchange dominated at long distances, there are multiple pion ($\pi\pi$, $\pi\pi\pi$, etc.) exchange, heavy meson (ρ, ω, σ, etc.) exchange at short distances as well. With these potentials, we solve the two-body

Schrödinger equation with channel-couplings and discuss the existence of bound and/or resonant states of $\mathrm{P}^{(*)}\bar{\mathrm{P}}^{(*)}$.

In this section, we study $\mathrm{P}^{(*)}\bar{\mathrm{P}}^{(*)}$ systems, with exotic quantum numbers which cannot be accessed by quarkonia. The first group is for isosinglet states with $I = 0$. We recall that the possible J^{PC} of quarkonia are $J^{PC} = 0^{-+}$ (η_b), 0^{++} ($\chi_{\mathrm{b}0}$) for $J = 0$, J^{--} (Υ), J^{+-} ($\mathrm{h_b}$), J^{++} ($\chi_{\mathrm{b}1}$) for odd $J \geq 1$, and J^{--}, J^{-+}, J^{++} ($\chi_{\mathrm{b}2}$) for even $J \geq 2$, where examples of bottomonia are shown in the parentheses. However, there cannot be $J^{PC} = 0^{--}$ and 0^{+-}, J^{-+} with odd $J \geq 1$, and J^{+-} with even $J \geq 2$ in the quarkonia. These quantum numbers are called exotic J^{PC}, and it has been discussed that they are the signals for exotics including the $\mathrm{P}^{(*)}\bar{\mathrm{P}}^{(*)}$ systems and glueballs. The second group is for isospin triplet states with $I = 1$. It is obvious that the quarkonia themselves cannot be isotriplet. To have a finite isospin, there must be additional light quark degrees of freedom [41]. In this regard, $\mathrm{P}^{(*)}$ and $\bar{\mathrm{P}}^{(*)}$ mesons have isospin half, and therefore the $\mathrm{P}^{(*)}\bar{\mathrm{P}}^{(*)}$ composite systems can be isospin triplet. We observe that, near the thresholds, the $\mathrm{P}^{(*)}\bar{\mathrm{P}}^{(*)}$ systems can access to more various quantum numbers than the $\mathrm{Q}\bar{\mathrm{Q}}$ systems. In this section, we focus on the bottom sector ($\mathrm{P} = \mathrm{B}$ and $\mathrm{P}^* = \mathrm{B}^*$), because the heavy quark symmetry works better than the charm sector.

In the previous works, Ericson and Karl estimated the OPEP in hadronic molecules within strangeness sector and indicated the importance of tensor interaction in this system [42]. Törnqvist analyzed one pion exchange force between two mesons for many possible quantum numbers in [43, 44]. Inspired by the discovery of X(3872), the hadronic molecular model has been developed by many authors [14, 15, 45, 46, 47, 48, 49]. For $\mathrm{Z_b}$'s many works have already been done since the Belle's discovery. As candidates of exotic states, molecular structure has been studied [50, 51, 52, 53, 54, 55, 56], and also tetraquark structure [57, 58, 59, 60, 61, 62]. The existence of $\mathrm{Z_b}$'s has also been investigated in the decays of $\Upsilon(5S)$ [63, 64, 65, 66]. Our study based on the molecular picture of $\mathrm{P}^{(*)}\bar{\mathrm{P}}^{(*)}$ differs from the previous works in that we completely take into account the degeneracy of pseudoscalar meson B and a vector meson B^* due to the heavy quark symmetry, and fully consider channel-couplings of $\mathrm{B}^{(*)}$ and $\bar{\mathrm{B}}^{(*)}$. In the previous publications, the low lying molecular states around $\mathrm{Z_b}$'s which can be produced from the decay of $\Upsilon(5S)$ were studied systematically and qualitatively [18, 67]. Our present work covers them also.

This section is organized as followings. In 4.1.2, we introduce (i) the π exchange potential and (ii) the $\pi\rho\,\omega$ potential between $\mathrm{B}^{(*)}$ and $\bar{\mathrm{B}}^{(*)}$ mesons. To obtain the potentials, we

respect the heavy quark symmetry for the $B^{(*)}B^{(*)}\pi$, $B^{(*)}B^{(*)}\rho$ and $B^{(*)}B^{(*)}\omega$ vertices. In section 4.1.3, we classify all the possible states composed by a pair of $B^{(*)}$ and $\bar{B}^{(*)}$ mesons with exotic quantum numbers $I^G(J^{PC})$ with isospin I, G-parity, total angular momentum J, parity P and charge conjugation C. (C in $I = 1$ is defined only for states of $I_z = 0$.) In section 4.1.4, we solve numerically the Schrödinger equations with channel-couplings and discuss the bound and/or resonant states of the $B^{(*)}\bar{B}^{(*)}$ systems. We employ the hadronic molecular picture and only consider the $B^{(*)}\bar{B}^{(*)}$ states. In practice, there are bottomonium and light meson states which couple to these states. The effect of these couplings as quantum corrections is estimated in section 4.1.5. In 4.1.6, we discuss the possible decay modes of these states. 4.1.7 is devoted to summary.

4.1.2 Interactions with heavy quark symmetry

$B^{(*)}$ mesons have a heavy anti-quark $\bar{b}$ and a light quark q = u, d. The dynamics of the $B^{(*)}\bar{B}^{(*)}$ systems is given by the two symmetries: the heavy quark symmetry for heavy quarks and chiral symmetry for light quarks. These two symmetries provide the vertices of π meson and of vector meson ($v = \rho, \omega$) with open heavy flavor (bottom) mesons P and P^* (P for B and P^* for B^*)

$$\mathcal{L}_{\pi HH} = g\,\mathrm{tr}\bar{H}_a H_b \gamma_\nu \gamma_5 A^\nu_{ba}, \tag{4.1}$$

$$\mathcal{L}_{vHH} = -i\beta \mathrm{tr}\bar{H}_a H_b v^\mu (\rho_\mu)_{ba} + i\lambda \mathrm{tr}\bar{H}_a H_b \sigma_{\mu\nu} F_{\mu\nu}(\rho)_{ba}\,, \tag{4.2}$$

where the multiplet field H containing P and P^* is defined by

$$H_a = \frac{1+\not{v}}{2}\left[P^*_{a\mu}\gamma^\mu - P_a\gamma_5\right], \tag{4.3}$$

with the four velocity v_μ of the heavy mesons [32]. The conjugate field is defined by $\bar{H}_a = \gamma_0 H_a^\dagger \gamma_0$, and the index a denotes up and down flavors. The axial current is given by $A_\mu \simeq \frac{i}{f_\pi}\partial_\mu \hat{\pi}$ with the pion field

$$\hat{\pi} = \begin{pmatrix} \frac{\pi^0}{\sqrt{2}} & \pi^+ \\ \pi^- & -\frac{\pi^0}{\sqrt{2}} \end{pmatrix}, \tag{4.4}$$

where $f_\pi = 135$ MeV is the pion decay constant. The coupling constant $|g| = 0.59$ for πPP^* is determined with reference to the observed decay width $\Gamma = 96$ keV for $D^* \to D\pi$ [68], assuming that the charm quark is sufficiently heavy. The coupling constant g for

πBB* would be different from the one for πDD* because of $1/m_{\rm Q}$ corrections with the heavy quark mass $m_{\rm Q}$ [69]. However the lattice simulation in the heavy quark limit suggests a similar value as adopted above [70], allowing us to use the common value for D and B. The coupling of $\pi P^* P^*$, which is difficult to access from experiments, is also fixed thanks to the heavy quark symmetry. Note that the coupling of πPP does not exist due to the parity conservation. The coupling constants β and λ are determined by the radiative decays of D* meson and semileptonic decays of B meson with vector meson dominance as $\beta = 0.9$ and $\lambda = 0.56$ GeV^{-1} by following Ref. [71]. The vector (ρ and ω) meson field is defined by

$$\rho_\mu = i\frac{g_V}{\sqrt{2}}\hat{\rho_\mu}\,, \tag{4.5}$$

with

$$\hat{\rho_\mu} = \begin{pmatrix} \frac{\rho^0}{\sqrt{2}} + \frac{\omega}{\sqrt{2}} & \rho^+ \\ \rho^- & -\frac{\rho^0}{\sqrt{2}} + \frac{\omega}{\sqrt{2}} \end{pmatrix}_\mu , \tag{4.6}$$

and its field tensor by

$$F_{\mu\nu}(\rho) = \partial_\mu \rho_\nu - \partial_\nu \rho_\mu + [\rho_\mu, \rho_\nu]\,, \tag{4.7}$$

where $g_V = 5.8$ is the coupling constant for $\rho \to \pi\pi$ decay.

From Eq. (4.1), we obtain the πPP^* and $\pi P^* P^*$ vertices

$$\mathcal{L}_{\pi PP^*} = 2\frac{g}{f_\pi}(P_a^\dagger P^*_{b\,\mu} + P^{*\,\dagger}_{a\,\mu} P_b)\partial^\mu \hat{\pi}_{ab}\,, \tag{4.8}$$

$$\mathcal{L}_{\pi P^* P^*} = 2i\frac{g}{f_\pi}\epsilon^{\alpha\beta\mu\nu} v_\alpha P^{*\,\dagger}_{a\,\beta} P^*_{b\,\mu} \partial_\nu \hat{\pi}_{ab}\,. \tag{4.9}$$

The $\pi\bar{P}\bar{P}^*$ and $\pi\bar{P}^*\bar{P}^*$ vertices are obtained by changing the sign of the πPP^* and $\pi P^* P^*$ vertices in Eqs. (4.8) and (4.9). Similarly, from Eq. (4.2) we derive the vPP, vPP^* and vP^*P^* vertices ($v = \rho,\, \omega$) as

$$\mathcal{L}_{vPP} = -\sqrt{2}\beta g_V P_b P_a^\dagger v\cdot\hat{\rho}_{ba}\,, \tag{4.10}$$

$$\mathcal{L}_{vPP^*} = -2\sqrt{2}\lambda g_V v_\mu \epsilon^{\mu\nu\alpha\beta}\left(P_a^\dagger P^*_{b\,\beta} - P^{*\,\dagger}_{a\,\beta} P_b\right)\partial_\nu(\hat{\rho}_\alpha)_{ba}\,, \tag{4.11}$$

$$\begin{aligned}\mathcal{L}_{vP^*P^*} &= \sqrt{2}\beta g_V P^*_b P^{*\dagger}_a v\cdot\hat{\rho}_{ba} \\ &\quad + i2\sqrt{2}\lambda g_V P^{*\,\dagger}_{a\,\mu} P^*_{b\,\nu}(\partial^\mu(\hat{\rho}^\nu)_{ba} - \partial^\nu(\hat{\rho}^\mu)_{ba})\,.\end{aligned} \tag{4.12}$$

Due to the G-parity, the signs of vertices for $v\bar{P}\bar{P}$, $v\bar{P}\bar{P}^*$ and $v\bar{P}^*\bar{P}^*$ are opposite to those of vPP, vPP^* and vP^*P^*, respectively, for $v=\omega$, while they are the same for $v=\rho$.

It is important that the scatterings $P^{(*)}\bar{P}^{(*)} \to P^{(*)}\bar{P}^{(*)}$ include not only diagonal components $P\bar{P}^* \to P^*\bar{P}$ and $P^*\bar{P}^* \to P^*\bar{P}^*$ but also off-diagonal components $P\bar{P} \to P^*\bar{P}^*$ and $P\bar{P}^* \to P^*\bar{P}^*$. The OPEPs for $P\bar{P}^* \to P^*\bar{P}$ and $P^*\bar{P}^* \to P^*\bar{P}^*$ are given from the vertices (4.8) and (4.9) in the heavy quark limit as

$$V^{\pi}_{P_1\bar{P}_2^*\to P_1^*\bar{P}_2} = -\left(\sqrt{2}\frac{g}{f_\pi}\right)^2 \frac{1}{3}\left[\vec{\varepsilon}_1^{\,*}\cdot\vec{\varepsilon}_2\, C(r;m_\pi)+S_{\varepsilon_1^*,\varepsilon_2}\, T(r;m_\pi)\right]\vec{\tau}_1\cdot\vec{\tau}_2, \quad (4.13)$$

$$V^{\pi}_{P_1^*\bar{P}_2^*\to P_1^*\bar{P}_2^*} = -\left(\sqrt{2}\frac{g}{f_\pi}\right)^2 \frac{1}{3}\left[\vec{T}_1\cdot\vec{T}_2\, C(r;m_\pi)+S_{T_1,T_2}\, T(r;m_\pi)\right]\vec{\tau}_1\cdot\vec{\tau}_2, \quad (4.14)$$

and the OPEPs for $P\bar{P} \to P^*\bar{P}^*$ and $P\bar{P}^* \to P^*\bar{P}^*$ are given as

$$V^{\pi}_{P_1\bar{P}_2\to P_1^*\bar{P}_2^*} = -\left(\sqrt{2}\frac{g}{f_\pi}\right)^2 \frac{1}{3}\left[\vec{\varepsilon}_1^{\,*}\cdot\vec{\varepsilon}_2^{\,*}\, C(r;m_\pi)+S_{\varepsilon_1^*,\varepsilon_2^*}\, T(r;m_\pi)\right]\vec{\tau}_1\cdot\vec{\tau}_2, \quad (4.15)$$

$$V^{\pi}_{P_1\bar{P}_2^*\to P_1^*\bar{P}_2^*} = \left(\sqrt{2}\frac{g}{f_\pi}\right)^2 \frac{1}{3}\left[\vec{\varepsilon}_1^{\,*}\cdot\vec{T}_2\, C(r;m_\pi)+S_{\varepsilon_1^*,T_2}\, T(r;m_\pi)\right]\vec{\tau}_1\cdot\vec{\tau}_2. \quad (4.16)$$

Here three polarizations are possible for P^* as defined by $\vec{\varepsilon}^{\,(\pm)} = \left(\mp 1/\sqrt{2}, \pm i/\sqrt{2}, 0\right)$ and $\vec{\varepsilon}^{\,(0)} = (0,0,1)$, and the spin-one operator $\vec{T}$ is defined by $T^i_{\lambda'\lambda} = i\varepsilon^{ijk}\varepsilon_j^{(\lambda')\dagger}\varepsilon_k^{(\lambda)}$. As a convention, we assign $\vec{\varepsilon}^{\,(\lambda)}$ for an incoming vector particle and $\vec{\varepsilon}^{\,(\lambda)*}$ for an outgoing vector particle. Here $\vec{\tau}_1$ and $\vec{\tau}_2$ are isospin operators for $P_1^{(*)}$ and $\bar{P}_2^{(*)}$. We define the tensor operators

$$S_{\varepsilon_1^*,\varepsilon_2} = 3(\vec{\varepsilon}^{\,(\lambda_1)*}\cdot\hat{r})(\vec{\varepsilon}^{\,(\lambda_2)}\cdot\hat{r}) - \vec{\varepsilon}^{\,(\lambda_1)*}\cdot\vec{\varepsilon}^{\,(\lambda_2)}, \quad (4.17)$$

$$S_{T_1,T_2} = 3(\vec{T}_1\cdot\hat{r})(\vec{T}_2\cdot\hat{r}) - \vec{T}_1\cdot\vec{T}_2, \quad (4.18)$$

$$S_{\varepsilon_1^*,\varepsilon_2^*} = 3(\vec{\varepsilon}^{\,(\lambda_1)*}\cdot\hat{r})(\vec{\varepsilon}^{\,(\lambda_2)*}\cdot\hat{r}) - \vec{\varepsilon}^{\,(\lambda_1)*}\cdot\vec{\varepsilon}^{\,(\lambda_2)*}, \quad (4.19)$$

$$S_{\varepsilon_1^*,T_2} = 3(\vec{\varepsilon}^{\,(\lambda_1)*}\cdot\hat{r})(\vec{T}_2\cdot\hat{r}) - \vec{\varepsilon}^{\,(\lambda_1)*}\cdot\vec{T}_2. \quad (4.20)$$

The ρ meson exchange potentials are derived by using the same notation of the OPEPs and the vertices in Eqs. (4.10)-(4.12),

$$V^v_{P_1\bar{P}_2\to P_1\bar{P}_2} = \left(\frac{\beta g_V}{2m_v}\right)^2 \frac{1}{3} C(r;m_v)\vec{\tau}_1\cdot\vec{\tau}_2, \tag{4.21}$$

$$V^v_{P_1\bar{P}^*_2\to P_1\bar{P}^*_2} = \left(\frac{\beta g_V}{2m_v}\right)^2 \frac{1}{3} C(r;m_v)\vec{\tau}_1\cdot\vec{\tau}_2, \tag{4.22}$$

$$V^v_{P_1\bar{P}^*_2\to P^*_1\bar{P}_2} = (2\lambda g_V)^2 \frac{1}{3}\left[2\vec{\varepsilon}^{\,*}_1\cdot\vec{\varepsilon}_2\, C(r;m_v) - S_{\varepsilon^*_1,\varepsilon_2}\, T(r;m_v)\right]\vec{\tau}_1\cdot\vec{\tau}_2, \tag{4.23}$$

$$\begin{aligned} V^v_{P^*_1\bar{P}^*_2\to P^*_1\bar{P}^*_2} &= (2\lambda g_V)^2 \frac{1}{3}\left[2\vec{T}_1\cdot\vec{T}_2\, C(r;m_v) - S_{T_1,T_2}\, T(r;m_v)\right]\vec{\tau}_1\cdot\vec{\tau}_2 \\ &\quad + \left(\frac{\beta g_V}{2m_v}\right)^2 \frac{1}{3} C(r;m_v)\vec{\tau}_1\cdot\vec{\tau}_2, \end{aligned} \tag{4.24}$$

$$V^v_{P_1\bar{P}_2\to P^*_1\bar{P}^*_2} = (2\lambda g_V)^2 \frac{1}{3}\left[2\vec{\varepsilon}^{\,*}_1\cdot\vec{\varepsilon}^{\,*}_2\, C(r;m_v) - S_{\varepsilon^*_1,\varepsilon^*_2}\, T(r;m_v)\right]\vec{\tau}_1\cdot\vec{\tau}_2, \tag{4.25}$$

$$V^v_{P_1\bar{P}^*_2\to P^*_1\bar{P}^*_2} = -(2\lambda g_V)^2 \frac{1}{3}\left[2\vec{\varepsilon}^{\,*}_1\cdot\vec{T}_2\, C(r;m_v) - S_{\varepsilon^*_1,T_2}\, T(r;m_v)\right]\vec{\tau}_1\cdot\vec{\tau}_2, \tag{4.26}$$

for $v=\rho$. The ω exchange potentials are obtained by changing the overall sign from the above equations with $v=\omega$ and by removing the isospin factor $\vec{\tau}_1\cdot\vec{\tau}_2$.

To estimate the size effect of mesons, we introduce a form factor $(\Lambda^2-m_h^2)/(\Lambda^2+\vec{q}^{\,2})$ in the momentum space at vertices of hPP, hPP^* and hP^*P^* ($h=\pi$, ρ and ω). Here $\vec{q}$ and m_h are momentum and mass of the exchanged meson, and Λ is the cut-off parameter. Then, $C(r;m_h)$ and $T(r;m_h)$ are defined as

$$C(r;m_h) = \int \frac{\mathrm{d}^3\vec{q}}{(2\pi)^3}\frac{m_h^2}{\vec{q}^{\,2}+m_h^2} e^{i\vec{q}\cdot\vec{r}}\, F(\vec{q};m_h), \tag{4.27}$$

$$T(r;m_h)S_{12}(\hat{r}) = \int \frac{\mathrm{d}^3\vec{q}}{(2\pi)^3}\frac{-\vec{q}^{\,2}}{\vec{q}^{\,2}+m_h^2} S_{12}(\hat{q}) e^{i\vec{q}\cdot\vec{r}} F(\vec{q};m_h), \tag{4.28}$$

with $S_{12}(\hat{x}) = 3(\vec{\sigma}_1\cdot\hat{x})(\vec{\sigma}_2\cdot\hat{x}) - \vec{\sigma}_1\cdot\vec{\sigma}_2$, and $F(\vec{q};m_h) = (\Lambda^2-m_h^2)^2/(\Lambda^2+\vec{q}^{\,2})^2$. The cut-off Λ is determined from the size of $\mathrm{B}^{(*)}$ based on the quark model as discussed in Refs. [72, 73]. There, the cut-off parameter is $\Lambda = 1070$ MeV when the π exchange potential is employed, while $\Lambda = 1091$ MeV when the $\pi\rho\omega$ potential is employed.

As a brief summary, we emphasize again that, according to the heavy quark symmetry, not only the $\mathrm{B}\bar{\mathrm{B}}^* \to \mathrm{B}^*\bar{\mathrm{B}}$ and $\mathrm{B}^*\bar{\mathrm{B}}^* \to \mathrm{B}^*\bar{\mathrm{B}}^*$ transitions but also the $\mathrm{B}\bar{\mathrm{B}} \to \mathrm{B}^*\bar{\mathrm{B}}^*$ and $\mathrm{B}\bar{\mathrm{B}}^* \to \mathrm{B}^*\bar{\mathrm{B}}^*$ transitions become important as channel-couplings. In the next section, we will see that the latter two transitions supply the strong tensor force, through the channel mixing B and B^* as well as different angular momentum, such as L and $L\pm 2$.

4.1.3 Classification of the $\mathrm{B}^{(*)}\bar{\mathrm{B}}^{(*)}$ states

TABLE 4.1: The exotic quantum numbers which cannot be assigned to bottomonia $\mathrm{b\bar{b}}$ are indicated by $\surd$. The 0^{+-} state cannot be neither bottomonium nor $\mathrm{B}^{(*)}\bar{\mathrm{B}}^{(*)}$ states.

J^{PC}	components	exoticness	
		$I=0$	$I=1$
0^{+-}	——	$\surd$	$\surd$
0^{++}	$\mathrm{B\bar{B}}(^1S_0)$, $\mathrm{B^*\bar{B}^*}(^1S_0)$, $\mathrm{B^*\bar{B}^*}(^5D_0)$	$\chi_{\mathrm{b}0}$	$\surd$
0^{--}	$\frac{1}{\sqrt{2}}\left(\mathrm{B\bar{B}^*}+\mathrm{B^*\bar{B}}\right)(^3P_0)$	$\surd$	$\surd$
0^{-+}	$\frac{1}{\sqrt{2}}\left(\mathrm{B\bar{B}^*}-\mathrm{B^*\bar{B}}\right)(^3P_0)$, $\mathrm{B^*\bar{B}^*}(^3P_0)$	η_{b}	$\surd$
1^{+-}	$\frac{1}{\sqrt{2}}\left(\mathrm{B\bar{B}^*}-\mathrm{B^*\bar{B}}\right)(^3S_1)$, $\frac{1}{\sqrt{2}}\left(\mathrm{B\bar{B}^*}-\mathrm{B^*\bar{B}}\right)(^3D_1)$, $\mathrm{B^*\bar{B}^*}(^3S_1)$, $\mathrm{B^*\bar{B}^*}(^3D_1)$	$\mathrm{h_b}$	$\surd$
1^{++}	$\frac{1}{\sqrt{2}}\left(\mathrm{B\bar{B}^*}+\mathrm{B^*\bar{B}}\right)(^3S_1)$, $\frac{1}{\sqrt{2}}\left(\mathrm{B\bar{B}^*}+\mathrm{B^*\bar{B}}\right)(^3D_1)$, $\mathrm{B^*\bar{B}^*}(^5D_1)$	$\chi_{\mathrm{b}1}$	$\surd$
1^{--}	$\mathrm{B\bar{B}}(^1P_1)$, $\frac{1}{\sqrt{2}}\left(\mathrm{B\bar{B}^*}+\mathrm{B^*\bar{B}}\right)(^3P_1)$, $\mathrm{B^*\bar{B}^*}(^1P_1)$, $\mathrm{B^*\bar{B}^*}(^5P_1)$, $\mathrm{B^*\bar{B}^*}(^5F_1)$	Υ	$\surd$
1^{-+}	$\frac{1}{\sqrt{2}}\left(\mathrm{B\bar{B}^*}-\mathrm{B^*\bar{B}}\right)(^3P_1)$, $\mathrm{B^*\bar{B}^*}(^3P_1)$	$\surd$	$\surd$
2^{+-}	$\frac{1}{\sqrt{2}}\left(\mathrm{B\bar{B}^*}-\mathrm{B^*\bar{B}}\right)(^3D_2)$, $\mathrm{B^*\bar{B}^*}(^3D_2)$	$\surd$	$\surd$
2^{++}	$\mathrm{B\bar{B}}(^1D_2)$, $\frac{1}{\sqrt{2}}\left(\mathrm{B\bar{B}^*}+\mathrm{B^*\bar{B}}\right)(^3D_2)$, $\mathrm{B^*\bar{B}^*}(^1D_2)$, $\mathrm{B^*\bar{B}^*}(^5S_2)$, $\mathrm{B^*\bar{B}^*}(^5D_2)$, $\mathrm{B^*\bar{B}^*}(^5G_2)$	$\chi_{\mathrm{b}2}$	$\surd$
2^{-+}	$\frac{1}{\sqrt{2}}\left(\mathrm{B\bar{B}^*}-\mathrm{B^*\bar{B}}\right)(^3P_2)$, $\frac{1}{\sqrt{2}}\left(\mathrm{B\bar{B}^*}-\mathrm{B^*\bar{B}}\right)(^3F_2)$, $\mathrm{B^*\bar{B}^*}(^3P_2)$, $\mathrm{B^*\bar{B}^*}(^3F_2)$	$\eta_{\mathrm{b}2}$	$\surd$
2^{--}	$\frac{1}{\sqrt{2}}\left(\mathrm{B\bar{B}^*}+\mathrm{B^*\bar{B}}\right)(^3P_2)$, $\frac{1}{\sqrt{2}}\left(\mathrm{B\bar{B}^*}+\mathrm{B^*\bar{B}}\right)(^3F_2)$, $\mathrm{B^*\bar{B}^*}(^5P_2)$, $\mathrm{B^*\bar{B}^*}(^5F_2)$	$\psi_{\mathrm{b}2}$	$\surd$

We classify all the possible quantum numbers $I^G(J^{PC})$ with isospin I, G-parity, total angular momentum J, parity P and charge conjugation C for the states which can be composed by a pair of $\mathrm{B}^{(*)}$ and $\bar{\mathrm{B}}^{(*)}$ mesons. The charge conjugation C is defined for $I=0$ or $I_z=0$ components for $I=1$, and is related to the G-parity by $G=(-1)^I C$. In the present discussion, we restrict upper limit of the total angular momentum as $J\leq 2$, because too higher angular momentum will be disfavored to form bound or resonant states. The $\mathrm{B}^{(*)}\bar{\mathrm{B}}^{(*)}$ components in the wave functions for various J^{PC} are listed in Table 4.5. We use the notation $^{2S+1}L_J$ to denote the total spin S and relative angular momentum L of the two body states of $\mathrm{B}^{(*)}$ and $\bar{\mathrm{B}}^{(*)}$ mesons. We note that there are not only $\mathrm{B\bar{B}}$ and $\mathrm{B^*\bar{B}^*}$ components but also $\mathrm{B\bar{B}^*}\pm\mathrm{\bar{B}B^*}$ components. The $J^{PC}=0^{+-}$ state cannot be generated by a combination of $\mathrm{B}^{(*)}$ and $\bar{\mathrm{B}}^{(*)}$ mesons [1]. For $I=0$, there are many $\mathrm{B}^{(*)}\bar{\mathrm{B}}^{(*)}$ states whose quantum number J^{PC} are the same as those of the quarkonia as shown in the third row of $I=0$. In the present study, however, we do

[1] The $J^{PC}=0^{+-}$ state cannot be given also in the quarkonium picture.

not consider these states, because we have not yet included mixing terms between the quarkonia and the $B^{(*)}\bar{B}^{(*)}$ states. This problem will be left as future works. Therefore, for $I = 0$, we consider only the exotic quantum numbers $J^{PC} = 0^{--}$, 1^{-+} and 2^{+-}. The states of $I = 1$ are clearly not accessible by quarkonia. We investigate all possible J^{PC} states listed in Table 4.5.

From Eqs. (4.13)-(4.16) and (4.42)-(4.47), we obtain the potentials with channel-couplings for each quantum number $I^G(J^{PC})$. For each state, the Hamiltonian is given as a sum of the kinetic energy and the potential with channel-couplings in a form of a matrix. Breaking of the heavy quark symmetry is taken into account by mass difference between B and B^* mesons in the kinetic term. The explicit forms of the Hamiltonian for each $I^G(J^{PC})$ are presented in Appendix A. For example, the $J^{PC} = 1^{+-}$ state has four components, $\frac{1}{\sqrt{2}}\left(B\bar{B}^* - B^*\bar{B}\right)(^3S_1)$, $\frac{1}{\sqrt{2}}\left(B\bar{B}^* - B^*\bar{B}\right)(^3D_1)$, $B^*\bar{B}^*(^3S_1)$, $B^*\bar{B}^*(^3D_1)$ and hence it gives a potential in the form of 4×4 matrix as Eqs. (A.6), (A.58) and (A.28).

4.1.4 Numerical results

To obtain the solutions of the $B^{(*)}\bar{B}^{(*)}$ states, we solve numerically the Schrödinger equations which are second-order differential equations with channel-couplings. As numerics, the renormalized Numerov method developed in Ref. [74] is adopted. The resonant states are found from the phase shift δ as a function of the scattering energy E. The resonance position E_r is defined by an inflection point of the phase shift $\delta(E)$ and the resonance width by $\Gamma_r = 2/(d\delta/dE)_{E=E_r}$ following Ref. [75]. To check consistency of our method with others, we also use the complex scaling method (CSM). We obtain an agreement in results between the renormalized Nemerov method and the CSM.

In Table 4.2, we summarize the result of the obtained bound and resonant states, and their possible decay modes to quarkonium and light flavor meson. For decay modes, the ρ meson can be either real or virtual depending on the mass of the decaying particle, depending on the resonance energy which is either sufficient or not to emit the real state of ρ or ω meson. $\rho^*(\omega^*)$ indicates that it is a virtual state in radiative decays assuming the vector meson dominance. We show the mass spectrum of these states in Fig 4.1.

Let us see the states of isospin $I = 1$. Interestingly, having the present potential we find the twin states in the $I^G(J^{PC}) = 1^+(1^{+-})$ near the $B\bar{B}^*$ and $B^*\bar{B}^*$ thresholds; a bound state slightly below the $B\bar{B}^*$ threshold, and a resonant state slightly above the $B^*\bar{B}^*$ threshold. The binding energy is 8.5 MeV, and the resonance energy and decay width

are 50.4 MeV and 15.1 MeV, respectively, from the $B\bar{B}^*$ threshold. The twin states are obtained when the $\pi\rho\omega$ potential is used. We interpret them as the $Z_b(10610)$ and $Z_b(10650)$ observed in the Belle experiment [2, 17]. It should be emphasized that the interaction in the present study has been determined in the previous works without knowing the experimental data of Z_b's [72, 73].

Several comments are in order. First, the bound state of lower energy has been obtained in the coupled channel method of $B\bar{B}^*$ and $B^*\bar{B}^*$ channels. In reality, however, they also couple to other lower channels such as πh_b, $\pi\Upsilon$ and so on as shown in Table 4.5. Once these decay channels are included, the bound state will be a resonant state with a finite width. A qualitative discussion will be given in Section 5. Second, when the π exchange potential is used, only the lower bound state is obtained but the resonant state is not. However, we have verified that a small change in the π exchange potential generates, as well as the bound state, the corresponding resonant state also. Therefore, the pion dominance is working for the $B\bar{B}^*$ and $B^*\bar{B}^*$ systems. (See also the discussion in Appendix C.) Third, it would provide a direct evidence of these states to be $B\bar{B}^*$ and $B^*\bar{B}^*$ molecules if the $B\bar{B}^*$ and $B^*\bar{B}^*$ decays are observed in experiments. Whether the energies are below or above the thresholds is also checked by the observation of these decays.

In other channels, we further predict the $B^{(*)}\bar{B}^{(*)}$ bound and resonant states. The $I^G(J^{PC}) = 1^-(0^{++})$ state is a bound state with binding energy 6.5 MeV from the $B\bar{B}$ threshold for the π exchange potential, while no structure for the $\pi\rho\omega$ potential. The existence of this state depends on the details of the potential, while the states in the other quantum numbers are rather robust. Let us see the results for the latter states from the $\pi\rho\omega$ potentials. For $1^+(0^{--})$ and $1^-(1^{++})$, we find bound states with binding energy 9.8 MeV and 1.9 MeV from the $B\bar{B}^*$ threshold, respectively. These bound states appear also for the π exchange potential, though the binding energy of the $1^-(1^{++})$ state becomes larger. The $1^-(2^{++})$ state is a resonant state with the resonance energy 62.7 MeV and the decay width 8.4 MeV. The $1^+(1^{--})$ states are twin resonances with the resonance energy 7.1 MeV and the decay width 37.4 MeV for the first resonance, and the resonance energy 58.6 MeV and the decay width 27.7 MeV for the second. The resonance energies are measured from the $B\bar{B}$ threshold. The $1^+(2^{--})$ states also form twin resonances with the resonance energy 2.0 MeV and the decay width 3.9 MeV for the first resonance and the resonance energy 44.1 MeV and the decay width 2.8 MeV for the second, where the resonance energies have are measured from the $B\bar{B}^*$ threshold.

Next we discuss the result for the states of isospin $I = 0$. In general, the interaction in these states are either repulsive or only weakly attractive as compared to the cases of $I = 1$. The fact that there are less channel-couplings explains less attraction partly. Because of this, we find only one resonant state with $I^G(J^{PC}) = 0^+(1^{-+})$, as shown in Fig 4.1 and in Table 4.3. The $0^+(1^{-+})$ state is a resonant state with the resonance energy 17.8 MeV and the decay width 30.1 MeV for the $\pi\rho\omega$ potential.

In the present study, all the states appear in the threshold regions and therefore are all weakly bound or resonant states. The present results are consequences of unique features of the bottom quark sector; the large reduced mass of the $\mathrm{B}^{(*)}\bar{\mathrm{B}}^{(*)}$ systems and the strong tensor force induced by the mixing of B and B^* with small mass splitting. In fact, in the charm sector, our model does not predict any bound or resonant states in the region where we research numerically. Because the reduced mass is smaller and the mass splitting between D and D^* is larger.

TABLE 4.2: The energies E can be either pure real for bound states or complex for resonances. The real parts are measured from the thresholds as indicated in the second column. The imaginary parts are half of the decay widths of the resonances, $\Gamma/2$. In the last two columns, decay channels of a quarkonium and a light flavor meson are indicated. Asterisk of ρ^* indicates that the decay occurs only with a virtual ρ while subsequently transit to a real photon via vector meson dominance.

$I^G(J^{PC})$	threshold	E [MeV]		decay channels	
		π-potential	$\pi\rho\omega$-potential	s-wave	p-wave
$1^+(0^{+-})$	—	—	—	—	$\mathrm{h_b}+\pi$, $\chi_{\mathrm{b}0,1,2}+\rho$
$1^-(0^{++})$	$\mathrm{B\bar{B}}$	-6.5	no	$\eta_\mathrm{b}+\pi$, $\Upsilon+\rho$	$\mathrm{h_b}+\rho^*$, $\chi_{\mathrm{b}1}+\pi$
$1^+(0^{--})$	$\mathrm{B\bar{B}^*}$	-9.9	-9.8	$\chi_{\mathrm{b}1}+\rho^*$	$\eta_\mathrm{b}+\rho$, $\Upsilon+\pi$
$1^-(0^{-+})$	$\mathrm{B\bar{B}^*}$	no	no	$\mathrm{h_b}+\rho$, $\chi_{\mathrm{b}0}+\pi$	$\Upsilon+\rho$
$1^+(1^{+-})$	$\mathrm{B\bar{B}^*}$	-7.7	-8.5 $50.4-i15.1/2$	$\Upsilon+\pi$	$\mathrm{h_b}+\pi$, $\chi_{\mathrm{b}1}+\rho^*$
$1^-(1^{++})$	$\mathrm{B\bar{B}^*}$	-16.7	-1.9	$\Upsilon+\rho$	$\mathrm{h_b}+\rho^*$, $\chi_{\mathrm{b}0,1}+\pi$
$1^+(1^{--})$	$\mathrm{B\bar{B}}$	$7.0-i37.9/2$ $58.8-i30.0/2$	$7.1-i37.4/2$ $58.6-i27.7/2$	$\mathrm{h_b}+\pi$, $\chi_{\mathrm{b}0,1,2}+\rho^*$	$\eta_\mathrm{b}+\rho$, $\Upsilon+\pi$
$1^-(1^{-+})$	$\mathrm{B\bar{B}^*}$	no	no	$\mathrm{h_b}+\rho$, $\chi_{\mathrm{b}1}+\pi$	$\eta_\mathrm{b}+\pi$, $\Upsilon+\rho$
$1^+(2^{+-})$	$\mathrm{B\bar{B}^*}$	no	no	—	$\mathrm{h_b}+\pi$, $\chi_{\mathrm{b}0,1,2}+\rho$
$1^-(2^{++})$	$\mathrm{B\bar{B}}$	$63.5-i8.3/2$	$62.7-i8.4/2$	$\Upsilon+\rho$	$\mathrm{h_b}+\rho^*$, $\chi_{\mathrm{b}1,2}+\pi$
$1^-(2^{-+})$	$\mathrm{B\bar{B}^*}$	no	no	$\mathrm{h_b}+\rho$	$\Upsilon+\rho$
$1^+(2^{--})$	$\mathrm{B\bar{B}^*}$	$2.0-i4.1/2$ $44.2-i2.5/2$	$2.0-i3.9/2$ $44.1-i2.8/2$	$\chi_{\mathrm{b}1}+\rho^*$	$\eta_\mathrm{b}+\rho$, $\Upsilon+\pi$

TABLE 4.3: (Same convention as Table II.)

$I^G(J^{PC})$	threshold	E [MeV]		decay channels	
		π-potential	$\pi\rho\omega$-potential	s-wave	p-wave
$0^-(0^{--})$	$B\bar{B}^*$	no	no	$\chi_{b1}+\omega$	$\eta_b+\omega$, $\Upsilon+\eta$
$0^+(1^{-+})$	$B\bar{B}^*$	$28.6-i91.6/2$	$17.8-i30.1/2$	$h_b+\omega^*$, $\chi_{b1}+\eta$	$\eta_b+\eta$, $\Upsilon+\omega$
$0^-(2^{+-})$	$B\bar{B}^*$	no	no	—	$h_b+\eta$, $\chi_{b0,1,2}+\omega$

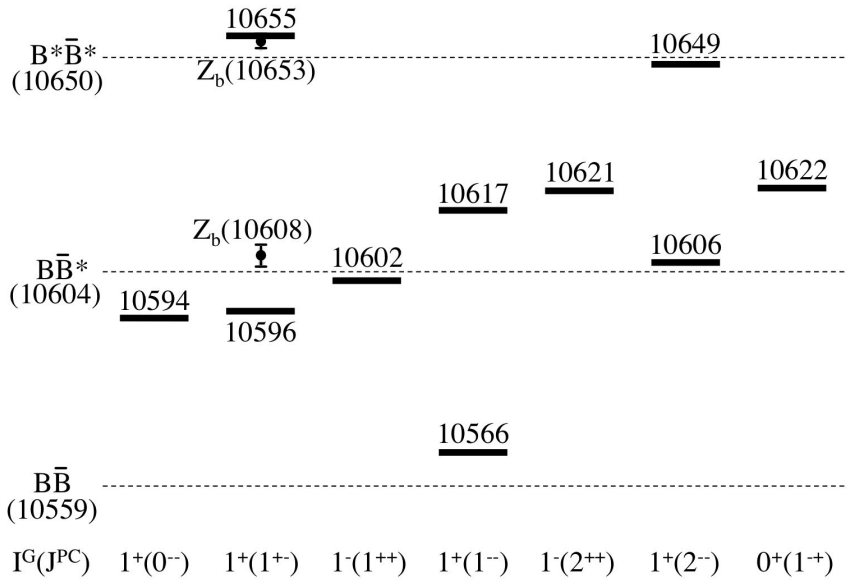

FIGURE 4.1: The dots with error bars denote the position of the experimentally observed Z_b's where $M(Z_b(10610)) = 10607.2$ MeV and $M(Z_b(10650)) = 10652.2$ MeV. Solid lines are for our predictions for the energies of the bound and resonant states when the $\pi\rho\omega$ potential is employed. Mass values are shown in units of MeV.

4.1.5 Effects of the coupling to decay channels

We have employed the hadronic molecular picture and only considered the $B^{(*)}\bar{B}^{(*)}$ states so far. In reality, however, the $B^{(*)}\bar{B}^{(*)}$ states couple to a bottomonium and a light meson state which is predominantly a pion, as Z_b's were discovered in the decay channels of $\Upsilon(nS)\pi$ $(n = 1, 2, 3)$ and $h_b(mP)\pi$ $(m = 1, 2)$ [2, 17]. In this section, we estimate the effects of such channel coupling to the $B^{(*)}\bar{B}^{(*)}$ states. We give a qualitative estimation

for the lowest $\mathrm{B}^{(*)}\bar{\mathrm{B}}^{(*)}$ state in $1^+(1^{+-})$ corresponding to $\mathrm{Z_b}(10610)^{\pm}$. Similar effects are expected for other states.

To this purpose, we employ the method of Pennington and Wilson [76]. They calculated charmonium mass-shifts for including the effect of open and nearby closed channels and we apply their calculation procedure for $\mathrm{Z_b}$ mass-shift. The bare bound state propagator $i/[s-m_0^2]$, where m_0 is the mass of the bare state, is dressed by the contribution of hadron loops $\Pi(s)$. Therefore, the full propagator can be written as

$$\begin{aligned} G_z(s) = \frac{i}{s-\mathcal{M}^2(s)} &= \frac{i}{s-m_0^2-\Pi(s)} \\ &= \frac{i}{s-m_0^2-\sum_{n=1}\Pi_n(s)}\,, \end{aligned} \tag{4.29}$$

where s is the square of the momentum carried by the propagator. $\mathcal{M}(s)$ is the complex mass function and the real part of this give the "renormalized" mass. Since the $\mathrm{Z_b}$ has five decay channels, the hadron loops $\Pi(s)$ is a sum of each decay channel n (Fig.4.2). Each hadron loop $\Pi_n(s)$ (Fig.4.2) is obtained by using the dispersion relation in terms of its imaginary part. All hadronic channels contribute to its mass at least in principle. Because the dispersion integral diverges, we have to subtract the square of mass function $\mathcal{M}(s_0)$ at suitable point s_0 from $\mathcal{M}(s)$. We shall discuss the choice of s_0 shortly. Now, we can write the loop function in a once subtracted form as

$$\Delta\Pi_n(s,s_0) \equiv \Pi_n(s) - \Pi_n(s_0) = \frac{(s-s_0)}{\pi}\int_{s_n}^{\infty} ds' \frac{\mathrm{Im}\Pi_n(s')}{(s'-s)(s'-s_0)}\,. \tag{4.30}$$

Then we arrive at the mass-shift δM as

$$\sum_{n=1}\Delta\Pi_n(s,s_0) = \mathcal{M}^2(s) - m_0^2 \equiv \delta M^2(s)\,. \tag{4.31}$$

Since an imaginary part of a loop function is proportional to the two-body phase space, we take $\mathrm{Im}\Pi_n$ in the form for $s \geq s_n$ as

$$\mathrm{Im}\Pi_n(s) = -g_n^2\left(\frac{2q_{cm}}{\sqrt{s}}\right)^{2L+1}\exp\left(-\frac{q_{cm}^2}{\Lambda^2}\right), \tag{4.32}$$

where g_n is the coupling of $\mathrm{Z_b}$ to a decay channel n (a bottomonium and a pion), L is the orbital angular momentum between a bottomonium and a pion. q_{cm} is the magnitude

of the three momentum of a pion in the center of mass frame and is related to q_{cm} by

$$q_{cm} = \left(\frac{s + m_\pi^2 - M_{b\bar{b}}^2}{2\sqrt{s}} \right)^2 - m_\pi^2 \,. \tag{4.33}$$

In eq (4.32), following [76], we have introduced the Gaussian-type form factor with a cut-off parameter Λ which is related to the interaction range R. We set $\Lambda = 1000$ MeV as a typical hadron scale; this value corresponds to $R \sim 0.5$ fm by using the relation $R \simeq \sqrt{6}/\Lambda$, which correspond the size of B meson. Coupling g_n is determined from the partial decay width Γ_n, by $\Gamma_n(s) = -\mathrm{Im}\Pi_n(s)/\sqrt{s}$. Then partial decay widths for each decay channel are given from the experimental data (See Table 3.1).

The subtraction point s_0 determines the renormalization point where the loop correction vanishes. In Ref. [76], the subtraction point was chosen at the mass of J/ψ. Since J/ψ is a deeply bound state of a $c\bar{c}$ pair where the charmonium description works well without a $\mathrm{D\bar{D}}$ loop. Now in our situation, there is no such a physical bottomonium like state decaying into a pion and a bottomonium. However, as in the case of J/ψ we expect that the renormalization point of the vanishing loop is located at an energy which is significantly below the thresholds of the particle in the loop. We adopt such an energy at $\sqrt{s_0} = 9000$ MeV, 600 MeV below the $\pi\Upsilon(1S)$, which is similar to the mass difference of J/ψ and $\mathrm{D\bar{D}}$.

The resulting mass-shift δM due to each coupling is given in Table 4.4. The $\Upsilon(1S)\pi$ coupling only contributes the mass correction as repulsive. This cause is the wide large phase space for this channel, but the contribution of this channel is very small, $\delta M_{\Upsilon(1S)\pi} = 0.026$. Therefore, the mass correction of the $\Upsilon(1S)\pi$ coupling is approximately negligible. The other couplings work as attractive,$\delta M < 0$. The mass correction due to $h_b(2P)\pi$ coupling is largest in the five decay channels, however this is still less than 1 MeV. The total mass-shift is $\delta M = -1.5$ MeV, which is slightly attractive. This means that the $\Upsilon(nS)\pi$ and $h_b(mP)\pi$ couplings will attract the mass of $B\bar{B}^*$ bound state with $1^+(1^+)$ into their thresholds. But the value of the total mass correction is quite small compared with the dependence of other considerable ambiguity in the present model such as the cutoff parameter and coupling constants for each vertex. Then this effect will be a minor role.

To summarize this section, we have estimated loop contributions to the mass of the $\mathrm{B^{(*)}\bar{B}^{(*)}}$ molecules. We find small attractive corrections, which will be negligible in the presence model. It is unthinkable that the loop contributions are direct cause of making

the bound state to the resonance state as observed Z_b state. Thus, what makes Z_b as a resonance state is still open question and needs further consideration.

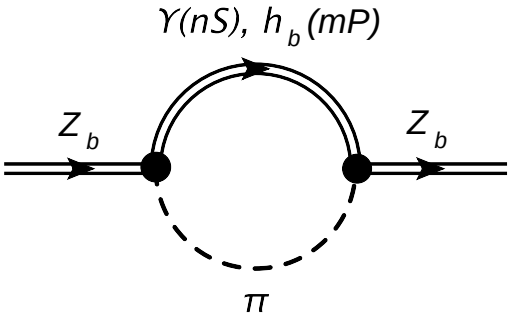

FIGURE 4.2: The diagram corresponding to a loop function $\Pi_n(s)$ of channel n.

TABLE 4.4: The first and the second row show the threshold masses and the coupling strengths of channel n. M_{th} and δM are given in units of MeV.

	$\Upsilon(1S)\pi$	$\Upsilon(2S)\pi$	$\Upsilon(3S)\pi$	$h_b(1P)\pi$	$h_b(2P)\pi$	total
M_{th}	9600	10163	10495	10038	10399	—
g_n	99.1	338	334	2041	4716	—
δM	0.026	-0.074	-0.28	-0.23	-0.97	-1.5

4.1.6 Search for heavy meson molecules in decays from $\Upsilon(5S)$

As twin Z_b's were observed from $\Upsilon(5S)$ decay, $\Upsilon(5S)$ decay is a useful source to search the exotic states around the $B^{(*)}\bar{B}^{(*)}$ energy region. $\Upsilon(5S)$ can decay to a $I^G(J^{PC}) = 1^+(1^{+-})$ state by a single pion emission in s-wave, and a $1^+(0^{--})$, $1^+(1^{--})$ or $1^+(2^{--})$ state by a single pion emission in p-wave. We recall that the twin Z_b's with $I^G(J^{PC}) = 1^+(1^{+-})$ were observed in the s-wave channel [2, 17]. In the present study, we further predict the bound state in $I^G(J^{PC}) = 1^+(0^{--})$, and another twin resonant states in $I^G(J^{PC}) = 1^+(1^{--})$ and $1^+(2^{--})$ as summarized in Table 4.2. As for the exotic J^{PC} states in isosinglet, the resonant state in $I^G(J^{PC}) = 0^+(1^{-+})$ can be observed from $\Upsilon(5S)$ by ω emission in p-wave as shown in Table 4.3.

The radiative decay of $\Upsilon(5S)$ is also an interesting channel as discussed in Ref. [67]. In radiative decay, $\Upsilon(5S)$ decays to the $I^G(J^{PC}) = 1^-(0^{++})$, $1^-(1^{++})$ and $1^-(2^{++})$ states with a photon emission in s-wave. These channels can be also produced in hadronic transitions with emission of ρ meson from higher Υ-like bottomonim states. In the

present study, we predict the bound states in $I^G(J^{PC}) = 1^-(0^{++})$ and $1^-(1^{++})$ and a resonant states in $1^-(2^{++})$ as summarized in Table 4.2.

As a consequence, we will be able to study the $\mathrm{B}^{(*)}\bar{\mathrm{B}}^{(*)}$ bound and resonant states with positive G-parity in a pion emission from $\Upsilon(5S)$ and with negative G-parity in a photon emission from $\Upsilon(5S)$. It will be an interesting subject for experiments to search these states in $\Upsilon(5S)$ decays.

4.1.7 Summary

In this section, we have systematically studied the possibility of the $\mathrm{B}^{(*)}\bar{\mathrm{B}}^{(*)}$ bound and resonant states having exotic quantum numbers $I^G(J^{PC})$. These states are consisted of at least four quarks, because their quantum numbers cannot be assigned by the quarkonium picture and hence they are genuinely exotic states. We have constructed the potential of the $\mathrm{B}^{(*)}\bar{\mathrm{B}}^{(*)}$ states using the effective Lagrangian respecting the heavy quark symmetry. Because of the degeneracy in masses of B and B^* mesons, the channel mixing, such as $\mathrm{B}\bar{\mathrm{B}}^*$-$\mathrm{B}^*\bar{\mathrm{B}}$, $\mathrm{B}^*\bar{\mathrm{B}}^*$-$\mathrm{B}^*\bar{\mathrm{B}}^*$, $\mathrm{B}\bar{\mathrm{B}}$-$\mathrm{B}^*\bar{\mathrm{B}}^*$ and $\mathrm{B}\bar{\mathrm{B}}^*$-$\mathrm{B}^*\bar{\mathrm{B}}^*$, plays an important role to form the $\mathrm{B}^{(*)}\bar{\mathrm{B}}^{(*)}$ bound and/or resonant states. We have numerically solved the Schrödinger equation with the channel-couplings for the $\mathrm{B}^{(*)}\bar{\mathrm{B}}^{(*)}$ states with $I^G(J^{PC})$ for $J \leq 2$.

As a result, in $I = 1$, we have found that the $I^G(J^{PC}) = 1^+(1^{+-})$ states have a bound state with binding energy 8.5 MeV, and a resonant state with the resonance energy 50.4 MeV and the decay width 15.1 MeV. We have successfully reproduced the positions of $\mathrm{Z_b}(10610)$ and $\mathrm{Z_b}(10650)$ observed by Belle. Therefore, the twin resonances of $\mathrm{Z_b}$'s can be interpreted as the $\mathrm{B}^{(*)}\bar{\mathrm{B}}^{(*)}$ molecular type states. It should be noted that the $\mathrm{B}\bar{\mathrm{B}}^*$-$\mathrm{B}^*\bar{\mathrm{B}}$, $\mathrm{B}\bar{\mathrm{B}}^*$-$\mathrm{B}^*\bar{\mathrm{B}}^*$ and $\mathrm{B}^*\bar{\mathrm{B}}$-$\mathrm{B}^*\bar{\mathrm{B}}^*$ mixing effects are important, because many structures disappear without the mixing effects. We have obtained the other possible $\mathrm{B}^{(*)}\bar{\mathrm{B}}^{(*)}$ states in $I = 1$. We have found one bound state in each $1^+(0^{--})$ and $1^-(1^{++})$, one resonant state in $1^-(2^{++})$ and twin resonant states in each $1^+(1^{--})$ and $1^+(2^{--})$. It is remarkable that another two twin resonances can exist in addition to the $\mathrm{Z_b}$'s. We have also studied the $\mathrm{B}^{(*)}\bar{\mathrm{B}}^{(*)}$ states in $I = 0$ and found one resonant state in $0^+(1^{-+})$. We have checked the differences between the results from the π exchange potential and those from the $\pi\rho\,\omega$ potential, and found that the difference is small. Therefore, the one pion exchange potential dominates as the interaction in the $\mathrm{B}^{(*)}\bar{\mathrm{B}}^{(*)}$ bound and resonant states.

We have estimated the effects of the coupling to decay channels by means of dispersion relations. Total mass-shift is $\delta M = -0.97$ MeV, which is slightly attractive. This value is negligible under the degree of accuracy on the current model. Therefore, we conclude that the molecular picture of $\mathrm{B}^{(*)}\bar{\mathrm{B}}^{(*)}$ will be a good approximation for the first step. More systematic analyses will be left for future works.

For experimental studies, the $\Upsilon(5S)$ decay is a useful tool to search the $\mathrm{B}^{(*)}\bar{\mathrm{B}}^{(*)}$ states. $\Upsilon(5S)$ can decay to the $\mathrm{B}^{(*)}\bar{\mathrm{B}}^{(*)}$ states with $1^+(0^{--})$, $1^+(1^{--})$ and $1^+(2^{--})$ by a single pion emission in p-wave and the state with $0^+(1^{-+})$ by ω emission in p-wave. $\Upsilon(5S)$ can also decay to the $\mathrm{B}^{(*)}\bar{\mathrm{B}}^{(*)}$ states with $1^-(0^{++})$, $1^-(1^{++})$ and $1^-(2^{++})$ by radiative decays. In the future, various exotic states would be observed around the thresholds from $\Upsilon(5S)$ decays in accelerator facilities such as Belle and also would be searched in the relativistic heavy ion collisions in RHIC and LHC [77, 78]. If these states are fit in our predictions, they will be good candidates of the $\mathrm{B}^{(*)}\bar{\mathrm{B}}^{(*)}$ molecular states.

4.2 PP molecules

In this section, we study exotic mesons with double charm and bottom flavor ($|C| = |B| = 2$), whose quark configurations are $QQ\bar{q}\bar{q}$ or $\bar{Q}\bar{Q}qq$. These states are genuinely exotic states because these quark configurations have no annihilation process of quark and antiquark. We take a hadronic picture by considering the molecular states composed of a pair of heavy mesons, such as DD, DD^* and $\mathrm{D}^*\mathrm{D}^*$ for charm flavor, and BB, BB^* and $\mathrm{B}^*\mathrm{B}^*$ for bottom flavor. The interactions between heavy mesons are derived from the heavy quark effective theory. All molecular states are classified by $I(J^P)$ quantum numbers, and are systematically studied up to the total angular momentum $J \leq 2$. By solving the coupled channel Schrödinger equations, due to the strong tensor force of one pion exchanging, we find bound and/or resonant states of various quantum numbers.

4.2.1 Introduction for PP molecules

As candidates of flavor exotics, a new hadron state $\mathrm{T_{QQ}}$, whose quark content is $QQ\bar{q}\bar{q}$, has been discussed theoretically [44, 79, 80, 81, 82, 83, 84, 85, 86, 87, 88, 89, 90, 91, 92, 93, 94, 95, 96, 97, 98, 99, 100, 101, 102, 103, 104, 105, 106]. $\mathrm{T_{QQ}}$ is a system containing two heavy quarks and it is genuinely a flavor exotic which cannot be assigned

by a normal hadron. Here, we discuss the energy spectrum of the possible bound and/or resonant states of T_{QQ}.

In phenomenological studies, there exist two approaches to T_{QQ} state. In one approach, T_{QQ} is considered as a tetraquark state, in which the effective degrees of freedom are constituent quarks [79, 80, 81, 82, 83, 84, 85, 86, 87, 88, 89, 90, 91, 92, 93, 94, 95, 96, 97, 98, 99, 100, 101, 102, 103]. It is shown that T_{QQ} may be a stable object due to the strong attraction in qq which may form a stable scalar diquark [107, 108, 109]. As a result, T_{QQ} may be a deeply bound state, which does not decay through the strong interaction [94, 95, 96]. If the diquark developed, the study of T_{QQ} is also useful to understand the color superconductivity in high density quark matter [110, 111, 112]. The tetraquark states such as T^1_{cc}, T^1_{cb} and T^1_{bb} states with $I(J^P) = 0(1^+)$ as well as T^0_{cb} with $I(J^P) = 0(0^+)$ have been discussed also as stable objects [95, 96].

Another approach is the hadronic molecule picture. When four quarks ($\bar{Q}\bar{Q}qq$) are present, they may form hadronic clusters ($\bar{Q}q$) which may alternatively become relevant degrees of freedom instead of diquarks [44, 104, 105, 106]. The hadronic molecule picture is applied to the energy region close to the thresholds. In the T_{QQ} system, two mesons composed by $\bar{Q}q$, the pseudoscalar meson $P \sim (\bar{Q}q)_{\text{spin}\,0}$ and the vector meson $P^* \sim (\bar{Q}q)_{\text{spin}\,1}$, can become effective degrees of freedom as constituents. In the heavy quark limit, the pseudoscalar meson P and the vector meson P^* become degenerate in mass, and hence both of them should be considered. Hereafter we introduce the notation $P^{(*)}$ for P and P^*. Indeed, we will show that the mass degeneracy of the P and P^* activates the one-pion exchange potential between two $P^{(*)}$'s, and the bound and/or resonant $P^{(*)}P^{(*)}$ states are formed.

The tetraquark picture and the hadronic molecule picture are quite different. The tetraquark picture is applied to the deeply bound state. To apply this picture to the shallow bound states or resonant states, slightly below or above thresholds respectively, is not appropriate, because the continuous $P^{(*)}$ states above thresholds are not taken into account. On the other hand, the hadronic molecule picture can be applied to the shallow and resonant states, while it cannot be applied to the deeply bound states. Though there have been several studies for bound states of $P^{(*)}P^{(*)}$ in the hadronic molecule picture, resonant states of $P^{(*)}P^{(*)}$ have not been studied yet. Moreover, the quantum numbers $I(J^P)$ which have been discussed are limited only $J \leq 1$. To be more problematic, several channels in coupled channel problem have been neglected. The last point is very important in the heavy quark systems. In the heavy quark limit,

we need to consider the mass degeneracy of P and P* which provides more number of channels than discussed in the literature. In the present work, we discuss both bound and resonant states of P$^{(*)}$P$^{(*)}$ systematically for various quantum numbers $I(J^P)$ up to $J \leq 2$ by considering the fully coupled channel problem. The systematic analysis of the energy spectrum for various quantum numbers is important to investigate the dynamics governing the systems. Indeed, it will be shown that there are several new shallow bound and/or resonant states, which were not found in other studies, thanks to the strong attraction induced from the channel couplings even for larger J or angular momentum.

This section is organized as follows. In 4.2.2, we give the interaction between two P$^{(*)}$ mesons with respecting the heavy quark symmetry and chiral symmetry. We introduce the two types of potentials, the π exchange potential and $\pi\rho\,\omega$ exchange potential. In section 4.2.3, we classify all the P$^{(*)}$P$^{(*)}$ systems up to $J = 2$, and search the bound and/or resonant states by applying the potentials and solving the Schrödinger equations numerically. In section 4.2.4, we compare our results from the hadronic molecule picture with the previous results from the tetraquark picture. We summarize our discussions in the final section.

4.2.2 Interaction with two mesons with doubly heavy flavor

The dynamics of the hadronic molecule of P$^{(*)}$P$^{(*)}$ respects two important symmetries; the heavy quark symmetry and chiral symmetry. The heavy quark symmetry induces the mass degeneracy of P and P* in the heavy quark limit. Because of this, we have to consider the channels of degenerate pairs, such as PP, PP*, P*P and P*P*, leading to the mixing of them; PP*-P*P, P*P*-P*P*, PP-P*P*, PP*-P*P*.

As for the meson-exchange interaction between two P$^{(*)}$'s, the one pion exchange potential (OPEP) exists at long distances. The existence of a pion is a robust consequence of spontaneous breaking of chiral symmetry [113]. The OPEP is provided by the PP$^*\pi$ and P*P$^*\pi$ vertices whose coupling strengths are equally weighted thanks to the heavy quark symmetry. We note that there is no PPπ vertex because of the parity conservation. It should be noted that the existence of both PP$^*\pi$ and P*P$^*\pi$ vertices thanks to the heavy quark symmetry provide the channel mixing in PP, PP*, P*P and P*P* at long distance in the following discussions. At short distances, heavier mesons exchange potential, which provide similar channel mixing, should also be considered.

To derive the $\mathrm{P}^{(*)}\mathrm{P}^{(*)}$ potential, we employ the effective Lagrangians based on the heavy quark symmetry and chiral symmetry [27, 33, 34, 35, 38, 71]. The interaction Lagrangians are given in the same way as $P\bar{P}$ molecules. The only difference appears at the sign of couplings.

The OPEPs are derived by the interaction Lagrangians (4.8) and (4.9) as follows:

$$V^{\pi}_{P_1P_2^*\to P_1^*P_2} = \left(\sqrt{2}\frac{g}{f_\pi}\right)^2 \frac{1}{3}\left[\vec{\varepsilon}_1^{\,*}\cdot\vec{\varepsilon}_2\, C(r;m_\pi)+S_{\varepsilon_1^*,\varepsilon_2}\, T(r;m_\pi)\right]\vec{\tau}_1\cdot\vec{\tau}_2, \tag{4.34}$$

$$V^{\pi}_{P_1^*P_2^*\to P_1^*P_2^*} = \left(\sqrt{2}\frac{g}{f_\pi}\right)^2 \frac{1}{3}\left[\vec{T}_1\cdot\vec{T}_2\, C(r;m_\pi)+S_{T_1,T_2}\, T(r;m_\pi)\right]\vec{\tau}_1\cdot\vec{\tau}_2, \tag{4.35}$$

$$V^{\pi}_{P_1P_2\to P_1^*P_2^*} = \left(\sqrt{2}\frac{g}{f_\pi}\right)^2 \frac{1}{3}\left[\vec{\varepsilon}_1^{\,*}\cdot\vec{\varepsilon}_2^{\,*}\, C(r;m_\pi)+S_{\varepsilon_1^*,\varepsilon_2^*}\, T(r;m_\pi)\right]\vec{\tau}_1\cdot\vec{\tau}_2, \tag{4.36}$$

$$V^{\pi}_{P_1P_2^*\to P_1^*P_2^*} = -\left(\sqrt{2}\frac{g}{f_\pi}\right)^2 \frac{1}{3}\left[\vec{\varepsilon}_1^{\,*}\cdot\vec{T}_2\, C(r;m_\pi)+S_{\varepsilon_1^*,T_2}\, T(r;m_\pi)\right]\vec{\tau}_1\cdot\vec{\tau}_2, \tag{4.37}$$

where m_π is the pion mass. Here three polarizations are introduced for P^* as defined by $\vec{\varepsilon}^{\,(\pm)}=\left(\mp 1/\sqrt{2}, -i/\sqrt{2}, 0\right)$ and $\vec{\varepsilon}^{\,(0)}=(0,0,1)$, and the spin-one operator $\vec{T}$ is defined by $T^i_{\lambda'\lambda}=i\varepsilon^{ijk}\varepsilon_j^{(\lambda')\dagger}\varepsilon_k^{(\lambda)}$. As a convention, we assign $\vec{\varepsilon}^{\,(\lambda)}$ for an incoming vector particle and $\vec{\varepsilon}^{\,(\lambda)*}$ for an outgoing vector particle. Here $\vec{\tau}_1$ and $\vec{\tau}_2$ are isospin operators for $\mathrm{P}_1^{(*)}$ and $\mathrm{P}_2^{(*)}$; $\vec{\tau}_1\cdot\vec{\tau}_2=-3$ and 1 for the $I=0$ and $I=1$ channels, respectively. We define the tensor operators

$$S_{\varepsilon_1^*,\varepsilon_2} = 3(\vec{\varepsilon}^{\,(\lambda_1)*}\cdot\hat{r})(\vec{\varepsilon}^{\,(\lambda_2)}\cdot\hat{r})-\vec{\varepsilon}^{\,(\lambda_1)*}\cdot\vec{\varepsilon}^{\,(\lambda_2)}, \tag{4.38}$$

$$S_{T_1,T_2} = 3(\vec{T}_1\cdot\hat{r})(\vec{T}_2\cdot\hat{r})-\vec{T}_1\cdot\vec{T}_2, \tag{4.39}$$

$$S_{\varepsilon_1^*,\varepsilon_2^*} = 3(\vec{\varepsilon}^{\,(\lambda_1)*}\cdot\hat{r})(\vec{\varepsilon}^{\,(\lambda_2)*}\cdot\hat{r})-\vec{\varepsilon}^{\,(\lambda_1)*}\cdot\vec{\varepsilon}^{\,(\lambda_2)*}, \tag{4.40}$$

$$S_{\varepsilon_1^*,T_2} = 3(\vec{\varepsilon}^{\,(\lambda_1)*}\cdot\hat{r})(\vec{T}_2\cdot\hat{r})-\vec{\varepsilon}^{\,(\lambda_1)*}\cdot\vec{T}_2, \tag{4.41}$$

where $\hat{r}=\vec{r}/r$ is a unit vector between the two mesons.

The ρ meson exchange potentials are similarly obtained from the interaction Lagrangians (4.10)-(4.12),

$$V^{\rho}_{P_1P_2\to P_1P_2} = \left(\frac{\beta g_V}{2m_\rho}\right)^2 \frac{1}{3} C(r;m_\rho)\vec{\tau}_1\cdot\vec{\tau}_2, \tag{4.42}$$

$$V^{\rho}_{P_1P_2^*\to P_1P_2^*} = \left(\frac{\beta g_V}{2m_\rho}\right)^2 \frac{1}{3} C(r;m_\rho)\vec{\tau}_1\cdot\vec{\tau}_2, \tag{4.43}$$

$$V^{\rho}_{P_1P_2^*\to P_1^*P_2} = (2\lambda g_V)^2 \frac{1}{3}\left[2\vec{\varepsilon}_1^{\,*}\cdot\vec{\varepsilon}_2\, C(r;m_\rho) - S_{\varepsilon_1^*,\varepsilon_2}\, T(r;m_\rho)\right]\vec{\tau}_1\cdot\vec{\tau}_2, \tag{4.44}$$

$$\begin{aligned} V^{\rho}_{P_1^*P_2^*\to P_1^*P_2^*} &= (2\lambda g_V)^2 \frac{1}{3}\left[2\vec{T}_1\cdot\vec{T}_2\, C(r;m_\rho) - S_{T_1,T_2}\, T(r;m_\rho)\right]\vec{\tau}_1\cdot\vec{\tau}_2 \\ &\quad + \left(\frac{\beta g_V}{2m_\rho}\right)^2 \frac{1}{3} C(r;m_\rho)\vec{\tau}_1\cdot\vec{\tau}_2, \end{aligned} \tag{4.45}$$

$$V^{\rho}_{P_1P_2\to P_1^*P_2^*} = (2\lambda g_V)^2 \frac{1}{3}\left[2\vec{\varepsilon}_1^{\,*}\cdot\vec{\varepsilon}_2^{\,*}\, C(r;m_\rho) - S_{\varepsilon_1^*,\varepsilon_2^*}\, T(r;m_\rho)\right]\vec{\tau}_1\cdot\vec{\tau}_2, \tag{4.46}$$

$$V^{\rho}_{P_1P_2^*\to P_1^*P_2^*} = -(2\lambda g_V)^2 \frac{1}{3}\left[2\vec{\varepsilon}_1^{\,*}\cdot\vec{T}_2\, C(r;m_\rho) - S_{\varepsilon_1^*,T_2}\, T(r;m_\rho)\right]\vec{\tau}_1\cdot\vec{\tau}_2. \tag{4.47}$$

The ω meson exchange potentials are obtained by replacing the mass of ρ meson with the one of ω meson and by removing the isospin factor $\vec{\tau}_1\cdot\vec{\tau}_2$. The OPEP's of $\mathrm{P}^{(*)}\mathrm{P}^{(*)}$ differ from the ones of $\mathrm{P}^{(*)}\bar{\mathrm{P}}^{(*)}$ in that the overall signs are changed due to G-parity. The situation is the same with ω meson exchange potentials, while ρ meson exchange potentials of $\mathrm{P}^{(*)}\bar{\mathrm{P}}^{(*)}$ are not changed because the G-parity is even [5].

In the above equations, $C(r;m_h)$ and $T(r;m_h)$ are defined as

$$C(r;m_h) = \int \frac{\mathrm{d}^3\vec{q}}{(2\pi)^3}\frac{m_h^2}{\vec{q}^{\,2}+m_h^2} e^{i\vec{q}\cdot\vec{r}}\, F(\vec{q};m_h), \tag{4.48}$$

$$T(r;m_h)S_{12}(\hat{r}) = \int \frac{\mathrm{d}^3\vec{q}}{(2\pi)^3}\frac{-\vec{q}^{\,2}}{\vec{q}^{\,2}+m_h^2} S_{12}(\hat{q}) e^{i\vec{q}\cdot\vec{r}} F(\vec{q};m_h), \tag{4.49}$$

with $S_{12}(\hat{x}) = 3(\vec{\sigma}_1\cdot\hat{x})(\vec{\sigma}_2\cdot\hat{x}) - \vec{\sigma}_1\cdot\vec{\sigma}_2$. We introduce the monopole type form factor at each vertex to take into account of the size effect of $\mathrm{P}^{(*)}$ mesons. Then the function reflected form factors is defined as

$$F(\vec{q};m_h) = \left(\frac{\Lambda_\mathrm{P}^2 - m_h^2}{\Lambda_\mathrm{P}^2 + \vec{q}^{\,2}}\right)^2, \tag{4.50}$$

where m_h and $\vec{q}$ are the mass and three-momentum of the exchanged meson h $(=\pi,\rho,\omega)$ and Λ_P is the cut-off parameter. The cut-off parameter Λ_P are determined from the size of P estimated from the constituent quark model as discussed in Refs. [5, 72, 73, 114]. The cut-off parameters are $\Lambda_\mathrm{D} = 1121$ MeV and $\Lambda_\mathrm{B} = 1070$ MeV when the π exchange

potential is employed, while $\Lambda_{\rm D} = 1142$ MeV and $\Lambda_{\rm B} = 1091$ MeV when the $\pi\rho\omega$ is employed.

Up to now we have given the meson-exchange potentials between two $\mathrm{P}^{(*)}$ mesons. We should note that the potentials contain spin operators and tensor operators, hence that the potentials for each quantum number are different. In the next section, we classify all the $\mathrm{P}^{(*)}\mathrm{P}^{(*)}$ states up to $J = 2$ and give the corresponding potentials in matrix forms.

4.2.3 Bound and resonant states

Let us classify all the possible quantum numbers of the $\mathrm{P}^{(*)}\mathrm{P}^{(*)}$ systems with isospin I, total angular momentum J ($J \leq 2$), and parity P. We need also principal quantum number $n = 0, 1, \ldots$, if there exist several bound states for a given $I(J^P)$. We show the quantum numbers $I(J^P)$ and the channels in the wave functions in Table 4.5. It is noted that the wave functions must be symmetric under the exchange of the two $\mathrm{P}^{(*)}$ mesons. We use the notation $^{2S+1}L_J$ to indicate the states with the internal spins S and angular momentum L. For example, the $I(J^P) = 0(1^+)$ state is a superposition of four channels; $\frac{1}{\sqrt{2}}\left(\mathrm{PP}^* - \mathrm{P}^*\mathrm{P}\right)(^3S_1)$, $\frac{1}{\sqrt{2}}\left(\mathrm{PP}^* - \mathrm{P}^*\mathrm{P}\right)(^3D_1)$, $\mathrm{P}^*\mathrm{P}^*(^3S_1)$ and $\mathrm{P}^*\mathrm{P}^*(^3D_1)$. All the possible channels should be mixed for a given the quantum number. In the previous studies, the channel mixing were not fully considered [44, 105, 106]. Here we pay an attention to that the approximate mass degeneracy of P and P^* plays a crucial role to mix the channels. Otherwise the attraction from the mixing effect becomes suppressed. We note that the tensor force is also important to mix the channels with different angular momenta, L and $L \pm 2$. As a result, we obtain the Hamiltonian in a matrix form with the basis of those coupled channels. The explicit forms of the Hamiltonian for each $I(J^P)$ are summarized in Appendix A.

Now we are ready to solve the coupled channel Schrödinger equations for each quantum number. The renormalized Numerov method [74] is adopted to numerically solve the coupled second-order differential equations. The resonant states are identified by the behavior of the phase shift δ as a function of the scattering energy E. The resonance position E_r is defined by an inflection point of the phase shift $\delta(E)$ and the resonance width by $\Gamma_r = 2/(d\delta/dE)_{E=E_r}$ following Refs. [5, 73, 75]. To check the consistency of our numerical calculations, we also adopt the complex scaling method (CSM), in which the resonant state is defined as a pole in the complex energy plane [75]. We obtain an agreement in the results of the renormalized Nemerov method and the CSM.

We summarize our numerical results for $\mathrm{D}^{(*)}\mathrm{D}^{(*)}$ bound/resonant states in Table 4.6 and Fig 4.3. In $\mathrm{D}^{(*)}\mathrm{D}^{(*)}$ states, we find several bound and/or resonant states in $I = 0$, while there is no bound state in $I = 1$. In general, the attractive force of pion exchange in $I = 1$ is three times weaker than in $I = 0$ due to the isospin factor. As a numerical result, $\mathrm{D}^{(*)}\mathrm{D}^{(*)}$ bound states in $I = 1$ are not obtained but only resonant states are.

Let us look at our results one by one for each quantum number in detail. In the following text, most of the numerical values are those for the case of the $\pi\rho\omega$ potential, because the results from the $\pi\rho\omega$ potential are generally not so different from those from the π potential, except for the $0(2^-)$ state. The energies are measured from the threshold, which is defined to be the lowest mass among the channels for a given quantum number as tabulated in Table 4.5. For example, we adopt the DD^* mass as threshold for $I(J^P) = 0(0^-)$, while, the DD mass for $I(J^P) = 0(1^-)$.

$0(0^-)$ This state has only one channel of DD^* (see Table .4.5) and the pion exchange potential is attractive as shown in Eq. (A.57). As a result, the very deep bound state of DD^* is generated with binding energy 132.1 MeV measured from the DD^* threshold.

$0(1^+)$ The pion exchange potential is repulsive for diagonal components as shown in Eq. (A.58). However this state has four components and the mixing of the S- and D-waves causes the strong tensor attraction from the off-diagonal components of the potential. Consequently, there is a deeply bound state of mostly DD^* with binding energy 62.3 MeV measured from the DD^* threshold.

$0(1^-)$ There are twin shape resonances of DD with the resonance energy 17.8 MeV and the decay width 41.6 MeV for the first resonance, and the resonance energy 152.8 MeV and the decay width 10.6 MeV for the second. The resonance energies are measured from the DD threshold. Those resonances are formed by the centrifugal barrier in the P-wave.

$0(2^+)$ This state contains only D-wave components of DD^* and $\mathrm{D}^*\mathrm{D}^*$. The potential is weakly attractive. Nevertheless, due to the centrifugal barrier in the D-wave, there is a shape resonance of DD^* scattering at the energy 33.7 MeV from the DD^* threshold, but the decay width 196.3 MeV is very wide.

$0(2^-)$ When the OPEP is employed, there are twin resonant states with the resonance energy 0.1 MeV and the decay width 0.02 MeV for the first resonance, and the

resonance energy 118.0 MeV and the decay width 23.4 MeV for the second from the DD^* threshold. When the effects of ρ and ω meson exchange are included, the first resonance becomes a weakly bound state with the binding energy 4.3 MeV, because the ρ meson exchange enhances the central force attraction of the pion exchange. The ω meson exchange plays a minor role due to the isospin factor, although this contribution suppresses the attractive central force. The second resonant state with the resonance energy 112.1 MeV and the decay width 26.6 MeV is not affected very much. From the analysis of wave function components of the two bound states, we have verified that the lower and higher states are dominated by DD^* and D^*D^*, respectively.

$1(0^-)$ This is the only $I = 1$ state in $D^{(*)}D^{(*)}$. The interaction in $I = 1$ are either repulsive or only weakly attractive as already discussed. Nevertheless, due to the P-wave centrifugal barrier, we find twin shape resonances; the resonance energy 2.3 MeV and the decay width 37.4 MeV for the first resonance, and the resonance energy 144.2 MeV and the decay width 34.4 MeV for the second, from the DD^* threshold.

Here several comments are in order. First, we have obtained several bound and/or resonant state even for $J = 2$. Here the long range force by the OPEP becomes effective for the extended objects with large angular momenta. It is also interesting to have "twin states" for several quantum numbers, $0(1^-)$, $0(2^-)$ and $1(0^-)$. We have to note that the channel couplings by D and D^* are important to produce the obtained energy spectrum. Indeed, if we cut the channel coupling, we confirm that many of the states disappear. Thus, we consider that the pattern of the energy spectrum is reflected by the dynamics of the fully coupled channels.

Second, the present formalism of the hadronic molecule picture cannot be applied to compact objects. When the two $P^{(*)}$ mesons overlap spatially, we need to consider the internal structure of $P^{(*)}$, which is not included in the present hadronic picture. Therefore we shall adopt 1 fm or larger for the size of the bound state to be interpreted as a molecular state. The size of 1 fm is twice of typical radius of $P^{(*)} \sim 0.5$ fm. For instance, the $I(J^P) = 0(2^-)$ bound state with the binding energy -4.3 Mev is identified with a molecular state because it has the size 1.6 fm, while the $I(J^P) = 0(0^-)$ bound state with -132.1 MeV is not because its size is 0.8 fm. We emphasize, however, that this criterion is not definitive but gives only qualitative guide.

Next we discuss the $B^{(*)}B^{(*)}$ states. We use the same coupling constants, and change only the masses of heavy mesons with small difference of the cutoff parameters. The results are summarized in Table 4.7 and Figs. 4.4 and 4.5. At first glance, we find that the $B^{(*)}B^{(*)}$ states have many bound and resonant states in comparison with the $D^{(*)}D^{(*)}$ states. There are two reasons. First, the kinetic term is suppressed in the Hamiltonian because the reduced mass becomes larger in the bottom sector. Second, the effect of channel-couplings becomes more important, because a pseudoscalar meson B and a vector meson B^* become more degenerate thanks to the heavy quark symmetry; similar discussion has been done in Refs. [5, 72, 73]. We note that, as a consequence of the strong attraction, several new states appear in the $B^{(*)}B^{(*)}$ states in isospin triplet; $I(J^P) = 1(0^+)$, $1(1^-)$, $1(2^+)$ and $1(2^-)$. The corresponding states are not obtained in the $D^{(*)}D^{(*)}$ states.

As noted in the charm sector, the deeply bound states will not be within the scope of the hadronic molecule picture. In the bottom sector, due to more attraction, more bound states are generated. For example, we have three states ($n = 0$, 1, 2) in the $0(0^-)$ state. However, the $n = 0$, 1 states are too compact (0.5 fm and 0.9 fm, respectively) to be considered as hadronic molecules. The $n = 2$ state is an extended object (2.5 fm), and hence can be considered as the hadronic molecule. Similarly, it would not be conclusive yet to consider hadronic molecules for the following states with radii less than 1 fm; the $n = 0$ state in $0(1^+)$, the $n = 0$, 1 states in $0(1^-)$, the $n = 0$ state in $0(2^+)$, the $n = 0$, 1 states in $0(2^-)$ and the $n = 0$ state in $1(0^+)$.

4.2.4 Hadronic molecules and tetraquarks

In the present study, we have considered T_{QQ} as a hadronic molecule composed by $P^{(*)}P^{(*)}$ in which one pion exchange potential induces a dominant attraction. On the other hand, as mentioned in the introduction, T_{QQ} can also be considered as a tetraquark $\bar{Q}\bar{Q}qq$ in which a diquark qq provides a strong binding energy. The different features between the hadronic molecule and tetraquark pictures are seen in their sizes. For hadronic molecules to be valid, hadron constituents are sufficiently far apart such that their identities as hadrons must be maintained. They can not be too close to overlap each other. Therefore, masses of hadronic molecules should appear around their threshold regions. In contrast, tetraquarks may be strongly bound and become compact objects as genuine quark objects. Thus, their natures are differentiated in the masses, small binding energy of order ten MeV or less, or larger one. Although it is tempting to seek

TABLE 4.5: Possible channels of $\mathrm{P}^{(*)}\mathrm{P}^{(*)}(^{2S+1}L_J)$ for a set of quantum numbers I and J^P for $J \leq 2$.

I	J^P	components
0	0^-	$\frac{1}{\sqrt{2}}(\mathrm{PP^*}+\mathrm{P^*P})(^3P_0)$
	1^+	$\frac{1}{\sqrt{2}}(\mathrm{PP^*}-\mathrm{P^*P})(^3S_1)$, $\frac{1}{\sqrt{2}}(\mathrm{PP^*}-\mathrm{P^*P})(^3D_1)$, $\mathrm{P^*P^*}(^3S_1)$, $\mathrm{P^*P^*}(^3D_1)$
	1^-	$\mathrm{PP}(^1P_1)$, $\frac{1}{\sqrt{2}}(\mathrm{PP^*}+\mathrm{P^*P})(^3P_1)$, $\mathrm{P^*P^*}(^1P_1)$, $\mathrm{P^*P^*}(^5P_1)$, $\mathrm{P^*P^*}(^5F_1)$
	2^+	$\frac{1}{\sqrt{2}}(\mathrm{PP^*}-\mathrm{P^*P})(^3D_2)$, $\mathrm{P^*P^*}(^3D_2)$
	2^-	$\frac{1}{\sqrt{2}}(\mathrm{PP^*}+\mathrm{P^*P})(^3P_2)$, $\frac{1}{\sqrt{2}}(\mathrm{PP^*}+\mathrm{P^*P})(^3F_2)$, $\mathrm{P^*P^*}(^5P_2)$, $\mathrm{P^*P^*}(^5F_2)$
1	0^+	$\mathrm{PP}(^1S_0)$, $\mathrm{P^*P^*}(^1S_0)$, $\mathrm{P^*P^*}(^5D_0)$
	0^-	$\frac{1}{\sqrt{2}}(\mathrm{PP^*}-\mathrm{P^*P})(^3P_0)$, $\mathrm{P^*P^*}(^3P_0)$
	1^+	$\frac{1}{\sqrt{2}}(\mathrm{PP^*}+\mathrm{P^*P})(^3S_1)$, $\frac{1}{\sqrt{2}}(\mathrm{PP^*}+\mathrm{P^*P})(^3D_1)$, $\mathrm{P^*P^*}(^5D_1)$
	1^-	$\frac{1}{\sqrt{2}}(\mathrm{PP^*}-\mathrm{P^*P})(^3P_1)$, $\mathrm{P^*P^*}(^3P_1)$
	2^+	$\mathrm{PP}(^1D_2)$, $\frac{1}{\sqrt{2}}(\mathrm{PP^*}+\mathrm{P^*P})(^3D_2)$, $\mathrm{P^*P^*}(^1D_2)$, $\mathrm{P^*P^*}(^5S_2)$, $\mathrm{P^*P^*}(^5D_2)$, $\mathrm{P^*P^*}(^5G_2)$
	2^-	$\frac{1}{\sqrt{2}}(\mathrm{PP^*}-\mathrm{P^*P})(^3P_2)$, $\frac{1}{\sqrt{2}}(\mathrm{PP^*}-\mathrm{P^*P})(^3F_2)$, $\mathrm{P^*P^*}(^3P_2)$, $\mathrm{P^*P^*}(^3F_2)$

TABLE 4.6: The energies E can be either pure real for bound states or complex for resonances. The real parts are measured from the thresholds as indicated in the third columns. The imaginary parts are half of the decay widths of the resonances, $\Gamma/2$. The values in the parentheses for the bound states are matter radii (relative distance of the two constituents) in units of fm.

I	J^P	threshold	E [MeV]	
			π-potential	π, ρ, ω-potential
0	0^-	$\mathrm{DD^*}$	-50.2 (1.0)	-132.1 (0.8)
	1^+	$\mathrm{DD^*}$	-45.7 (0.9)	-62.3 (0.8)
	1^-	DD	$175.4-i\frac{37.4}{2}$ $19.4-i\frac{63.0}{2}$	$152.8-i\frac{10.6}{2}$ $17.8-i\frac{41.6}{2}$
	2^+	$\mathrm{DD^*}$	$34.5-i\frac{183.1}{2}$	$33.7-i\frac{196.3}{2}$
	2^-	$\mathrm{DD^*}$	$118.0-i\frac{23.4}{2}$ $0.1-i\frac{0.02}{2}$	$112.1-i\frac{26.6}{2}$ -4.3 (1.6)
1	0^+	DD	no	no
	0^-	$\mathrm{DD^*}$	$143.8-i\frac{40.0}{2}$ $3.7-i\frac{27.7}{2}$	$144.2-i\frac{34.4}{2}$ $2.3-i\frac{37.4}{2}$
	1^+	$\mathrm{DD^*}$	no	no
	1^-	$\mathrm{DD^*}$	no	no
	2^+	DD	$289.4-i\frac{10.9}{2}$	no
	2^-	$\mathrm{DD^*}$	no	no

TABLE 4.7: The energies of $B^{(*)}B^{(*)}$ states with $I(J^P)$ with $J \leq 2$. (Same convention as Table 4.6.)

I	J^P	threshold	$E - i\Gamma/2$ [MeV]	
			π-potential	π, ρ, ω-potential
0	0^-	BB^*	-32.0 (1.2) -178.0 (0.6)	-3.3 (2.5) -77.5 (0.9) -305.9 (0.5)
	1^+	BB^*	-25.7 (1.2) -179.7 (0.5)	-33.6 (1.1) -201.5 (0.5)
	1^-	BB	$52.8 - i\frac{12.8}{2}$ $1.9 - i\frac{3.3}{2}$ -39.1 (0.8) -125.5 (0.6)	$35.0 - i\frac{11.8}{2}$ -3.1 (1.6) -98.9 (0.6) -164.4 (0.5)
	2^+	BB^*	$5.5 - i\frac{5.9}{2}$ -51.2 (0.8)	$5.7 - i\frac{13.2}{2}$ -60.6 (0.8)
	2^-	BB^*	$26.9 - i\frac{20.2}{2}$ $7.6 - i\frac{4.3}{2}$ -68.7 (0.8) -147.5 (0.6)	$26.9 - i\frac{20.2}{2}$ $7.6 - i\frac{4.3}{2}$ $0.5 - i\frac{8.5}{2}$ -84.1 (0.7) -196.5 (0.6)
1	0^+	BB	-18.1 (0.9),	-33.9 (0.5)
	0^-	BB^*	$46.7 - i\frac{1.9}{2}$ $0.7 - i\frac{3.0}{2}$ -50.5 (0.8)	$38.5 - i\frac{4.6}{2}$ -5.9 (1.4)
	1^+	BB^*	-38.1 (0.8)	no
	1^-	BB^*	no	$11.7 - i\frac{11.0}{2}$
	2^+	BB	$23.0 - i\frac{4.4}{2}$	$62.4 - i\frac{52.5}{2}$
	2^-	BB^*	$63.7 - i\frac{7.6}{2}$ $2.0 - i\frac{3.3}{2}$	$2.3 - i\frac{4.7}{2}$

for a framework to cover both scales, such a problem is out of scope of the present study. Instead, we compare the results from the two pictures and just clarify the differences between them.

In the hadronic molecule picture by $P^{(*)}P^{(*)}$, as presented in the previous section, we obtain, not only the bound states, but also the resonant states in many $I(J^P)$ quantum numbers. Both in charm and bottom sectors, it is remarkable that there are even the twin states in several quantum numbers, $0(1^-)$, $0(2^-)$ and $1(0^-)$.

In the tetraquark picture including a diquark model [95, 96, 99, 101], in contrast, only two bound states in $I(J^P) = 0(1^+)$ and $1(2^-)$ have been predicted until now, as discussed for an example in Refs. [99, 100, 101] as recent works. For $0(1^+)$, the predicted binding energy can be around 70 MeV from the DD^* threshold. For $1(2^-)$, the predicted binding

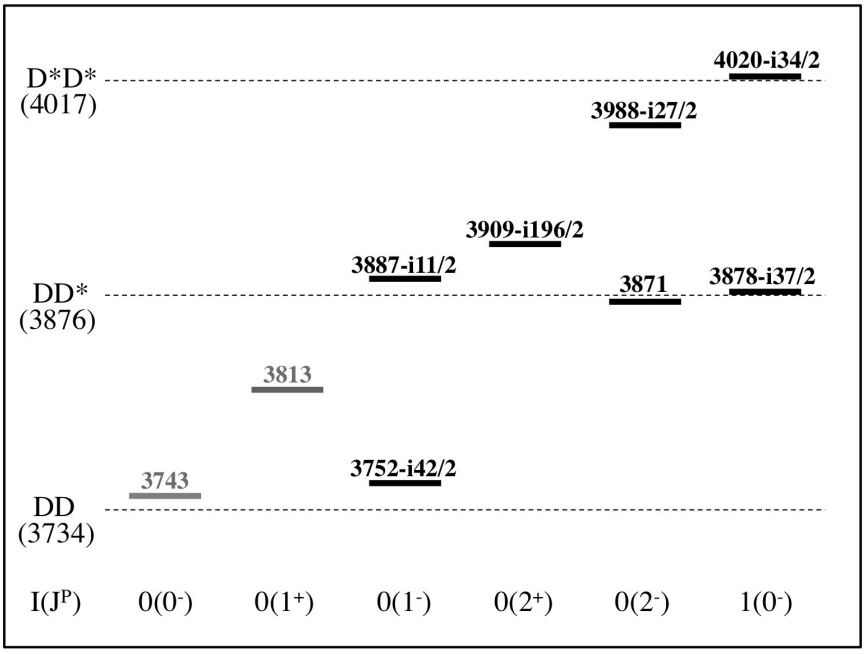

FIGURE 4.3: Solid lines are for our predictions with numerical values as denoted above the lines, and the values in parentheses below the lines denote the decay width Γ of the resonances when the $\pi\rho\omega$ potential is employed. Mass values are given in units of MeV. Compact objects which can not be regarded as molecular states are shown with grey lines.

energy can be around 27 MeV. The mass of the $0(1^+)$ states in the tetraquark picture is accidentally close to our value 62 MeV in the hadronic molecule picture. However, this comparison should be considered more carefully. Because the size of the $0(1^+)$ state is 0.8 fm from Table 4.6, the D and D^* mesons composing the $0(1^+)$ state would be overlapped spatially if the size of each D and D^* meson is a scale of about 1 fm. In such a compact object, the quark degrees of freedom may become active to contribute to the dynamics like the tetraquark picture. However, such an effect is out of the scope of the present hadronic molecule picture. The $1(2^-)$ state cannot be found in our present study.

In any cases, the feature in the energy spectrum in the $D^{(*)}D^{(*)}$ molecule picture is that there are many shallow bound states and resonances in $0(1^-)$, $0(2^+)$, $0(2^-)$ and $1(0^-)$, which are not found in the tetraquark picture. Thus, we observe that the energy spectrum of the hadronic molecule picture by $P^{(*)}P^{(*)}$ is qualitatively different from that of the tetraquark picture.

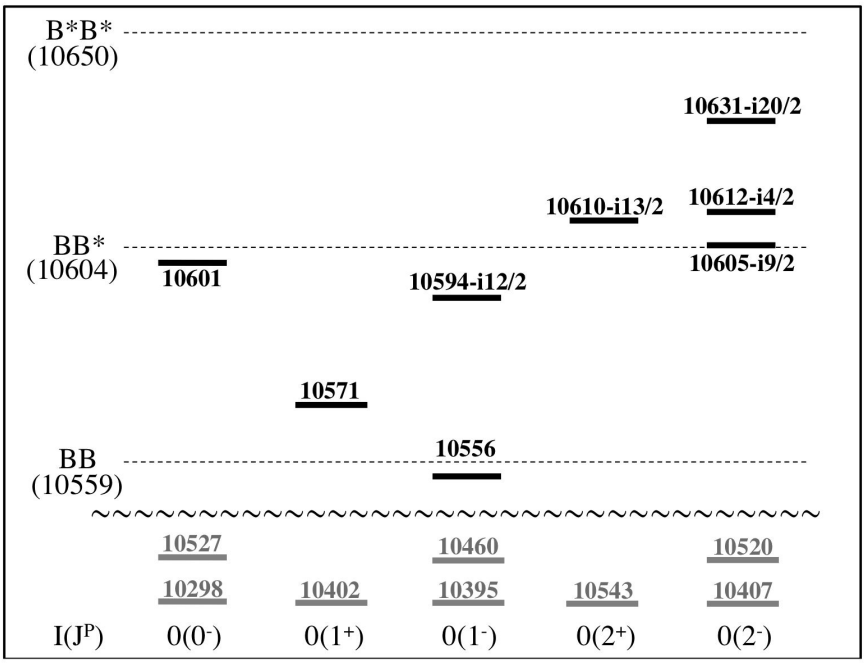

FIGURE 4.4: Compact objects which can not be regarded as molecular states are shown below the wavy line, but their location do not reflect correct energy scale. (Same convention as Fig. 4.3.)

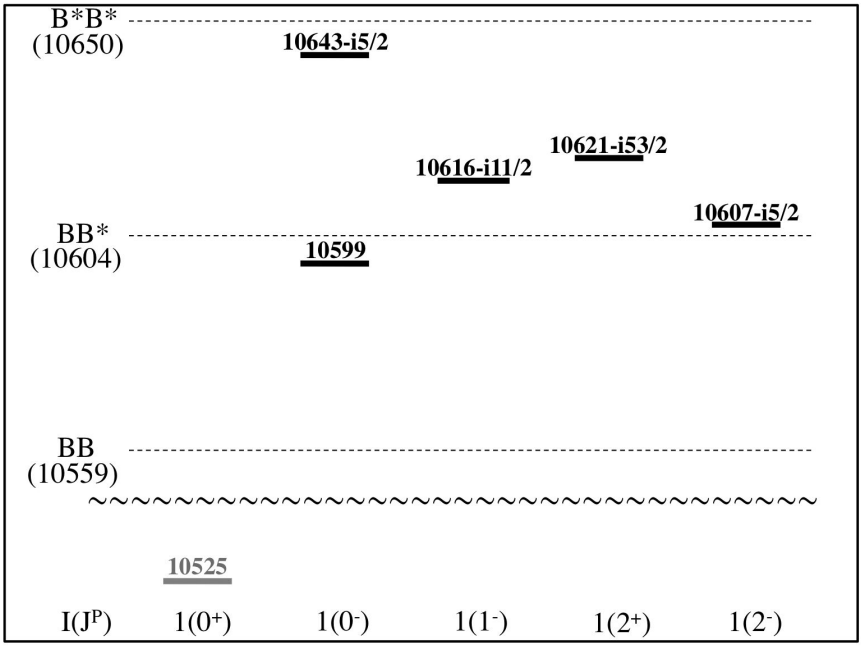

FIGURE 4.5: The $B^{(*)}B^{(*)}$ bound and resonant states around the thresholds with $I(J^P)$ in $I = 1$. (Same convention as Fig. 4.3.)

4.2.5 Summary

We have discussed exotic mesons with double charm and bottom flavor whose quark content $\bar{Q}\bar{Q}qq$ is genuinely exotic. We have taken the hadronic picture, and considered molecular states of two heavy mesons $P^{(*)}$'s (a pseudoscalar meson P = D, B, and a vector meson $P^* = D^*, B^*$). With respecting the heavy quark and chiral symmetries, we have constructed the π exchange potential and the $\pi\rho\,\omega$ exchange potential between the two heavy mesons. To investigate the bound and/or resonant states, we have numerically solved the coupled channel Schrödinger equations for the $P^{(*)}P^{(*)}$ states with $I(J^P)$ for $J \leq 2$.

As results, we have found many bound and/or resonant states in both charm and bottom sectors. The $D^{(*)}D^{(*)}$ bound and resonant states have moderate energies and decay widths around the thresholds in several channels with quantum numbers; $0(0^-)$, $0(1^+)$, $0(1^-)$, $0(2^+)$, $0(2^-)$ and $1(0^-)$. The $B^{(*)}B^{(*)}$ states have more bound and resonant states with various quantum numbers. Several new states appear in the $B^{(*)}B^{(*)}$ states in isotriplet states, such as $1(0^+)$, $1(1^-)$, $1(2^+)$ and $1(2^-)$, which cannot be found in the charm sector. By contrast to the $D^{(*)}D^{(*)}$ states, some $B^{(*)}B^{(*)}$ states are very compact objects with a large binding energy much below the thresholds. Perhaps, these states cannot survive as hadronic molecules and more consideration of quark dynamics such as tetraquarks is required.

The energy spectrum for quantum numbers $I(J^P)$ will help us to study the structure of the exotic states with $\bar{Q}\bar{Q}qq$. In the present hadronic molecule picture, many shallow bound states and resonant states appear around the thresholds in several quantum numbers. Indeed, they were not found in the tetraquark picture. It is interesting to note that, around the thresholds for $0(1^-)$, $0(2^+)$, $0(2^-)$ and $1(0^-)$, the shape of energy spectrum in those states in the charm sector seems to that in he bottom sector. It may indicate a universal behavior of the energy spectrum around the thresholds.

Experimental studies of those exotic hadrons should be performed in the coming future. The double charm production in accelerator facilities will help us to search them [115]. Recently it has been discussed that the quark-gluon plasma in the relativistic heavy ion collisions could produce much abundance of exotic hadrons including the exotic mesons with double charm [77, 78]. Those experimental studies will shed a light on the nature of the exotic mesons with double charm and bottom flavor, and provide important hints to the fundamental questions of the strong interaction in hadron physics.

Chapter 5

Spin selection rules for decays and productions of Z_b resonances and other $B\bar{B}$ molecules

We discuss decays and productions of possible molecular states formed by bottom mesons B (B^*) and $\bar{B}$ ($\bar{B}^*$). The twin resonances, $Z_b^{\pm,0}(10610)$ and $Z_b^{\pm}(10650)$, are such candidates. The spin wave functions of the molecular states are rearranged into those of heavy and light spin degrees of freedom by using the re-coupling formula of angular momentum. By applying the heavy quark symmetry we derive model independent relations among various decay and production rates, which can be tested in experiments.

5.1 Introduction

We have seen in the previous chapter that the two Z_b states are a good candidates of the $B^{(*)}\bar{B}^*$ molecule from the point of view of potential model. In addition, the potential model predicts undiscovered exotic hadrons around the $B^{(*)}\bar{B}^{(*)}$ thresholds, which appear as $B^{(*)}\bar{B}^*$ molecules. To verify whether these theoretically expected states exist or not in experiments, it is useful to study their production and decay properties.

Z_b's were found under the processes, $\Upsilon(5S) \to Z_b\pi \to Z_b\Upsilon(nS)\pi\pi(n = 1, 2, 3)$ and $\Upsilon(5S) \to Z_b\pi \to Z_b h_b(mP)\pi\pi(m = 1, 2)$. It is well known that $\Upsilon(5S)$ decays via Z_b resonances are exotic in terms of heavy quark spin selection rules. We assume that $\Upsilon(5S)$

and $\Upsilon(nS)$ are spin triplet states of $Q\bar{Q}$, whereas $h_b(mP)$ are spin singlet states. At first glance, one may expect that spin flip processes, $Z_b \to h_b(mP)\pi$, should be suppressed compared with non-spin flip processes, $Z_b \to \Upsilon(nS)\pi$, because of the large mass of b quark. Nevertheless, two kinds of decays occur with comparable rate [1, 2] This puzzle is related to the spin structure of Z_b .[18, 31], which will be discussed in this chapter.

In this chapter, we derive relative rates of vaious transition when we consider that $B^{(*)}\bar{B}^{(*)}$ molecular states obey the heavy quark symmetry. The heavy quark symmetry allows only the processes where heavy quark spin is conserved, leading to selection rules among certain classes of transitions. To derive them, we consider the spin structure of the mesons by means of spin re-coupling formula which is equivalent to Fierz rearrangement. By rearranging the two heavy quarks in $B^{(*)}$ and $\bar{B}^{(*)}$ mesons of a molecular state, we can separate the heavy quark spin and the spin of light degrees of freedom in heavy quark limit.

This chapter is organized as follows. First we define the conserved quantities in heavy quark limit, namely the spin of heavy quarks and that of light degrees of freedom in Section 5.2. In Section 5.3, We show the examples of spin selection rules for the bottomonium decays, and discuss some symmetry breaking case for bottomonium decays. We analyze the spin structures of Z_b resonances, and study the decay properties of Z_b in Section 5.4. After that, we also analyze the spin structures of the predicted $B^{(*)}\bar{B}^{(*)}$ molecules to give the decay properties of them in Section 5.5.

5.2 Heavy quark spin symmetry

5.2.1 Heavy quark spin symmetry

In the heavy effective theory, the effective Lagrangian for heavy quark field Q_v is given as

$$\mathcal{L}_{\rm HQET} = \bar{Q}_v v\cdot iDQ_v + \bar{Q}_v \frac{(iD_\perp)^2}{2m_Q} Q_v - c(\mu) g_s \bar{Q}_v \frac{\sigma_{\mu\nu}G^{\mu\nu}}{4m_Q} Q_v + \mathcal{O}(1/m_Q^2), \tag{5.1}$$

where $D_\perp^\mu = D^\mu - v^\mu v\cdot D$,$G^{\mu\nu} = [D^\mu D^\nu]/ig_s$, and $\sigma^{\mu\nu} = i[\gamma^\mu,\gamma^\nu]/2$. Here, the covariant derivative is defined as $D_\mu = \partial_\mu + ig_s A_\mu^a t^a$ with the gluon field A_μ^a, the gauge coupling g_s, and $t_a = \lambda_a/2$ with the Gell-Mann matrices $\lambda_a (a = 1,\cdots,8)$. $c(\mu)$ is the Wilson coefficient with the typical QCD parameter μ. This is the effective Lagrangian in the

heavy quark effective theory (HQET). In the heavy quark mass limit $m_Q \to \infty$, only the first term survives, whereas the other terms including the spin-flip terms $\sigma_{\mu\nu}G^{\mu\nu}$ are suppressed by $1/m_Q$. This implies that the spin of a heavy quark is a conserved quantity in heavy quark limit, which is called heavy quark spin symmetry.

As a consequence, we can define the new conserved quantity, namely the spin of light degrees freedom (light spin for short). In general, the total angular momentum $\mathbf{J}$ of a hadron is a conserved quantity. The spin of heavy quark $\mathbf{S}_H$ is also conserved in the limit of heavy quark mass, $m_Q \to \infty$. Then the light spin $\mathbf{S}_l$ defiened by

$$\mathbf{S}_l \equiv \mathbf{J} - \mathbf{S}_H \,, \tag{5.2}$$

is also conserved. Generally speaking, the light spin has complex structure. For instance, a $Q\bar{q}$ meson includes an anti-quark $\bar{q}$, gluons, an arbitrary number of $q\bar{q}$ pairs and angular momentum $\mathbf{L}$ as the light degrees of freedom. Although they are not conserved separately, the sum of them is conserved in the heavy quark limit. This quantity is referred to simply as "light spin" because it includes all degrees of freedom except for the heavy quark spin. Therefore, we can describe the spin structure of a hadron containing heavy quarks in terms of the good quantum numbers $\mathbf{S}_H$ and $\mathbf{S}_l$. Thus the wavefunction of a heavy meson as hadron is described by $\mathbf{S}_H \otimes \mathbf{S}_l$, which we call heavy quark spin (HQS) basis. It should be noted that this expression is clearly written with the conserved quantities unlike the ordinal expressions such as $Q\bar{q}(^{2S+1}L_J)$.

5.2.2 Spin structures for open flavor heavy mesons

Here, we consider the spin structures of ordinary heavy mesons which is described as $Q\bar{q}$, $Q\bar{Q}$ $(q = u, d)$. THe heavy meson containing a heavy quark is the examplest example of the heavy quark spin doublet. For HQS basis, the notation is $(\mathbf{S}_H \otimes \mathbf{S}_l)_J$, where S_l is the light spin degrees of freedom. The ground states are composed of a heavy quark $S_H = 1/2^+$ and the light-spin $S_l = 1/2^-$, which makes a heavy quark spin doublet as,

$$\begin{cases} |P\rangle = |(\frac{1}{2}{}_H^+ \otimes \frac{1}{2}{}_l^-)_0\rangle \\ |P^*\rangle = |(\frac{1}{2}{}_H^+ \otimes \frac{1}{2}{}_l^-)_1\rangle \end{cases} . \tag{5.3}$$

These states are degenerate in the heavy quark mass limit $m_Q \to \infty$ because of the suppression of spin-spin interaction between a heavy quark and a light spin. For particle

basis, the notation is $|Q\bar{q}(^{2S+1}L_J)\rangle$, where L is orbital angular momentum, S is the total spin of the pair of quarks and J is total angular momentum. Then P stands for a pseudo scalar meson $|P\rangle = |Q\bar{q}(^1S_0)\rangle$ and P^* for a vector meson $|P^*\rangle = |Q\bar{q}(^3S_1)\rangle$. P and P^* correspond to D and D^* if Q is a charm quark and $\bar{B}$ and $\bar{B}^*$ if Q is a bottom quark. The first excited states have an orbital angular momentum $L = 1$ between a heavy quark and a light antiquark. These states make two kinds of doublets, since $L = 1$ and the spin of a constituent antiquark s_l can give light-spin $1/2^+$ and $3/2^+$. They are

$$\begin{cases} |P_0^*\rangle = |(\frac{1}{2}^+_H \otimes \frac{1}{2}^+_l)_0\rangle \\ |P_1^*\rangle = |(\frac{1}{2}^+_H \otimes \frac{1}{2}^+_l)_1\rangle \end{cases} , \quad \begin{cases} |P_1\rangle = |(\frac{1}{2}^+_H \otimes \frac{3}{2}^+_l)_1\rangle \\ |P_2^*\rangle = |(\frac{1}{2}^+_H \otimes \frac{3}{2}^+_l)_2\rangle \end{cases} . \tag{5.4}$$

For P_0^* and P_2^*, the HQS basis corresponds to the particle basis one for one as $|(\frac{1}{2}^+_H \otimes \frac{1}{2}^+_l)_0\rangle = |Q\bar{q}(^3P_0)\rangle$ and $|(\frac{1}{2}^+_H \otimes \frac{3}{2}^+_l)_2\rangle = |Q\bar{q}(^3P_2)\rangle$. In contrast, P_1 and P_1^* are mixture states of $Q\bar{q}(^1P_1)$ and $Q\bar{q}(^3P_1)$, because the spin-spin interaction among Q and $\bar{q}$ is suppressed in the heavy quark limit. For the purpose to see this relation, it is instructive to consider the spin recouplings. In general, the HQS basis are deconstruct to the particle basis with standard spin recoupling formula. This decomposition is written as

$$|[\alpha]^{(s_l,L)}_{j^P}\rangle = \sum_S \hat{j}\hat{s_Q}\hat{L}\hat{S} \begin{Bmatrix} L & s_l & j \\ 0 & s_Q & s_Q \\ L & S & J \end{Bmatrix} |Q\bar{q}(^{2S+1}L_J)\rangle , \tag{5.5}$$

where we use the 9-j symbol and $\hat{S} = \sqrt{2S+1}$. In terms of Eq. 5.5, we derive the relations

$$|(\frac{1}{2}^+_H \otimes \frac{1}{2}^+_l)_1\rangle = -\frac{1}{\sqrt{3}}|Q\bar{q}(^1P_1)\rangle + \sqrt{\frac{2}{3}}|Q\bar{q}(^3P_1)\rangle , \tag{5.6}$$

$$|(\frac{1}{2}^+_H \otimes \frac{3}{2}^+_l)_1\rangle = \sqrt{\frac{2}{3}}|Q\bar{q}(^1P_1)\rangle + \frac{1}{\sqrt{3}}|Q\bar{q}(^3P_1)\rangle , \tag{5.7}$$

In reality, however, $(\frac{1}{2}^+_H \otimes \frac{1}{2}^+_l)_1$ and $(\frac{1}{2}^+_H \otimes \frac{3}{2}^+_l)_1$ will be separated, and it is good approximation that $|P_1^*\rangle \sim |(\frac{1}{2}^+_H \otimes \frac{1}{2}^+_l)_1\rangle$ and $|(\frac{1}{2}^+_H \otimes \frac{3}{2}^+_l)_1\rangle$ as far as we consider the decay properties (see also the next section).

We summarize the properties of the lowest-mass mesons containing a heavy quark in Tables. 5.1 and 5.2. Actually, since spin-spin interaction between spin of a heavy quark and light-spin doesn't vanish because of finite mass of a heavy quark, the masses of doublet mesons are slightly separated. But we can see that HQS is a good approximation

in charm and bottom sector from the tables. Spin structures make clear understanding regarding the mass spectrum of heavy hadrons.

TABLE 5.1: The lowest-mass mesons containing a c quark

Meson	J^P	Mass (MeV)	HQS basis $(S_H^P \otimes S_l^P)_J$	particle basis $Q\bar{q}(^{2S+1}L_J)$
D^+	0^-	1869.62	$(\frac{1}{2}^+_H \otimes \frac{1}{2}^-_l)_0$	$c\bar{d}(^1S_0)$
D^{*+}	1^-	2010.29	$(\frac{1}{2}^+_H \otimes \frac{1}{2}^-_l)_1$	$c\bar{d}(^3S_1)$
D^0	0^-	1864.86	$(\frac{1}{2}^+_H \otimes \frac{1}{2}^-_l)_0$	$c\bar{u}(^1S_0)$
D^{*0}	1^-	2006.99	$(\frac{1}{2}^+_H \otimes \frac{1}{2}^-_l)_1$	$c\bar{u}(^3S_1)$
D_s^+	0^-	1968.50	$(\frac{1}{2}^+_H \otimes \frac{1}{2}^-_l)_0$	$c\bar{s}(^1S_0)$
D_s^{*+}	1^-	2112.3	$(\frac{1}{2}^+_H \otimes \frac{1}{2}^-_l)_1$	$c\bar{s}(^3S_1)$
D_0^*	0^+	2318	$(\frac{1}{2}^+_H \otimes \frac{1}{2}^+_l)_0$	$c\bar{q}(^3P_0)$
D_1^*	1^+		$(\frac{1}{2}^+_H \otimes \frac{1}{2}^+_l)_1$	$c\bar{q}(^3P_1)$
D_1	1^+	2424	$(\frac{1}{2}^+_H \otimes \frac{3}{2}^+_l)_1$	$c\bar{q}(^1P_1)$
D_2^*	2^+	2461	$(\frac{1}{2}^+_H \otimes \frac{3}{2}^+_l)_2$	$c\bar{q}(^3P_2)$

5.2.3 Heavy quarkonium

Next, we consider the spin structure of heavy quarkonium ($\bar{Q}Q$). Because spin-spin interaction between two heavy quarks is suppressed in heavy quark limit $m_Q \to \infty$, $S_Q^{PC} = 0^{-+}$ and 1^{--} states generally degenerate as

$$\begin{cases} |0^{-+}_H \otimes S_l^{PC}\rangle \\ |1^{--}_H \otimes S_l^{PC}\rangle \end{cases}, \tag{5.8}$$

where P is the parity and C charge parity. This is general consequence and the degenerate is hold at any S_l taken. The lowest case is seen when $S_l^{PC} = 0_l^{++}$ is taken. It makes the doublet as follows,

$$\begin{cases} |Q\bar{Q}(^1S_0)\rangle = |(0^{--}_H \otimes 0^{++}_l)_0\rangle \\ |Q\bar{Q}(^3S_1)\rangle = |(1^{--}_H \otimes 0^{++}_l)_1\rangle \end{cases}. \tag{5.9}$$

TABLE 5.2: The lowest-mass mesons containing a b quark

Meson	J^P	Mass (MeV)	HQS basis $(S_H^P \otimes S_l^P)_J$	particle basis $Q\bar{q}(^{2S+1}L_J)$
$\bar{B}^0$	0^-	5279.58	$(\frac{1}{2}^+_H \otimes \frac{1}{2}^-_l)_0$	$b\bar{d}(^1S_0)$
$\bar{B}^{*0}$	1^-	5325.2	$(\frac{1}{2}^+_H \otimes \frac{1}{2}^-_l)_1$	$b\bar{d}(^3S_1)$
$\bar{B}^-$	0^-	5279.26	$(\frac{1}{2}^+_H \otimes \frac{1}{2}^-_l)_0$	$b\bar{u}(^1S_0)$
$\bar{B}^{*-}$	1^-	5325.2	$(\frac{1}{2}^+_H \otimes \frac{1}{2}^-_l)_1$	$b\bar{u}(^3S_1)$
$\bar{B}_s^0$	0^-	5366.77	$(\frac{1}{2}^+_H \otimes \frac{1}{2}^-_l)_0$	$b\bar{s}(^1S_0)$
$\bar{B}_s^{*0}$	1^-	5415.4	$(\frac{1}{2}^+_H \otimes \frac{1}{2}^-_l)_1$	$b\bar{s}(^3S_1)$
$\bar{B}_0^*$	0^+		$(\frac{1}{2}^+_H \otimes \frac{1}{2}^+_l)_0$	$b\bar{q}(^3P_0)$
$\bar{B}_1^*$	1^+		$(\frac{1}{2}^+_H \otimes \frac{1}{2}^+_l)_1$	$b\bar{q}(^3P_1)$
$\bar{B}_1$	1^+	5723.5	$(\frac{1}{2}^+_H \otimes \frac{3}{2}^+_l)_1$	$b\bar{q}(^1P_1)$
$\bar{B}_2^*$	2^+	5743	$(\frac{1}{2}^+_H \otimes \frac{3}{2}^+_l)_2$	$b\bar{q}(^3P_2)$

This doublet corresponds $\eta_c - J/\Psi$ for $Q = c$ and $\eta_b - \Upsilon$ for $Q = b$. We can see that the doublet is a special case on a heavy quarkonium. The light spin S_l^{PC} equals the quantum number of the relative angular momentum between two quarks in a heavy quarkonium case. Thus, when the light spin $S_l = 0$ is taken, the positive parity P and charge conjugation C should be positive. In general, when the arbitrary natural number is taken as light-spin $S_l = j(j \neq 0)$, a heavy quarkonium forms quartet as follows

$$\begin{cases} |Q\bar{Q}(j^{-PC})\rangle = |(0_H^{-+} \otimes j_l^{PC})_j\rangle \\ |Q\bar{Q}(\mathbf{J}^{-P-C})\rangle = |(1_H^{--} \otimes j_l^{PC})_{\mathbf{J}}\rangle \end{cases}, \tag{5.10}$$

where the total angular momentum is $\mathbf{J} = j-1, j, j+1$. The three states $|Q\bar{Q}(\mathbf{J}^{-P-C})\rangle$ also degenerate in heavy quark mass limit, because spin dependent interactions between the heavy quark spins and the light-spin are also suppressed. As an example, we consider the quartet for $S_l = 1_l$ as follows,

$$\begin{cases} |Q\bar{Q}(^1P_1)\rangle = |(0_H^{-+} \otimes 1_l^{--})_1\rangle \\ |Q\bar{Q}(^3P_J)\rangle = |(1_H^{--} \otimes 1_l^{--})_J\rangle \end{cases}. \tag{5.11}$$

The $Q\bar{Q}(^1P_1)$ state corresponds h_c for charm quark $Q = c$ and h_b for bottom quark $Q = b$, whereas $Q\bar{Q}(^3P_J)$ states can be regarded as $\chi_{bJ}(J = 0, 1, 2)$ for $Q = c$ and χ_{bJ} for $Q = b$. The properties of heavy quarkonia are summarized in Tables .5.3 and 5.4.

The spin structures of excited heavy quarkonia are basically the same as of the ground state ones. Around the thresholds, however, they can couple to other states such as open flavor channels. As a result of the mixing states, the simple assign of the spin structures will break down. This example will be discussed later.

TABLE 5.3: The lowest-mass charmonia

Meson	J^{PC}	Mass (MeV)	HQS basis $(S_H^{PC} \otimes S_l^{PC})_J$	particle basis $c\bar{c}(^{2S+1}L_J)$
η_c	0^{-+}	2983.7	$(0_H^{-+} \otimes 0_l^{++})_0$	$c\bar{c}(^1S_0)$
J/Ψ	1^{--}	3096.92	$(1_H^{--} \otimes 0_l^{++})_1$	$c\bar{c}(^3S_1)$
h_c	1^{+-}	3525.38	$(0_H^{-+} \otimes 1_l^{--})_1$	$c\bar{c}(^1P_1)$
χ_{c0}	0^{++}	3414.75	$(1_H^{--} \otimes 1_l^{--})_0$	$c\bar{c}(^3P_0)$
χ_{c1}	1^{++}	3510.66	$(1_H^{--} \otimes 1_l^{--})_1$	$c\bar{c}(^3P_1)$
χ_{c2}	2^{++}	3556.20	$(1_H^{--} \otimes 1_l^{--})_2$	$c\bar{c}(^3P_2)$

TABLE 5.4: The lowest-mass bottomonia

Meson	J^{PC}	Mass (MeV)	HQS basis $(S_H^{PC} \otimes S_l^{PC})_J$	particle basis $b\bar{b}(^{2S+1}L_J)$
η_b	0^{-+}	9398.0	$(0_H^{-+} \otimes 0_l^{++})_0$	$b\bar{b}(^1S_0)$
Υ	1^{--}	9460.30	$(1_H^{--} \otimes 0_l^{++})_1$	$b\bar{b}(^3S_1)$
h_b	1^{+-}	9899.3	$(0_H^{-+} \otimes 1_l^{--})_1$	$b\bar{b}(^1P_1)$
χ_{b0}	0^{++}	9859.44	$(1_H^{--} \otimes 1_l^{--})_0$	$b\bar{b}(^3P_0)$
χ_{b1}	1^{++}	9892.78	$(1_H^{--} \otimes 1_l^{--})_1$	$b\bar{b}(^3P_1)$
χ_{b2}	2^{++}	9912.21	$(1_H^{--} \otimes 1_l^{--})_2$	$b\bar{b}(^3P_2)$

5.3 Relation of the spin structure and decays

We consider decays of a heavy meson in terms of heavy quark spin symmetry. The spin structures provide useful information about not only the mass spectrum but decays of a heavy meson. We show some examples in this section.

5.3.1 Strong decays of heavy-light mesons

In many cases, excited heavy mesons containing a heavy quark decay into a ground state doublet, $P - P^*$, with a single pion emission. In generall, the strong decays are restricted by parity, angular momentum conservation and kinematics. In addition to them, the heavy quark spin selection rule becomes important in heavy quark limit. Now we consider the four kinds of decays, $(D_1, D_2^*) \to (D, D^*) + \pi$. It is an instructive exercise to derive these symmetry relations [27]. The spin structures of excited doublet, (D_1, D_2^*), are given as follows,

$$|D_1\rangle = |(\frac{1}{2}^+_H \otimes \frac{3}{2}^+_l)_1\rangle\,, \tag{5.12}$$

$$|D_2^*\rangle = |(\frac{1}{2}^+_H \otimes \frac{3}{2}^+_l)_2\rangle\,, \tag{5.13}$$

from Table 5.1. These two multiplets have opposite parity and the pion has negative parity, so the pion must be in an even partial wave with $L = 0, 2$ by parity and quantum numbers conservation. $D_2^* \to D + \pi$ and $D_2^* \to D^* + \pi$ must occur through the $L = 2$ partial wave, while $D_1 \to D^* + \pi$ seems to be able to decay with both $L = 0$ and $L = 2$ partial wave. But $L = 0$ for $D_1 \to D^* + \pi$ decay is forbidden due to the heavy quark spin selection rule. The wave function of $D^* + \pi(L = 0)$ is uniquely given as

$$|D^*\pi(L = 0)\rangle = |(\frac{1}{2}^+_H \otimes \frac{1}{2}^+_l)_1\rangle\,. \tag{5.14}$$

Since the light-spin of D_1 is $S_l = 3/2_l$, $D_1 \to D^* + \pi$ is forbidden inspite of allowing by kinematics and quantum number conservation. This is the first example of the heavy quark spin selection rule.

Next, we consider the decays with $L = 2$ partial wave. The transition amplitude for $D_1 \to D^{(*)} + \pi$ can be written by

$$\mathcal{M}[D_1 \to D^{(*)} + \pi] = \langle D^{(*)}\pi(L = 2)|H_{eff}|D_1\rangle\,, \tag{5.15}$$

where D_1 can be replaced by D_2^* for $D_2^* \to D^{(*)} + \pi$. Here H_{eff} is the effective strong interaction Hamiltonian, which conserves the spin of the heavy quark and light-spin separately. From the point of view of heavy quark symmetry, H_{eff} should be replaced by the common coupling constant g_{eff} when we postulate that these decays occur with

contact interaction. Thus the amplitude is given as

$$\mathcal{M}[D_1 \to D^{(*)} + \pi] = g_{eff} \langle D^{(*)}\pi(L=2)|D_1\rangle \,, \tag{5.16}$$

then the transition amplitude depend only on the overlap of the wavefunctions between the initial and final states. Thus the decay width is given as follows

$$\Gamma(D_1 \to D^{(*)} + \pi) \sim g_{eff}^2 |\langle D^{(*)}\pi(L=2)|D_1\rangle|^2, \tag{5.17}$$

Because the wavefunction of the outgoing pion with $L = 2$ is given as $(0_H^+ \otimes 2_l^-)_2$, the wavefunction of $|D\pi(L=2)\rangle$ is calculated by means of spin-recoupling formula as follows,

$$\begin{aligned} |D\pi(L=2)\rangle &= (\frac{1}{2}{}^+_H \otimes \frac{1}{2}{}^-_l)_0 \otimes (0_H^+ \otimes 2_l^-)_2 \\ &= \sum_{S_l} \hat{0}\hat{2}\frac{\hat{1}}{2}\hat{S}_l \begin{Bmatrix} \frac{1}{2} & \frac{1}{2} & 0 \\ 0 & 2 & 2 \\ \frac{1}{2} & S_l & 2 \end{Bmatrix} \\ &= -\sqrt{\frac{2}{5}}\left(\frac{1}{2}{}^+_H \otimes \frac{3}{2}{}^+_l\right)_2 + \sqrt{\frac{3}{5}}\left(\frac{1}{2}{}^+_H \otimes \frac{5}{2}{}^+_l\right)_2, \end{aligned} \tag{5.18}$$

where we abbreviate $|(S_H^P \otimes S_l^P)_J\rangle$ to $(S_H^P \otimes S_l^P)_J$. We derive the spin structures of $|D^*\pi(L=2)\rangle$ in the same way,

$$|D^*\pi(L=2)\rangle_{J=1} = \left(\frac{1}{2}{}^+_H \otimes \frac{3}{2}{}^+_l\right)_1, \tag{5.19}$$

$$|D^*\pi(L=2)\rangle_{J=2} = \sqrt{\frac{3}{5}}\left(\frac{1}{2}{}^+_H \otimes \frac{3}{2}{}^+_l\right)_2 + \sqrt{\frac{2}{5}}\left(\frac{1}{2}{}^+_H \otimes \frac{5}{2}{}^+_l\right)_2. \tag{5.20}$$

These spin structures imply that the ratio of the $L = 2$ decay rates are given by

$$\begin{array}{ccccccc} \Gamma(D_1 \to D\pi) & : & \Gamma(D_1 \to D^*\pi) & : & \Gamma(D_2^* \to D\pi) & : & \Gamma(D_2^* \to D^*\pi) \\ 0 & : & 1 & : & \frac{2}{5} & : & \frac{3}{5}, \end{array} \tag{5.21}$$

where $\Gamma(D_1 \to D\pi)$ is forbidden by angular momentum and parity conservation. The relation Eq. 5.21 holds in the exact heavy quark limit. It is important to take into account the difference of the phase spaces to compare the experimental values. The decay rates are proportional to the final state three-momentum $|\mathbf{p}_\pi|^{2L+1}$ for small $\mathbf{p}_\pi$,

then $|\mathbf{p}_\pi|^5$ for $L = 2$. In the $m_c \to \infty$ limit, the D_1, D_2^* are degenerate and the D and D^* are also degenerate. Hence the effect of the difference of phase spaces does not affect the ratios. For the physical value of m_c, the D^*-D mass splitting is ~ 145 MeV, which is not negligible. Including the $|\mathbf{p}_\pi|^5$, the relative decay rates are given as

$$\begin{array}{ccccccc} \Gamma(D_1 \to D\pi) & : & \Gamma(D_1 \to D^*\pi) & : & \Gamma(D_2^* \to D\pi) & : & \Gamma(D_2^* \to D^*\pi) \\ 0 & : & 1 & : & 2.3 & : & 0.93 \end{array}.$$

As a consequence, we obtain the ratio $\mathrm{Br}(D_2^* \to D\pi)/\mathrm{Br}(D_2^* \to D^*\pi) \cong 2.5$, which is consistent with the experimental value 2.4 for D_2^{*0} decay. In contrast, the ratio 1.9 for $D_2^{*\pm}$ decay is not so far from the theoretical prediction.

This argument can apply the B_1 and B_2^* decays in the same way. The only difference is the pion three momentum $|\mathbf{p}_\pi|^5$. Including the $|\mathbf{p}_\pi|^5$, the relative decay rates for B_1 and B_2^* decays are

$$\begin{array}{ccccccc} \Gamma(B_1 \to B\pi) & : & \Gamma(B_1 \to B^*\pi) & : & \Gamma(B_2^* \to B\pi) & : & \Gamma(B_2^* \to B^*\pi) \\ 0 & : & 1 & : & 0.91 & : & 0.78 \end{array}.$$

The phase space effect can't be effective in the relative ratios compared with the charm mesons, because the heavy quark symmetry is the good approximation at the bottom quark mass and the $B^* - B$ mass splitting is small, ~ 45 MeV. We obtain the prediction for the ratio $\mathrm{Br}(B_2^* \to B\pi)/\mathrm{Br}(B_2^* \to B^*\pi) \cong 1.2$, which is unobserved in experiments and will be testable in the future.

Next we argue the D_0^* and D_1^*. Phenomenologically, the decay is suppressed by the phase space factor $\sim (|\mathbf{p}_\pi|/\Lambda)^{2L+1}$, for the partial wave L. The Λ is the scale parameter of typical hadron interactions. The fact that the scale $\Lambda \sim 1$ GeV makes possible to understand why the doublet D_0^* and D_1^* is difficult to observe. They can decay into the ground state doublet D and D^* with a single pion emission in partial wave $L = 0$ because of the conservation of light spin $S_l = 1/2_l$. Thus the decay widths should be wider than the D_1 and D_2^* decay widths by roughly $(\Lambda/|\mathbf{p}_\pi|)^4 \sim 20 - 40$. Because the D_1 and D_2^* widths are $\Gamma(D_1^0) = 27.4$ MeV and $\Gamma(D_2^{*0}) = 49.0$ MeV, D_0^* and D_1^* should be broad, with widths greater than 300 MeV, which makes it difficult to observe them. The measured width of the $D_1^* = 384$ MeV.

5.3.2 Heavy quarkonium decay

The heavy quark spin selection rules bring out the properties of heavy quarkonia $Q\bar{Q}$. As a simple example, the heavy quark spin of heavy quarkonia implies that heavy quark triplet states, Υ, χ_{bJ} for $Q = b$, are forbidden to decay into heavy quark singlet states, η_b, h_b for $Q = b$. The excited Υ's can decay into both $\Upsilon\pi\pi$ and $\eta_b\pi\pi$ from the point of view of quantum number conservation law, however spin selection rule only allows the decay $\Upsilon \to \Upsilon\pi\pi$.

In many cases excited heavy quarkonia $Q\bar{Q}$ decay to the open flavor channels such as $P\bar{P}, P\bar{P}^*$ and $P^*\bar{P}^*$ if their masses are above the thresholds. Here, we estimate the decay ratio of $\Upsilon(5S) \to B\bar{B}, B\bar{B}^*, B^*\bar{B}^*$. The $\Upsilon(5S)$ should be assigned as $1^-_H \otimes 0^+_l$ states, whose quantum numbers are 1^{--}. Because $\Upsilon(5S)$ with mass of approximately 10.87 GeV is well above the thresholds for non-strange $B^{(*)}$ mesons, so that spin symmetry breaking due to the mixing with the open flavor channels should not be large. This state is of a special interest due to a large reproduction rate in the e^+e^- annihilation. In this channel, there are four different P-wave states of pair of B mesons with $J^{PC} = 1^{--}$: $B\bar{B}(^1P_1)$, $\frac{1}{\sqrt{2}}(B\bar{B}^* + B^*\bar{B})(^3P_1)$, $B^*\bar{B}^*(^1P_1)$ and $B^*\bar{B}^*(^5P_1)$. The states $B^*\bar{B}^*(^1P_1)$ and $B^*\bar{B}^*(^5P_1)$ correspond to two possible values of the total spin S of the $B^{*|}\bar{B}^*$ mason pair. It is convenient to write the four possible combinations as follows:

$$\psi_{10} = \left|1^{--}_H \otimes 0^{++}_l\right\rangle \tag{5.22}$$

$$\psi_{11} = \left|1^{--}_H \otimes 1^{++}_l\right\rangle_{J=1} \tag{5.23}$$

$$\psi_{12} = \left|1^{--}_H \otimes 2^{++}_l\right\rangle_{J=1} \tag{5.24}$$

$$\psi_{01} = \left|0^{-+}_H \otimes 1^{+-}_l\right\rangle. \tag{5.25}$$

The first three of these combinations involve the heavy quark triplet states with three kinds of light spin, whereas the forth combination is a heavy quark singlet state with the light spin uniquely assigned $S_l = 1$. Using spin recoupling formula, we decompose

the wave functions in Eqs. 5.22-5.25 to heavy and light spin:

$$B\bar{B}(^1P_1) = \frac{1}{2\sqrt{3}}\psi_{10} - \frac{1}{2}\psi_{11} + \frac{\sqrt{5}}{2\sqrt{3}}\psi_{12} + \frac{1}{2}\psi_{01} \quad (5.26)$$

$$\frac{1}{\sqrt{2}}(B\bar{B}^* + B^*\bar{B})(^3P_1) = -\frac{1}{\sqrt{3}}\psi_{10} + \frac{1}{2}\psi_{11} + \frac{\sqrt{5}}{2\sqrt{3}}\psi_{12} \quad (5.27)$$

$$B^*\bar{B}^*(^1P_1) = -\frac{1}{6}\psi_{10} + \frac{1}{2\sqrt{3}}\psi_{11} - \frac{\sqrt{5}}{6}\psi_{12} + \frac{\sqrt{3}}{2}\psi_{01} \quad (5.28)$$

$$B^*\bar{B}^*(^5P_1) = \frac{\sqrt{5}}{3}\psi_{10} + \frac{\sqrt{5}}{2\sqrt{3}}\psi_{11} + \frac{1}{6}\psi_{12}. \quad (5.29)$$

Since $\Upsilon(5S)$ corresponds the structure $1_H^{--} \otimes 0_l^{++}$, in the limit of exact heavy quark spin conservation the relative amplitudes for production of the four states from $\Upsilon(5S)$ are given by the coefficients of ψ_{10} in Eqs. 5.26-5.29

$$\begin{array}{ccccccccc} A(\Upsilon(5S) \to B\bar{B}) & : & A(\Upsilon(5S) \to B\bar{B}^*) & : & A(\Upsilon(5S) \to (B^*\bar{B}^*)_{S=0}) & : & A(\Upsilon(5S) \to (B^*\bar{B}^*)_{S=2}) \\ \frac{1}{2\sqrt{3}} & : & -\frac{1}{\sqrt{3}} & : & -\frac{1}{6} & : & \frac{\sqrt{5}}{3}, \end{array} \quad (5.30)$$

where $B\bar{B}^*$ stands for $\frac{1}{\sqrt{2}}(B\bar{B}^* + B^*\bar{B})$. This relation was found in Ref. [116, 117]. These ratios give the decay ratios for each channel as

$$\begin{array}{ccccccccc} \Gamma(\Upsilon(5S) \to B\bar{B}) & : & \Gamma(\Upsilon(5S) \to B\bar{B}^*) & : & \Gamma(\Upsilon(5S) \to (B^*\bar{B}^*)_{S=0}) & : & \Gamma(\Upsilon(5S) \to (B^*\bar{B}^*)_{S=2}) \\ 1 & : & 4 & : & \frac{1}{3} & : & \frac{20}{3} \end{array}, \quad (5.31)$$

where we neglect the phase space factor $\vec{p}^{\,3}$, which is the three-momentum of outgoing particle. If the states of the vector meson pairs, $B^*\bar{B}^*(^1P_1)$ and $B^*\bar{B}^*(^5P_1)$ are not resolved and only the total yield of the meson is measured, the ratio for the decay widths is given by

$$\begin{array}{ccccccc} \Gamma(\Upsilon(5S) \to B\bar{B}) & : & \Gamma(\Upsilon(5S) \to B\bar{B}^*) & : & \Gamma(\Upsilon(5S) \to B^*\bar{B}^*) \\ 1 & : & 4 & : & 7 \end{array}, \quad (5.32)$$

This relation, which is pointed out long ago [118], is a direct consequence of the heavy quark symmetry. This result can be tested in experiments and enables to discuss the structure of hadrons.

The available data give the branching fractions of decay

$$\begin{array}{ccccc} \Gamma_{exp}(\Upsilon(5S)\to B\bar{B}) & : & \Gamma_{exp}(\Upsilon(5S)\to B\bar{B}^*) & : & \Gamma_{exp}(\Upsilon(5S)\to B^*\bar{B}^*) \\ 1 & : & 2.5 & : & 7 \end{array}, \tag{5.33}$$

which is not so far from the result in Eq. (5.32).

5.4 The Z_b decay property

Now we consider $Z_b(10610)$ and $Z_b(10650)$. We assume that the main component of the wave function of $Z_b(10610)$ is $\frac{1}{\sqrt{2}}(B\bar{B}^* - B^*\bar{B})(^3S_1)$ and that of the $Z_b(10650)$ is $B^*\bar{B}^*(^3S_1)$. Because these masses are close to $B\bar{B}^*$ and $B^*\bar{B}^*$ thresholds respectively, and the rate of D-wave mixing is not large as the previous study indicates that the probability of $\frac{1}{\sqrt{2}}(B\bar{B}^* - B^*\bar{B})(^3D_1)$ is about 9% and that of $B^*\bar{B}^*(^3D_1)$ is about 6% in the total wave function of $Z_b(10610)$ [5]. Let us now employ the spin re-coupling formula with 9-j symbols to analyze the spin structure of $\frac{1}{\sqrt{2}}(B\bar{B}^* - B^*\bar{B})(^3S_1)$ and $B^*\bar{B}^*(^3S_1)$. This standard formula is written as

$$[[l_1,s_1]^{j_1},[l_2,s_2]^{j_2}]^J = \sum_{L,S}\hat{j}_1\hat{j}_2\hat{L}\hat{S}\begin{Bmatrix} l_1 & s_1 & j_1 \\ l_2 & s_2 & j_2 \\ L & S & J \end{Bmatrix}[[l_1,l_2]^L,[s_1,s_2]^S]^J\,, \tag{5.34}$$

where $[j_1,j_2]^J$ means that the angular momenta j_1 and j_2 are coupled to the total angular momentum J, and $\hat{J}=\sqrt{2J+1}$. By using this, the heavy and light spins of $B\bar{B}^*(^3S_1)$ and $B^*\bar{B}(^3S_1)$ are re-coupled as

$$\begin{aligned} |B\bar{B}^*(^3S_1)\rangle &= [[b\bar{q}]^0,[\bar{b}q]^1]^1 \\ &= \sum_{H,l}\hat{0}\hat{1}\hat{H}\hat{l}\begin{Bmatrix} 1/2 & 1/2 & 0 \\ 1/2 & 1/2 & 1 \\ H & l & 1 \end{Bmatrix}\left[[b\bar{b}]^H,[\bar{q}q]^l\right]^1 \\ &= \frac{1}{2}\left[[b\bar{b}]^0,[\bar{q}q]^1\right]^1 - \frac{1}{2}\left[[b\bar{b}]^1,[\bar{q}q]^0\right]^1 + \frac{1}{\sqrt{2}}\left[[b\bar{b}]^1,[\bar{q}q]^1\right]^1 \\ &= \frac{1}{2}(0_H^-\otimes 1_l^-) - \frac{1}{2}(1_H^-\otimes 0_l^-) + \frac{1}{\sqrt{2}}(1_H^-\otimes 1_l^-)\,, \end{aligned} \tag{5.35}$$

$$
\begin{aligned}
|B^*\bar{B}(^3S_1)\rangle &= [[b\bar{q}]^1,[\bar{b}q]^0]^1 \\
&= -\frac{1}{2}(0^-_H\otimes 1^-_l)+\frac{1}{2}(1^-_H\otimes 0^-_l)+\frac{1}{\sqrt{2}}(1^-_H\otimes 1^-_l)\,, \qquad (5.36)
\end{aligned}
$$

which give the spin structure of $\frac{1}{\sqrt{2}}(B\bar{B}^*-B^*\bar{B})(^3S_1)$. For $B^*\bar{B}^*(^3S_1)$, we have

$$
\begin{aligned}
|B^*\bar{B}^*(^3S_1)\rangle &= \left[[b\bar{q}]^1,[\bar{b}q]^1\right]^1 \\
&= \sum_{H,l}\hat{1}\hat{1}\hat{H}\hat{l}\begin{Bmatrix} 1/2 & 1/2 & 1 \\ 1/2 & 1/2 & 1 \\ H & l & 1 \end{Bmatrix}\left[[b\bar{b}]^H,[\bar{q}q]^l\right]^1 \\
&= \frac{1}{\sqrt{2}}\left[[b\bar{b}]^0,[\bar{q}q]^1\right]^1+\frac{1}{\sqrt{2}}\left[[b\bar{b}]^1,[\bar{q}q]^0\right]^1 \\
&= \frac{1}{\sqrt{2}}(0^-_H\otimes 1^-_l)+\frac{1}{\sqrt{2}}(1^-_H\otimes 0^-_l)\,. \qquad (5.37)
\end{aligned}
$$

If the structure of Z_b's is dominated by $B^{(*)}\bar{B}^*(^3S_1)$, their spin configurations are given from (5.35)-(5.37) as

$$
\begin{aligned}
|Z_b(10610)\rangle &= \frac{1}{\sqrt{2}}(0^-_H\otimes 1^-_l)-\frac{1}{\sqrt{2}}(1^-_H\otimes 0^-_l)\,, \qquad (5.38)\\
|Z_b(10650)\rangle &= \frac{1}{\sqrt{2}}(0^-_H\otimes 1^-_l)+\frac{1}{\sqrt{2}}(1^-_H\otimes 0^-_l)\,. \qquad (5.39)
\end{aligned}
$$

It is important to note that Z_b's have the same fraction of a heavy quark spin singlet component and a triplet component. A usual bottomonium cannot have two kinds of heavy quark spin states. For instance, $\Upsilon(nS)$ is a spin-triplet bottomonium ($|\Upsilon(nS)\rangle = 1^-_H\otimes 0^+_l$) and $h_b(kP)$ is a spin-singlet bottomonium ($|h_b(kP)\rangle = 0^-_H\otimes 1^-_l$). Naively, it is expected that $\Upsilon\to h_b\pi\pi$ decay is suppressed because this process needs spin flip of a heavy quark. However, the experimental data shows that $\Upsilon(5S)\to h_b(kP)\pi\pi$ decays have almost same probabilities as $\Upsilon(5S)\to\Upsilon(nS)\pi\pi$ [1]. This can be explained by the wave function of (5.38) and (5.39). In fact, if a two pion emission process from $\Upsilon(5S)$ occurs through Z_b, the first term of (5.38) or (5.39) allows the decay into $h_b(kP)\pi\pi$ while the second term into $\Upsilon(nS)\pi\pi$. These arguments have been already made by Fierz transformation in [18, 67]. Here we have shown the same results in terms of the spin re-coupling formula (5.34), which is also applied to other processes in a straightforward manner.

Next we consider the neutral resonance $Z_b^0(10610)$ recently observed in the processes $\Upsilon(5S)\to\pi^0\pi^0\Upsilon(1S,2S)$ by Belle group [4]. It is possible for $Z_b^0(10610)$ to decay into

$\Upsilon\pi^0$, $h_b\pi^0$, $\eta_b\gamma(\rho^0)$ and $\chi_{bJ}\gamma$ $(J = 1, 2, 3)$ from the viewpoint of the conservation of quantum numbers and kinematics. In general, the decay $\Upsilon(5S) \to \eta_b\pi^0\gamma(\rho^0)$ should be suppressed because this process requires heavy quark spin flip. However, going through Z_b, the decay into the singlet bottomonium state is allowed.

$Z_b^0(10610)$ can decay into χ_{bJ} $(J = 1, 2, 3)$ by a photon emission. The radiative transition into a bottomonium is a new decay pattern for Z_b, which cannot be seen in charged $Z_b^\pm$. It can be used to investigate the structure and interaction of Z_b. Here, we estimate the ratio of decays $Z_b^0 \to \chi_{bJ}\gamma$. To do this, we derive the spin structure of $\chi_{bJ}\gamma$. Since $Z_b^0(10610)$ has $I(J^{PC}) = 1(1^{+-})$ as a possible isospin partner of $Z_b^\pm(10610)$, the orbital angular momentum, for instance, between χ_{b0} and photon must be $L = 1$, which corresponds to an M1 multipole transition. Therefore, the spin structure of the photon can be written as $|\gamma(M1)\rangle = 0_H^+ \otimes 1_l^+$. The spin structure of χ_{b0} is $|\chi_{b0}\rangle = (1_H^- \otimes 1_l^-)|_{J=0}$. Applying the re-coupling formula to the spin of χ_{b0} and photon, we find

$$\begin{aligned} |\chi_{b0}\gamma(M1)\rangle &= (1_H^- \otimes 1_l^-)|_{J=0} \otimes (0_H^+ \otimes 1_l^+) \\ &= \frac{1}{3}(1_H^- \otimes 0_l^-) - \frac{1}{\sqrt{3}}(1_H^- \otimes 1_l^-)|_{J=1} + \frac{\sqrt{5}}{3}(1_H^- \otimes 2_l^-)|_{J=1}\,. \end{aligned} \quad (5.40)$$

The same consideration is applied to the decay $Z_b^0(10610) \to \chi_{b1}\gamma$, where M1 and E2 transitions are possible. Assuming $|\gamma(E2)\rangle = 0_H^+ \otimes 2_l^-$, the spin structures of these decay channels are given by

$$|\chi_{b1}\gamma(M1)\rangle = -\frac{1}{\sqrt{3}}(1_H^- \otimes 0_l^-) + \frac{1}{2}(1_H^- \otimes 1_l^-)|_{J=1} + \frac{15}{6}(1_H^- \otimes 2_l^-)|_{J=1}\,, \quad (5.41)$$

$$|\chi_{b1}\gamma(E2)\rangle = -\frac{1}{2}(1_H^- \otimes 1_l^-)|_{J=1} + \frac{\sqrt{3}}{2}(1_H^- \otimes 2_l^-)|_{J=1}\,. \quad (5.42)$$

The decay $Z_b^0(10610) \to \chi_{b2}\gamma$ can also occur in M1 and E2 transitions and the spin structures of these states are given by

$$|\chi_{b2}\gamma(M1)\rangle = \frac{\sqrt{5}}{3}(1_H^- \otimes 0_l^-) + \frac{\sqrt{15}}{6}(1_H^- \otimes 1_l^-)|_{J=1} + \frac{1}{6}(1_H^- \otimes 2_l^-)|_{J=1}\,, \quad (5.43)$$

$$|\chi_{b2}\gamma(E2)\rangle = \frac{\sqrt{3}}{2}(1_H^- \otimes 1_l^-)|_{J=1} + \frac{1}{2}(1_H^- \otimes 2_l^-)|_{J=2}\,. \quad (5.44)$$

Because $Z_b^0(10610)$ has the structure (5.38), its radiative decay is possible only through M1 transitions, and (5.40)-(5.44) imply that the decay ratio is given as

$$\begin{array}{ccccc} \Gamma(Z_b^0 \to \chi_{b0}\gamma) & : & \Gamma(Z_b^0 \to \chi_{b1}\gamma) & : & \Gamma(Z_b^0 \to \chi_{b2}\gamma) \\ 1 & : & 3 & : & 5 \end{array} . \tag{5.45}$$

Note that the differences of the phase spaces are not included here, and furthermore overlaps of the meson wave functions are assumed to be the same, which is the case when the spatial wave functions of χ_{bJ} have the same node quantum number. Considering the phase space factors proportional to the cube of the photon energy ω_J^3, we find the relation for $Z_b^0(10610) \to \chi_{bJ}(1P)$

$$\begin{array}{ccccc} \Gamma(Z_b^0 \to \chi_{b0}(1P)\gamma) & : & \Gamma(Z_b^0 \to \chi_{b1}(1P)\gamma) & : & \Gamma(Z_b^0 \to \chi_{b2}(1P)\gamma) \\ 1.0 & : & 2.6 & : & 4.1 \end{array} , \tag{5.46}$$

and for $Z_b^0(10610) \to \chi_{bJ}(2P)$

$$\begin{array}{ccccc} \Gamma(Z_b^0 \to \chi_{b0}(2P)\gamma) & : & \Gamma(Z_b^0 \to \chi_{b1}(2P)\gamma) & : & \Gamma(Z_b^0 \to \chi_{b2}(2P)\gamma) \\ 1.0 & : & 2.5 & : & 3.8 \end{array} , \tag{5.47}$$

which can be compared with experimental data. This decay is also studied with NREFT by Cleven's model [119], which obtains the ratios 1:2.5:3.7 for the $\chi_{bJ}(1P)$ states and 1:2.1:2.9 for the $\chi_{bJ}(2P)$ states. It appears that their analysis lends support to our predictions. So far we have assumed that $Z_b(10610)$ wave function is dominated by ${}^3S_1$ of $\frac{1}{\sqrt{2}}(B\bar{B}^* - B^*\bar{B})$. It should be noted that a ${}^3D_1$ component exists with a small fraction in the $\frac{1}{\sqrt{2}}(B\bar{B}^* - B^*\bar{B})$ molecular state [5]. The spin structure of $\frac{1}{\sqrt{2}}(B\bar{B}^* - B^*\bar{B})({}^3D_1)$ is $\frac{1}{\sqrt{2}}(0_H^- \otimes 1_l^-) + \frac{1}{\sqrt{2}}(1_H^- \otimes 2_l^-)|_{J=1}$, which modifies slightly the relations (5.46) and (5.47). Moreover, it implies that E2 transition in the processes $Z_b^0 \to \chi_{bJ}\gamma$ must occur mediated by the D-wave component. This is also an interesting point to be studied in experiments with higher statistics.

TABLE 5.5: Various properties of W_{bJ}^{++} states. Masses are taken from the predicted values from [5].

W_{bJ}^{PC}	$I^G(J^{PC})$	Main component	Mass [MeV]
W_{b0}^{++}	$1^-(0^{++})$	$B\bar{B}(^1S_0)$	-
$W_{b0}^{\prime++}$	$1^-(0^{++})$	$B^*\bar{B}^*(^1S_0)$	-
W_{b1}^{++}	$1^-(1^{++})$	$\frac{1}{\sqrt{2}}(B\bar{B}^* + B^*\bar{B})(^3S_1)$	10602
W_{b2}^{++}	$1^-(2^{++})$	$B^*\bar{B}^*(^5S_2)$	10621

5.5 Other heavy meson molecules

5.5.1 Heavy meson molecules with negative G-parity

In this section, we discuss the decay properties of the predicted $B^{(*)}\bar{B}^{(*)}$ meson molecules, which can be accessed by $\Upsilon(5S)$ decays. We introduce the notations W_{bJ}^{PC} for the lowest state and $W_{bJ}^{\prime PC}$ for the first excited state. First, we consider the isotriplet $B^{(*)}\bar{B}^{(*)}$ molecules having G-parity: W_{b0}^{++}, $W_{b0}^{\prime++}$, W_{b1}^{++} and W_{b2}^{++}. Their decay and production properties are first studied by Voloshin [67]. These states can be produced by the radiative transitions from $\Upsilon(5S)$. We summarize the W_{bJ}^{++} properties in Table 5.5: quantum numbers, the main component and the mass. The masses are estimated values from the potential model [5]. Actually, potential model does not reproduce any bound and resonance states in $I^G(J^{PC}) = 1^-(0^{++})$. Some studies, however, argue the presence of the W_{b0}^{++} and $W_{b0}^{\prime++}$. According their claim, we postulate them, whose main components are $B\bar{B}(^1S_0)$ for W_{b0}^{++} and $B^*\bar{B}^*(^1S_0)$ for $W_{b0}^{\prime++}$, in this section.

Using the spin-recoupling formula, we can obtain the spin structures for W_{bJ}^{++}:

$$W_{b0}^{++} \quad : \quad \frac{1}{2}(0_H^- \otimes 0_l^-) + \frac{\sqrt{3}}{2}(1_H^+ \otimes 1_l^+)|_{J=0} \tag{5.48}$$

$$W_{b0}^{\prime++} \quad : \quad \frac{\sqrt{3}}{2}(0_H^- \otimes 0_l^-) - \frac{1}{2}(1_H^+ \otimes 1_l^+)|_{J=0} \tag{5.49}$$

$$W_{b1}^{++} \quad : \quad (1_H^- \otimes 1_l^+)|_{J=1} \tag{5.50}$$

$$W_{b2}^{++} \quad : \quad (1_H^- \otimes 1_l^+)|_{J=2} \tag{5.51}$$

At first glance, W_{b1}^{++} and W_{b2}^{++} are pure heavy quark spin triplet states. This fact suggests that these states cannot decay into the channels of spin singlet bottomonia such as $\epsilon_b\pi$, $h_b\gamma$. In contrast, W_{b0}^{++} and $W_{b0}^{\prime++}$ will decay to $\eta_b\pi$ in a S-wave. The

relative decay ratio is expected from the spin structures:

$$\begin{array}{ccc} \Gamma(W_{b0}^{++} \to \eta_b \pi) & : & \Gamma(W_{b0}^{\prime ++} \to \eta_b \pi) \\ 1 & : & 3 \end{array}, \tag{5.52}$$

when we neglect the difference of the phase space. Because this decay occurs in S-wave, this factor will be negligible. Assuming that the masses are $M(B\bar{B}) = 10599$ MeV for $M(W_{b0^{++}})$ and $M(B^*\bar{B}^*)10650$ MeV for $M(W_{b0'^{++}})$ although our potential model does not predict these states, we derive the decay ratio taking into account the phase space:

$$\begin{array}{ccc} \Gamma(W_{b0}^{++} \to \eta_b \pi) & : & \Gamma(W_{b0}^{\prime ++} \to \eta_b \pi) \\ 1.0 & : & 3.2 \end{array}, \tag{5.53}$$

which shows that the phase space factor hardly contributes this decay ratio.

All of W_{bJ}^{++} can decay to $\Upsilon\rho$ in a S-wave via the $(1_H^+ \otimes 0_l^+)$ component. The relative decay ratio of them are given as

$$\begin{array}{ccccccc} \Gamma(W_{b0}^{++} \to \Upsilon\rho) & : & \Gamma(W_{b0}^{\prime ++} \to \Upsilon\rho) & : & \Gamma(W_{b1}^{++} \to \Upsilon\rho) & : & \Gamma(W_{b2}^{++} \to \Upsilon\rho) \\ \frac{3}{4} & : & \frac{1}{4} & : & 1 & : & 1 \end{array} \tag{5.54}$$

Since these decays occur in a S-wave, the effect of the phase space will be small as the result on $\epsilon_b\pi$ decays.

The wavefunctions of W_{bJ}^{++} also make it possible to estimate the production properties. The W_{bJ}^{++} can be accessed from $\Upsilon(5S)$ radiative decay as predicted in . The spin structure of $\Upsilon(5S)$ will be $(1_H^- \otimes 0_l^+)$ as denoted . To see the production properties, we need to know the wave functions of $(W_{bJ}^{++}\gamma)_{J=1}$ in HQS basis. Because $\Upsilon(5S)$ radiative decay to W_{bJ}^{++} corresponds to $E1$ transition, the wavefunction of the γ is regarded as $0_H^+ \otimes 1_l^-$. Thus the spin structures of $W_{bJ}^{++}\gamma$ is given as

$$\begin{aligned}
|W_{b0}^{++}\gamma(E1)\rangle &= \frac{1}{2}(0_H^- \otimes 1_l^-) + \frac{1}{2\sqrt{3}}(1_H^- \otimes 0_l^-) - \frac{1}{2}(1_H^- \otimes 1_l^-)|_{J=1} + \frac{\sqrt{5}}{2\sqrt{3}}(1_H^- \otimes 2_l^-)|_{J=1} \\
|W_{b0}^{\prime ++}\gamma(E1)\rangle &= \frac{\sqrt{3}}{2}(0_H^- \otimes 1_l^-) - \frac{1}{6}(1_H^- \otimes 0_l^-) + \frac{1}{2\sqrt{3}}(1_H^- \otimes 1_l^-)|_{J=1} - \frac{\sqrt{5}}{6}(1_H^- \otimes 2_l^-)|_{J=1} \\
|W_{b1}^{++}\gamma(E1)\rangle &= -\frac{1}{\sqrt{3}}(1_H^- \otimes 0_l^-) + \frac{1}{2}(1_H^- \otimes 1_l^-)|_{J=1} + \frac{\sqrt{5}}{2\sqrt{3}}(1_H^- \otimes 2_l^-)|_{J=1} \\
|W_{b2}^{++}\gamma(E1)\rangle &= \frac{\sqrt{5}}{3}(1_H^- \otimes 0_l^-) + \frac{\sqrt{5}}{2\sqrt{3}}(1_H^- \otimes 1_l^-)|_{J=1} + \frac{1}{6}(1_H^- \otimes 2_l^-)|_{J=2}
\end{aligned} \tag{5.55}$$

TABLE 5.6: Various properties of W_{bJ}^{--} states found in [5].

W_{bJ}^{PC}	$I^G(J^{PC})$	Main component	Mass [MeV]
W_{b0}^{--}	$1^+(0^{--})$	$\frac{1}{\sqrt{2}}(B\bar{B}^* + B^*\bar{B})(^3P_0)$	10594
$W_{b1}^{\prime--}$	$1^+(1^{--})$	$\frac{1}{\sqrt{2}}(B\bar{B}^* + B^*\bar{B})(^3P_1)$	10617
W_{b1}^{--}	$1^+(1^{--})$	$B\bar{B}(^1P_1)$	10566
$W_{b2}^{\prime--}$	$1^+(2^{--})$	$B^*\bar{B}^*(^5P_2)$	10649
W_{b2}^{--}	$1^+(2^{--})$	$\frac{1}{\sqrt{2}}(B\bar{B}^* + B^*\bar{B})(^3P_2)$	10606

Since the $\Upsilon(5S)$ is $1_H^- \otimes 0_l^+$ state, these productions must occur through the $1_H^- \otimes 0_l^+$ component. Hence, the relative production rate of $\Upsilon(5S) \to W_{bJ}^{++}\gamma$ is obtained as

$$\begin{array}{ccccccc} f(W_{b0}^{++}\gamma) & : & f(W_{b0}^{\prime++}\gamma) & : & f(W_{b1}^{++}\gamma) & : & f(W_{b2}^{++}\gamma) \\ \frac{3}{4}w_0^3 & : & \frac{1}{4}w_2^3 & : & 3w_1^3 & : & 5w_2^3 \end{array}, \tag{5.56}$$

where $w_{0,1,2}$ are the photon energies in the corresponding transitions: $W_0 \sim 305$ MeV, $W_1 \sim 260$ MeV and $W_2 \sim 215$ MeV. Taking account the kinematical factors w^3, we estimate the ratio of the rates approximately as 8.5:1:21:20, which will be proper rather than the result 5.56 one ignores the kinematical effect. In both cases, heavy quark spin suggests that $W_{b0}^{\prime++}$ is suppressed compared with W_{b2}^{++}.

5.5.2 Heavy meson molecules with positive G-parity

Now, we consider production and decay properties of recently predicted isotriplet $B^{(*)}\bar{B}^{(*)}$ molecular states having positive G-parity [5]. These states can be produced by one pion emission in P-wave from $\Upsilon(5S)$. We summarize various properties including the quantum numbers, the main components of wave functions and the masses of W_{bJ}^{--} in Table 5.6. We note that, in principle, $B^*\bar{B}^*(^1P_1)$ and $B^*\bar{B}^*(^5P_1)$ in $I^G(J^{PC}) = 1^+(1^{--})$ states can be mixed. As a result of the previous study, however, it has been shown that W_{b1}^{--} and $W_{b1}^{\prime--}$ are close to each threshold of $B\bar{B}$ and $B\bar{B}^*$, and so $B^*\bar{B}^*$ components are suppressed. There could be also coupled channels $\frac{1}{\sqrt{2}}(B\bar{B}^* + B^*\bar{B})(^3F_2)$ and $B^*\bar{B}^*(^5F_2)$ components in $1^+(2^{--})$ states. However, we expect that the probabilities of these components are small due to high angular momentum. Hence, the main components of W_{bJ}^{--} are those given in Table 5.6. The corresponding spin structures of W_{bJ}^{--}

states are given as

$$W_{b0}^{--} \;:\; (1_H^- \otimes 1_l^+)|_{J=0}\,, \tag{5.57}$$

$$W_{b1}'^{--} \;:\; -\frac{1}{\sqrt{3}}(1_H^- \otimes 0_l^+) + \frac{1}{2}(1_H^- \otimes 1_l^+)|_{J=1} + \frac{\sqrt{5}}{2\sqrt{3}}(1_H^- \otimes 2_l^+)|_{J=1}\,, \tag{5.58}$$

$$W_{b1}^{--} \;:\; \frac{1}{2}(0_H^- \otimes 1_l^+) + \frac{1}{2\sqrt{3}}(1_H^- \otimes 0_l^+) - \frac{1}{2}(1_H^- \otimes 1_l^+)|_{J=1} + \frac{\sqrt{5}}{2\sqrt{3}}(1_H^- \otimes 2_l^+)|_{J=1}\,, \tag{5.59}$$

$$W_{b2}'^{--} \;:\; \frac{\sqrt{3}}{2}(1_H^- \otimes 1_l^+)|_{J=2} + \frac{1}{2}(1_H^- \otimes 2_l^+)|_{J=2}\,, \tag{5.60}$$

$$W_{b2}^{--} \;:\; -\frac{1}{2}(1_H^- \otimes 1_l^+)|_{J=2} + \frac{\sqrt{3}}{2}(1_H^- \otimes 2_l^+)|_{J=2}\,. \tag{5.61}$$

Remarkably, the heavy quark spin singlet state exists only in W_{b1}^{--}. Therefore decays of W_{bJ}^{--} into a heavy quark spin singlet state of bottomonium and light hadrons are forbidden except for W_{b1}^{--}, although their quantum numbers and kinematics allow them. Only W_{b1}^{--} can decay into $h_b\pi$ or $\eta_b\rho(\gamma)$. In contrast, all W_{bJ}^{--} can decay into a heavy quark spin triplet state, e.g. $\Upsilon\pi$ in P-wave ($|\Upsilon\pi\rangle_{P\text{-}wave} = (1_H^- \otimes 1_l^+)|_{J=0,1,2}$). The decay ratio of the processes $W_{bJ}^{--} \to \Upsilon\pi$ is obtained as

$$\begin{array}{ccccccccccc} \Gamma(W_{b0}^{--} \to \Upsilon\pi) & : & \Gamma(W_{b1}'^{--} \to \Upsilon\pi) & : & \Gamma(W_{b1}^{--} \to \Upsilon\pi) & : & \Gamma(W_{b2}'^{--} \to \Upsilon\pi) & : & \Gamma(W_{b2}^{--} \to \Upsilon\pi) \\ 4 & : & 1 & : & 1 & : & 3 & : & 1 \end{array} \tag{5.62}$$

The decay processes $\Upsilon(5S) \to W_{bJ}^{--}\pi \to \Upsilon(nS)\pi\pi$ are not yet observed, though they are similar to $\Upsilon(5S) \to Z_b\pi \to \Upsilon(nS)\pi\pi$. However we expect that the production rates of W_{bJ}^{--} is small compared with that of Z_b, since the W_{bJ}^{--} transition is mediated by a pion emission in P-wave. High statistics and refined analysis of experiments will establish the presence or absence of W_{bJ}^{--} and their production and decay properties. Finally, the production ratio of W_{bJ}^{--} from $\Upsilon(5S)$ is obtained as

$$\begin{array}{ccccccccccc} f(W_{b0}^{--}\pi) & : & f(W_{b1}'^{--}\pi) & : & f(W_{b1}^{--}\pi) & : & f(W_{b2}'^{--}\pi) & : & f(W_{b2}^{--}\pi) \\ 2 & : & 9 & : & 4.5 & : & 9 & : & 12 \end{array}\,, \tag{5.63}$$

where we find the production rate of W_{b2}^{--} is favored, while the production of W_{b0}^{--} is suppressed. Considering the phase space factors proportional to the cube of the pion momentum $\vec{q}_\pi$, the relation for the production ratio (5.63) is modified as

$$\begin{array}{ccccccccccc} f(W_{b0}^{--}\pi) & : & f(W_{b1}'^{--}\pi) & : & f(W_{b1}^{--}\pi) & : & f(W_{b2}'^{--}\pi) & : & f(W_{b2}^{--}\pi) \\ 2.0 & : & 6.3 & : & 6.4 & : & 3.5 & : & 10.0 \end{array}\,. \tag{5.64}$$

This result shows that the phase space corrections will not drastically change the result (5.63) except for $W_{b2}'^{--}\pi$. The production ratio of $W_{b2}'^{--}\pi$ is most affected, because the mass of $W_{b2}'^{--}$ is close to $\Upsilon(5S)$ and hence the phase space is reduced in comparison with those of other states.

5.6 Summary

In summary, we have derived the model independent relations among various decay and production rates for possible $B^{(*)}\bar{B}^{(*)}$ molecular states under the heavy quark symmetry. Part of decay properties of $Z_b(10610)$ and $Z_b(10650)$ are well explained and the possible decay patterns for neutral $Z_b^0(10610)$ are discussed in the present framework. We have shown that the W_{bJ}^{--} decay into a spin singlet bottomonium is forbidden except for W_{b1}^{--}. We have also predicted the production rate of various W_{bJ}^{--} through the one pion emission of $\Upsilon(5S)$. All of them can be tested experimentally and will provide important information to further understand the exotic structure of the new particles.

Chapter 6

Decays of $Z_b \to \Upsilon\pi$ via triangle diagrams in heavy meson molecules

Bottomonium-like resonances $Z_b(10610)$ and $Z_b'(10650)$ are good candidates of hadronic molecules composed of $B\bar{B}^*$ (or $B^*\bar{B}$) and $B^*\bar{B}^*$, respectively. Considering $Z_b^{(\prime)}$ as heavy meson molecules, we investigate the decays of $Z_b^{(\prime)+} \to \Upsilon(nS)\pi^+$ in terms of the heavy meson effective theory. We find that the intermediate $B^{(*)}$ and $\bar{B}^{(*)}$ meson loops and the form factors play a significant role to reproduce the experimental values of the decay widths. We also predict the decay widths of $Z_c^+ \to J/\psi\pi^+$ and $\psi(2S)\pi^+$ for a charmonium-like resonance Z_c which has been reported recently in experiments.

6.1 Introduction

Two charged bottomonium-like resonances $Z_b(10610)$ and $Z_b'(10650)$ were reported in the processes $\Upsilon(5S) \to \Upsilon(nS)\pi^+\pi^-$ $(n = 1, 2, 3)$ and $\Upsilon(5S) \to h_b(mP)\pi^+\pi^-$ $(m = 1, 2)$ [2, 17]. Their quantum numbers are $I^G(J^P) = 1^+(1^+)$, which indicates that the quark content of $Z_b^{(\prime)}$ must be four quarks as minimal constituents such as $|b\bar{b}u\bar{d}\rangle$. The reported masses and decay widths of the two resonances are $M(Z_b(10610)) = 10607.4 \pm 2.0$ MeV, $\Gamma(Z_b(10610)) = 18.4 \pm 2.4$ MeV and $M(Z_b(10650)) = 10652.2 \pm 1.5$ MeV, $\Gamma(Z_b(10650)) = 11.5 \pm 2.2$ MeV, showing that the masses are very close to the $B\bar{B}^*$ (or $B^*\bar{B}$) and $B^*\bar{B}^*$

thresholds, respectively. In view of these facts, Z_b and Z_b' are likely molecular states of two $B^{(*)}$ and $\bar{B}^{(*)}$ mesons [5, 18, 31].

More recently, Belle reported the branching fractions of each channel in three-body decays from $\Upsilon(5S)$ [3], the results of which are summarized in Table. 6.1. They show a remarkable feature of $Z_b^{(\prime)}$. One is that the dominant decay processes are channels to open flavor mesons, $\mathrm{Br}(\mathrm{Z_b^+} \to \mathrm{B^+\bar{B}^{*0}}+\mathrm{B^{*+}\bar{B}^0}) = 0.860$ and $\mathrm{Br}(Z_b'^+ \to B^{*+}\bar{B}^{*0}) = 0.734$. This is consistent with the naive consideration from the molecular picture. Another point is in the ratios of the decay widths to a bottomonium and a pion, where it is important to notice the following two facts. Firstly, $h_b(mP)\pi^+$ decays are not suppressed in spite of their spin-flip processes of heavy quarks from $\Upsilon(5S)$. In general, the spin-nonconserved decay in the strong interaction should be suppressed due to a large mass of b quark. Nevertheless, the spin-conserved decay $Z_b^{(\prime)+} \to \Upsilon(nS)\pi^+$ and spin-nonconserved one $Z_b^{(\prime)+} \to h_b(mP)\pi^+$ occur in comparable ratios. The previous studies suggest that molecular picture explains well this behavior [18, 31]: if the $Z_b^{(\prime)}$ is a molecular state, the wave function is a mixture state of heavy quark spin singlet and triplet. Then, $Z_b^{(\prime)}$ is possible to decay into both channels. Secondly, the decay ratios are not simply proportional to the magnitudes of the phase space. In particular, the branching fraction of $Z_b^{(\prime)+} \to \Upsilon(nS)\pi^+$ is only approximately ten percents of the one of $Z_b^{(\prime)+} \to \Upsilon(2S)\pi^+$ although the phase space of $\Upsilon(1S)\pi^+$ is larger than the one of $\Upsilon(2S)\pi^+$. In fact, $\Gamma(Z_b^{(\prime)+} \to \Upsilon(3S)\pi^+)$ is approximately half a size of $\Gamma(Z_b^{(\prime)+} \to \Upsilon(2S)\pi^+)$, which is still wider than the $\Gamma(Z_b^{(\prime)+} \to \Upsilon(1S)\pi^+)$. The mechanism of this behavior is not still elucidated completely and needs detailed considerations. In this paper, we focus on the strong decays $Z_b^{(\prime)+} \to \Upsilon(nS)\pi^+$ and analyze their decay widths as hadronic molecules. This study will also provide a perspective for the internal structure of $Z_b^{(\prime)}$. Our approach also applies to the decays of $Z_c(3900)$, which is charged charmonium-like resonance reported both by the BESIII Collaboration [19] and by the Belle collaboration [20].

6.2 Formalism

To start the discussion, we assume that the main components of Z_b and Z_b' are molecular states of $\frac{1}{\sqrt{2}}(B\bar{B}^* - B^*\bar{B})(^3S_1)$ and $B^*\bar{B}^*(^3S_1)$, namely,

$$|Z_b\rangle = \frac{1}{\sqrt{2}}|B\bar{B}^* - B^*\bar{B}\rangle \ , \tag{6.1}$$

$$|Z_b'\rangle = |B^*\bar{B}^*\rangle \ . \tag{6.2}$$

TABLE 6.1: Branching ratios (Br) of various decay channels from $Z_b(10610)$ and $Z_b'(10650)$.

channel	Br of Z_b	Br of Z_b',
$\Upsilon(1S)\pi^+$	0.32 ± 0.09	0.24 ± 0.07
$\Upsilon(2S)\pi^+$	4.38 ± 1.21	2.40 ± 0.63
$\Upsilon(3S)\pi^+$	2.15 ± 0.56	1.64 ± 0.40
$h_b(1P)\pi^+$	2.81 ± 1.10	7.43 ± 2.70
$h_b(2P)\pi^+$	2.15 ± 0.56	14.8 ± 6.22
$B^+\bar{B}^{*0} + B^{*+}\bar{B}^0$	86.0 ± 3.6	$-$
$B^{*+}\bar{B}^{*0}$	$-$	73.4 ± 7.0

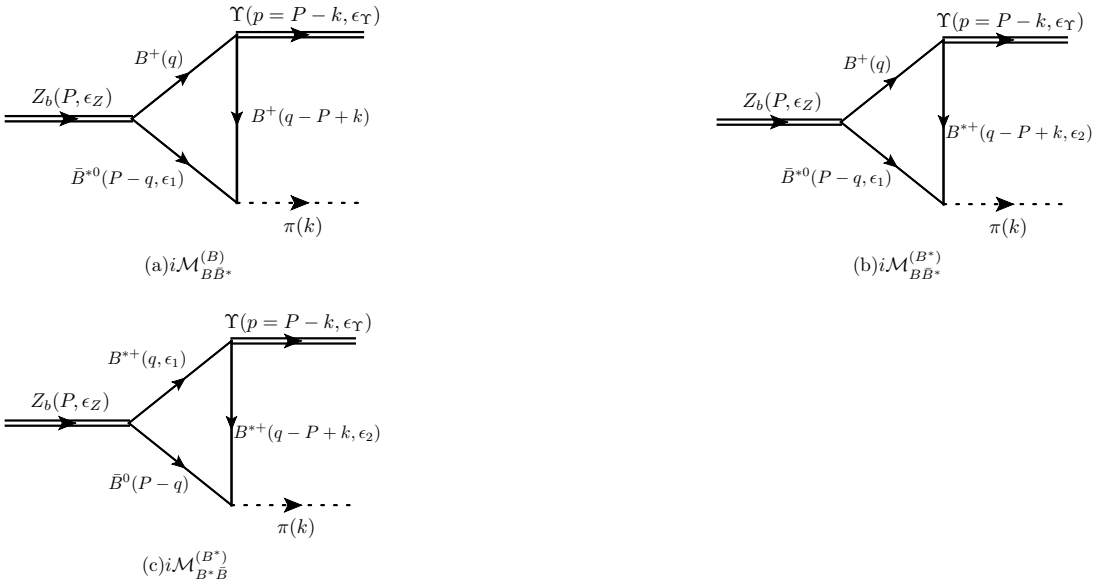

FIGURE 6.1: Feynman diagrams for $Z_b^+ \to \Upsilon(nS)\pi^+$.

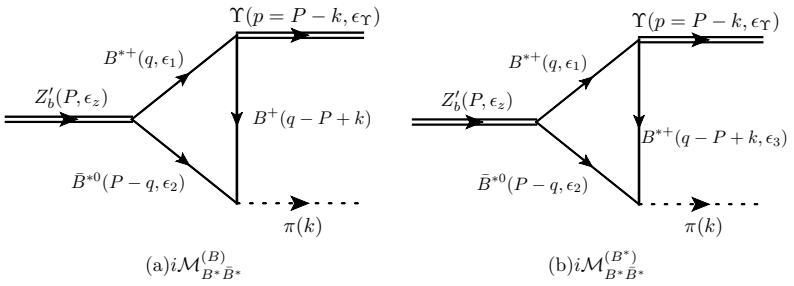

FIGURE 6.2: Feynman diagrams for $Z_b'^+ \to \Upsilon(nS)\pi^+$.

Such a simple molecular picture will give a good description, because those masses are close to the $B\bar{B}^*$ (or $B^*\bar{B}$) and $B^*\bar{B}^*$ thresholds, respectively, and the ratio of D-wave mixing is not large. In fact, the explicit calculations based on the hadronic model in our previous study indicate that the probability of the $\frac{1}{\sqrt{2}}(B\bar{B}^* - B^*\bar{B})(^3D_1)$ component is approximately 9 % and the $B^*\bar{B}^*(^3D_1)$ component is approximately 6 % in the total wave function of Z_b [5]. In the hadronic molecular picture, the diagrams contributing to the decay $Z_b^{(\prime)+} \to \Upsilon(nS)\pi^+$ are described with the intermediate $B^{(*)}$ and $\bar{B}^{(*)}$ meson loops at lowest order [119, 120] as shown in Figs. 6.1 and 6.2. Since B^+ and $\bar{B}^0$ are interchangeable, the total transition amplitudes are given by the twice of the sum of each channel as follows,

$$\mathcal{M}_{Z_b} = 2(\mathcal{M}^{(B)}_{B\bar{B}^*} + \mathcal{M}^{(B^*)}_{B\bar{B}^*} + \mathcal{M}^{(B^*)}_{B^*\bar{B}}), \tag{6.3}$$

$$\mathcal{M}_{Z_b'} = 2(\mathcal{M}^{(B)}_{B^*\bar{B}^*} + \mathcal{M}^{(B^*)}_{B^*\bar{B}^*}). \tag{6.4}$$

To calculate the transition amplitudes, we need the couplings from the effective Lagrangians. We adopt the phenomenological Lagrangians at vertices of $Z_b^{(\prime)}$ and $B^{(*)}$ mesons, which are

$$\mathcal{L}_{ZBB^*} = g_{ZBB^*} M_z Z^\mu (B B^{*\dagger}_\mu + B^*_\mu B^\dagger), \tag{6.5}$$

$$\mathcal{L}_{Z'B^*B^*} = i g_{Z'B^*B^*} \epsilon^{\mu\nu\alpha\beta} \partial_\mu Z'_\nu B^*_\alpha B^{*\dagger}_\beta, \tag{6.6}$$

where the coupling constants g_{ZBB^*} and $g_{Z'B^*B^*}$ are determined from the experimentally observed decay widths for the process to open heavy flavor channels from $Z_b^{(\prime)}$. The experimental results are $\Gamma(Z_b^+ \to B^+\bar{B}^{*0} + B^{*+}\bar{B}^0) = 15.82\,\text{MeV}$ and $\Gamma(Z_b'^+ \to B^{*+}\bar{B}^{*0}) = 8.44\,\text{MeV}$. The decay widths are given with the effective Lagrangians 6.5 and 6.6 as follows,

$$\Gamma(Z_b^+ \to B^+\bar{B}^{*0} + B^{*+}\bar{B}^0) = \frac{g^2_{ZBB^*}}{4\pi} |\vec{q}_{cm}|, \tag{6.7}$$

$$\Gamma(Z_b'^+ \to B^{*+}\bar{B}^{*0}) = \frac{g_{Z'B^*B^*}}{4\pi} |\vec{q}_{cm}|, \tag{6.8}$$

where q_{cm} is the final state three-momentum of the $B(B^*)$ meson, $q_{cm} = 118$ MeV and $q_{cm} = 98$ MeV are for $\Gamma(Z_b^+ \to B^+\bar{B}^{*0} + B^{*+}\bar{B}^0)$ and $\Gamma(Z_b'^+ \to B^{*+}\bar{B}^{*0})$, respectively. We obtain $g_{BB^*Z_b} = 1.30$ and $g_{B^*B^*Z_b'} = 1.04$ to reproduce the observed values. For the other vertices, we employ the effective Lagrangians reflecting both heavy quark

symmetry and chiral symmetry [121],

$$\mathcal{L}_{BB^*\pi} = -ig_{BB^*\pi}(B_i\partial_\mu\pi_{ij}B_j^{\dagger *\mu} - B_i^{*\mu}\partial_\mu\pi_{ij}B_j^\dagger)\,, \tag{6.9}$$

$$\mathcal{L}_{B^*B^*\pi} = \frac{1}{2}g_{B^*B^*\pi}\epsilon^{\mu\nu\alpha\beta}B^*_{i\mu}\overleftrightarrow{\partial}_\alpha\bar{B}^*_{j\beta}\partial_\nu\pi_{ij}\,, \tag{6.10}$$

$$\mathcal{L}_{BB\Upsilon} = ig_{BB\Upsilon}\Upsilon_\mu(\partial^\mu BB^\dagger - B\partial^\mu B^\dagger)\,, \tag{6.11}$$

$$\mathcal{L}_{BB^*\Upsilon} = -g_{BB^*\Upsilon}\epsilon^{\mu\nu\alpha\beta}\partial_\mu\Upsilon_\nu(\partial_\alpha B^*_\beta B^\dagger + B\partial_\alpha B^{*\dagger}_\beta)\,, \tag{6.12}$$

$$\begin{aligned}\mathcal{L}_{B^*B^*\Upsilon} = -ig_{B^*B^*\Upsilon}\Big\{&\Upsilon^\mu(\partial_\mu B^{*\nu}B^{*\dagger}_\nu - B^{*\nu}\partial_\mu B^{*\dagger}_\nu) + (\partial_\mu\Upsilon_\nu B^{*\nu} - \Upsilon_\nu\partial_\mu B^{*\nu})B^{*\dagger\nu} \\ &+B^{*\mu}(\Upsilon^\nu\partial_\mu B^{*\dagger}_\nu - \partial_\mu\Upsilon^\nu B^{*\dagger\nu})\Big\}\,,\end{aligned} \tag{6.13}$$

where $B^{(*)} = (B^{(*)0}, B^{(*)+})$. The two coupling constants $g_{BB^*\pi}$ and $g_{B^*B^*\pi}$ are expressed by a single parameter g thanks to heavy quark symmetry as follows:

$$g_{BB^*\pi} = \frac{2g}{f_\pi}\sqrt{m_B m_{B^*}}\,, \qquad g_{B^*B^*\pi} = \frac{g_{BB^*\pi}}{\sqrt{m_B m_{B^*}}}\,, \tag{6.14}$$

where $f_\pi = 132$ MeV is a pion decay constant. Since the decay $B^* \to B\pi$ is kinematically forbidden, it is impossible to determine the coupling g from experiments. Therefore, using the experimental information in the charm sector and the heavy quark symmetry, we adopt approximately $g = 0.59$ when the observed decay width $\Gamma = 96$ keV for $D^* \to D\pi$ is used. The coupling $g_{BB\Upsilon(nS)}$ of $\Upsilon(nS)$ and B is estimated on the assumption of vector meson dominance (VMD) [122]. VMD gives the coupling constant $g_{BB\Upsilon(nS)} = M_{\Upsilon(nS)}/f_{\Upsilon(nS)}$, where $f_{\Upsilon(nS)}$ is a leptonic decay constant defined by $\langle 0|\bar{b}\gamma^\mu b|\Upsilon(nS)(p,\epsilon)\rangle = f_{\Upsilon(nS)}M_{\Upsilon(nS)}\epsilon^\mu$. Here $f_{\Upsilon(nS)}$ is determined from the leptonic decays $\Upsilon(nS) \to e^+e^-$ as

$$\Gamma(\Upsilon(nS) \to e^+e^-) = \frac{4\pi\alpha_{\rm EM}^2}{27}\frac{f^2_{\Upsilon(nS)}}{M_{\Upsilon(nS)}} \tag{6.15}$$

where $\alpha_{\rm EM} = 137.036$ is the fine-structure constant. In terms of this relation, the decay constants are given as $f_{\Upsilon(1S)} = 715$ MeV, $f_{\Upsilon(2S)} = 497.5$ MeV and $f_{\Upsilon(3S)} = 430.2$ MeV, where the masses and decay widths are taken from Particle Data Group (PDG) [28]. Finally, we obtain $g_{BB\Upsilon(1S)} = 13.2$, $g_{BB\Upsilon(2S)} = 20.1$ and $g_{BB\Upsilon(3S)} = 24.7$. The other couplings $g_{BB^*\Upsilon(nS)}$ and $g_{B^*B^*\Upsilon(nS)}$ are related with $g_{BB\Upsilon(nS)}$ as

$$\frac{g_{BB\Upsilon(nS)}}{M_B} = \frac{g_{BB^*\Upsilon(nS)}}{\sqrt{M_B M_{B^*}}} = -\frac{g_{B^*B^*\Upsilon(nS)}}{M_{B^*}}\,. \tag{6.16}$$

All the above arguments are valid in the heavy quark mass limit. We neglect $1/m_Q$

corrections assuming that the mass of the bottom quark is sufficiently heavy. The next higher order is determined by the ratio $\Lambda_{QCD}/m_b = \mathcal{O}(0.1)$ and the expected corrections should be at the level of approximately 10 %.

In terms of the effective Lagrangians, we derive explicitly the transition amplitudes for $Z_b^{(\prime)} \to \Upsilon(nS) + \pi^+$ as follows:

$$
\begin{aligned}
i\mathcal{M}^{(B)}_{BB^*} = \quad & (i)^3 \int \frac{d^4q}{(2\pi)^4} [i g_{ZBB^*} M_Z \epsilon_Z \cdot \epsilon_1][g_{BB\Upsilon(nS)} (\epsilon_\Upsilon \cdot (2q-p))][g_{BB^*\pi}(\epsilon_1 \cdot k)] \\
\times \quad & \frac{1}{(q)^2 - m_B^2} \frac{1}{(P-q)^2 - m_{B^*}^2} \frac{1}{(q-p)^2 - m_B^2} \mathcal{F}(\vec{q}^{\,2}, \vec{k}^{\,2}) \,, \qquad (6.17) \\
i\mathcal{M}^{(B^*)}_{BB^*} = \quad & (i)^3 \int \frac{d^4q}{(2\pi)^4} [i g_{ZBB^*} M_Z \epsilon_Z \cdot \epsilon_1][g_{BB^*\Upsilon(nS)} i\epsilon_{\alpha\beta\gamma\delta} v^\alpha \epsilon_\Upsilon^\beta \epsilon_2^\gamma (2q-p)^\delta] \\
\times \quad & [i\epsilon_{abcd} g_{B^*B^*\pi} M_{B^*} v^a \epsilon_2^b k^c \epsilon_1^d] \\
\times \quad & \frac{1}{(q)^2 - m_B^2} \frac{1}{(P-q)^2 - m_{B^*}^2} \frac{1}{(q-p)^2 - m_{B^*}^2} \mathcal{F}(\vec{q}^{\,2}, \vec{k}^{\,2}) \,, \qquad (6.18) \\
i\mathcal{M}^{(B^*)}_{B^*B} = \quad & (i)^3 \int \frac{d^4q}{(2\pi)^4} [i g_{ZBB^*} M_Z \epsilon_Z \cdot \epsilon_1][g_{BB^*\pi}(\epsilon_2 \cdot k)] \\
\times \quad & \left[g_{B^*B^*\Upsilon(nS)} \left\{ (\epsilon_\Upsilon \cdot \epsilon_2)(\epsilon_1 \cdot (2q-p)) + (\epsilon_\Upsilon \cdot \epsilon_1)(\epsilon_2 \cdot (2q-p)) - (\epsilon_1 \cdot \epsilon_2)(\epsilon_\Upsilon \cdot (2q-p)) \right\} \right] \\
\times \quad & \frac{1}{(q)^2 - m_{B^*}^2} \frac{1}{(P-q)^2 - m_B^2} \frac{1}{(q-p)^2 - m_{B^*}^2} \mathcal{F}(\vec{q}^{\,2}, \vec{k}^{\,2}) \,, \qquad (6.19)
\end{aligned}
$$

$$
\begin{aligned}
i\mathcal{M}^{(B)}_{B^*B^*} = \quad & (i)^3 \int \frac{d^4q}{(2\pi)^4} [i g_{Z'B^*B^*} \epsilon_{\mu\nu\alpha\beta} P^\mu \epsilon_z^\nu \epsilon_1^\alpha \epsilon_2^\beta] \\
\times \quad & [i g_{B^*B^*\Upsilon(nS)} \epsilon_{\delta\tau\theta\phi} v^\delta \epsilon_\Upsilon^\tau \epsilon_1^\theta (2q-p)^\phi][g_{BB^*\pi}(\epsilon_2 \cdot k)] \\
\times \quad & \frac{1}{(q)^2 - m_{B^*}^2} \frac{1}{(P-q)^2 - m_{B^*}^2} \frac{1}{(q-p)^2 - m_B^2} \mathcal{F}(\vec{q}^{\,2}, \vec{k}^{\,2}) \,, \qquad (6.20) \\
i\mathcal{M}^{(B^*)}_{B^*B^*} = \quad & (i)^3 \int \frac{d^4q}{(2\pi)^4} [i g_{Z'B^*B^*} \epsilon_{\mu\nu\alpha\beta} P^\mu \epsilon_z^\nu \epsilon_1^\alpha \epsilon_2^\beta][i g_{B^*B^*\pi} \epsilon_{0\tau\theta\phi} M_{B^*} \epsilon_3^\tau k^\theta \epsilon_2] \\
\times \quad & \left[g_{B^*B^*\Upsilon(nS)} \left\{ (\epsilon_\Upsilon \cdot \epsilon_1)(\epsilon_3 \cdot (2q-p)) + (\epsilon_\Upsilon \cdot \epsilon_3)(\epsilon_1 \cdot (2q-p)) - (\epsilon_1 \cdot \epsilon_3)(\epsilon_\Upsilon \cdot (2q-p)) \right\} \right] \\
\times \quad & \frac{1}{(q)^2 - m_{B^*}^2} \frac{1}{(P-q)^2 - m_{B^*}^2} \frac{1}{(q-p)^2 - m_{B^*}^2} \mathcal{F}(\vec{q}^{\,2}, \vec{k}^{\,2}) \,, \qquad (6.21)
\end{aligned}
$$

where P (p, k) is the momentum of $Z_b^{(\prime)}$ ($\Upsilon(nS)$, π meson), and q is the momentum in the loop integrals. We use the polarization vectors ϵ_Z and ϵ_Υ for $Z_b^{(\prime)}$ and Υ as well as $\epsilon_{1,2,3}$ for the propagating B^* and $\bar{B}^*$ mesons in the loops. To calculate the square of the absolute value of the transition amplitudes, we use the approximation for the polarization vector of the B^* meson as $\epsilon^0_{B^*} \simeq 0$ and use the sum over the polarizations λ as $\sum_\lambda \epsilon^\mu_{B^*} \epsilon^\nu_{B^*} = \delta^{\mu\nu}$ ($\mu, \nu = 1, 2, 3$) and 0 for other μ and ν, because the absolute value

of three-momentum $\vec{q}$ is assumed to be much smaller than the mass of $B^{(*)}$ meson in heavy quark limit [123].

In the above loop calculations, in order to reflect the finite range of the interaction, we use the form factor $\mathcal{F}(\vec{q}^{\,2}, \vec{k}^{\,2})$ as follows,

$$\mathcal{F}(\vec{q}^{\,2}, \vec{k}^{\,2}) = \frac{\Lambda_Z^2}{\vec{q}^{\,2} + \Lambda_Z^2} \frac{\Lambda^2}{\vec{k}^{\,2} + \Lambda^2} \frac{\Lambda^2}{\vec{k}^{\,2} + \Lambda^2} \,. \tag{6.22}$$

The introduction of the form factor is important. At the initial vertex of $Z_b B\bar{B}^*(B^*\bar{B})$, the amplitude is expressed by the Fourier transform of the bound state amplitude which is dictated by the interaction range. In the other vertices, the amplitudes are expressed as Fourier transforms of the wave function for the internal structure of B and $\bar{B}^*$ mesons at the momentum carried by the outgoing Υ and π. In both cases, the Fourier components are functions of the relevant momentum, and are suppressed for higher momentum. The form factor of Eq. (6.22) takes into account those effects.

6.3 Numerical method

To calculate the decay widths with given amplitudes, we need to introduce some numerical methods. Here, we demonstrate the two methods: standard numerical formula picking up the residues of the poles and the formula of Passarino-Veltman integrals.

6.3.1 Numerical formula picking up poles

The outline of this numerical procedure is as follows: we integrate the amplitudes with q^0 analytically and pick up poles in the propagators. Since the masses of $Z_b^{(\prime)}$ are located above the $B\bar{B}^*$ (or $B^*\bar{B}$) and $B^*\bar{B}^*$ thresholds, respectively, the integrals have singular points. To treat them properly, we divide the integrals into real and imaginary parts by using the principle value of the integral. In the end, it becomes possible to integrate with three-momentum $\vec{q}$ numerically. Here, we discuss this procedure in detail. To begin with, let us consider a simple example, a one-loop integral with three propagators as

$$J \equiv \int \frac{d^4q}{(2\pi)^4} \frac{1}{q^2 - m_1^2 + i\epsilon} \frac{1}{(q - P + k)^2 - m_2^2 + i\epsilon} \frac{1}{(P - q)^2 - m_3^2 + i\epsilon} \tag{6.23}$$

where we neglect the coupling constants and the components of the numerator on the propagators and note that Total four momentum is $P = (\sqrt{s}, \mathbf{0})$ in the center of mass frame and $\boldsymbol{P} = \boldsymbol{q} + \boldsymbol{k}$ to conserve the momentum. On-shell energies of the internal $B^{(*)}$ mesons are difined as $E_i(\boldsymbol{q}) = \sqrt{M_i + \boldsymbol{q}^2}$. The pion energies are $E_\pi(\boldsymbol{k}) = \sqrt{m_\pi^2 + \boldsymbol{k}^2}$. The poles locate at

$$Z_1^{\mp} = \pm E_1(\boldsymbol{q}) \mp i\epsilon, \quad Z_2^{\mp} = \sqrt{s} - E_\pi(\boldsymbol{k}) \pm E_2(\boldsymbol{q}+\boldsymbol{k}) \mp i\epsilon, \quad Z_3^{\mp} = \sqrt{s} \pm E_3(\boldsymbol{q}) \mp i\epsilon \tag{6.24}$$

Closing the integration contour downward, we pick up the residues of poles in the lower half-plane: Z_1^-, Z_2^- and Z_3^-. After this procedure, J is obtained as

$$\begin{aligned} J &= \frac{2\pi i}{2\pi}\int \frac{d^3q}{(2\pi)^3}\left\{\frac{1}{2E_1(\boldsymbol{q})}\frac{1}{(E_1(\boldsymbol{q})-\sqrt{s}+k_0)^2-(E_2(\boldsymbol{q}+\boldsymbol{k}))^2}\frac{1}{(E_1(\boldsymbol{q})-\sqrt{s})^2-(E_3(\boldsymbol{q}))^2}\right. \\ &+\frac{1}{(\sqrt{s}-k_0+E_2(\boldsymbol{q}+\boldsymbol{k}))^2-(E_1(\boldsymbol{q}))^2}\frac{1}{2E_2(\boldsymbol{q}+\boldsymbol{k})}\frac{1}{(-k_0+E_2(\boldsymbol{q}+\boldsymbol{k}))^2-(E_3(\boldsymbol{q}))^2} \\ &\left.+\frac{1}{(\sqrt{s}+E_3(\boldsymbol{q}))^2-(E_1(\boldsymbol{q}))^2}\frac{1}{(k_0+E_3(\boldsymbol{q}))^2-(E_2(\boldsymbol{q}+\boldsymbol{k}))^2}\frac{1}{2E_2(\boldsymbol{q})}\right\}, \end{aligned} \tag{6.25}$$

where $J \equiv J(\sqrt{s}, \boldsymbol{q}, \boldsymbol{k}, m_1, m_2, m_3)$ For the sake of simplisity, we write the J as

$$J = i\int \frac{d^3q}{(2\pi)^3} J_1(\sqrt{s}, \boldsymbol{q}, \boldsymbol{k}, m_1, m_2, m_3) + J_2(\sqrt{s}, \boldsymbol{q}, \boldsymbol{k}, m_1, m_2, m_3) + J_3(\sqrt{s}, \boldsymbol{q}, \boldsymbol{k}, m_1, m_2, m_3), \tag{6.26}$$

where

$$\begin{aligned} J_1(\sqrt{s}, \boldsymbol{q}, \boldsymbol{k}, m_1, m_2, m_3) &= \frac{1}{2E_1(\boldsymbol{q})}\frac{1}{(E_1(\boldsymbol{q})-\sqrt{s}+E_\pi(\boldsymbol{k}))^2-(E_2(\boldsymbol{q}+\boldsymbol{k}))^2} \\ &\times\frac{1}{(E_1(\boldsymbol{q})-\sqrt{s})^2-(E_3(\boldsymbol{q}))^2}, \end{aligned} \tag{6.27}$$

$$\begin{aligned} J_2(\sqrt{s}, \boldsymbol{q}, \boldsymbol{k}, m_1, m_2, m_3) &= \frac{1}{(\sqrt{s}-E_\pi(\boldsymbol{k})+E_2(\boldsymbol{q}+\boldsymbol{k}))^2-(E_1(\boldsymbol{q}))^2}\frac{1}{2E_2(\boldsymbol{q}+\boldsymbol{k})} \\ &\times\frac{1}{(-E_\pi(\boldsymbol{k})+E_2(\boldsymbol{q}+\boldsymbol{k}))^2-(E_3(\boldsymbol{q}))^2}, \end{aligned} \tag{6.28}$$

$$J_3(\sqrt{s}, \boldsymbol{q}, \boldsymbol{k}, m_1, m_2, m_3) = \frac{1}{(\sqrt{s}+E_3(\boldsymbol{q}))^2-(E_1(\boldsymbol{q}))^2}\frac{1}{(E_\pi(\boldsymbol{k})+E_3(\boldsymbol{q}))^2-(E_2(\boldsymbol{q}+\boldsymbol{k}))^2}\frac{1}{2E_2(\boldsymbol{q})}. \tag{6.29}$$

It should be noted that the first term of J only has a pole on the real axis in the q^3 plane, which is given as

$$Z_{J_1}(\sqrt{s}, m_1, m_3) = \frac{\sqrt{m_1^4 - 2m_1^2 m_3^2 + m_3^4 - 2m_1^2(\sqrt{s})^2 - 2m_3^2(\sqrt{s})^2 + (\sqrt{s})^4}}{2\sqrt{s}}, \quad (6.30)$$

where Z_{J_1} is a function of $\sqrt{s}$, m_1 and m_3, and irrelevant with the m_2, which is the internal $B^{(*)}$ meson between the Υ and the pion. Because the presence of the pole Z_{J_1} is releated with the phase space of $Z_b^{(\prime)} \to B^* \bar{B}^{(*)}$ decays, the pole appears when the condition $\sqrt{s} > m_1 + m_3$. Since $Z_b^{(\prime)}$ are resonance states, the poles are on the real axis at $Z_{J_1}(M_Z, m_B, m_{B^*}) = 119$ MeV and $Z_{J_1}(M_{Z'}, m_{B^*}, m_{B^*}) = 98$ MeV, which correspond the final state momenta of the $B(B^*)$ mesons for the $Z_b^+ \to B^+\bar{B}^{*0} + B^{*+}\bar{B}^0$ and $Z_b^{\prime +} \to B^{*+}\bar{B}^{*0}$, respectively. It is useful to divide J_1 into real and imagiranly parts. Using

$$\lim_{\epsilon \to +0} \frac{1}{x - a \pm i\epsilon} = \text{P.V.}\frac{1}{x-a} \mp i\pi\delta(x-a) \quad (6.31)$$

where P.V. stands for the principle value of the integral. Then we can calculate J numerically.

6.3.2 Passarino-Veltman integral

Here, we introduce the calculation method by means of Passarino-Veltman formula. Passarino-Veltman integral formalism is a useful tool to calculate one loop Feynman integrals. Here we briefly introduce this scheme for the case of triangle diagrams and more general case is discussed in Appendix B. We can write the general one-loop tensor integral which appers in a triangle diagram as

$$C_3^{\mu_1\mu_2\mu_P} \equiv \frac{(2\pi\mu)^{4-d}}{i\pi^2} \int d^d k \frac{k^{\mu_1} k^{\mu_2} k^{\mu_P}}{D_0 D_1 D_2}, \quad (6.32)$$

where we follow for the momenta the conventions of Fig. 6.3, with

$$D_i = (k + r_i)^2 - m_i^2 + i\epsilon, \quad (6.33)$$

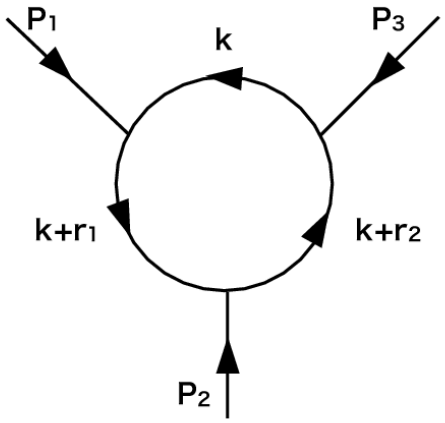

FIGURE 6.3: The diagram of general one-loop integrals with three vertices.

and the momenta r_i are related with the external momenta (all taking to be incoming) through the relations,

$$r_1 = p_1 \tag{6.34}$$

$$r_2 = p_1 + p_2 r_0 \quad = \quad p_1 + p_2 + p_3 = 0, \tag{6.35}$$

where the last one is a consequence of momentum conservation.

Here we deifine the notation for scalar integral of a triangle loop diagram as

$$C_0(r_{10}^2, r_{12}^2, r_{20}^2, m_0^2, m_1^2, m_2^2) = \frac{(2\pi\mu)^\epsilon}{i\pi^2} \int d^d k \prod_{i=0}^{2} \frac{1}{[(k+r_i)^2 - m_i^2]}, \tag{6.36}$$

where $r_{ij}^2 = (r_i - r_j)$. Since $r_0 = 0$ on our conventions, $r_{i0}^2 = r_i^2$. For simplicity, in this expressions the $i\epsilon$ part of the denominator factors are suppressed. We can also write the

general on-loop tensor integral as follows:

$$C^{\mu} \equiv \frac{(2\pi\mu)^{4-d}}{i\pi^2}\int d^d k k^{\mu}\prod_{i=0}^{2}\frac{1}{[(k+r_i)^2-m_i^2]} \tag{6.37}$$

$$C^{\mu\nu} \equiv \frac{(2\pi\mu)^{4-d}}{i\pi^2}\int d^d k k^{\mu}k^{\nu}\prod_{i=0}^{2}\frac{1}{[(k+r_i)^2-m_i^2]} \tag{6.38}$$

$$C^{\mu\nu\rho} \equiv \frac{(2\pi\mu)^{4-d}}{i\pi^2}\int d^d k k^{\mu}k^{\nu}k^{\rho}\prod_{i=0}^{2}\frac{1}{[(k+r_i)^2-m_i^2]}. \tag{6.39}$$

These integrals can be decomposed in terms of reduced functions as follows:

$$C^{\mu} = r_1^{\mu}C_1 + r_2^{\mu}C_2 \tag{6.40}$$

$$C^{\mu\nu} = g^{\mu\nu}C_{00} + \sum_{i=1}^{2} r_i^{\mu}r_j^{\nu}C_{ij} \tag{6.41}$$

$$C^{\mu\nu\rho} = \sum_{i=1}^{2}(g^{\mu\nu}r_i^{\rho} + g^{\nu\rho}r_i^{\mu} + g^{\rho\mu}r_i^{\nu})C_{00i} + \sum_{i,j,k=1}^{2} r_i^{\mu}r_j^{\nu}r_k^{\rho}C_{ijk} \tag{6.42}$$

These reduced functions are easily calculated numerically in terms of Dimensional regularization scheme with Feynman paramters (see also Appendix B).

Using this scheme, we can discribe the amplitudes in a concise way:

$$i\mathcal{M}^{(B)}_{BB^*} = \frac{(i)^4}{(4\pi)^2}M_Z g_{ZBB^*}g_{BB\Upsilon_{nS}}g_{BB^*\pi}[(\boldsymbol{\epsilon}_Z\cdot\boldsymbol{k})(\epsilon^a_{\Upsilon}(2C_a + p_a C_0))] \tag{6.43}$$

$$i\mathcal{M}^{(B^*)}_{BB^*} = \frac{(i)^6}{(4\pi)^2}M_Z M_B g_{ZBB^*}g_{BB^*\Upsilon}g_{B^*B^*\pi}[(2C^a k_a + C_0 p^a k_a)(\boldsymbol{\epsilon}_Z\cdot\boldsymbol{\epsilon}_{\Upsilon} - \boldsymbol{\epsilon}_{\Upsilon}\cdot\boldsymbol{k})] \tag{6.44}$$

$$\begin{aligned} i\mathcal{M}^{(B^*)}_{B^*B} = {} & \frac{(i)^4}{(4\pi)^2}M_Z g_{ZBB^*}g_{BB^*\pi}g_{B^*B^*\Upsilon(nS)}\,[(\epsilon_{Za}(2C^a + C_0p^a))(\boldsymbol{\epsilon}_{\Upsilon}\cdot\boldsymbol{k}) \\ & + (\boldsymbol{\epsilon}_Z\cdot\boldsymbol{\epsilon}_{\Upsilon})(2C^a k_a + C_0 p^a k_a) - (\boldsymbol{\epsilon}_Z\cdot\boldsymbol{k})(\epsilon_{\Upsilon a}(2C^a + C_0p^a))] \end{aligned} \tag{6.45}$$

$$\begin{aligned} i\mathcal{M}^{(B)}_{B^*B^*} = {} & \frac{(i)^6}{(4\pi)^2}g_{Z'B^*B^*}g_{BB^*\Upsilon(nS)}g_{BB^*\pi}M_{Z'}\,[(\boldsymbol{\epsilon}_{Z'}\cdot\boldsymbol{\epsilon}_{\Upsilon})(2C^a + C_0p^a)k_a - \epsilon_{Za}(2C^a + C_0p^a)(\boldsymbol{\epsilon}_{\Upsilon}\cdot\boldsymbol{k}) \\ & + ((\boldsymbol{\epsilon}_Z\cdot\boldsymbol{\epsilon}_{\Upsilon}) - (\boldsymbol{\epsilon}_Z\cdot\boldsymbol{p})(\boldsymbol{\epsilon}_{\Upsilon}\cdot\boldsymbol{k}))\,(C_0 + \frac{2C^{\nu\to 0}}{M_{\Upsilon}})\Big], \end{aligned} \tag{6.46}$$

$$\begin{aligned} i\mathcal{M}^{(B^*)}_{B^*B^*} = {} & \frac{(i)^6}{(4\pi)^2}g_{Z'B^*B^*}g_{B^*B^*\Upsilon(nS)}g_{B^*B^*\pi}M_{Z'}m_{B^*} \\ & \times[(\boldsymbol{\epsilon}_{Z'}\cdot\boldsymbol{\epsilon}_{\Upsilon})(2C^a + C_0p^a)k_a + \epsilon_{Za}(2C^a + C_0p^a)(\boldsymbol{\epsilon}_{\Upsilon}\cdot\boldsymbol{k})] \end{aligned} \tag{6.47}$$

where $a = 1, 2, 3$ and C^a and C_0 are the notation which are used in the Passarino-Veltman integrals formalism. We calculate these amplitudes and confirm that Passalino-Veltman integral scheme is consistent with our numerical formula explained in .

6.4 Numerical results

We obtain the decay widths from the given amplitudes in Eqs. (6.3) and (6.4). Numerical procedure has beed discussed before section.

Tables 6.2 and 6.3 present the numerical results for the partial decay widths of $Z_b^{(\prime)}$. When the form factors are ignored, the decay widths are solely proportional to $|\vec{k}|^5$, namely $\Gamma(Z_b^{(\prime)} \to \Upsilon(nS)\pi^+) \propto |\vec{k}|^5$. This is much inconsistent with the experimental fact, because the loop integrals without form factors include the high-momentum contributions which are not acceptable in the low energy hadron dynamics. In contrast, given the form factor, our calculations are qualitatively consistent with the experimental results: (i) the decay to $\Upsilon(1S)\pi^+$ is strongly suppressed, (ii) the decay to $\Upsilon(2S)\pi^+$ occurs with the highest probability and (iii) the branching fraction of the decay to $\Upsilon(3S)\pi^+$ is smaller than the one of $\Upsilon(2S)\pi^+$ but is still larger than the one of $\Upsilon(1S)\pi^+$, $f(2S\pi^+) > f(3S\pi^+) \gg f(1S\pi^+)$. We determine the cutoff parameters $\Lambda_Z = 1000$ MeV and $\Lambda = 600$ MeV to reproduce the experimental values. To see the cutoff dependence, we change Λ_Z as $\Lambda_Z = 1000$, 1050, 1100 and 1150 MeV and verified that the results do not change much. The main reason for the suppression of the $\Upsilon(1S)\pi^+$ decay is in the form factor depending on the final state momentum $\vec{k}$ ($\vec{p}$). The final state momentum of $\Upsilon(1S)\pi^+$ is $\vec{k} \sim 1100$MeV, which is large compared with the one of other channels, $\vec{k} \sim 600$MeV for $\Upsilon(2S)\pi^+$ and $\vec{k} \sim 300$ MeV for $\Upsilon(3S)\pi^+$. In contrast, this effect is minor for $\Upsilon(3S)\pi^+$ decay due to the small final state momentum. The cutoff Λ_Z does not influence the relative decay ratio between the $\Upsilon(nS)\pi^+$ decays, because this factor only regularize the internal momenta q, which is irrelevant to the final state momenta.

We find that counting rule with a heavy quark mass is valid when the form factor is introduced. Recall that the loop integral $J \equiv J(\sqrt{s}, \boldsymbol{q}, \boldsymbol{k}, m_1, m_2, m_3)$ is decomposed to the three parts, J_1, J_2, J_3. Now consider the power counting scheme in the $Z_b \to \Upsilon(nS)\pi$ decays . The mass of Z_b and $M_{B^{(*)}}$ count as m_Q^2 and m_Q. Because the form factor suppress the high momentum contributions either the internal momentum $\boldsymbol{q}$ and the outgoing momentum $\boldsymbol{k}$, they can be neglected, $\boldsymbol{k}, \boldsymbol{q} \ll m_Q$. Then $E_{B^{(*)}}$ and E_π count

TABLE 6.2: $\Lambda = 600$ MeV is fixed. The left column shows the results without the form factors.

Λ_Z	-	1000	1050	1100	1150	Exp.
$\Upsilon(1S)\pi^+$	96.3	0.074	0.079	0.083	0.087	0.059 ± 0.017
$\Upsilon(2S)\pi^+$	20.0	0.47	0.50	0.52	0.55	0.81 ± 0.22
$\Upsilon(3S)\pi^+$	0.498	0.14	0.14	0.15	0.15	0.40 ± 0.10

TABLE 6.3: The partial decay widths of $Z_b(10650)^+$. $\Lambda = 600$ MeV is fixed. The unit is MeV.

Λ_Z	-	1000	1050	1100	1150	Exp.
$\Upsilon(1S)\pi^+$	71.3	0.044	0.046	0.049	0.051	0.028 ± 0.008
$\Upsilon(2S)\pi^+$	17.6	0.31	0.33	0.34	0.36	0.28 ± 0.07
$\Upsilon(3S)\pi^+$	0.858	0.18	0.19	0.20	0.21	0.19 ± 0.05

as m_Q and ~ 0. Using this rule we can count the each component as follows:

$$J_1(M_{Z^{(\prime)}}, \boldsymbol{q}, \boldsymbol{k}, m_{B^{(*)}}, m_{B^{(*)}}, m_{B^{(*)}}) \sim \frac{1}{m_Q} \tag{6.48}$$

$$J_2(M_{Z^{(\prime)}}, \boldsymbol{q}, \boldsymbol{k}, m_{B^{(*)}}, m_{B^{(*)}}, m_{B^{(*)}}) \sim \frac{1}{m_Q^9} \tag{6.49}$$

$$J_3(M_{Z^{(\prime)}}, \boldsymbol{q}, \boldsymbol{k}, m_{B^{(*)}}, m_{B^{(*)}}, m_{B^{(*)}}) \sim \frac{1}{m_Q^9} \tag{6.50}$$

Thus, J_2 and J_3 are strongly suppressed, whereas J_1 is dominant in the loop integral J. This counting rule holds as far as $k, q \ll m_Q$.

6.5 Decays of $Z_c(3900)$

Finally, we briefly discuss the decays of $Z_c(3900)$ in the similar formalism, which has been recently observed in the $J/\psi\pi^+$ invariant mass spectrum of $Y(4260) \to J/\psi\pi^+\pi^-$ decay by the BESIII Collaboration [19]. The reported mass and decay width are $M(Z_c) = 3899.0 \pm 3.6 \pm 4.9$ MeV and $\Gamma(Z_c) = 46 \pm 10 \pm 20$ MeV. Belle collaboration also has reported $Z_c(3900)$ with mass $M(Z_c) = 3894.5 \pm 6.6 \pm 4.5$ MeV and decay width $\Gamma(Z_c) = 63 \pm 24 \pm 26$ MeV [20]. Since Z_c has the decay properties and the mass spectrum both of which are similar to the Z_b case, it is expected that Z_c would be the heavy-flavor partner of Z_b. Thus, our model can apply to the analysis of the decays $Z_c \to J/\psi\pi^+$ and

TABLE 6.4: The partial decay widths of Z_c^+. $\Lambda = 600$ MeV is fixed. The unit is MeV.

Λ_Z	-	1000	1050	1100	1150	Exp.
$J/\psi\pi^+$	39.0	0.66	0.69	0.71	0.73	-
$\psi(2S)\pi^+$	0.305	0.18	0.17	0.17	0.18	-

$\psi(2S)\pi^+$. In the present situation in experiments, branching fractions of Z_c have not still been observed. Besides, the decay $Z_c \to \psi(2S)$, which is allowed kinematically, is unconfirmed. For these reasons, the numerical predictions are of benefit to the future experiments.

We apply the triangle diagram to the decays of $Z_c(3900)$. We assume that Z_c is a superposition state of $D\bar{D}^*$ and $D^*\bar{D}$, namely

$$|Z_c\rangle = \frac{1}{\sqrt{2}}|D\bar{D}^* - D^*\bar{D}\rangle \ . \tag{6.51}$$

The main difference between $Z_c^+ \to \psi(nS)\pi^+$ and $Z_b^+ \to \Upsilon(nS)\pi^+$ is the coupling constants for each vertex and masses of the hadrons. As numerical inputs for Z_c, we use the averaged masses and decay widths reported by BESIII and Belle. Considering that the branching fraction of $Z_b^+ \to B^+\bar{B}^{*0} + B^{*+}\bar{B}^0$ is known to be 86.0 %, we assume the one of $Z_c^+ \to D^+\bar{D}^{*0} + D^{*+}\bar{D}^0$ is also approximately 86 % from the view of the heavy-flavor symmetry. Then, we have the coupling $g_{Z_cDD^*} = 2.23$ for Z_cDD^* vertex. The couplings $g_{DDJ/\psi} = 7.43$ and $g_{DD\psi(2S)} = 12.4$ are employed with VMD. Table 6.4 shows the numerical results for the partial decay widths of Z_c. The width of $Z_c^+ \to \psi(2S)\pi^+$ is narrower than the one of $Z_c^+ \to J/\psi\pi^+$, owing to the small final state momentum. The predicted branching fractions are $f(Z_c^+ \to J/\psi\pi^+) = 1.2 - 1.3$ % and $f(Z_c^+ \to \psi(2S)\pi^+) = 0.31 - 0.33$ %, which will be testable for future experiments. Although $f(Z_c^+ \to \psi(2S)\pi^+)$ and $f(Z_b^+ \to \Upsilon(1S))\pi^+$ are almost same probabilities in our calculations, the main factors are different: the former is the narrow final phase space, the latter is the suppression due to the form factor.

6.6 Summary

In summary, we have studied the $Z_b^{(\prime)+} \to \Upsilon(nS)\pi^+$ decays in a picture of the heavy meson molecule. Assuming that $Z_b^{(\prime)}$ is the $B^*\bar{B}^{(*)}$ molecular state, we have considered the transition amplitudes given by the triangle diagrams with $B^{(*)}$ and $\bar{B}^{(*)}$ meson loops at lowest order based on the heavy meson effective theory. The couplings of g_{ZBB^*} and

$g_{Z'B^*B^*}$ are fixed to reproduce correctly the observed decay widths from $Z_b^{(\prime)}$ to the open flavor channels. To treat the effect of the finite range of the hadron interactions and regularize the loop integrals in the transition amplitudes suitably, we introduce the phenomenological form factors with the cutoff parameters Λ_Z and Λ. The numerical result with $\Lambda_z = 1000$ MeV and $\Lambda = 600$ MeV is qualitatively consistent with the experimental data. Our results suggest that, if $Z_b^{(\prime)}$ have molecular type structures, the form factor should play a crucial role in the transition amplitudes. Our model also applies the decays, $Z_c^+ \to J/\psi\pi^+, \psi(2S)\pi^+$. We roughly estimate the branching fractions as $f(Z_c^+ \to J/\psi\pi^+) \sim 1.3$ % and $f(Z_c^+ \to \psi(2S)\pi^+) \sim 0.32$ %, which is testable for the future experiments in high energy accelerator facilities, such as KEK-Belle, BES and so on. In the foreseeable future, our formulation will apply to the other exotic decays, such as $Z_b^{(\prime)+} \to \eta_b\rho^+$, $Z_b^{(\prime)0} \to \eta_b\gamma$ and so on, which can be also studied in future experiments.

Chapter 7

Spin degeneracy of the heavy meson molecules

We study the properties of heavy meson molecules, which contain two heavy quarks, in exact heavy quark mass limit. Spin multiplet structure of them are elucidated in terms of heavy quark symmetry. Using potential model, we analyze the spectrum and decay properties of them. The properties of some exotic hadrons are also discussed in the point of view of heavy quark spin symmetry.

7.1 Introduction

The heavy quark spin symmetry is the one of the important aspects of heavy quark symmetry. This is the fundamental property of the heavy hadrons, which plays a crucial role to understand the mass spectrum of the heavy hadrons.

As we have already discussed in Chapter 5, the heavy quark spin symmetry cause the mass degeneracy of heavy hadrons. As an example, B and B^* mesons degenerate in heavy quark limit due to the suppression of the spin-spin interactions between heavy and light quarks. As an another important aspect in heavy hadrons, there are spin selection rules. This rule, which is a result of heavy quark symmetry, provides the information of the decay and production properties of heavy hadrons as discussed in Chapter 5.

In principle, it is expected that the heavy quark spin symmetry also cause the mass degeneracy in any multi-hadron systems with heavy quarks, because this symmetry also holds in multi hadron systems [124]. However, the properties of heavy meson molecules in heavy quark limit are not still elucidated and spin partners of them are not understood. This chapter focuses on heavy meson molecules containing two heavy quarks in heavy quark limit in terms of heavy quark spin symmetry and discuss their various properties.

To begin with, we reconsider the heavy quarkonia $Q\bar{Q}$ in heavy quark limit. The wave-functions of heavy hadrons are expressed with conserved quantities, the heavy quark spin S_Q and the light spin S_l, as $|S_H \otimes S_l\rangle$, which we call "HQS basis" expressions. The lowest states of heavy quarkonia are $Q\bar{Q}(^1S_0)$ and $Q\bar{Q}(^3S_1)$ in the particle basis. They degenerate in heavy quark limit and their wave functions are given with HQS basis as follows:

$$\begin{cases} |Q\bar{Q}(^1S_0)\rangle = |(0_H^{--} \otimes 0_l^{++})_0\rangle \\ |Q\bar{Q}(^3S_1)\rangle = |(1_H^{--} \otimes 0_l^{++})_1\rangle \end{cases} . \tag{7.1}$$

They are doublet and correspond η-J/Ψ for $Q = c$ and η_b-Υ for $Q = b$. It should be noted that their decay and production properties are opposite although their masses are same. Because the heavy quark spin must be conserved in the strong decays, $|(0_H^{--} \otimes 0_l^{++})_0\rangle$ state decays only to heavy quark singlet states and $|(1_H^{--} \otimes 0_l^{++})_1\rangle$ state can decay to heavy quark triplet states. We call such degenerate states the spin doublet of "type α".

$S_l = 0$ is a special case and now we consider the the heavy hadrons, whose light spin is taken as the arbitrary natural number $S_l = j(j \neq 0)$. The $(1_H \otimes j_l)_{\mathbf{J}}$ state, where $\mathbf{J} = j-1, j, j+1$, degenerate in the heavy quark mass limit, because spin dependent interaction between the heavy quark spins and light-spin are suppressed. The important thing is that the differences of their decay properties are mostly depend on their kinematics and total angular momenta, because these three states can equally decay into heavy quark triplet states. We call such degenerate states the spin triplet of "type β". In the $Q\bar{Q}$ case, the $(1_H \otimes j_l)_{\mathbf{J}}$ state also degenerates with the $(0_H \otimes j_l)_j$ state, which is classified as type α.

This classification will be also valid in heavy meson molecules containing two heavy quarks, however the degeneracy of them are more complicated problems. The wave functions of them can be mixture state of heavy quark singlet and triplet states as seen in the spin structure of Z_b in Section 5. Thus the spin structure of the bound states

depend on dynamics. To consider the spectrum of heavy meson molecules, we need some model to describe the dynamics. Here, we employ the OPEP model and discuss the mass spectra of the heavy meson molecules.

This chapter is organized as follows. First we show the expressions of the wave function of the heavy meson molecules in HQS basis in Section 7.2. The spin multiplets of heavy meson molecules are shown in Chapter 7.3. We consider the specific candidates of heavy meson molecules in terms of heavy quark spin symmetry and also discuss the effects of this symmetry breaking in Section 7.4.

7.2 The expressions in HQS basis

We discuss the spin structures of heavy meson molecules, $QQ\bar{q}\bar{q}$ and $Q\bar{Q}q\bar{q}$. We assume that the heavy meson molecules are composed by two heavy mesons $P \sim (Q\bar{q})_{S=0}(\bar{P} \sim (\bar{Q}q)_{S=0})$ and $P^* \sim (Q\bar{q})_{S=1}(\bar{P}^* \sim (\bar{Q})q)_{S=1}$. The heavy meson molecules, $P^{(*)}\bar{P}^{(*)}$ and $P^{(*)}P^{(*)}$, are classified with the quantum numbers: total angular momentum J, parity P, (charge parity C) and isospin $I = 0, 1$. The relevant corresponding channels for $P\bar{P}$ states given quantum numbers J^{PC} up to $J = 2$ are summarized in Table 7.1, where charge parity C is defined for $I_Z = 0$ components for $I = 0$. In the same way, we summarize the channels for PP states given quantum numbers $I(J^P)$ up to $J = 2$ in Table 7.2. The wave functions of the heavy meson molecules can be decomposed to the heavy quark spin and light degrees of freedom (light spin in short) as already discussed in Chapter 5. In this section, we show the transformation of the particle basis to HQS basis in the case of the heavy meson molecule.

7.2.1 $P\bar{P}$ states

Here, we discuss the spin structure of $P\bar{P}$ states. As an example, let us consider the transformation to HQS basis for $P^{(*)}\bar{P}^{(*)}$ states with $J^{PC} = 1^{+-}$ and $I = 0$. From Table 7.1, there are four channels in this states as follows:

$$\frac{1}{\sqrt{2}}(P\bar{P}^* - P^*\bar{P})({}^3S_1), \frac{1}{\sqrt{2}}(P\bar{P}^* - P^*\bar{P})({}^3D_1), P^*\bar{P}^*({}^3S_1), P^*\bar{P}({}^3D_1). \tag{7.2}$$

In general, heavy quark spin symmetry guarantee that the wave functions with particle basis are decoupled to the heavy quark spin and the light spin. Then the wave functions

TABLE 7.1: Relevant coupled channels for $P^{(*)}\bar{P}^{(*)}$ states for given quantum numbers J^{PC}.

J^{PC}	components
0^{+-}	——
0^{++}	$\mathrm{P}\bar{\mathrm{P}}(^1S_0)$, $\mathrm{P}^*\bar{\mathrm{P}}^*(^1S_0)$, $\mathrm{P}^*\bar{\mathrm{P}}^*(^5D_0)$
0^{--}	$\frac{1}{\sqrt{2}}\left(\mathrm{P}\bar{\mathrm{P}}^* + \mathrm{P}^*\bar{\mathrm{P}}\right)(^3P_0)$
0^{-+}	$\frac{1}{\sqrt{2}}\left(\mathrm{P}\bar{\mathrm{P}}^* - \mathrm{P}^*\bar{\mathrm{P}}\right)(^3P_0)$, $\mathrm{P}^*\bar{\mathrm{P}}^*(^3P_0)$
1^{+-}	$\frac{1}{\sqrt{2}}\left(\mathrm{P}\bar{\mathrm{P}}^* - \mathrm{P}^*\bar{\mathrm{P}}\right)(^3S_1)$, $\frac{1}{\sqrt{2}}\left(\mathrm{P}\bar{\mathrm{P}}^* - \mathrm{P}^*\bar{\mathrm{P}}\right)(^3D_1)$, $\mathrm{P}^*\bar{\mathrm{P}}^*(^3S_1)$, $\mathrm{P}^*\bar{\mathrm{P}}^*(^3D_1)$
1^{++}	$\frac{1}{\sqrt{2}}\left(\mathrm{P}\bar{\mathrm{P}}^* + \mathrm{P}^*\bar{\mathrm{P}}\right)(^3S_1)$, $\frac{1}{\sqrt{2}}\left(\mathrm{P}\bar{\mathrm{P}}^* + \mathrm{P}^*\bar{\mathrm{P}}\right)(^3D_1)$, $\mathrm{P}^*\bar{\mathrm{P}}^*(^5D_1)$
1^{--}	$\mathrm{P}\bar{\mathrm{P}}(^1P_1)$, $\frac{1}{\sqrt{2}}\left(\mathrm{P}\bar{\mathrm{P}}^* + \mathrm{P}^*\bar{\mathrm{P}}\right)(^3P_1)$, $\mathrm{P}^*\bar{\mathrm{P}}^*(^1P_1)$, $\mathrm{P}^*\bar{\mathrm{P}}^*(^5P_1)$, $\mathrm{P}^*\bar{\mathrm{P}}^*(^5F_1)$
1^{-+}	$\frac{1}{\sqrt{2}}\left(\mathrm{P}\bar{\mathrm{P}}^* - \mathrm{P}^*\bar{\mathrm{P}}\right)(^3P_1)$, $\mathrm{P}^*\bar{\mathrm{P}}^*(^3P_1)$
2^{+-}	$\frac{1}{\sqrt{2}}\left(\mathrm{P}\bar{\mathrm{P}}^* - \mathrm{P}^*\bar{\mathrm{P}}\right)(^3D_2)$, $\mathrm{P}^*\bar{\mathrm{P}}^*(^3D_2)$
2^{++}	$\mathrm{P}\bar{\mathrm{P}}(^1D_2)$, $\frac{1}{\sqrt{2}}\left(\mathrm{P}\bar{\mathrm{P}}^* + \mathrm{P}^*\bar{\mathrm{P}}\right)(^3D_2)$, $\mathrm{P}^*\bar{\mathrm{P}}^*(^1D_2)$, $\mathrm{P}^*\bar{\mathrm{P}}^*(^5S_2)$, $\mathrm{P}^*\bar{\mathrm{P}}^*(^5D_2)$, $\mathrm{P}^*\bar{\mathrm{P}}^*(^5G_2)$
2^{-+}	$\frac{1}{\sqrt{2}}\left(\mathrm{P}\bar{\mathrm{P}}^* - \mathrm{P}^*\bar{\mathrm{P}}\right)(^3P_2)$, $\frac{1}{\sqrt{2}}\left(\mathrm{P}\bar{\mathrm{P}}^* - \mathrm{P}^*\bar{\mathrm{P}}\right)(^3F_2)$, $\mathrm{P}^*\bar{\mathrm{P}}^*(^3P_2)$, $\mathrm{P}^*\bar{\mathrm{P}}^*(^3F_2)$
2^{--}	$\frac{1}{\sqrt{2}}\left(\mathrm{P}\bar{\mathrm{P}}^* + \mathrm{P}^*\bar{\mathrm{P}}\right)(^3P_2)$, $\frac{1}{\sqrt{2}}\left(\mathrm{P}\bar{\mathrm{P}}^* + \mathrm{P}^*\bar{\mathrm{P}}\right)(^3F_2)$, $\mathrm{P}^*\bar{\mathrm{P}}^*(^5P_2)$, $\mathrm{P}^*\bar{\mathrm{P}}^*(^5F_2)$

TABLE 7.2: Possible channels of $\mathrm{P}^{(*)}\mathrm{P}^{(*)}(^{2S+1}L_J)$ for a set of quantum numbers I and J^P for $J \leq 2$.

I	J^P	components
0	0^-	$\frac{1}{\sqrt{2}}(\mathrm{PP}^* + \mathrm{P}^*\mathrm{P})(^3P_0)$
	1^+	$\frac{1}{\sqrt{2}}\left(\mathrm{PP}^* - \mathrm{P}^*\mathrm{P}\right)(^3S_1)$, $\frac{1}{\sqrt{2}}\left(\mathrm{PP}^* - \mathrm{P}^*\mathrm{P}\right)(^3D_1)$, $\mathrm{P}^*\mathrm{P}^*(^3S_1)$, $\mathrm{P}^*\mathrm{P}^*(^3D_1)$
	1^-	$\mathrm{PP}(^1P_1)$, $\frac{1}{\sqrt{2}}\left(\mathrm{PP}^* + \mathrm{P}^*\mathrm{P}\right)(^3P_1)$, $\mathrm{P}^*\mathrm{P}^*(^1P_1)$, $\mathrm{P}^*\mathrm{P}^*(^5P_1)$, $\mathrm{P}^*\mathrm{P}^*(^5F_1)$
	2^+	$\frac{1}{\sqrt{2}}\left(\mathrm{PP}^* - \mathrm{P}^*\mathrm{P}\right)(^3D_2)$, $\mathrm{P}^*\mathrm{P}^*(^3D_2)$
	2^-	$\frac{1}{\sqrt{2}}\left(\mathrm{PP}^* + \mathrm{P}^*\mathrm{P}\right)(^3P_2)$, $\frac{1}{\sqrt{2}}\left(\mathrm{PP}^* + \mathrm{P}^*\mathrm{P}\right)(^3F_2)$, $\mathrm{P}^*\mathrm{P}^*(^5P_2)$, $\mathrm{P}^*\mathrm{P}^*(^5F_2)$
1	0^+	$\mathrm{PP}(^1S_0)$, $\mathrm{P}^*\mathrm{P}^*(^1S_0)$, $\mathrm{P}^*\mathrm{P}^*(^5D_0)$
	0^-	$\frac{1}{\sqrt{2}}\left(\mathrm{PP}^* - \mathrm{P}^*\mathrm{P}\right)(^3P_0)$, $\mathrm{P}^*\mathrm{P}^*(^3P_0)$
	1^+	$\frac{1}{\sqrt{2}}\left(\mathrm{PP}^* + \mathrm{P}^*\mathrm{P}\right)(^3S_1)$, $\frac{1}{\sqrt{2}}\left(\mathrm{PP}^* + \mathrm{P}^*\mathrm{P}\right)(^3D_1)$, $\mathrm{P}^*\mathrm{P}^*(^5D_1)$
	1^-	$\frac{1}{\sqrt{2}}\left(\mathrm{PP}^* - \mathrm{P}^*\mathrm{P}\right)(^3P_1)$, $\mathrm{P}^*\mathrm{P}^*(^3P_1)$
	2^+	$\mathrm{PP}(^1D_2)$, $\frac{1}{\sqrt{2}}\left(\mathrm{PP}^* + \mathrm{P}^*\mathrm{P}\right)(^3D_2)$, $\mathrm{P}^*\mathrm{P}^*(^1D_2)$, $\mathrm{P}^*\mathrm{P}^*(^5S_2)$, $\mathrm{P}^*\mathrm{P}^*(^5D_2)$, $\mathrm{P}^*\mathrm{P}^*(^5G_2)$
	2^-	$\frac{1}{\sqrt{2}}\left(\mathrm{PP}^* - \mathrm{P}^*\mathrm{P}\right)(^3P_2)$, $\frac{1}{\sqrt{2}}\left(\mathrm{PP}^* - \mathrm{P}^*\mathrm{P}\right)(^3F_2)$, $\mathrm{P}^*\mathrm{P}^*(^3P_2)$, $\mathrm{P}^*\mathrm{P}^*(^3F_2)$

for HQS basis are described with the product of heavy quark spin and light spin, $(S_Q \otimes S_l)_J$, where J is total angular momentum. In the heavy meson molecule case, the light spin is given as $S_l = S_q + L$, where S_q is total spin of light quarks and L is the orbital angular momentum. To specify the light spin structures, we use the notation $|S_Q, S_q, L, S_l; J\rangle$ for HQS basis. It should be noted that S_Q, S_l and J are conserved quantities, whereas S_q and L are not good quantum numbers. Using the notation $|S_Q, S_q, L, S_l; J\rangle$, we write the explicit wave functions for $P^{(*)}\bar{P}^{(*)}$ states with 1^{+-} and $I = 0$ as

$$|0_H, 1_q, 0_L, 1_l; 1\rangle\,, |0_H, 1_q, 2_L, 1_l; 1\rangle\,, |1_H, 0_q, 0_L, 0_l; 1\rangle\,, |1_H, 0_1, 2_L, 2_l; 1\rangle\,. \tag{7.3}$$

We find three kind of independent components in this channel. The particle basis is transformed to HQS basis with spin recoupling formula. We write the transformation with unitary matrix U_{JPC} as

$$\begin{pmatrix} |\frac{1}{\sqrt{2}}(P\bar{P}^* - P^*\bar{P})(^3S_1)\rangle \\ |\frac{1}{\sqrt{2}}(P\bar{P}^* - P^*\bar{P})(^3D_1)\rangle \\ |P^*\bar{P}^*(^3S_1)\rangle \\ |P^*\bar{P}^*(^3D_1)\rangle \end{pmatrix} = U_{1^{+-}} \begin{pmatrix} |0_H, 1_q, 0_L, 1_l; 1\rangle \\ |0_H, 1_q, 2_L, 1_l; 1\rangle \\ |1_H, 0_q, 0_L, 0_l; 1\rangle \\ |1_H, 0_1, 2_L, 2_l; 1\rangle \end{pmatrix}, \tag{7.4}$$

where the explicit form is given by

$$U_{1^{+-}} = \begin{pmatrix} \frac{1}{\sqrt{2}} & 0 & -\frac{1}{\sqrt{2}} & 0 \\ 0 & \frac{1}{\sqrt{2}} & 0 & -\frac{1}{\sqrt{2}} \\ \frac{1}{\sqrt{2}} & 0 & \frac{1}{\sqrt{2}} & 0 \\ 0 & \frac{1}{\sqrt{2}} & 0 & \frac{1}{\sqrt{2}} \end{pmatrix}. \tag{7.5}$$

In the same way, we show the transformation from particle basis to HQS basis for other states as follows:

$$\begin{pmatrix} |P\bar{P}(^1S_0)\rangle \\ |P^*\bar{P}^*(^1S_0)\rangle \\ |P^*\bar{P}^*(^5D_0)\rangle \end{pmatrix} = U_{0^{++}} \begin{pmatrix} |0_H, 0_q, 0_L, 0_l; 0\rangle \\ |1_H, 1_q, 0_L, 1_l; 0\rangle \\ |1_H, 1_q, 2_L, 1_l; 0\rangle \end{pmatrix}, \tag{7.6}$$

$$U_{0^{++}} = \begin{pmatrix} \frac{1}{2} & \frac{\sqrt{3}}{2} & 0 \\ \frac{\sqrt{3}}{2} & -\frac{1}{2} & 0 \\ 0 & 0 & 1 \end{pmatrix}, \tag{7.7}$$

for $J^{PC} = 0^{++}$.

$$\begin{pmatrix} |\frac{1}{\sqrt{2}}(P\bar{P}^* - P^*\bar{P})(^3P_0)\rangle \\ |P^*\bar{P}^*(^3P_0)\rangle \end{pmatrix} = U_{0^{-+}} \begin{pmatrix} |0_H, 1_q, 1_L, 0_l; 0\rangle \\ |1_H, 0_q, 1_L, 1_l; 0\rangle \end{pmatrix}, \tag{7.8}$$

$$U_{0^{-+}} = \begin{pmatrix} \frac{1}{\sqrt{2}} & -\frac{1}{\sqrt{2}} \\ \frac{1}{\sqrt{2}} & \frac{1}{\sqrt{2}} \end{pmatrix}, \tag{7.9}$$

for 0^{-+},

$$|\frac{1}{\sqrt{2}}(P\bar{P}^* + P^*\bar{P})(^3P_0)\rangle = U_{0^{--}} |1_H, 1_q, 1_L, 1_l; 0\rangle, \tag{7.10}$$

$$U_{0^{--}} = 1, \tag{7.11}$$

for 0^{--},

$$\begin{pmatrix} |\frac{1}{\sqrt{2}}(P\bar{P}^* - P^*\bar{P})(^3S_1)\rangle \\ |\frac{1}{\sqrt{2}}(P\bar{P}^* - P^*\bar{P})(^3D_1)\rangle \\ |P^*\bar{P}^*(^3S_1)\rangle \\ |P^*\bar{P}^*(^3D_1)\rangle \end{pmatrix} = U_{1^{+-}} \begin{pmatrix} |0_H, 1_q, 0_L, 1_l; 1\rangle \\ |0_H, 1_q, 2_L, 1_l; 1\rangle \\ |1_H, 0_q, 0_L, 0_l; 1\rangle \\ |1_H, 0_1, 2_L, 2_l; 1\rangle \end{pmatrix} \tag{7.12}$$

$$U_{1^{+-}} = \begin{pmatrix} \frac{1}{\sqrt{2}} & 0 & -\frac{1}{\sqrt{2}} & 0 \\ 0 & \frac{1}{\sqrt{2}} & 0 & -\frac{1}{\sqrt{2}} \\ \frac{1}{\sqrt{2}} & 0 & \frac{1}{\sqrt{2}} & 0 \\ 0 & \frac{1}{\sqrt{2}} & 0 & \frac{1}{\sqrt{2}} \end{pmatrix}, \tag{7.13}$$

for 1^{+-},

$$\begin{pmatrix} |\frac{1}{\sqrt{2}}(P\bar{P}^* + P^*\bar{P})(^3S_1)\rangle \\ |\frac{1}{\sqrt{2}}(P\bar{P}^* + P^*\bar{P})(^3D_1)\rangle \\ |P^*\bar{P}^*(^5D_1)\rangle \end{pmatrix} = U_{1^{++}} \begin{pmatrix} |1_H, 1_q, 0_L, 1_l; 1\rangle \\ |1_H, 1_q, 2_L, 1_l; 1\rangle \\ |1_H, 1_q, 2_L, 2_l; 1\rangle \end{pmatrix} \tag{7.14}$$

$$U_{1^{++}} = \begin{pmatrix} 1 & 0 & 0 \\ 0 & -\frac{1}{2} & \frac{\sqrt{3}}{2} \\ 0 & \frac{\sqrt{3}}{2} & \frac{1}{2} \end{pmatrix}, \tag{7.15}$$

for 1^{++}

$$\begin{pmatrix} |\frac{1}{\sqrt{2}}(P\bar{P}^* - P^*\bar{P})(^3P_1)\rangle \\ |P^*\bar{P}^*(^3P_1)\rangle \end{pmatrix} = U_{1^{-+}} \begin{pmatrix} |0_H, 1_q, 1_L, 1_l; 1\rangle \\ |1_H, 0_q, 1_L, 1_l; 1\rangle \end{pmatrix} \tag{7.16}$$

$$U_{1^{-+}} = \begin{pmatrix} \frac{1}{\sqrt{2}} & -\frac{1}{\sqrt{2}} \\ \frac{1}{\sqrt{2}} & \frac{1}{\sqrt{2}} \end{pmatrix}, \tag{7.17}$$

for 1^{-+},

$$\begin{pmatrix} |P\bar{P}(^1P_1)\rangle \\ |\frac{1}{\sqrt{2}}(P\bar{P}^* + P^*\bar{P})(^3P_1)\rangle \\ |P^*\bar{P}^*(^1P_1)\rangle \\ |P^*\bar{P}^*(^5P_1)\rangle \\ |P^*\bar{P}^*(^5F_1)\rangle \end{pmatrix} = U_{1^{--}} \begin{pmatrix} |1_H, 1_q, 1_L, 0_l; 1\rangle \\ |0_H, 0_q, 1_L, 1_l; 1\rangle \\ |1_H, 1_q, 1_L, 1_l; 1\rangle \\ |1_H, 1_q, 1_L, 2_l; 1\rangle \\ |1_H, 1_1, 3_L, 2_l; 1\rangle \end{pmatrix} \tag{7.18}$$

$$U_{1^{--}} = \begin{pmatrix} \frac{1}{2\sqrt{3}} & \frac{1}{2} & -\frac{1}{2} & \frac{\sqrt{\frac{5}{3}}}{2} & 0 \\ -\frac{1}{\sqrt{3}} & 0 & \frac{1}{2} & \frac{\sqrt{\frac{5}{3}}}{2} & 0 \\ -\frac{1}{6} & \frac{\sqrt{3}}{2} & \frac{1}{2\sqrt{3}} & -\frac{\sqrt{5}}{6} & 0 \\ \frac{\sqrt{5}}{3} & 0 & \frac{\sqrt{\frac{5}{3}}}{2} & \frac{1}{6} & 0 \\ 0 & 0 & 0 & 0 & 1 \end{pmatrix}, \tag{7.19}$$

for 1^{--},

$$\begin{pmatrix} |\frac{1}{\sqrt{2}}(P\bar{P}^* - P^*\bar{P})(^3D_2)\rangle \\ |P^*\bar{P}^*(^3D_2)\rangle \end{pmatrix} = U_{2^{+-}} \begin{pmatrix} |0_H, 1_q, 2_L, 2_l; 2\rangle \\ |1_H, 0_q, 2_L, 2_l; 2\rangle \end{pmatrix} \tag{7.20}$$

$$U_{2^{+-}} = \begin{pmatrix} \frac{1}{\sqrt{2}} & -\frac{1}{\sqrt{2}} \\ \frac{1}{\sqrt{2}} & \frac{1}{\sqrt{2}} \end{pmatrix}, \tag{7.21}$$

for 2^{+-},

$$\begin{pmatrix} |P\bar{P}(^1D_2)\rangle \\ |\frac{1}{\sqrt{2}}(P\bar{P}^* + P^*\bar{P})(^3D_2)\rangle \\ |P^*\bar{P}^*(^1D_2)\rangle \\ |P^*\bar{P}^*(^5S_2)\rangle \\ |P^*\bar{P}^*(^5D_2)\rangle \\ |P^*\bar{P}^*(^5G_2)\rangle \end{pmatrix} = U_{2^{++}} \begin{pmatrix} |1_H, 1_q, 0_L, 1_l; 2\rangle \\ |1_H, 1_q, 2_L, 1_l; 2\rangle \\ |0_H, 0_q, 2_L, 2_l; 2\rangle \\ |1_H, 1_q, 2_L, 2_l; 2\rangle \\ |1_H, 1_q, 2_L, 3_l; 2\rangle \\ |1_H, 1_q, 4_L, 3_l; 2\rangle \end{pmatrix} \tag{7.22}$$

$$U_{2^{++}} = \begin{pmatrix} 0 & \frac{\sqrt{\frac{3}{5}}}{2} & \frac{1}{2} & -\frac{1}{2} & \frac{\sqrt{\frac{7}{5}}}{2} & 0 \\ 0 & -\frac{3}{2\sqrt{5}} & 0 & \frac{1}{2\sqrt{3}} & \sqrt{\frac{7}{15}} & 0 \\ 0 & -\frac{1}{2\sqrt{5}} & \frac{\sqrt{3}}{2} & \frac{1}{2\sqrt{3}} & -\frac{\sqrt{\frac{7}{15}}}{2} & 0 \\ 1 & 0 & 0 & 0 & 0 & 0 \\ 0 & \frac{\sqrt{\frac{7}{5}}}{2} & 0 & \frac{\sqrt{\frac{7}{3}}}{2} & \frac{1}{\sqrt{15}} & 0 \\ 0 & 0 & 0 & 0 & 0 & 1 \end{pmatrix} \tag{7.23}$$

for 2^{++},

$$\begin{pmatrix} |\frac{1}{\sqrt{2}}(P\bar{P}^* - P^*\bar{P})(^3P_2)\rangle \\ |\frac{1}{\sqrt{2}}(P\bar{P}^* - P^*\bar{P})(^3F_2)\rangle \\ |P^*\bar{P}^*(^3P_2)\rangle \\ |P^*\bar{P}^*(^3F_2)\rangle \end{pmatrix} = U_{2^{-+}} \begin{pmatrix} |1_H, 0_q, 1_L, 1_l; 2\rangle \\ |0_H, 1_q, 1_L, 2_l; 2\rangle \\ |0_H, 1_q, 3_L, 2_l; 2\rangle \\ |1_H, 0_q, 3_L, 3_l; 2\rangle \end{pmatrix}, \tag{7.24}$$

$$U_{2^{-+}} = \begin{pmatrix} -\frac{1}{\sqrt{2}} & \frac{1}{\sqrt{2}} & 0 & 0 \\ 0 & 0 & \frac{1}{\sqrt{2}} & -\frac{1}{\sqrt{2}} \\ \frac{1}{\sqrt{2}} & \frac{1}{\sqrt{2}} & 0 & 0 \\ 0 & 0 & \frac{1}{\sqrt{2}} & \frac{1}{\sqrt{2}} \end{pmatrix}, \tag{7.25}$$

for 2^{-+},

$$\begin{pmatrix} |\frac{1}{\sqrt{2}}(P\bar{P}^* + P^*\bar{P})(^3P_2)\rangle \\ |\frac{1}{\sqrt{2}}(P\bar{P}^* + P^*\bar{P})(^3F_2)\rangle \\ |P^*\bar{P}^*(^5P_2)\rangle \\ |P^*\bar{P}^*(^5F_2)\rangle \end{pmatrix} = U_{2^{--}} \begin{pmatrix} |1_H, 1_q, 1_L, 1_l; 2\rangle \\ |1_H, 1_q, 1_L, 2_l; 2\rangle \\ |1_H, 1_q, 3_L, 2_l; 2\rangle \\ |1_H, 1_q, 3_L, 3_l; 2\rangle \end{pmatrix}, \tag{7.26}$$

$$U_{2^{--}} = \begin{pmatrix} -\frac{1}{2} & \frac{\sqrt{3}}{2} & 0 & 0 \\ 0 & 0 & -\frac{1}{\sqrt{3}} & \sqrt{\frac{2}{3}} \\ \frac{\sqrt{3}}{2} & \frac{1}{2} & 0 & 0 \\ 0 & 0 & \sqrt{\frac{2}{3}} & \frac{1}{\sqrt{3}} \end{pmatrix}, \tag{7.27}$$

for 2^{--}. The decomposition for higher J states will be given similarly. This relation is independent the interaction between two heavy mesons and holds as far as we consider the heavy quark symmetry.

7.2.2 PP states

In the same way of the transformation for $P\bar{P}$ states, we can expand the wave function for PP states with HQS basis. The explicit expressions are summarized in Appendix D.

7.3 Spin multiplets of heavy meson molecules with potential model

Now we discuss the dynamics of $P\bar{P}$ states in heavy quark limit and analysis their eigen values. We consider the one pion exchange potential (OPEP) as a long range force. Because we see that pion force is dominant in the heavy meson molecules in chapter 4, this is a good approximation for a first step.

7.3.1 The properties of $P^{(*)}\bar{P}^{(*)}$ states for $J^{PC} = 1^{+-}$ in heavy quark limit

To begin with, we consider the $P^{(*)}\bar{P}^{(*)}$ with $J^{PC} = 1^{+-}$. The following argument are also valid in other molecules. The Hamiltonian for this state is given from Eqs. A.6 and

A.58 as

$$H_{1^{+-}} = \begin{pmatrix} K_0 + C & -\sqrt{2}T & -2C & -\sqrt{2}T \\ -\sqrt{2}T & K_2 + C + T & -\sqrt{2}T & -2C + T \\ -2C & -\sqrt{2}T & K_0 + C & -\sqrt{2}T \\ -\sqrt{2}T & -2C + T & -\sqrt{2}T & K_2 + C + T \end{pmatrix} \vec{\tau_1} \cdot \vec{\tau_2}, \tag{7.28}$$

where τ_1 and τ_2 are isospin of $P^{(*)}$. Then $\tau_1 \cdot \tau_2 = -3$ for $I = 0$ states and $\tau_1 \cdot \tau_2 = 1$ for $I = 1$ states. K_l is kinetic term and defined as

$$K_l = -\frac{1}{2\mu}\left(\frac{\partial^2}{\partial r^2} + \frac{2}{r}\frac{\partial}{\partial r} - \frac{l(l+1)}{r^2}\right), \tag{7.29}$$

for angular momentum l with reduced mass $\mu = m_{P^{(*)}} m_{P^{(*)}}/(m_{P^{(*)}} + m_{P^{(*)}}) \to \infty$ in the heavy quark limit. C and T are center and tensor force for OPEP, respectively. They are

$$C = (\sqrt{2}\frac{g}{f_\pi})^2 \frac{C(r)}{3}, \tag{7.30}$$

$$T = (\sqrt{2}\frac{g}{f_\pi})^2 \frac{T(r)}{3}. \tag{7.31}$$

The function $C(r)$ and $T(r)$ are

$$C(r) = \int \frac{d^3\vec{q}}{(2\pi)^3} \frac{m_\pi^2}{\vec{q}^2 + m_\pi^2} e^{i\vec{q}\cdot\vec{r}} F(\vec{q}), \tag{7.32}$$

$$S_{12}(\hat{r})T(r) = \int \frac{d^3\vec{q}}{(2\pi)^3} \frac{-\vec{q}^2}{\vec{q}^2 + m_\pi^2} S_{12}(\hat{q}) e^{i\vec{q}\cdot\vec{r}} F(\vec{q}), \tag{7.33}$$

with $\hat{q} = \vec{q}/|\vec{q}|$, where $F(\vec{q})$ is the dipole-type form factor from Eqs. (4.27) and (4.28). Recall that the mixing terms between $B\bar{B}^*$ and $B^*\bar{B}^*$ appear as a result of HQS. As a rule, tensor force is stronger than center force with typical cut-off parameter. By its very nature, the attraction force on heavy meson molecules is mainly controlled by the tensor force.

Now we rewrite the Hamiltonian $H_{1^{+-}}$ in the HQS basis with the unitary matrix $U_{1^{+-}}$ as

$$
\begin{aligned}
H^{HQ}_{1^{+-}} &= U^{-1}_{1^{+-}} H_{1^{+-}} U_{1^{+-}} \\
&= \left(\begin{array}{cc|c|c} K_0 - C & -2\sqrt{2}T & 0 & 0 \\ -2\sqrt{2}T & K_2 - C + 2T & 0 & 0 \\ \hline 0 & 0 & K_0 + 3C & 0 \\ \hline 0 & 0 & 0 & K_2 + 3C \end{array}\right) \vec{\tau_1} \cdot \vec{\tau_2} \qquad (7.34) \\
&= \left(\begin{array}{c|c|c} H^{(0,1)}_{1^{+-}} & 0 & 0 \\ \hline 0 & H^{(1,0)}_{1^{+-}} & 0 \\ \hline 0 & 0 & H^{(1,2)}_{1^{+-}} \end{array}\right) \vec{\tau_1} \cdot \vec{\tau_2}, \qquad (7.35)
\end{aligned}
$$

where $H^{HQ}_{1^{+-}}$ means the Hamiltonian described by HQS basis. We define the Hamiltonian $H^{(S_H,S_l)}_{J^{PC}}$, where S_H and S_l are heavy quark and the light spin, respectively. The Hamiltonian $H^{HQ}_{1^{+-}}$ is given as the block-diagonal forms, because the Hamiltonians $H^{(0,1)}_{1^{+-}}$, $H^{(1,0)}_{1^{+-}}$ and $H^{(1,2)}_{1^{+-}}$ cannot interact each other in the heavy quark limit.

Since the kinetic term is always repulsive and suppressed due to the infinite reduced mass, $\mu \to \infty$, whether the states are bound or not is depend on the potential. Therefore, it is useful to see the potential part of Hamiltonian. First, we consider the $I = 1$ state, which corresponds $\vec{\tau_1} \cdot \vec{\tau_2} = 1$. The potential of $H^{(1,0)}_{1^{+-}}$ and $H^{(1,2)}_{1^{+-}}$ are $3C$, which is clearly repulsive. In contrast, the diagonalized potential of $H^{(0,1)}_{1^{+-}}$ has both attractive and repulsive channels. This eigenvalues are approximately $E = K + 3C + 6T$ and $E = K + 3C - 6T$ under the condition, $K_0 \approx K_2 \approx K$, which is given by the infinite reduced mass. As a result, we can conclude that $P^{(*)}\bar{P}^{(*)}$ state in $I(J^{PC}) = 1(1^{+-})$ have only one bound state in the $H^{(0,1)}_{1^{+-}}$ channel with eigenvalue $E \sim K + 3C - 6T$. Next, consider the $I = 1$ state. In this case, the coefficient is $\vec{\tau_1} \cdot \vec{\tau_2} = -3$, which is three times larger than the case of $I = 0$. As is clear from the Hamiltonian (D.31), the potentials of $H^{(1,0)}_{1^{+-}}$ and $H^{(1,2)}_{1^{+-}}$ are attractive and the eigenvalues of them are given as $E = K_0 - 9C$ and $E = K_2 - 9C$, respectively. The eigen values of $H^{(0,1)}_{1^{+-}}$ are approximately given as $E = 3C - 12T$ and $E = 3C + 6T$. Thus the deepest bound state is in $H^{(0,1)}_{1^{+-}}$ with eigenvalue $E = 3C - 12T$.

The spin degenerate states must exist as a consequence of HQS. As an example, we consider the spin partners for $H^{(1,0)}_{1^{+-}}$. This state do not have the spin partner as a type β because of $S_H = 0^{-+}$. We can identify the spin partners as a type α by replacing

$S_H = 0^{-+}$ to 1^{--}. The spin partners should be $H^{(1,1)}_{0^{++}}, H^{(1,1)}_{1^{++}}$ and $H^{(1,1)}_{2^{++}}$. To confirm this argument, we also rewrite the Hamiltonians, $H_{0^{++}}, H_{1^{++}}$ and $H_{2^{++}}$, as follows:

$$
\begin{aligned}
H^{HQ}_{0^{++}} &= U^{-1}_{0^{++}} H_{0^{++}} U_{0^{++}} \\
&= \left(\begin{array}{c|cc} K_0+3C & 0 & 0 \\ \hline 0 & K_0-C & -2\sqrt{2}T \\ 0 & -2\sqrt{2}T & K_2-C+2T \end{array}\right) \vec{\tau_1}\cdot\vec{\tau_2} && (7.36) \\
&= \left(\begin{array}{c|c} H^{(1,0)}_{0^{++}} & 0 \\ \hline 0 & H^{(1,1)}_{0^{++}} \end{array}\right) \vec{\tau_1}\cdot\vec{\tau_2}, && (7.37) \\
H^{HQ}_{1^{++}} &= U^{-1}_{1^{++}} H_{1^{++}} U_{1^{++}} \\
&= \left(\begin{array}{cc|c} K_0-C & -2\sqrt{2}T & 0 \\ -2\sqrt{2}T & K_2-C+2T & 0 \\ \hline 0 & 0 & K_2-C-2T \end{array}\right) \vec{\tau_1}\cdot\vec{\tau_2} && (7.38) \\
&= \left(\begin{array}{c|c} H^{(1,1)}_{1^{++}} & 0 \\ \hline 0 & H^{(1,2)}_{1^{++}} \end{array}\right) \vec{\tau_1}\cdot\vec{\tau_2}, && (7.39) \\
H^{HQ}_{2^{++}} &= U^{-1}_{2^{++}} H_{2^{++}} U_{2^{++}} \\
&= \left(\begin{array}{cc|c|c|cc} K_0-C & -2\sqrt{2}T & 0 & 0 & 0 & 0 \\ -2\sqrt{2}T & K_2-C+2T & 0 & 0 & 0 & 0 \\ \hline 0 & 0 & K_2+3C & 0 & 0 & 0 \\ \hline 0 & 0 & 0 & K_2-C-2T & 0 & 0 \\ \hline 0 & 0 & 0 & 0 & K_2-C+\frac{4}{7}T & -\frac{12\sqrt{3}}{7}T \\ 0 & 0 & 0 & 0 & -\frac{12\sqrt{3}}{7}T & K_4-C+\frac{10}{7}T \end{array}\right) \\
&\quad \times \vec{\tau_1}\cdot\vec{\tau_2} && (7.40) \\
&= \left(\begin{array}{c|c|c|c} H^{(1,1)}_{2^{++}} & 0 & 0 & 0 \\ \hline 0 & H^{(0,2)}_{2^{++}} & 0 & 0 \\ \hline 0 & 0 & H^{(1,2)}_{2^{++}} & 0 \\ \hline 0 & 0 & 0 & H^{(1,3)}_{2^{++}} \end{array}\right) \vec{\tau_1}\cdot\vec{\tau_2}. && (7.41)
\end{aligned}
$$

From the above Eqs. (D.24)-(7.41), we can confirm that the Hamiltonians $H^{(1,1)}_{0^{++}}$, $H^{(1,1)}_{1^{++}}$, $H^{(1,1)}_{2^{++}}$ and $H^{(0,1)}_{1^{+-}}$ are equivalent in the heavy quark limit. Thus they degenerate to forthlets.

It is important to consider the decay properties of the $P^{(*)}\bar{P}^{(*)}$ states. $H^{(0,1)}_{1^{+-}}$ states is possible to decay into the the heavy quark singlet with a light meson such as $\epsilon_b\rho(\gamma)$ and $h_b\pi$. In contrast, $H^{(1,1)}_{0^{++}}$, $H^{(1,1)}_{1^{++}}$ and $H^{(1,1)}_{2^{++}}$, which are degenerate with $H^{(0,1)}_{1^{+-}}$ as spin

partner type α, decay into the heavy quark triplet with a light meson, such as $\Upsilon\rho$ and $\chi_{bJ}\pi$. Their decay ratios will be assigned by means of the heavy quark spin selection rule.

7.3.2 The $P^{(*)}\bar{P}^{(*)}$ states

Here, we show the complete results of the mass degeneracy of the $P^{(*)}\bar{P}^{(*)}$ states up to $J < 2$. As shown in the previous section, their spin partners are divided into two types: type α and type β. The spin partner of type α is caused from the suppression of spin-spin interaction between heavy quarks. The direct cause of the presence of type β spin partners is the suppression of the spin dependent interaction between heavy quark and light spins. As a result, the doublets appear when the $S_l = 0$ as type α, whereas the $P^{(*)}\bar{P}^{(*)}$ with $S_l \neq 0$ are forthlets states involving type α and β.

Tabs. 7.3 and 7.4 show the spin multiplets of $P^{(*)}\bar{P}^{(*)}$ molecules. The explicit Hamiltonians are summarized in Appendix D. The first left column shows the quantum numbers of $P\bar{P}$ molecules. The second column write the Hamiltonians for each states with the notation $H^{(S_H,S_l)}_{J^{PC}}$. Third column denotes the potential, but take care that the 2×2 matrix potential is diagonalized. The spin partner for each Hamiltonians are shown in the forth and fifth column from left. The rightmost column denotes that the potential of Hamiltonian is attractive or not with which check mark written in the case of the attractive channel. For example, consider the $P\bar{P}$ with $J^{PC} = 0^{++}$ for $I = 1$ states. This state has two kind of Hamiltonians, $H^{(0,0)}_{0^{++}}$ and $H^{(1,1)}_{0^{++}}$. The potential of $H^{(0,0)}_{0^{++}}$ is $3C$, thus this channel is not attractive. Since the light spin S_l of $H^{(0,0)}_{0^{++}}$ is zero, it has only spin partner type α, $H^{(1,0)}_{1^{+-}}$. The diagonalized potentials of $H^{(1,1)}_{0^{++}}$ are $-C - 2T$ and $-C + 4T$, thus it has one attractive channel, which denotes with check mark in the rightmost column. For this Hamiltonian, the spin partner type α is $H^{(0,1)}_{1^{+-}}$ and type β are $H^{(1,1)}_{1^{++}}$ and $H^{(1,1)}_{2^{++}}$.

The multiplets are classified as two classes. The doublets appear when the light spin of Hamiltonian is zero, because they do not have the partner, type β. In the case of $s_l \neq 0$, since the Hamiltonians have the spin partners as type β, they degenerate as forthlets.

For $I = 0$ states in Table 7.3, there are two kind of attractive potentials: $-9C$ and $3C - 12T$. Because the central potential is weak compared with tensor force, whether the attractive potential $-9C$ forms the bound state is sensitive problem. The potential

TABLE 7.3: Spin multiplets of $P\bar{P}$ molecules for $I = 0$ states.

J^{PC}	$H^{(S_H,S_l)}_{J^{PC}}$	Potential	Spin partner		attractive
			type α	type β	
0^{++}	$H^{(0,0)}_{0^{++}}$	$-9C$	$H^{(1,0)}_{1^{+-}}$		$\surd$
	$H^{(1,1)}_{0^{++}}$	$3C+6T, 3C-12T$	$H^{(0,1)}_{1^{+-}}$	$H^{(1,1)}_{1^{++}}$, $H^{(1,1)}_{2^{++}}$	$\surd$
0^{-+}	$H^{(0,0)}_{0^{-+}}$	$3C-12T$	$H^{(1,0)}_{1^{--}}$		$\surd$
	$H^{(1,1)}_{0^{-+}}$	$-9C$	$H^{(0,1)}_{1^{--}}$	$H^{(1,1)}_{1^{-+}}$, $H^{(1,1)}_{2^{-+}}$	$\surd$
0^{--}	$H^{(1,1)}_{0^{--}}$	$3C+12T$	$H^{(0,1)}_{1^{-+}}$	$H^{(1,1)}_{1^{--}}$, $H^{(1,1)}_{2^{--}}$	
1^{+-}	$H^{(0,1)}_{1^{+-}}$	$3C+6T$, $3C-12T$	$H^{(1,1)}_{0^{++}}$, $H^{(1,1)}_{1^{++}}$, $H^{(1,1)}_{2^{++}}$		$\surd$
	$H^{(1,0)}_{1^{+-}}$	$-9C$	$H^{(0,0)}_{0^{++}}$		$\surd$
	$H^{(1,2)}_{1^{+-}}$	$-9C$	$H^{(0,2)}_{2^{++}}$	$H^{(1,2)}_{2^{+-}}$, $H^{(1,2)}_{3^{+-}}$	$\surd$
1^{++}	$H^{(1,1)}_{1^{++}}$	$3C+6T, 3C-12T$	$H^{(0,1)}_{1^{+-}}$	$H^{(1,1)}_{0^{++}}$,$H^{(1,1)}_{2^{++}}$	$\surd$
	$H^{(1,2)}_{1^{++}}$	$3C+6T$	$H^{(0,2)}_{2^{+-}}$	$H^{(1,2)}_{2^{++}}$, $H^{(1,2)}_{3^{++}}$	
1^{-+}	$H^{(0,1)}_{1^{-+}}$	$3C+6T$	$H^{(1,1)}_{0^{--}}$, $H^{(1,1)}_{1^{--}}$, $H^{(1,1)}_{2^{--}}$		
	$H^{(1,1)}_{1^{-+}}$	$-9C$	$H^{(0,1)}_{1^{--}}$	$H^{(1,1)}_{0^{-+}}$, $H^{(1,1)}_{2^{-+}}$	$\surd$
1^{--}	$H^{(1,0)}_{1^{--}}$	$3C-12T$	$H^{(0,0)}_{0^{-+}}$		$\surd$
	$H^{(0,1)}_{1^{--}}$	$-9C$	$H^{(1,1)}_{0^{-+}}$, $H^{(1,1)}_{1^{-+}}$, $H^{(1,1)}_{2^{-+}}$		$\surd$
	$H^{(1,1)}_{1^{--}}$	$3C+6T$	$H^{(0,1)}_{1^{-+}}$	$H^{(1,1)}_{0^{--}}$ $H^{(1,1)}_{2^{--}}$	
	$H^{(1,2)}_{1^{--}}$	$3C+6T, 3C-12T$	$H^{(0,2)}_{2^{-+}}$	$H^{(1,2)}_{2^{--}}$, $H^{(1,2)}_{3^{--}}$	$\surd$
2^{+-}	$H^{(0,2)}_{2^{+-}}$	$3C+6T$	$H^{(1,2)}_{1^{++}}$, $H^{(1,2)}_{2^{++}}$,$H^{(1,2)}_{3^{++}}$		
	$H^{(1,2)}_{2^{+-}}$	$-9C$	$H^{(1,2)}_{2^{++}}$	$H^{(1,2)}_{1^{+-}}$,$H^{(1,2)}_{3^{+-}}$	$\surd$
2^{++}	$H^{(1,1)}_{2^{++}}$	$3C+6T$,$3C-12T$	$H^{(0,1)}_{1^{+-}}$	$H^{(1,1)}_{0^{++}}$,$H^{(1,1)}_{1^{++}}$	$\surd$
	$H^{(0,2)}_{2^{++}}$	$-9C$	$H^{(1,2)}_{1^{+-}}$, $H^{(1,2)}_{2^{+-}}$,$H^{(1,2)}_{3^{+-}}$		$\surd$
	$H^{(1,2)}_{2^{++}}$	$3C+6T$	$H^{(0,2)}_{2^{+-}}$	$H^{(1,2)}_{1^{++}}$, $H^{(1,2)}_{3^{++}}$	
	$H^{(1,3)}_{2^{++}}$	$3C+6T$, $3C-12T$	$H^{(0,3)}_{3^{+-}}$	$H^{(1,3)}_{3^{++}}$, $H^{(1,3)}_{3^{++}}$,$H^{(1,3)}_{4^{++}}$	$\surd$
2^{-+}	$H^{(1,1)}_{2^{-+}}$	$-9C$	$H^{(0,1)}_{1^{--}}$	$H^{(1,1)}_{0^{-+}}$, $H^{(1,1)}_{1^{-+}}$	$\surd$
	$H^{(0,2)}_{2^{-+}}$	$3C+6T$,$3C-12T$	$H^{(1,2)}_{1^{--}}$, $H^{(1,2)}_{2^{--}}$,$H^{(1,2)}_{3^{--}}$		$\surd$
	$H^{(1,3)}_{2^{-+}}$	$-9C$	$H^{(0,3)}_{3^{--}}$		$\surd$
2^{--}	$H^{(1,1)}_{2^{--}}$	$3C+6T$	$H^{(0,1)}_{1^{-+}}$	$H^{(1,1)}_{1^{-+}}$,$H^{(1,1)}_{1^{--}}$	
	$H^{(1,2)}_{2^{--}}$	$3C+6T$,$3C-12T$	$H^{(0,2)}_{2^{-+}}$	$H^{(1,2)}_{1^{--}}$, $H^{(1,2)}_{3^{--}}$	$\surd$
	$H^{(1,3)}_{2^{--}}$	$3C+6T$	$H^{(0,3)}_{2^{-+}}$	$H^{(1,3)}_{3^{--}}$, $H^{(1,3)}_{4^{--}}$	

$3C-12T$ forms the deeply bound state. The most deeply bound states appear in $H^{(1,1)}_{0^{++}}, H^{(0,1)}_{1^{+-}}, H^{(1,1)}_{1^{++}}$ and $H^{(1,1)}_{2^{++}}$ as a forthlet.

For $I = 1$ states in Table 7.3, the potential $-C-2T$ is the only attractive channel. The most deeply bound states exist in $H^{(1,1)}_{0^{++}}, H^{(0,1)}_{1^{+-}}, H^{(1,1)}_{1^{++}}$ and $H^{(1,1)}_{2^{++}}$ as a forthlet, which is a similar result of $I = 0$ states.

TABLE 7.4: Spin multiplets of $P\bar{P}$ molecules for $I = 1$ states

J^{PC}	$H^{(S_H,S_l)}_{J^{PC}}$	Potential	Spin partner		attractive
			type α	type β	
0^{++}	$H^{(0,0)}_{0^{++}}$	$3C$	$H^{(1,0)}_{1^{+-}}$		
	$H^{(1,1)}_{0^{++}}$	$-C-2T,\ -C+4T$	$H^{(0,1)}_{1^{+-}}$	$H^{(1,1)}_{1^{++}},\ \ H^{(1,1)}_{2^{++}}$	$\surd$
0^{-+}	$H^{(0,0)}_{0^{-+}}$	$-C+4T$	$H^{(1,0)}_{1^{--}}$		
	$H^{(1,1)}_{0^{-+}}$	$3C$	$H^{(0,1)}_{1^{--}}$	$H^{(1,1)}_{1^{-+}},\ \ H^{(1,1)}_{2^{-+}}$	
0^{--}	$H^{(1,1)}_{0^{--}}$	$-C-2T$	$H^{(0,1)}_{1^{-+}}$	$H^{(1,1)}_{1^{--}},\ \ H^{(1,1)}_{2^{--}}$	$\surd$
1^{+-}	$H^{(0,1)}_{1^{+-}}$	$-C-2T,\ \ -C+4T$	$H^{(1,1)}_{0^{++}},\ H^{(1,1)}_{1^{++}},\ H^{(1,1)}_{2^{++}}$		$\surd$
	$H^{(1,0)}_{1^{+-}}$	$3C$	$H^{(0,0)}_{0^{++}}$		
	$H^{(1,2)}_{1^{+-}}$	$3C$	$H^{(0,2)}_{2^{++}}$	$H^{(1,2)}_{2^{+-}},\ H^{(1,2)}_{3^{+-}}$	
1^{++}	$H^{(1,1)}_{1^{++}}$	$-C-2T, -C+4T$	$H^{(0,1)}_{1^{+-}}$	$H^{(1,1)}_{0^{++}}, H^{(1,1)}_{2^{++}}$	$\surd$
	$H^{(1,2)}_{1^{++}}$	$-C-2T$	$H^{(0,2)}_{2^{+-}}$	$H^{(1,2)}_{2^{++}},\ H^{(1,2)}_{3^{++}}$	$\surd$
1^{-+}	$H^{(0,1)}_{1^{-+}}$	$-C-2T$	$H^{(1,1)}_{0^{--}},\ H^{(1,1)}_{1^{--}},\ H^{(1,1)}_{2^{--}}$		$\surd$
	$H^{(1,1)}_{1^{-+}}$	$3C$	$H^{(0,1)}_{1^{--}}$	$H^{(1,1)}_{0^{-+}},\ H^{(1,1)}_{2^{-+}}$	
1^{--}	$H^{(1,0)}_{1^{--}}$	$-C+4T$	$H^{(0,0)}_{0^{-+}}$		
	$H^{(0,1)}_{1^{--}}$	$3C$	$H^{(1,1)}_{0^{-+}},\ H^{(1,1)}_{1^{-+}},\ H^{(1,1)}_{2^{-+}}$		
	$H^{(1,1)}_{1^{--}}$	$-C-2T$	$H^{(0,1)}_{1^{-+}}$	$H^{(1,1)}_{0^{--}}\ H^{(1,1)}_{2^{--}}$	$\surd$
	$H^{(1,2)}_{1^{--}}$	$-C-2T, -C+4T$	$H^{(0,2)}_{2^{-+}}$	$H^{(1,2)}_{2^{--}},\ H^{(1,2)}_{3^{--}}$	$\surd$
2^{+-}	$H^{(0,2)}_{2^{+-}}$	$-C-2T$	$H^{(1,2)}_{1^{++}},\ H^{(1,2)}_{2^{++}}, H^{(1,2)}_{3^{++}}$		$\surd$
	$H^{(1,2)}_{2^{+-}}$	$3C$	$H^{(1,2)}_{2^{++}}$	$H^{(1,2)}_{1^{+-}}, H^{(1,2)}_{3^{+-}}$	
2^{++}	$H^{(1,1)}_{2^{++}}$	$-C-2T, -C+4T$	$H^{(0,1)}_{1^{+-}}$	$H^{(1,1)}_{0^{++}}, H^{(1,1)}_{1^{++}}$	$\surd$
	$H^{(0,2)}_{2^{++}}$	$3C$	$H^{(1,2)}_{1^{+-}},\ H^{(1,2)}_{2^{+-}}, H^{(1,2)}_{3^{+-}}$		
	$H^{(1,2)}_{2^{++}}$	$-C-2T$	$H^{(0,2)}_{2^{+-}}$	$H^{(1,2)}_{1^{++}},\ H^{(1,2)}_{3^{++}}$	$\surd$
	$H^{(1,3)}_{2^{++}}$	$-C-2T,\ -C+4T$	$H^{(0,3)}_{3^{+-}}$	$H^{(1,3)}_{3^{++}},\ H^{(1,3)}_{3^{++}}, H^{(1,3)}_{4^{++}}$	$\surd$
2^{-+}	$H^{(1,1)}_{2^{-+}}$	$3C$	$H^{(0,1)}_{1^{--}}$	$H^{(1,1)}_{0^{-+}},\ H^{(1,1)}_{1^{-+}}$	
	$H^{(0,2)}_{2^{-+}}$	$-C-2T, -C+4T$	$H^{(1,2)}_{1^{--}},\ H^{(1,2)}_{2^{--}}, H^{(1,2)}_{3^{--}}$		$\surd$
	$H^{(1,3)}_{2^{-+}}$	$3C$	$H^{(0,3)}_{3^{--}}$		
2^{--}	$H^{(1,1)}_{2^{--}}$	$-C-2T$	$H^{(0,1)}_{1^{-+}}$	$H^{(1,1)}_{1^{-+}}, H^{(1,1)}_{1^{--}}$	$\surd$
	$H^{(1,2)}_{2^{--}}$	$-C-2T, -C+4T$	$H^{(0,2)}_{2^{-+}}$	$H^{(1,2)}_{1^{--}},\ H^{(1,2)}_{3^{--}}$	$\surd$
	$H^{(1,3)}_{2^{--}}$	$-C-2T$	$H^{(0,3)}_{2^{-+}}$	$H^{(1,3)}_{3^{--}},\ H^{(1,3)}_{4^{--}}$	$\surd$

7.3.3 The $P^{(*)}P^{(*)}$ states

The degenerates of the $P^{(*)}P^{(*)}$ states are studied in the same way of the analysis of the $P^{(*)}\bar{P}^{(*)}$ states. The results are summarized in Tabs. 7.5 and 7.6. The the $P^{(*)}\bar{P}^{(*)}$ states are classified with the quantum numbers, $I(J^P)$.

The main difference from the $P\bar{P}$ is that PP states do not have spin partner of type α. Because, if the heavy quark spin $S_Q = 0$ is replaced $S_Q = 1$ in the wave function, the isospin should be also switched over to retain the wave functions in symmetric. As a result, the multiplets are classified as two classes. One is the singlet, which appears in the case of $S_l = 0$. When the light spin in the Hamiltonian is not zero, this Hamiltonian forms triplet as type β.

Table 7.5 shows the properties of PP states for $I = 0$ in the heavy quark limit. The attractive potential is only $-3C - 6T$ and the other potential, $9C$ and $-3C - 12T$, are repulsive. We can see the bound states in every channels with respective quantum numbers. The most deeply bound state exists in $H^{(0,1)}_{0(1^+)}$, which is a singlet. In the $0(2^-)$ channel, there are three bound states with similar eigenvalues in the heavy quark limit.

The various properties of PP states for $I = 1$ are shown in Table 7.6. Although the potentials with $-3C$ are attractive, the Hamiltonians with this potential will not form the bound states in the real situation because of the weakness of the center force. The most deeply bound states are triplets in $H^{(1,1)}_{1(0^+)}, H^{(1,1)}_{1(1^+)}$ and $H^{(1,1)}_{1(2^+)}$.

7.4 Specific candidates of heavy meson molecules

So far, we have only considered $P^{(*)}\bar{P}^{(*)}$ molecules in heavy quark mass limit. Some $P^{(*)}\bar{P}^{(*)}$ molecules would correspond to the observed exotic hadrons such as $X(3872)$, $X(3940)$ and Z_b. In reality, however, the masses of the heavy quarks are finite: $M_c = 1.275$ GeV and $M_b = 4.18$ GeV. Hence, the heavy mesons are finite, which imply that the heavy meson molecules appear with heavy quark symmetry breaking to a certain extent. In other words, there should be a gap between our model and real situations.

In this chapter, we discuss the relation between specific candidates of heavy meson molecules and our model expectations. We also perform the numerical calculations to consider the The heavy quark symmetry breaking effect.

TABLE 7.5: Spin multiplets of PP molecules for $I = 0$ states

$I(J^P)$	$H^{S_H,S_l}_{I(J^P)}$	Potential	Spin partner		attractive
			type α	type β	
$0(0^-)$	$H^{(1,1)}_{0(0^-)}$	$-3C-6T$	—	$H^{(1,1)}_{0(1^-)}$,$H^{(1,1)}_{0(2^-)}$	$\surd$
$0(1^+)$	$H^{(0,1)}_{0(1^+)}$	$-3C-6T,-3C+12T$	—	—	$\surd$
	$H^{(1,0)}_{0(1^+)}$	$9C$	—	—	
	$H^{(1,2)}_{0(1^+)}$	$9C$	—	$H^{(1,2)}_{0(2^+)}, H^{(1,2)}_{0(3^+)}$	
$0(1^-)$	$H^{(1,0)}_{0(1^-)}$	$-3C+12T$	—	—	
	$H^{(0,1)}_{0(1^-)}$	$9C$	—	—	
	$H^{(1,1)}_{0(1^-)}$	$-3C-6T$	—	$H^{(1,1)}_{0(0^-)}$,$H^{(1,1)}_{0(2^-)}$	$\surd$
	$H^{(1,2)}_{0(1^-)}$	$-3C-6T,-3C+12T$	—	$H^{(1,2)}_{0(2^-)}, H^{(1,2)}_{0(3^-)}$	$\surd$
$0(2^+)$	$H^{(0,2)}_{0(2^+)}$	$-3C-6T$	—	—	$\surd$
	$H^{(1,2)}_{0(2^+)}$	$9C$	—	$H^{(1,2)}_{0(1^+)}$,$H^{(1,2)}_{0(3^+)}$	
$0(2^-)$	$H^{(1,1)}_{0(2^-)}$	$-3C-6T$	—	$H^{(1,1)}_{0(0^-)}$, $H^{(1,1)}_{0(1^-)}$	$\surd$
	$H^{(1,2)}_{0(2^-)}$	$-3C-6T,-3C+12T$	—	$H^{(1,2)}_{0(1^-)}, H^{(1,2)}_{0(3^-)}$	$\surd$
	$H^{(1,3)}_{0(2^-)}$	$-3C-6T$	—	$H^{(1,3)}_{0(3^-)}, H^{(1,3)}_{0(4^-)}$	$\surd$

TABLE 7.6: Spin multiplets of PP molecules for $I = 1$ states

$I(J^P)$	$H^{S_H,S_l}_{I(J^P)}$	Potential	Spin partner		attractive
			type α	type β	
$1(0^+)$	$H^{(0,0)}_{1(0^+)}$	$-3C$	—	—	$\surd$
	$H^{(1,1)}_{1(0^+)}$	$C+2T, C-4T$	—	$H^{(1,1)}_{1(1^+)}, H^{(1,1)}_{1(2^+)}$	$\surd$
$1(0^-)$	$H^{(0k0)}_{1(0^-)}$	$C-4T$	—	—	$\surd$
	$H^{(1,1)}_{1(0^-)}$	$-3C$	—	$H^{(1,1)}_{1(1^-))}, H^{(1,1)}_{1(2^-)}$	$\surd$
$1(1^+)$	$H^{(1,1)}_{1(1^+)}$	$C+2T, C-4T$	—	$H^{(1,1)}_{1(0^+)}$, $H^{(1,1)}_{1(2^+)}$	$\surd$
	$H^{(1,2)}_{1(1^+)}$	$C+2T$	—	$H^{(1,2)}_{1(2^+)}$,$H^{(1,2)}_{1(3^+)}$	
$1(1^-)$	$H^{(0,1)}_{1(1^-)}$	$C+2T$	—	—	
	$H^{(1,1)}_{1(1^-)}$	$-3C$	—	$H^{(1,1)}_{1(0^-)}$, $H^{(1,1)}_{1(2^-)}$	$\surd$
$1(2^+)$	$H^{(1,1)}_{1(2^+)}$	$C+2T, C-4T$	—	$H^{(1,1)}_{1(0^+)}$, $H^{(1,1)}_{1(1^+)}$	$\surd$
	$H^{(0,2)}_{1(2^+)}$	$-3C$	—	—	$\surd$
	$H^{(1,2)}_{1(2^+)}$	$C+2T$	—	$H(1,2)_{1(1^+)}$,$H^{(1,2)}_{1(3^+)}$	
	$H^{(1,3)}_{1(2^+)}$	$C+2T, C-4T$	—	$H^{(1,3)}_{1(3^+)}, H^{(1,3)}_{1(3^+)}$	$\surd$
$1(2^-)$	$H^{(1,1)}_{1(2^-)}$	$-3C$	—	$H^{(1,1)}_{1(0^-)}$, $H^{(1,1)}_{1(1^-)}$	$\surd$
	$H^{(0,2)}_{1(2^-)}$	$C+2T, C-4T$	—	—	$\surd$
	$H^{(1,3)}_{1(2^-)}$	$-3C$	—	$H^{(1,3)}_{1(3^-)}, H^{(1,3)}_{1(4^-)}$	$\surd$

7.4.1 $Z_b(10610)$ and $Z_b(10650)$

As already discussed in 4, Z_b's are strong candidates of $B^{(*)}\bar{B}^{(*)}$ states. Their masses are well explained as the $B^{(*)}\bar{B}^{(*)}$ states with $I^G(J^P) = 1^+(1^+)$ by means of the potential model. Now we consider this states in the heavy quark limit.

From Table 7.4, we can see that there are three sub-Hamiltonians in $1^+(1^+)$, $H^{(0,1)}_{1^{+-}}$, $H^{(1,0)}_{1^{+-}}$ and $H^{(1,2)}_{1^{+-}}$. But only $H^{(0,1)}_{1^{+-}}$ has attractive channel with diagonalized potential $-C-2T$. This fact is astonished for the following reasons. Since $H^{(0,1)}_{1^{+-}}$ has only one bound state, the potential model cannot reproduce the twin states as Z_b's. Moreover, the heavy quark spin of $H^{(0,1)}_{1^{+-}}$ indicate that the bound state of this state is impossible to decay into $\Upsilon\pi$ and be also produced from Υ. This result also run counter to the experimentally observed channels, $\Upsilon(5S) \to Z_b\pi \to \Upsilon(nS)\pi\pi$. These discrepancies may be related to the heavy quark symmetry breaking and we will consider this problem later. This state degenerates with the bound states belonging $H^{(1,1)}_{0^{++}}$, $H^{(1,1)}_{1^{++}}$ and $H^{(1,1)}_{2^{++}}$. For the $P^{(*)}\bar{P}^{(*)}$ states with $I^G(J^P) = 1^+(1^+)$, they are spin partners as type α. Therefore, the decay properties of them are different.

To see the detail of this state, we define the wave function for Z_b with particle basis as

$$\begin{aligned} |Z_b\rangle &= a\,|\frac{1}{\sqrt{2}}(B\bar{B}^* - B^*\bar{B})(^3S_1)\rangle + b\,|\frac{1}{\sqrt{2}}(B\bar{B}^* - B^*\bar{B})(^3D_1)\rangle + c\,|B^*\bar{B}^*(^3S_1)\rangle + d\,|B^*\bar{B}^*(^3D_1)\rangle \\ &= a'\,|0_H, 1_q, 0_L, 1_l; 1\rangle + b'\,|0_H, 1_q, 2_L, 1_l; 1\rangle + c'\,|1_H, 0_q, 0_L, 0_L; 1\rangle + d'\,|1_H, 0_l, 2_L, 2_l; 1\rangle\,, \end{aligned} \quad (7.42)$$

where $a^{(\prime)}$, $b^{(\prime)}$, $c^{(\prime)}$ and $d^{(\prime)}$ are coefficients of wave functions and they are normalized as $a^2+b^2+c^2+d^2 = a'^2+b'^2+c'^2+d'^2 = 1$. The coefficients are related with the unitary matrix $U_{1^{+-}}$ as follows:

$$\begin{cases} a' = \frac{1}{\sqrt{2}}a + \frac{1}{\sqrt{2}}c \\ b' = \frac{1}{\sqrt{2}}b + \frac{1}{\sqrt{2}}d \\ c' = -\frac{1}{\sqrt{2}}a + \frac{1}{\sqrt{2}}c \\ d' = -\frac{1}{\sqrt{2}}b + \frac{1}{\sqrt{2}}d. \end{cases} \quad (7.43)$$

The bound state should belong to the $H^{(0,1)}_{1^{+-}}$, hence $c' = d' = 0$. This implies the relations of the coefficients in the particle basis: $a = c$ and $b = d$. The coefficients a and b are depend on the dynamics.

To see the validity of this argument, we perform the numerical calculation with the potential model. We numerically solve the Hamiltonian, $H_{1^{+-}}$ in $I = 0$, where we adopt the values of the coupling constants and cutoff parameter used in 4. We input $m_B = m_{B^*} = 5 \times 10^{20}$ GeV as the effectively infinite masses of B and B' mesons. As a result, the bound state in obtained with the binding energy $E_v = -121$ MeV. The coefficients in particle basis are given as $a = c = \sqrt{0.35}$ and $b = d = \sqrt{0.15}$. Thus the coefficients in HQS basis are obtained as $a' = \sqrt{0.7}$, $b' = \sqrt{0.3}$ and $c' = d' = 0$. This result is consistent with the expectations from heavy quark symmetry and we can confirm that the $|Z_b\rangle$ state belongs to the $H^{(0,1)}_{1^{+-}}$.

Next, we numerically solve the total Hamiltonian of this state with inputs of the finite mass of $B^{(*)}$ mesons to see the effects of the heavy quark symmetry braking. As shown in Chapter 4, the one bound states are obtained with $E = -7.7$ MeV. The coefficients in particle basis are obtained as $a = \sqrt{0.76}$, $b = \sqrt{0.1}$, $c = \sqrt{0.1}$ and $d = \sqrt{0.04}$. Thus the coefficients in HQS basis are given as $a' = \sqrt{0.71}$, $b' = \sqrt{0.13}$, $c' = -\sqrt{0.15}$ and $d = -\sqrt{0.01}$. This result indicates that the bound state of $B^{(*)}\bar{B}^{(*)}$ states in $I^G(J^P) = 1^+(1^+)$ breaks the heavy quark symmetry with the rate $\sim$ 15 %. This breaking effect will make possible to produce the Z_b state from $\Upsilon(5S)$.

7.5 Summary

We have discussed the decoupling for the heavy quark and the total spin of light components in the multi-hadorns composed of the two heavy mesons in the heavy quark mass limit $m_Q \to \infty$. In this limit, these spins are conserved quantities. In the heavy meson molecule systems, the heavy quark symmetry plays an important role for the classification of the spectrum and the structure of the heavy hadrons.

Heavy quark symmetry cause the mass degeneracy of heavy hadorns. The degeneracy of heavy meson molecules are classified into two classes. One is the degeneracy of them due to the suppression of spin-spin interactions of two heavy quarks, which is called as the degeneracy of type α. The spin partners belonging the type α show the opposite decay properties. Second is that the degeneracy occurs due to the suppression of the spin-spin interactions between heavy quark and light spins.

We have found that the degeneracy of $P^{(*)}\bar{P}^{(*)}$ molecules are doublets or forthlets. The doublets exist as type α, whereas the forthlets occur involving type α and type β. The

most deeply bound states are in $H^{(S_H,S_l)_J PC} = H^{(1,1)}_{0^{++}}, H^{(0,1)}_{1^{+-}}, H^{(1,1)}_{1^{++}}$ and $H^{(1,1)}_{2^{++}}$ as a forthlet. In contrast, the degeneracy of $P^{(*)}\bar{P}^{(*)}$ occur only triplet as type β. There is no degeneracy as type α and some states belong the singlets.

We have also studied the relation of this analysis and Z_b as candidates of heavy meson molecules. In heavy quark limit, we have found only one bound state as $P^{(*)}\bar{P}^{(*)}$ states in $I^G(J^P) = 1^+(1^+)$. This state belongs $H^{(0,1)}_{1^{+-}}$ and has spin partners in $H^{(1,1)}_{0^{++}}, H^{(1,1)}_{1^{++}}$ and $H^{(1,1)}_{2^{++}}$. We have studied the heavy quark symmetry breaking in this state with numerical calculations. Our results suggest that the effects of heavy quark symmetry breaking makes possible to produce the Z_b state from $\Upsilon(5S)$ and decay from Z_b to $\Upsilon\pi$.

From the above results, we conclude that the heavy quark symmetry is a useful guiding principle to study the structure of the multi-hadron systems.

Chapter 8

Summary

In this thesis, we have studied the properties of heavy meson molecules from various point of view. They are strong candidates of new forms of hadrons.

In chapter 3, we overview the status of the twin resonances $Z_b(10610)$ and $Z_b(10650)$ observed in Belle. Their masses are located slightly above the respective thresholds, $B\bar{B}^*$ and $B^*\bar{B}^*$. Their quantum numbers, $I^G(J^P) = 1^+(1^+)$, indicate that the constituents of Z_b's must be not two quarks but at least four quarks. Their branching fractions of decays also show the exotic behaviors, which indicate that Z_b's cannot explained by the conventional quark models.

In chapter 4, we study the heavy hadron spectroscopy near the two heavy meson thresholds. We have employed $B(D)$ and $B^*(D^*)$ mesons as effective degrees of freedom near the thresholds, and systematically considered the possibility of $B^{(*)}\bar{B}^{(*)}$ bound and resonance states having exotic quantum numbers up to $J < 2$. The potential of them are constructed by using the effective Lagrangians respecting the heavy quark symmetry and the Schrödinger equation for the $B^{(*)}\bar{B}^{(*)}$ states with $J < 2$ are numerically solved. As a result, we have found the bound state with binding energy 8.5 MeV and resonance state with the resonance energy 50.4 MeV and the decay width 15.1 MeV in the $I^G(J^P) = 1^+(1^+)$ channel. These states correspond the masses of $Z_b(10610)$ and $Z_b(10650)$, respectively. Therefore, the twin resonances, Z_b's can be interpreted as the $B^{(*)}\bar{B}^{(*)}$ molecular type states. It should be noted that the mixing effects of pseudo scalar B and vector B^* mesons, which is consequence of heavy quark symmetry, play a crucial role to form the bound and resonance states. In addition to the states corresponding Z_b's, the potential model predicts other possible $B^{(*)}\bar{B}^{(*)}$ states in $I = 1$.

We have also discussed exotic mesons with double charm and bottom flavor, whose quark content $\bar{Q}\bar{Q}qq$ is genuinely exotic. As a result, we have found many bound and/or resonance states in both charm and bottom sectors. The $D^{(*)}D^{(*)}$ bound and resonance states have moderate binding energies and decay widths around the thresholds in several channels with quantum numbers, $0(0^-)$, $0(1^+)$, $0(1^-), 0(2^+), 0(2^-)$ and $1(0^-)$. The $B^{(*)}\bar{B}^{(*)}$ states have more bound and resonance states with various quantum numbers Some $B^{(*)}B^{(*)}$ states are very compact objects with a large binding energies much below the thresholds. Perhaps, these states cannot survive as hadronic molecules and more needs further considerations of quark dynamics such as tetraquark.

In Chapter 5, we have derived the model independent relations among various decay and production rates for possible $B^{(*)}\bar{B}^{(*)}$ molecular states under the heavy quark symmetry. Part of decay properties of $Z_b(10610)$ and $Z_b(10650)$ are well explained and the possible decay patterns for neutral $Z_b^0(10610)$ are discussed in the present framework. We have shown that the W_{bJ}^{--} decay into a spin singlet bottomonium is forbidden except for W_{b1}^{--}. We have also predicted the production rate of various W_{bJ}^{--} through the one pion emission of $\Upsilon(5S)$. All of them can be tested experimentally and will provide important information to further understand the exotic structure of the new particles.

In Chapter 6,we have studied the $Z_b^{(\prime)+} \to \Upsilon(nS)\pi^+$ decays in a picture of the heavy meson molecule. Assuming that $Z_b^{(\prime)}$ is the $B^*\bar{B}^{(*)}$ molecular state, we have considered the transition amplitudes given by the triangle diagrams with $B^{(*)}$ and $\bar{B}^{(*)}$ meson loops at lowest order based on the heavy meson effective theory. The couplings of g_{ZBB^*} and $g_{Z'B^*B^*}$ are fixed to reproduce correctly the observed decay widths from $Z_b^{(\prime)}$ to the open flavor channels. To treat the effect of the finite range of the hadron interactions and regularize the loop integrals in the transition amplitudes suitably, we introduce the phenomenological form factors with the cutoff parameters Λ_Z and Λ. The numerical result with $\Lambda_z = 1000$ MeV and $\Lambda = 600$ MeV is qualitatively consistent with the experimental data. Our results suggest that, if $Z_b^{(\prime)}$ have molecular type structures, the form factor should play a crucial role in the transition amplitudes. Our model also applies the decays, $Z_c^+ \to J/\psi\pi^+, \psi(2S)\pi^+$. We roughly estimate the branching fractions as $f(Z_c^+ \to J/\psi\pi^+) \sim 1.3$ % and $f(Z_c^+ \to \psi(2S)\pi^+) \sim 0.32$ %, which is testable for the future experiments in high energy accelerator facilities, such as KEK-Belle, BES and so on. In the foreseeable future, our formulation will apply to the other exotic decays, such as $Z_b^{(\prime)+} \to \eta_b\rho^+$, $Z_b^{(\prime)0} \to \eta_b\gamma$ and so on, which can be also studied in future experiments.

In chapter 7, we have discussed the decoupling for the heavy quark and the total spin of light components in the multi-hadorns composed of the two heavy mesons in the heavy quark mass limit $m_Q \to \infty$. In this limit, these spins are conserved quantities. Tn the heavy meson molecule systems, the heavy quark symmetry plays an important role for the classification of the spectrum and the structure of the heavy hadrons. Heavy quark symmetry cause the mass degeneracy of heavy hadorns. The degeneracy of heavy meson molecules are classified into two classes. One is the degeneracy of them due to the suppression of spin-spin interactions of two heavy quarks, which is called as the degeneracy of type α. The spin partners belonging the type α show the opposite decay properties. Second is that the degeneracy occurs due to the suppression of the spin-spin interactions between heavy quark and light spins.

We have found that the degeneracy of $P^{(*)}\bar{P}^{(*)}$ molecules are doublets or forthlets. The doublets exist as type α, whereas the forthlets occur involving type α and type β. The most deeply bound states are in $H^{(S_H,S_l)_{J^{PC}}} = H^{(1,1)}_{0^{++}}, H^{(0,1)}_{1^{+-}}, H^{(1,1)}_{1^{++}}$ and $H^{(1,1)}_{2^{++}}$ as a forthlet. In contrast, the degeneracy of $P^{(*)}\bar{P}^{(*)}$ occur only triplet as type β. There is no degeneracy as type α and some states belong the singlets. We have also studied the relation of this analysis and Z_b as candidates of heavy meson molecules. In heavy quark limit, we have found only one bound state as $P^{(*)}\bar{P}^{(*)}$ states in $I^G(J^P) = 1^+(1^+)$. This state belongs $H^{(0,1)}_{1^{+-}}$ and has spin partners in $H^{(1,1)}_{0^{++}}, H^{(1,1)}_{1^{++}}$ and $H^{(1,1)}_{2^{++}}$. We have studied the heavy quark symmetry breaking in this state with numerical calculations. Our results suggest that the effects of heavy quark symmetry breaking makes possible to produce the Z_b state from $\Upsilon(5S)$ and decay from Z_b to $\Upsilon\pi$. From the above results, we conclude that the heavy quark symmetry is a useful guiding principle to study the structure of the multi-hadron systems.

A key issue in this thesis is the study of the heavy meson molecules as exotic hadrons. They are strong candidates of new forms of matter. Around the thresholds, the heavy mesons arises as effective degrees of freedom, hence it is naturally expected that the molecules in the regions. The problem, however, is that the properties of heavy meson molecules are understood completely. This study have revealed the various properties of them such as the masses, production and decay properties. Our analysis of heavy meson molecules have predicted some candidates of exotic hadrons, which will be tested in future experiments. We hope that our study shed light on the understanding of exotic hadrons and fundamental dynamics of QCD.

Appendix A

Hamiltonian for heavy meson molecules

A.1 Hamiltonian for $P\bar{P}$ meson molecules

Here, we show the hamiltonians for exotic heavy mesons with hidden heavy quarks such as $B\bar{B}$ and $D\bar{D}$. The hamiltonian is a sum of the kinetic term and potential term as,

$$H_{JPC} = K_{JPC} + V^{\pi}_{JPC}, \tag{A.1}$$

for the π exchage potential only, and

$$H_{JPC} = K_{JPC} + \sum_{i=\pi,\rho,\omega} V^{i}_{JPC}, \tag{A.2}$$

for the $\pi\rho\omega$ potential.

The kinetic terms with including the explicit breaking of the heavy quark symmetry by the mass difference $m_{\mathrm{B}^*} - m_{\mathrm{B}}$ are

$$K_{0^{++}} = \mathrm{diag}\left(-\frac{1}{2\tilde{m}_{\mathrm{BB}}}\triangle_0, -\frac{1}{2\tilde{m}_{\mathrm{BB}^*}}\triangle_0 + 2\Delta m_{\mathrm{BB}^*}, -\frac{1}{2\tilde{m}_{\mathrm{BB}^*}}\triangle_2 + 2\Delta m_{\mathrm{BB}^*}\right), \tag{A.3}$$

$$K_{0^{--}} = \mathrm{diag}\left(-\frac{1}{2\tilde{m}_{\mathrm{BB}^*}}\triangle_1\right), \tag{A.4}$$

$$K_{0^{-+}} = \mathrm{diag}\left(-\frac{1}{2\tilde{m}_{\mathrm{BB}^*}}\triangle_1, -\frac{1}{2\tilde{m}_{\mathrm{B}^*\mathrm{B}^*}}\triangle_1 + \Delta m_{\mathrm{BB}^*}\right), \tag{A.5}$$

$$K_{1^{+-}} = \mathrm{diag}\left(-\frac{1}{2\tilde{m}_{\mathrm{BB}^*}}\triangle_0, -\frac{1}{2\tilde{m}_{\mathrm{BB}^*}}\triangle_2, -\frac{1}{2\tilde{m}_{\mathrm{B}^*\mathrm{B}^*}}\triangle_0 + \Delta m_{\mathrm{BB}^*}, -\frac{1}{2\tilde{m}_{\mathrm{B}^*\mathrm{B}^*}}\triangle_2 + \Delta m_{\mathrm{BB}^*}\right), \tag{A.6}$$

$$K_{1^{++}} = \mathrm{diag}\left(-\frac{1}{2\tilde{m}_{\mathrm{BB}^*}}\triangle_0, -\frac{1}{2\tilde{m}_{\mathrm{BB}^*}}\triangle_2, -\frac{1}{2\tilde{m}_{\mathrm{B}^*\mathrm{B}^*}}\triangle_2 + \Delta m_{\mathrm{BB}^*}\right), \tag{A.7}$$

$$\begin{aligned} K_{1^{--}} = \mathrm{diag}\Bigg(&-\frac{1}{2\tilde{m}_{\mathrm{BB}}}\triangle_0, -\frac{1}{2\tilde{m}_{\mathrm{BB}^*}}\triangle_1 + \Delta m_{\mathrm{BB}^*}, \\ &-\frac{1}{2\tilde{m}_{\mathrm{B}^*\mathrm{B}^*}}\triangle_1 + 2\Delta m_{\mathrm{BB}^*}, -\frac{1}{2\tilde{m}_{\mathrm{B}^*\mathrm{B}^*}}\triangle_1 + 2\Delta m_{\mathrm{BB}^*}, -\frac{1}{2\tilde{m}_{\mathrm{B}^*\mathrm{B}^*}}\triangle_3 + 2\Delta m_{\mathrm{BB}^*}\Bigg), \end{aligned} \tag{A.8}$$

$$K_{1^{-+}} = \mathrm{diag}\left(-\frac{1}{2\tilde{m}_{\mathrm{BB}^*}}\triangle_1, -\frac{1}{2\tilde{m}_{\mathrm{B}^*\mathrm{B}^*}}\triangle_1 + \Delta m_{\mathrm{BB}^*}\right), \tag{A.9}$$

$$K_{2^{+-}} = \mathrm{diag}\left(-\frac{1}{2\tilde{m}_{\mathrm{BB}^*}}\triangle_2, -\frac{1}{2\tilde{m}_{\mathrm{B}^*\mathrm{B}^*}}\triangle_2 + \Delta m_{\mathrm{BB}^*}\right), \tag{A.10}$$

$$\begin{aligned} K_{2^{++}} = \mathrm{diag}\Bigg(&-\frac{1}{2\tilde{m}_{\mathrm{BB}}}\triangle_2, -\frac{1}{2\tilde{m}_{\mathrm{BB}^*}}\triangle_2 + \Delta m_{\mathrm{BB}^*}, -\frac{1}{2\tilde{m}_{\mathrm{B}^*\mathrm{B}^*}}\triangle_2 + 2\Delta m_{\mathrm{BB}^*}, \\ &-\frac{1}{2\tilde{m}_{\mathrm{B}^*\mathrm{B}^*}}\triangle_0 + 2\Delta m_{\mathrm{BB}^*}, -\frac{1}{2\tilde{m}_{\mathrm{B}^*\mathrm{B}^*}}\triangle_2 + 2\Delta m_{\mathrm{BB}^*}, -\frac{1}{2\tilde{m}_{\mathrm{B}^*\mathrm{B}^*}}\triangle_4 + 2\Delta m_{\mathrm{BB}^*}\Bigg), \end{aligned} \tag{A.11}$$

$$K_{2^{-+}} = \mathrm{diag}\left(-\frac{1}{2\tilde{m}_{\mathrm{BB}^*}}\triangle_1, -\frac{1}{2\tilde{m}_{\mathrm{BB}^*}}\triangle_3, -\frac{1}{2\tilde{m}_{\mathrm{B}^*\mathrm{B}^*}}\triangle_1 + \Delta m_{\mathrm{BB}^*}, -\frac{1}{2\tilde{m}_{\mathrm{B}^*\mathrm{B}^*}}\triangle_3 + \Delta m_{\mathrm{BB}^*}\right), \tag{A.12}$$

$$K_{2^{--}} = \mathrm{diag}\left(-\frac{1}{2\tilde{m}_{\mathrm{BB}^*}}\triangle_1, -\frac{1}{2\tilde{m}_{\mathrm{BB}^*}}\triangle_3, -\frac{1}{2\tilde{m}_{\mathrm{B}^*\mathrm{B}^*}}\triangle_1 + \Delta m_{\mathrm{BB}^*}, -\frac{1}{2\tilde{m}_{\mathrm{B}^*\mathrm{B}^*}}\triangle_3 + \Delta m_{\mathrm{BB}^*}\right), \tag{A.13}$$

where $\triangle_l = \frac{\partial^2}{\partial r^2} + \frac{2}{r}\frac{\partial}{\partial r} - \frac{l(l+1)}{r^2}$ with integer $l \geq 0$, $1/\tilde{m}_{\mathrm{BB}} = 1/m_{\mathrm{B}} + 1/m_{\mathrm{B}}$, $1/\tilde{m}_{\mathrm{BB}^*} = 1/m_{\mathrm{B}} + 1/m_{\mathrm{B}^*}$, $1/\tilde{m}_{\mathrm{B}^*\mathrm{B}^*} = 1/m_{\mathrm{B}^*} + 1/m_{\mathrm{B}^*}$ and $\Delta m_{\mathrm{BB}^*} = m_{\mathrm{B}^*} - m_{\mathrm{B}}$.

The π exchange potentials for each J^{PC} states are

$$V^{\pi}_{0^{++}} = \begin{pmatrix} 0 & \sqrt{3}V_{\rm C} & -\sqrt{6}V_{\rm T} \\ \sqrt{3}V_{\rm C} & 2V_{\rm C} & \sqrt{2}V_{\rm T} \\ -\sqrt{6}V_{\rm T} & \sqrt{2}V_{\rm T} & -V_{\rm C}+2V_{\rm T} \end{pmatrix}, \tag{A.14}$$

$$V^{\pi}_{0^{--}} = (-V_{\rm C}-2V_{\rm T}), \tag{A.15}$$

$$V^{\pi}_{0^{-+}} = \begin{pmatrix} V_{\rm C}+2V_{\rm T} & -2V_{\rm C}+2V_{\rm T} \\ -2V_{\rm C}+2V_{\rm T} & V_{\rm C}+2V_{\rm T} \end{pmatrix}, \tag{A.16}$$

$$V^{\pi}_{1^{+-}} = \begin{pmatrix} V_{\rm C} & -\sqrt{2}V_{\rm T} & -2V_{\rm C} & -\sqrt{2}V_{\rm T} \\ -\sqrt{2}V_{\rm T} & V_{\rm C}+V_{\rm T} & -\sqrt{2}V_{\rm T} & -2V_{\rm C}+V_{\rm T} \\ -2V_{\rm C} & -\sqrt{2}V_{\rm T} & V_{\rm C} & -\sqrt{2}V_{\rm T} \\ -\sqrt{2}V_{\rm T} & -2V_{\rm C}+V_{\rm T} & -\sqrt{2}V_{\rm T} & V_{\rm C}+V_{\rm T} \end{pmatrix}, \tag{A.17}$$

$$V^{\pi}_{1^{++}} = \begin{pmatrix} -V_{\rm C} & \sqrt{2}V_{\rm T} & \sqrt{6}V_{\rm T} \\ \sqrt{2}V_{\rm T} & -V_{\rm C}-V_{\rm T} & \sqrt{3}V_{\rm T} \\ \sqrt{6}V_{\rm T} & \sqrt{3}V_{\rm T} & -V_{\rm C}+V_{\rm T} \end{pmatrix}, \tag{A.18}$$

$$V^{\pi}_{1^{--}} = \begin{pmatrix} 0 & 0 & \sqrt{3}V_{\rm C} & 2\sqrt{\frac{3}{5}}V_{\rm T} & -3\sqrt{\frac{2}{5}}V_{\rm T} \\ 0 & -V_{\rm C}+V_{\rm T} & 0 & 3\sqrt{\frac{3}{5}}V_{\rm T} & 3\sqrt{\frac{2}{5}}V_{\rm T} \\ \sqrt{3}V_{\rm C} & 0 & 2V_{\rm C} & -\frac{2}{\sqrt{5}}V_{\rm C} & \sqrt{\frac{6}{5}}V_{\rm T} \\ 2\sqrt{\frac{3}{5}}V_{\rm T} & 3\sqrt{\frac{2}{5}}V_{\rm T} & -\frac{2}{\sqrt{5}}V_{\rm C} & -V_{\rm C}+\frac{7}{5}V_{\rm T} & -\frac{\sqrt{6}}{5}V_{\rm T} \\ -3\sqrt{\frac{2}{5}}V_{\rm T} & 3\sqrt{\frac{2}{5}}V_{\rm T} & \sqrt{\frac{6}{5}}V_{\rm T} & -\frac{\sqrt{6}}{5}V_{\rm T} & -V_{\rm C}+\frac{8}{5}V_{\rm T} \end{pmatrix}, \tag{A.19}$$

$$V^{\pi}_{1^{-+}} = \begin{pmatrix} V_{\rm C}-V_{\rm T} & -2V_{\rm C}-V_{\rm T} \\ -2V_{\rm C}-V_{\rm T} & V_{\rm C}-V_{\rm T} \end{pmatrix}, \tag{A.20}$$

$$V^{\pi}_{2^{+-}} = \begin{pmatrix} V_{\rm C}-V_{\rm T} & -2V_{\rm C}-V_{\rm T} \\ -2V_{\rm C}-V_{\rm T} & V_{\rm C}-V_{\rm T} \end{pmatrix}, \tag{A.21}$$

$$V^{\pi}_{2^{++}} = \begin{pmatrix} 0 & 0 & \sqrt{3}V_{\rm C} & -\sqrt{\frac{6}{5}}V_{\rm T} & 2\sqrt{\frac{3}{7}}V_{\rm T} & -6\sqrt{\frac{3}{35}}V_{\rm T} \\ 0 & -V_{\rm C}+V_{\rm T} & 0 & -3\sqrt{\frac{2}{5}}V_{\rm T} & \frac{3}{\sqrt{7}}V_{\rm T} & \frac{12}{\sqrt{35}}V_{\rm T} \\ \sqrt{3}V_{\rm C} & 0 & 2V_{\rm C} & \sqrt{\frac{2}{5}}V_{\rm T} & -\frac{2}{\sqrt{7}}V_{\rm T} & \frac{6}{\sqrt{35}}V_{\rm T} \\ -\sqrt{\frac{6}{5}}V_{\rm T} & -3\sqrt{\frac{3}{5}}V_{\rm T} & \sqrt{\frac{2}{5}}V_{\rm T} & -V_{\rm C} & -\sqrt{\frac{14}{5}}V_{\rm T} & 0 \\ 2\sqrt{\frac{3}{7}}V_{\rm T} & \frac{3}{\sqrt{7}}V_{\rm T} & -\frac{2}{\sqrt{7}}V_{\rm T} & -\sqrt{\frac{14}{5}}V_{\rm T} & -V_{\rm C}-\frac{3}{7}V_{\rm T} & -\frac{12}{7\sqrt{5}}V_{\rm T} \\ -6\sqrt{\frac{3}{35}}V_{\rm T} & \frac{12}{\sqrt{35}}V_{\rm T} & \frac{6}{\sqrt{35}}V_{\rm T} & 0 & -\frac{12}{7\sqrt{5}}V_{\rm T} & -V_{\rm C}+\frac{10}{7}V_{\rm T} \end{pmatrix}, \tag{A.22}$$

$$V^{\pi}_{2^{-+}} = \begin{pmatrix} V_{\rm C}+\frac{1}{5}V_{\rm T} & -\frac{3\sqrt{6}}{5}V_{\rm T} & -2V_{\rm C}+\frac{1}{5}V_{\rm T} & -\frac{3\sqrt{6}}{5}V_{\rm T} \\ -\frac{3\sqrt{6}}{5}V_{\rm T} & V_{\rm C}+\frac{4}{5}V_{\rm T} & -\frac{3\sqrt{6}}{5}V_{\rm T} & -2V_{\rm C}+\frac{4}{5}V_{\rm T} \\ -2V_{\rm C}+\frac{1}{5}V_{\rm T} & -\frac{3\sqrt{6}}{5}V_{\rm T} & V_{\rm C}+\frac{1}{5}V_{\rm T} & -\frac{3\sqrt{6}}{5}V_{\rm T} \\ -\frac{3\sqrt{6}}{5}V_{\rm T} & -2V_{\rm C}+\frac{4}{5}V_{\rm T} & -\frac{3\sqrt{6}}{5}V_{\rm T} & V_{\rm C}+\frac{4}{5}V_{\rm T} \end{pmatrix}, \tag{A.23}$$

$$V^{\pi}_{2^{--}} = \begin{pmatrix} -V_{\rm C}-\frac{1}{5}V_{\rm T} & \frac{3\sqrt{6}}{5}V_{\rm T} & -\frac{3\sqrt{3}}{5}V_{\rm T} & \frac{6\sqrt{3}}{5}V_{\rm T} \\ \frac{3\sqrt{6}}{5}V_{\rm T} & -V_{\rm C}-\frac{4}{5}V_{\rm T} & -\frac{3\sqrt{2}}{5}V_{\rm T} & \frac{6\sqrt{2}}{5}V_{\rm T} \\ -\frac{3\sqrt{3}}{5}V_{\rm T} & -\frac{3\sqrt{2}}{5}V_{\rm T} & -V_{\rm C}-\frac{7}{5}V_{\rm T} & -\frac{6}{5}V_{\rm T} \\ \frac{6\sqrt{3}}{5}V_{\rm T} & \frac{6\sqrt{2}}{5}V_{\rm T} & -\frac{6}{5}V_{\rm T} & -V_{\rm C}+\frac{2}{5}V_{\rm T} \end{pmatrix}. \tag{A.24}$$

The ρ and ω potentials are

$$V^v_{0^{++}} = \begin{pmatrix} V^{v\prime}_{\rm C} & 2\sqrt{3}V^v_{\rm C} & \sqrt{6}V^v_{\rm T} \\ 2\sqrt{3}V^v_{\rm C} & 4V^v_{\rm C}+V^{v\prime}_{\rm C} & -\sqrt{2}V^v_{\rm T} \\ \sqrt{6}V^v_{\rm T} & -\sqrt{2}V^v_{\rm T} & -2V^v_{\rm C}-2V^v_{\rm T}+V^{v\prime}_{\rm C} \end{pmatrix}, \tag{A.25}$$

$$V^v_{0^{--}} = \left(-2V^v_{\rm C}+2V^v_{\rm T}+V^{v\prime}_{\rm C}\right), \tag{A.26}$$

$$V^v_{0^{-+}} = \begin{pmatrix} 2V^v_{\rm C}-2V^v_{\rm T}+V^{v\prime}_{\rm C} & -4V^v_{\rm C}-2V^v_{\rm T} \\ -4V^v_{\rm C}-2V^v_{\rm T} & 2V^v_{\rm C}-2V^v_{\rm T}+V^{v\prime}_{\rm C} \end{pmatrix}, \tag{A.27}$$

$$V^v_{1^{+-}} = \begin{pmatrix} 2V^v_{\rm C}+V^{v\prime}_{\rm C} & \sqrt{2}V^v_{\rm T} & -4V^v_{\rm C} & \sqrt{2}V^v_{\rm T} \\ \sqrt{2}V^v_{\rm T} & 2V^v_{\rm C}-V^v_{\rm T}+V^{v\prime}_{\rm C} & \sqrt{2}V^v_{\rm T} & -4V^v_{\rm C}-V^v_{\rm T} \\ -4V^v_{\rm C} & \sqrt{2}V^v_{\rm T} & 2V^v_{\rm C}+V^{v\prime}_{\rm C} & \sqrt{2}V^v_{\rm T} \\ \sqrt{2}V^v_{\rm T} & -4V^v_{\rm C}-V^v_{\rm T} & \sqrt{2}V^v_{\rm T} & 2V^v_{\rm C}-V^v_{\rm T}+V^{v\prime}_{\rm C} \end{pmatrix}, \tag{A.28}$$

$$V^v_{1^{++}} = \begin{pmatrix} -2V^v_{\rm C}+V^{v\prime}_{\rm C} & -\sqrt{2}V^v_{\rm T} & -\sqrt{6}V^v_{\rm T} \\ -\sqrt{2}V^v_{\rm T} & -2V^v_{\rm C}+V^v_{\rm T} & -\sqrt{3}V^v_{\rm T} \\ -\sqrt{6}V^v_{\rm T} & -\sqrt{3}V^v_{\rm T} & -2V^v_{\rm C}-V^v_{\rm T}+V^{v\prime}_{\rm C} \end{pmatrix}, \tag{A.29}$$

$$V^v_{1^{--}} = \begin{pmatrix} V^{v\prime}_{\rm C} & 0 & 2\sqrt{3}V^v_{\rm C} & -2\sqrt{\frac{3}{5}}V^v_{\rm T} & 3\sqrt{\frac{2}{5}}V^v_{\rm T} \\ 0 & -2V^v_{\rm C}-V^v_{\rm T}+V^{v\prime}_{\rm C} & 0 & -3\sqrt{\frac{3}{5}}V^v_{\rm T} & 3\sqrt{\frac{2}{5}}V^v_{\rm T} \\ 2\sqrt{3}V^v_{\rm C} & 0 & 4V^v_{\rm C}+V^{v\prime}_{\rm C} & -\frac{4}{\sqrt{5}}V^v_{\rm C} & -\sqrt{\frac{6}{5}}V^v_{\rm T} \\ -2\sqrt{\frac{3}{5}}V^v_{\rm T} & -3\sqrt{\frac{2}{5}}V^v_{\rm T} & -\frac{4}{\sqrt{5}}V^v_{\rm C} & -2V^v_{\rm C}-\frac{7}{5}V^v_{\rm T}+V^{v\prime}_{\rm C} & \frac{\sqrt{6}}{5}V^v_{\rm T} \\ 3\sqrt{\frac{2}{5}}V^v_{\rm T} & -3\sqrt{\frac{2}{5}}V^v_{\rm T} & -\sqrt{\frac{6}{5}}V^v_{\rm T} & \frac{\sqrt{6}}{5}V^v_{\rm T} & -2V^v_{\rm C}-\frac{8}{5}V^v_{\rm T}+V^{v\prime}_{\rm C} \end{pmatrix}, \tag{A.30}$$

$$V^v_{1^{-+}} = \begin{pmatrix} 2V^v_{\rm C}+V^v_{\rm T}+V^{v\prime}_{\rm C} & -4V^v_{\rm C}+-V^v_{\rm T} \\ -4V^v_{\rm C}+V^v_{\rm T} & 2V^v_{\rm C}+V^v_{\rm T}+V^{v\prime}_{\rm C} \end{pmatrix}, \tag{A.31}$$

$$V^v_{2^{+-}} = \begin{pmatrix} 2V^v_{\rm C}+V^v_{\rm T}+V^{v\prime}_{\rm C} & -4V^v_{\rm C}+V^v_{\rm T} \\ -4V^v_{\rm C}+V^v_{\rm T} & 2V^v_{\rm C}+V^v_{\rm T}+V^{v\prime}_{\rm C} \end{pmatrix}, \tag{A.32}$$

$$V^v_{2^{++}} = \begin{pmatrix} V^{v\prime}_{\rm C} & 0 & 2\sqrt{3}V^v_{\rm C} & \sqrt{\frac{6}{5}}V^v_{\rm T} & -2\sqrt{\frac{3}{7}}V^v_{\rm T} & 6\sqrt{\frac{3}{35}}V^v_{\rm T} \\ 0 & -2V^v_{\rm C}-V^v_{\rm T}+V^{v\prime}_{\rm C} & 0 & 3\sqrt{\frac{2}{5}}V^v_{\rm T} & -\frac{3}{\sqrt{7}}V^v_{\rm T} & -\frac{12}{\sqrt{35}}V^v_{\rm T} \\ 2\sqrt{3}V^v_{\rm C} & 0 & 4V^v_{\rm C}+V^{v\prime}_{\rm C} & -\sqrt{\frac{2}{5}}V^v_{\rm T} & \frac{2}{\sqrt{7}}V^v_{\rm T} & -\frac{6}{\sqrt{35}}V^v_{\rm T} \\ \sqrt{\frac{6}{5}}V^v_{\rm T} & -3\sqrt{\frac{3}{5}}V^v_{\rm T} & -\sqrt{\frac{2}{5}}V^v_{\rm T} & -2V^v_{\rm C}+V^{v\prime}_{\rm C} & \sqrt{\frac{14}{5}}V^v_{\rm T} & 0 \\ -2\sqrt{\frac{3}{7}}V^v_{\rm T} & -\frac{3}{\sqrt{7}}V^v_{\rm T} & \frac{2}{\sqrt{7}}V^v_{\rm T} & \sqrt{\frac{14}{5}}V^v_{\rm T} & -2V^v_{\rm C}+\frac{3}{7}V^v_{\rm T}+V^{v\prime}_{\rm C} & \frac{12}{7\sqrt{5}}V^v_{\rm T} \\ 6\sqrt{\frac{3}{35}}V^v_{\rm T} & -\frac{12}{\sqrt{35}}V^v_{\rm T} & -\frac{6}{\sqrt{35}}V^v_{\rm T} & 0 & \frac{12}{7\sqrt{5}}V^v_{\rm T} & -2V^v_{\rm C}-\frac{10}{7}V^v_{\rm T}+V^{v\prime}_{\rm C} \end{pmatrix}, \tag{A.33}$$

$$V^v_{2^{-+}} = \begin{pmatrix} 2V^v_{\rm C}-\frac{1}{5}V^v_{\rm T}+V^{v\prime}_{\rm C} & \frac{3\sqrt{6}}{5}V^v_{\rm T} & -4V^v_{\rm C}-\frac{1}{5}V^v_{\rm T} & \frac{3\sqrt{6}}{5}V^v_{\rm T} \\ \frac{3\sqrt{6}}{5}V^v_{\rm T} & 2V^v_{\rm C}-\frac{4}{5}V^v_{\rm T}+V^{v\prime}_{\rm C} & \frac{3\sqrt{6}}{5}V^v_{\rm T} & -4V^v_{\rm C}-\frac{4}{5}V^v_{\rm T} \\ -4V^v_{\rm C}-\frac{1}{5}V^v_{\rm T} & \frac{3\sqrt{6}}{5}V^v_{\rm T} & 2V^v_{\rm C}-\frac{1}{5}V^v_{\rm T}+V^{v\prime}_{\rm C} & \frac{3\sqrt{6}}{5}V^v_{\rm T} \\ \frac{3\sqrt{6}}{5}V^v_{\rm T} & -4V^v_{\rm C}-\frac{4}{5}V^v_{\rm T} & \frac{3\sqrt{6}}{5}V^v_{\rm T} & 2V^v_{\rm C}-\frac{4}{5}V^v_{\rm T}+V^{v\prime}_{\rm C} \end{pmatrix}, \tag{A.34}$$

$$V^v_{2^{--}} = \begin{pmatrix} -2V^v_{\rm C}+\frac{1}{5}V^v_{\rm T}+V^{v\prime}_{\rm C} & -\frac{3\sqrt{6}}{5}V^v_{\rm T} & \frac{3\sqrt{3}}{5}V^v_{\rm T} & -\frac{6\sqrt{3}}{5}V^v_{\rm T} \\ -\frac{3\sqrt{6}}{5}V^v_{\rm T} & -2V^v_{\rm C}+\frac{4}{5}V^v_{\rm T}+V^{v\prime}_{\rm C} & \frac{3\sqrt{2}}{5}V^v_{\rm T} & -\frac{6\sqrt{2}}{5}V^v_{\rm T} \\ \frac{3\sqrt{3}}{5}V^v_{\rm T} & \frac{3\sqrt{2}}{5}V^v_{\rm T} & -2V^v_{\rm C}+\frac{7}{5}V^v_{\rm T}+V^{v\prime}_{\rm C} & \frac{6}{5}V^v_{\rm T} \\ -\frac{6\sqrt{3}}{5}V^v_{\rm T} & -\frac{6\sqrt{2}}{5}V^v_{\rm T} & \frac{6}{5}V^v_{\rm T} & -2V^v_{\rm C}-\frac{2}{5}V^v_{\rm T}+V^{v\prime}_{\rm C} \end{pmatrix}. \tag{A.35}$$

where the central and tensor potentials are defined as,

$$V_{\rm C}^{\pi} = \left(\sqrt{2}\frac{g}{f_\pi}\right)^2 \frac{1}{3} C(r;m_\pi)\vec{\tau}_1\cdot\vec{\tau}_2\,, \tag{A.36}$$

$$V_{\rm T}^{\pi} = \left(\sqrt{2}\frac{g}{f_\pi}\right)^2 \frac{1}{3} T(r;m_\pi)\vec{\tau}_1\cdot\vec{\tau}_2\,, \tag{A.37}$$

$$V_{\rm C}^{\rho} = -\left(2\lambda g_V\right)^2 \frac{1}{3} C(r;m_\rho)\vec{\tau}_1\cdot\vec{\tau}_2\,, \tag{A.38}$$

$$V_{\rm C}^{\omega} = \left(2\lambda g_V\right)^2 \frac{1}{3} C(r;m_\omega)\,, \tag{A.39}$$

$$V_{\rm T}^{\rho} = -\left(2\lambda g_V\right)^2 \frac{1}{3} T(r;m_\rho)\vec{\tau}_1\cdot\vec{\tau}_2\,, \tag{A.40}$$

$$V_{\rm T}^{\omega} = \left(2\lambda g_V\right)^2 \frac{1}{3} T(r;m_\omega)\,, \tag{A.41}$$

$$V_{\rm C}^{\rho\prime} = \left(\frac{\beta g_V}{2m_\rho}\right)^2 \frac{1}{3} C(r;m_\rho)\vec{\tau}_1\cdot\vec{\tau}_2\,, \tag{A.42}$$

$$V_{\rm C}^{\omega\prime} = -\left(\frac{\beta g_V}{2m_\omega}\right)^2 \frac{1}{3} C(r;m_\omega)\,. \tag{A.43}$$

A.2 Hamiltonian for PP meson molecules

The Hamiltonian is a sum of the kinetic term and potential term as,

$$H_{I(J^P)} = K_{I(J^P)} + V^{\pi}_{I(J^P)}, \tag{A.44}$$

for the π exchange potential only, and

$$H_{I(J^P)} = K_{I(J^P)} + \sum_{i=\pi,\rho,\omega} V^{i}_{I(J^P)}, \tag{A.45}$$

for the $\pi\rho\,\omega$ potential.

The kinetic terms with including the explicit breaking of the heavy quark symmetry by the mass difference $\Delta m_{\mathrm{PP}^*} = m_{\mathrm{P}^*} - m_{\mathrm{P}}$ are

$$K_{0(0^-)} = \mathrm{diag}\left(-\frac{1}{2\tilde{m}_{\mathrm{PP}^*}}\triangle_1\right), \tag{A.46}$$

$$K_{0(1^+)} = \mathrm{diag}\left(-\frac{1}{2\tilde{m}_{\mathrm{PP}^*}}\triangle_0, -\frac{1}{2\tilde{m}_{\mathrm{PP}^*}}\triangle_2, -\frac{1}{2\tilde{m}_{\mathrm{P}^*\mathrm{P}^*}}\triangle_0 + \Delta m_{\mathrm{PP}^*}, -\frac{1}{2\tilde{m}_{\mathrm{P}^*\mathrm{P}^*}}\triangle_2 + \Delta m_{\mathrm{PP}^*}\right), \tag{A.47}$$

$$\begin{aligned} K_{0(1^-)} = \mathrm{diag}\Bigg(&-\frac{1}{2\tilde{m}_{\mathrm{PP}}}\triangle_0, -\frac{1}{2\tilde{m}_{\mathrm{PP}^*}}\triangle_1 + \Delta m_{\mathrm{PP}^*}, \\ &-\frac{1}{2\tilde{m}_{\mathrm{P}^*\mathrm{P}^*}}\triangle_1 + 2\Delta m_{\mathrm{PP}^*}, -\frac{1}{2\tilde{m}_{\mathrm{P}^*\mathrm{P}^*}}\triangle_1 + 2\Delta m_{\mathrm{PP}^*}, -\frac{1}{2\tilde{m}_{\mathrm{P}^*\mathrm{P}^*}}\triangle_3 + 2\Delta m_{\mathrm{PP}^*}\Bigg), \end{aligned} \tag{A.48}$$

$$K_{0(2^+)} = \mathrm{diag}\left(-\frac{1}{2\tilde{m}_{\mathrm{PP}^*}}\triangle_2, -\frac{1}{2\tilde{m}_{\mathrm{P}^*\mathrm{P}^*}}\triangle_2 + \Delta m_{\mathrm{PP}^*}\right), \tag{A.49}$$

$$K_{0(2^-)} = \mathrm{diag}\left(-\frac{1}{2\tilde{m}_{\mathrm{PP}^*}}\triangle_1, -\frac{1}{2\tilde{m}_{\mathrm{PP}^*}}\triangle_3, -\frac{1}{2\tilde{m}_{\mathrm{P}^*\mathrm{P}^*}}\triangle_1 + \Delta m_{\mathrm{PP}^*}, -\frac{1}{2\tilde{m}_{\mathrm{P}^*\mathrm{P}^*}}\triangle_3 + \Delta m_{\mathrm{PP}^*}\right), \tag{A.50}$$

$$K_{1(0^+)} = \mathrm{diag}\left(-\frac{1}{2\tilde{m}_{\mathrm{PP}}}\triangle_0, -\frac{1}{2\tilde{m}_{\mathrm{PP}^*}}\triangle_0 + 2\Delta m_{\mathrm{PP}^*}, -\frac{1}{2\tilde{m}_{\mathrm{PP}^*}}\triangle_2 + 2\Delta m_{\mathrm{PP}^*}\right), \tag{A.51}$$

$$K_{1(0^-)} = \mathrm{diag}\left(-\frac{1}{2\tilde{m}_{\mathrm{PP}^*}}\triangle_1, -\frac{1}{2\tilde{m}_{\mathrm{P}^*\mathrm{P}^*}}\triangle_1 + \Delta m_{\mathrm{PP}^*}\right), \tag{A.52}$$

$$K_{1(1^+)} = \mathrm{diag}\left(-\frac{1}{2\tilde{m}_{\mathrm{PP}^*}}\triangle_0, -\frac{1}{2\tilde{m}_{\mathrm{PP}^*}}\triangle_2, -\frac{1}{2\tilde{m}_{\mathrm{P}^*\mathrm{P}^*}}\triangle_2 + \Delta m_{\mathrm{PP}^*}\right), \tag{A.53}$$

$$K_{1(1^-)} = \mathrm{diag}\left(-\frac{1}{2\tilde{m}_{\mathrm{PP}^*}}\triangle_1, -\frac{1}{2\tilde{m}_{\mathrm{P}^*\mathrm{P}^*}}\triangle_1 + \Delta m_{\mathrm{PP}^*}\right), \tag{A.54}$$

$$\begin{aligned} K_{1(2^+)} = \mathrm{diag}\Bigg(&-\frac{1}{2\tilde{m}_{\mathrm{PP}}}\triangle_2, -\frac{1}{2\tilde{m}_{\mathrm{PP}^*}}\triangle_2 + \Delta m_{\mathrm{PP}^*}, -\frac{1}{2\tilde{m}_{\mathrm{P}^*\mathrm{P}^*}}\triangle_2 + 2\Delta m_{\mathrm{PP}^*}, \\ &-\frac{1}{2\tilde{m}_{\mathrm{P}^*\mathrm{P}^*}}\triangle_0 + 2\Delta m_{\mathrm{PP}^*}, -\frac{1}{2\tilde{m}_{\mathrm{P}^*\mathrm{P}^*}}\triangle_2 + 2\Delta m_{\mathrm{PP}^*}, -\frac{1}{2\tilde{m}_{\mathrm{P}^*\mathrm{P}^*}}\triangle_4 + 2\Delta m_{\mathrm{PP}^*}\Bigg), \end{aligned} \tag{A.55}$$

$$K_{1(2^-)} = \mathrm{diag}\left(-\frac{1}{2\tilde{m}_{\mathrm{PP}^*}}\triangle_1, -\frac{1}{2\tilde{m}_{\mathrm{PP}^*}}\triangle_3, -\frac{1}{2\tilde{m}_{\mathrm{P}^*\mathrm{P}^*}}\triangle_1 + \Delta m_{\mathrm{PP}^*}, -\frac{1}{2\tilde{m}_{\mathrm{P}^*\mathrm{P}^*}}\triangle_3 + \Delta m_{\mathrm{PP}^*}\right), \tag{A.56}$$

where $\triangle_l = \frac{\partial^2}{\partial r^2} + \frac{2}{r}\frac{\partial}{\partial r} - \frac{l(l+1)}{r^2}$ with integer $l \geq 0$, $1/\tilde{m}_{\mathrm{PP}} = 1/m_{\mathrm{P}} + 1/m_{\mathrm{P}}$, $1/\tilde{m}_{\mathrm{PP}^*} = 1/m_{\mathrm{P}} + 1/m_{\mathrm{P}^*}$, $1/\tilde{m}_{\mathrm{P}^*\mathrm{P}^*} = 1/m_{\mathrm{P}^*} + 1/m_{\mathrm{P}^*}$.

The π exchange potentials for each $I(J^P)$ states are

$$V^{\pi}_{0(0^-)} = \left(V^{\pi}_{\rm C} + 2V^{\pi}_{\rm T}\right), \tag{A.57}$$

$$V^{\pi}_{0(1^+)} = \begin{pmatrix} -V^{\pi}_{\rm C} & \sqrt{2}V^{\pi}_{\rm T} & 2V^{\pi}_{\rm C} & \sqrt{2}V^{\pi}_{\rm T} \\ \sqrt{2}V^{\pi}_{\rm T} & -V^{\pi}_{\rm C} - V^{\pi}_{\rm T} & \sqrt{2}V^{\pi}_{\rm T} & 2V^{\pi}_{\rm C} - V^{\pi}_{\rm T} \\ 2V^{\pi}_{\rm C} & \sqrt{2}V^{\pi}_{\rm T} & -V^{\pi}_{\rm C} & \sqrt{2}V^{\pi}_{\rm T} \\ \sqrt{2}V^{\pi}_{\rm T} & 2V^{\pi}_{\rm C} - V^{\pi}_{\rm T} & \sqrt{2}V^{\pi}_{\rm T} & -V^{\pi}_{\rm C} - V^{\pi}_{\rm T} \end{pmatrix}, \tag{A.58}$$

$$V^{\pi}_{0(1^-)} = \begin{pmatrix} 0 & 0 & -\sqrt{3}V^{\pi}_{\rm C} & -2\sqrt{\frac{3}{5}}V^{\pi}_{\rm T} & 3\sqrt{\frac{2}{5}}V^{\pi}_{\rm T} \\ 0 & V^{\pi}_{\rm C} - V^{\pi}_{\rm T} & 0 & -3\sqrt{\frac{3}{5}}V^{\pi}_{\rm T} & -3\sqrt{\frac{2}{5}}V^{\pi}_{\rm T} \\ -\sqrt{3}V^{\pi}_{\rm C} & 0 & -2V^{\pi}_{\rm C} & \frac{2}{\sqrt{5}}V^{\pi}_{\rm T} & -\sqrt{\frac{6}{5}}V^{\pi}_{\rm T} \\ -2\sqrt{\frac{3}{5}}V^{\pi}_{\rm T} & -3\sqrt{\frac{3}{5}}V^{\pi}_{\rm T} & \frac{2}{\sqrt{5}}V^{\pi}_{\rm T} & V^{\pi}_{\rm C} - \frac{7}{5}V^{\pi}_{\rm T} & \frac{\sqrt{6}}{5}V^{\pi}_{\rm T} \\ 3\sqrt{\frac{2}{5}}V^{\pi}_{\rm T} & -3\sqrt{\frac{2}{5}}V^{\pi}_{\rm T} & -\sqrt{\frac{6}{5}}V^{\pi}_{\rm T} & \frac{\sqrt{6}}{5}V^{\pi}_{\rm T} & V^{\pi}_{\rm C} - \frac{8}{5}V^{\pi}_{\rm T} \end{pmatrix}, \tag{A.59}$$

$$V^{\pi}_{0(2^+)} = \begin{pmatrix} -V^{\pi}_{\rm C} + V^{\pi}_{\rm T} & 2V^{\pi}_{\rm C} + V^{\pi}_{\rm T} \\ 2V^{\pi}_{\rm C} + V^{\pi}_{\rm T} & -V^{\pi}_{\rm C} + V^{\pi}_{\rm T} \end{pmatrix}, \tag{A.60}$$

$$V^{\pi}_{0(2^-)} = \begin{pmatrix} V^{\pi}_{\rm C} + \frac{1}{5}V^{\pi}_{\rm T} & -\frac{3\sqrt{6}}{5}V^{\pi}_{\rm T} & \frac{3\sqrt{3}}{5}V^{\pi}_{\rm T} & -\frac{6\sqrt{3}}{5}V^{\pi}_{\rm T} \\ -\frac{3\sqrt{6}}{5}V^{\pi}_{\rm T} & V^{\pi}_{\rm C} + \frac{4}{5}V^{\pi}_{\rm T} & \frac{3\sqrt{2}}{5}V^{\pi}_{\rm T} & -\frac{6\sqrt{2}}{5}V^{\pi}_{\rm T} \\ \frac{3\sqrt{3}}{5}V^{\pi}_{\rm T} & \frac{3\sqrt{2}}{5}V^{\pi}_{\rm T} & V^{\pi}_{\rm C} + \frac{7}{5}V^{\pi}_{\rm T} & \frac{6}{5}V^{\pi}_{\rm T} \\ -\frac{6\sqrt{3}}{5}V^{\pi}_{\rm T} & -\frac{6\sqrt{2}}{5}V^{\pi}_{\rm T} & \frac{6}{5}V^{\pi}_{\rm T} & V^{\pi}_{\rm C} - \frac{2}{5}V^{\pi}_{\rm T} \end{pmatrix}. \tag{A.61}$$

$$V^{\pi}_{1(0^+)} = \begin{pmatrix} 0 & -\sqrt{3}V^{\pi}_{\rm C} & \sqrt{6}V^{\pi}_{\rm T} \\ -\sqrt{3}V^{\pi}_{\rm C} & -2V^{\pi}_{\rm C} & -\sqrt{2}V^{\pi}_{\rm T} \\ \sqrt{6}V^{\pi}_{\rm T} & -\sqrt{2}V^{\pi}_{\rm T} & V^{\pi}_{\rm C} - 2V^{\pi}_{\rm T} \end{pmatrix}, \tag{A.62}$$

$$V^{\pi}_{1(0^-)} = \begin{pmatrix} -V^{\pi}_{\rm C} - 2V^{\pi}_{\rm T} & 2V^{\pi}_{\rm C} - 2V^{\pi}_{\rm T} \\ 2V^{\pi}_{\rm C} - 2V^{\pi}_{\rm T} & -V^{\pi}_{\rm C} - 2V^{\pi}_{\rm T} \end{pmatrix}, \tag{A.63}$$

$$V^{\pi}_{1(1^+)} = \begin{pmatrix} V^{\pi}_{\rm C} & -\sqrt{2}V^{\pi}_{\rm T} & -\sqrt{6}V^{\pi}_{\rm T} \\ -\sqrt{2}V^{\pi}_{\rm T} & V^{\pi}_{\rm C} + V^{\pi}_{\rm T} & -\sqrt{3}V^{\pi}_{\rm T} \\ -\sqrt{6}V^{\pi}_{\rm T} & -\sqrt{3}V^{\pi}_{\rm T} & V^{\pi}_{\rm C} - V^{\pi}_{\rm T} \end{pmatrix}, \tag{A.64}$$

$$V^{\pi}_{1(1^-)} = \begin{pmatrix} -V^{\pi}_{\rm C} + V^{\pi}_{\rm T} & -2V^{\pi}_{\rm C} - V^{\pi}_{\rm T} \\ -2V^{\pi}_{\rm C} - V^{\pi}_{\rm T} & -V^{\pi}_{\rm C} + V^{\pi}_{\rm T} \end{pmatrix}, \tag{A.65}$$

$$V^{\pi}_{1(2^+)} = \begin{pmatrix} 0 & 0 & -\sqrt{3}V^{\pi}_{\rm C} & \sqrt{\frac{6}{5}}V^{\pi}_{\rm T} & -2\sqrt{\frac{3}{7}}V^{\pi}_{\rm T} & 6\sqrt{\frac{3}{35}}V^{\pi}_{\rm T} \\ 0 & V^{\pi}_{\rm C} - V^{\pi}_{\rm T} & 0 & 3\sqrt{\frac{2}{5}}V^{\pi}_{\rm T} & -\frac{3}{\sqrt{7}}V^{\pi}_{\rm T} & -\frac{12}{\sqrt{35}}V^{\pi}_{\rm T} \\ -\sqrt{3}V^{\pi}_{\rm C} & 0 & -2V^{\pi}_{\rm C} & -\sqrt{\frac{2}{5}}V^{\pi}_{\rm T} & \frac{2}{\sqrt{7}}V^{\pi}_{\rm T} & -\frac{6}{\sqrt{35}}V^{\pi}_{\rm T} \\ \sqrt{\frac{6}{5}}V^{\pi}_{\rm T} & 3\sqrt{\frac{3}{5}}V^{\pi}_{\rm T} & -\sqrt{\frac{2}{5}}V^{\pi}_{\rm T} & V^{\pi}_{\rm C} & \sqrt{\frac{14}{5}}V^{\pi}_{\rm T} & 0 \\ -2\sqrt{\frac{3}{7}}V^{\pi}_{\rm T} & -\frac{3}{\sqrt{7}}V^{\pi}_{\rm T} & \frac{2}{\sqrt{7}}V^{\pi}_{\rm T} & \sqrt{\frac{14}{5}}V^{\pi}_{\rm T} & V^{\pi}_{\rm C} + \frac{3}{7}V^{\pi}_{\rm T} & \frac{12}{7\sqrt{5}}V^{\pi}_{\rm T} \\ 6\sqrt{\frac{3}{35}}V^{\pi}_{\rm T} & -\frac{12}{\sqrt{35}}V^{\pi}_{\rm T} & -\frac{6}{\sqrt{35}}V^{\pi}_{\rm T} & 0 & \frac{12}{7\sqrt{5}}V^{\pi}_{\rm T} & V^{\pi}_{\rm C} - \frac{10}{7}V^{\pi}_{\rm T} \end{pmatrix}, \tag{A.66}$$

$$V^{\pi}_{1(2^-)} = \begin{pmatrix} -V^{\pi}_{\rm C} - \frac{1}{5}V^{\pi}_{\rm T} & \frac{3\sqrt{6}}{5}V^{\pi}_{\rm T} & 2V^{\pi}_{\rm C} - \frac{1}{5}V^{\pi}_{\rm T} & \frac{3\sqrt{6}}{5}V^{\pi}_{\rm T} \\ \frac{3\sqrt{6}}{5}V^{\pi}_{\rm T} & -V^{\pi}_{\rm C} - \frac{4}{5}V^{\pi}_{\rm T} & \frac{3\sqrt{6}}{5}V^{\pi}_{\rm T} & 2V^{\pi}_{\rm C} - \frac{4}{5}V^{\pi}_{\rm T} \\ 2V^{\pi}_{\rm C} - \frac{1}{5}V^{\pi}_{\rm T} & \frac{3\sqrt{6}}{5}V^{\pi}_{\rm T} & -V^{\pi}_{\rm C} - \frac{1}{5}V^{\pi}_{\rm T} & \frac{3\sqrt{6}}{5}V^{\pi}_{\rm T} \\ \frac{3\sqrt{6}}{5}V^{\pi}_{\rm T} & 2V^{\pi}_{\rm C} - \frac{4}{5}V^{\pi}_{\rm T} & \frac{3\sqrt{6}}{5}V^{\pi}_{\rm T} & -V^{\pi}_{\rm C} - \frac{4}{5}V^{\pi}_{\rm T} \end{pmatrix}, \tag{A.67}$$

The ρ and ω potentials are

$$V^v_{0(0^-)} = \left(2V^v_{\rm C} - 2V^v_{\rm T} + V^{v\prime}_{\rm C}\right), \tag{A.68}$$

$$V^v_{0(1^+)} = \begin{pmatrix} -2V^v_{\rm C}+V^{v\prime}_{\rm C} & -\sqrt{2}V^v_{\rm T} & 4V^v_{\rm C} & -\sqrt{2}V^v_{\rm T} \\ -\sqrt{2}V^v_{\rm T} & -2V^v_{\rm C}+V^v_{\rm T}+V^{v\prime}_{\rm C} & -\sqrt{2}V^v_{\rm T} & 4V^v_{\rm C}+V^v_{\rm T} \\ 4V^v_{\rm C} & -\sqrt{2}V^v_{\rm T} & -2V^v_{\rm C}+V^{v\prime}_{\rm C} & -\sqrt{2}V^v_{\rm T} \\ -\sqrt{2}V^v_{\rm T} & 4V^v_{\rm C}+V^v_{\rm T} & -\sqrt{2}V^v_{\rm T} & -2V^v_{\rm C}+V^v_{\rm T}+V^{v\prime}_{\rm C} \end{pmatrix}, \tag{A.69}$$

$$V^v_{0(1^-)} = \begin{pmatrix} V^{v\prime}_{\rm C} & 0 & -2\sqrt{3}V^v_{\rm C} & 2\sqrt{\frac{3}{5}}V^v_{\rm T} & -3\sqrt{\frac{2}{5}}V^v_{\rm T} \\ 0 & 2V^v_{\rm C}+V^v_{\rm T}+V^{v\prime}_{\rm C} & 0 & 3\sqrt{\frac{3}{5}}V^v_{\rm T} & -3\sqrt{\frac{2}{5}}V^v_{\rm T} \\ -2\sqrt{3}V^v_{\rm C} & 0 & -4V^v_{\rm C}+V^{v\prime}_{\rm C} & -\frac{2}{\sqrt{5}}V^v_{\rm T} & \sqrt{\frac{6}{5}}V^v_{\rm T} \\ 2\sqrt{\frac{3}{5}}V^v_{\rm T} & 3\sqrt{\frac{3}{5}}V^v_{\rm T} & -\frac{2}{\sqrt{5}}V^v_{\rm T} & 2V^v_{\rm C}+\frac{7}{5}V^v_{\rm T}+V^{v\prime}_{\rm C} & -\frac{\sqrt{6}}{5}V^v_{\rm T} \\ -3\sqrt{\frac{2}{5}}V^v_{\rm T} & -3\sqrt{\frac{2}{5}}V^v_{\rm T} & \sqrt{\frac{6}{5}}V^v_{\rm T} & -\frac{\sqrt{6}}{5}V^v_{\rm T} & 2V^v_{\rm C}+\frac{8}{5}V^v_{\rm T}+V^{v\prime}_{\rm C} \end{pmatrix}, \tag{A.70}$$

$$V^v_{0(2^+)} = \begin{pmatrix} -2V^v_{\rm C}-V^v_{\rm T}+V^{v\prime}_{\rm C} & 4V^v_{\rm C}-V^v_{\rm T} \\ 4V^v_{\rm C}-V^v_{\rm T} & -2V^v_{\rm C}-V^v_{\rm T}+V^{v\prime}_{\rm C} \end{pmatrix}, \tag{A.71}$$

$$V^v_{0(2^-)} = \begin{pmatrix} 2V^v_{\rm C}-\frac{1}{5}V^v_{\rm T}+V^{v\prime}_{\rm C} & \frac{3\sqrt{6}}{5}V^v_{\rm T} & -\frac{3\sqrt{3}}{5}V^v_{\rm T} & \frac{6\sqrt{3}}{5}V^v_{\rm T} \\ \frac{3\sqrt{6}}{5}V^v_{\rm T} & 2V^v_{\rm C}-\frac{4}{5}V^v_{\rm T}+V^{v\prime}_{\rm C} & -\frac{3\sqrt{2}}{5}V^v_{\rm T} & \frac{6\sqrt{2}}{5}V^v_{\rm T} \\ -\frac{3\sqrt{3}}{5}V^v_{\rm T} & -\frac{3\sqrt{2}}{5}V^v_{\rm T} & 2V^v_{\rm C}-\frac{7}{5}V^v_{\rm T}+V^{v\prime}_{\rm C} & -\frac{6}{5}V^v_{\rm T} \\ \frac{6\sqrt{3}}{5}V^v_{\rm T} & \frac{6\sqrt{2}}{5}V^v_{\rm T} & -\frac{6}{5}V^v_{\rm T} & 2V^v_{\rm C}+\frac{2}{5}V^v_{\rm T}+V^{v\prime}_{\rm C} \end{pmatrix}, \tag{A.72}$$

$$V^v_{1(0^+)} = \begin{pmatrix} V^{v\prime}_{\rm C} & -2\sqrt{3}V^v_{\rm C} & -\sqrt{6}V^v_{\rm T} \\ -2\sqrt{3}V^v_{\rm C} & -4V^v_{\rm C}+V^{v\prime}_{\rm C} & \sqrt{2}V^v_{\rm T} \\ -\sqrt{6}V^v_{\rm T} & \sqrt{2}V^v_{\rm T} & 2V^v_{\rm C}+2V^v_{\rm T}+V^{v\prime}_{\rm C} \end{pmatrix}, \tag{A.73}$$

$$V^v_{1(0^-)} = \begin{pmatrix} -2V^v_{\rm C}+2V^v_{\rm T}+V^{v\prime}_{\rm C} & 4V^v_{\rm C}+2V^v_{\rm T} \\ 4V^v_{\rm C}+2V^v_{\rm T} & -2V^v_{\rm C}+2V^v_{\rm T}+V^{v\prime}_{\rm C} \end{pmatrix}, \tag{A.74}$$

$$V^v_{1(1^+)} = \begin{pmatrix} 2V^v_{\rm C}+V^{v\prime}_{\rm C} & \sqrt{2}V^v_{\rm T} & \sqrt{6}V^v_{\rm T} \\ \sqrt{2}V^v_{\rm T} & 2V^v_{\rm C}-V^v_{\rm T}+V^{v\prime}_{\rm C} & \sqrt{3}V^v_{\rm T} \\ \sqrt{6}V^v_{\rm T} & \sqrt{3}V^v_{\rm T} & 2V^v_{\rm C}+V^v_{\rm T}+V^{v\prime}_{\rm C} \end{pmatrix}, \tag{A.75}$$

$$V^v_{1(1^-)} = \begin{pmatrix} -2V^v_{\rm C}-V^v_{\rm T}+V^{v\prime}_{\rm C} & -4V^v_{\rm C}+V^v_{\rm T} \\ -4V^v_{\rm C}+V^v_{\rm T} & -2V^v_{\rm C}-V^v_{\rm T}+V^{v\prime}_{\rm C} \end{pmatrix}, \tag{A.76}$$

$$V^v_{1(2^+)} = \begin{pmatrix} V^{v\prime}_{\rm C} & 0 & -2\sqrt{3}V^v_{\rm C} & -\sqrt{\frac{6}{5}}V^v_{\rm T} & 2\sqrt{\frac{3}{7}}V^v_{\rm T} & -6\sqrt{\frac{3}{35}}V^v_{\rm T} \\ 0 & 2V^v_{\rm C}+V^v_{\rm T}+V^{v\prime}_{\rm C} & 0 & -3\sqrt{\frac{2}{5}}V^v_{\rm T} & \frac{3}{\sqrt{7}}V^v_{\rm T} & \frac{12}{\sqrt{35}}V^v_{\rm T} \\ -2\sqrt{3}V^v_{\rm C} & 0 & -4V^v_{\rm C}+V^{v\prime}_{\rm C} & \sqrt{\frac{2}{5}}V^v_{\rm T} & -\frac{2}{\sqrt{7}}V^v_{\rm T} & \frac{6}{\sqrt{35}}V^v_{\rm T} \\ -\sqrt{\frac{6}{5}}V^v_{\rm T} & 3\sqrt{\frac{3}{5}}V^v_{\rm T} & \sqrt{\frac{2}{5}}V^v_{\rm T} & 2V^v_{\rm C}+V^{v\prime}_{\rm C} & -\sqrt{\frac{14}{5}}V^v_{\rm T} & 0 \\ 2\sqrt{\frac{3}{7}}V^v_{\rm T} & \frac{3}{\sqrt{7}}V^v_{\rm T} & -\frac{2}{\sqrt{7}}V^v_{\rm T} & -\sqrt{\frac{14}{5}}V^v_{\rm T} & 2V^v_{\rm C}-\frac{3}{7}V^v_{\rm T}+V^{v\prime}_{\rm C} & -\frac{12}{7\sqrt{5}}V^v_{\rm T} \\ -6\sqrt{\frac{3}{35}}V^v_{\rm T} & \frac{12}{\sqrt{35}}V^v_{\rm T} & \frac{6}{\sqrt{35}}V^v_{\rm T} & 0 & -\frac{12}{7\sqrt{5}}V^v_{\rm T} & 2V^v_{\rm C}+\frac{10}{7}V^v_{\rm T}+V^{v\prime}_{\rm C} \end{pmatrix}, \tag{A.77}$$

$$V^v_{1(2^-)} = \begin{pmatrix} -2V^v_{\rm C}+\frac{1}{5}V^v_{\rm T}+V^{v\prime}_{\rm C} & -\frac{3\sqrt{6}}{5}V^v_{\rm T} & 4V^v_{\rm C}+\frac{1}{5}V^v_{\rm T} & -\frac{3\sqrt{6}}{5}V^v_{\rm T} \\ -\frac{3\sqrt{6}}{5}V^v_{\rm T} & -2V^v_{\rm C}+\frac{4}{5}V^v_{\rm T}+V^{v\prime}_{\rm C} & -\frac{3\sqrt{6}}{5}V^v_{\rm T} & 4V^v_{\rm C}+\frac{4}{5}V^v_{\rm T} \\ 4V^v_{\rm C}+\frac{1}{5}V^v_{\rm T} & -\frac{3\sqrt{6}}{5}V^v_{\rm T} & -2V^v_{\rm C}+\frac{1}{5}V^v_{\rm T}+V^{v\prime}_{\rm C} & -\frac{3\sqrt{6}}{5}V^v_{\rm T} \\ -\frac{3\sqrt{6}}{5}V^v_{\rm T} & 4V^v_{\rm C}+\frac{4}{5}V^v_{\rm T} & -\frac{3\sqrt{6}}{5}V^v_{\rm T} & -2V^v_{\rm C}+\frac{4}{5}V^v_{\rm T}+V^{v\prime}_{\rm C} \end{pmatrix}. \tag{A.78}$$

where the central and tensor potentials are defined as,

$$V_{\rm C}^{\pi} = \left(\sqrt{2}\frac{g}{f_\pi}\right)^2 \frac{1}{3} C(r;m_\pi)\vec{\tau}_1\cdot\vec{\tau}_2\,, \tag{A.79}$$

$$V_{\rm T}^{\pi} = \left(\sqrt{2}\frac{g}{f_\pi}\right)^2 \frac{1}{3} T(r;m_\pi)\vec{\tau}_1\cdot\vec{\tau}_2\,, \tag{A.80}$$

$$V_{\rm C}^{\rho} = (2\lambda g_V)^2 \frac{1}{3} C(r;m_\rho)\vec{\tau}_1\cdot\vec{\tau}_2\,, \tag{A.81}$$

$$V_{\rm C}^{\omega} = (2\lambda g_V)^2 \frac{1}{3} C(r;m_\omega)\,, \tag{A.82}$$

$$V_{\rm T}^{\rho} = (2\lambda g_V)^2 \frac{1}{3} T(r;m_\rho)\vec{\tau}_1\cdot\vec{\tau}_2\,, \tag{A.83}$$

$$V_{\rm T}^{\omega} = (2\lambda g_V)^2 \frac{1}{3} T(r;m_\omega)\,, \tag{A.84}$$

$$V_{\rm C}^{\rho\prime} = \left(\frac{\beta g_V}{2m_\rho}\right)^2 \frac{1}{3} C(r;m_\rho)\vec{\tau}_1\cdot\vec{\tau}_2\,, \tag{A.85}$$

$$V_{\rm C}^{\omega\prime} = \left(\frac{\beta g_V}{2m_\omega}\right)^2 \frac{1}{3} C(r;m_\omega)\,. \tag{A.86}$$

Appendix B

Passarino-Veltman Integrals

In this chapter, we present the Passarino-Veltman formalism, which is a useful tool to calculate the one loop integrals.

B.1 The general definition

We write the general forms of one-loop tensor intergral as

$$T_n^{\mu_1\cdots\mu_p} \equiv \frac{(2\pi\mu)^{4-d}}{i\pi^2}\int d^dk \frac{k^{\mu_1}\cdots k^{\mu_p}}{D_0D_1D_2\cdots D_{n-1}}\,, \tag{B.1}$$

where $d = 4-\epsilon$ is the space-time dimension shifted by ϵ. D_i comes from the momenta of propagators following the conventions of Fig. B.1 and given as

$$D_i = (k+r_i)^2 - m_i^2 + i\epsilon\,, \tag{B.2}$$

and the momenta r_i are related with the external momenta through the relations,

$$\begin{aligned} r_j &= \sum_{i=1}^{j} p_i \;;\; j = 1,\cdots,n-1 \\ r_0 &= \sum_{i=1}^{n} p_1 = 0. \end{aligned} \tag{B.3}$$

From all those integrals in Eq. (B.1), the scalar integrals are paticularly important, then we define the notations for them. It can be shown that there are only four independent

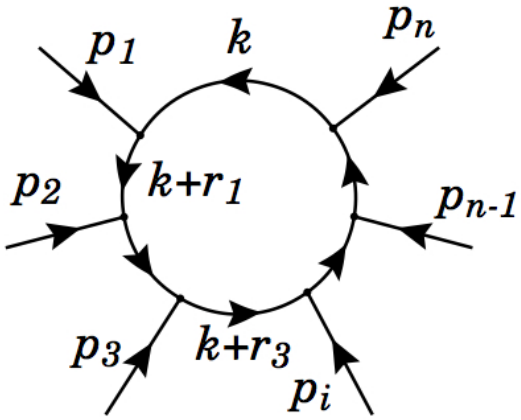

FIGURE B.1: The diagram of general one-loop integrals.

such integrals with $(4 - d = \epsilon)$ as follows:

$$A_0(m_0^2) = \frac{(2\pi\mu)^\epsilon}{i\pi^2}\int d^dk \frac{1}{k^2 - m_0}\,, \tag{B.4}$$

$$B_0(r_{10}^2, m_0^2, m_1^2) = \frac{(2\pi\mu)^\epsilon}{i\pi^2}\int d^dk \prod_{i=0}^{1}\frac{1}{[(k+r_i)^2 - m_i^2]} \tag{B.5}$$

$$C_0(r_{10}^2, r_{12}^2, r_{20}^2, m_0^2, m_1^2, m_2^2) = \frac{(2\pi\mu)^\epsilon}{i\pi^2}\int d^dk \prod_{i=0}^{2}\frac{1}{[(k+r_i)^2 - m_i^2]} \tag{B.6}$$

$$D_0(r_{10}^2, r_{12}^2, r_{23}^2, r_{30}^2, r_{20}^2, r_{13}^2, m_0^2, \cdots, m_3^2) = \frac{(2\pi\mu)^\epsilon}{i\pi^2}\int d^dk \prod_{i=0}^{3}\frac{1}{[(k+r_i)^2 - m_i^2]} \tag{B.7}$$

where

$$r_{ij}^2 = (r_i - r_j)^2 \quad ; \quad \forall i,j = (0, n-1) \tag{B.8}$$

Note that with our conventions $r_0 = 0$ and $r_{i0}^2 = r_i^2$. For sake of simplicity, the $i\epsilon$ part of the denomiantor factors is suppressed in all these expressions. The general one-loop tensor integrals are not independent, hence their decomposition is not unique. Following

the conventions used in [125], we write the tensor integrals as follows:

$$B^{\mu} \equiv \frac{(2\pi\mu)^{4-d}}{i\pi^2}\int d^d k k^{\mu}\prod_{i=1}^{1}\frac{1}{[(k+r_i)^2-m_i^2]} \tag{B.9}$$

$$B^{\mu\nu} \equiv \frac{(2\pi\mu)^{4-d}}{i\pi^2}\int d^d k k^{\mu}k^{\nu}\prod_{i=1}^{1}\frac{1}{[(k+r_i)^2-m_i^2]} \tag{B.10}$$

$$C^{\mu} \equiv \frac{(2\pi\mu)^{\epsilon}}{i\pi^2}\int d^d k k^{\mu}\prod_{i=0}^{2}\frac{1}{[(k+r_i)^2-m_i^2]} \tag{B.11}$$

$$C^{\mu\nu} \equiv \frac{(2\pi\mu)^{\epsilon}}{i\pi^2}\int d^d k k^{\mu}k^{\nu}\prod_{i=0}^{2}\frac{1}{[(k+r_i)^2-m_i^2]} \tag{B.12}$$

$$C^{\mu\nu\rho} \equiv \frac{(2\pi\mu)^{\epsilon}}{i\pi^2}\int d^d k k^{\mu}k^{\nu}k^{\rho}\prod_{i=0}^{2}\frac{1}{[(k+r_i)^2-m_i^2]} \tag{B.13}$$

$$D^{\mu} \equiv \frac{(2\pi\mu)^{\epsilon}}{i\pi^2}\int d^d k k^{\mu}\prod_{i=0}^{3}\frac{1}{[(k+r_i)^2-m_i^2]} \tag{B.14}$$

$$D^{\mu\nu} \equiv \frac{(2\pi\mu)^{\epsilon}}{i\pi^2}\int d^d k k^{\mu}k^{\nu}\prod_{i=0}^{3}\frac{1}{[(k+r_i)^2-m_i^2]} \tag{B.15}$$

$$D^{\mu\nu\rho} \equiv \frac{(2\pi\mu)^{\epsilon}}{i\pi^2}\int d^d k k^{\mu}k^{\nu}k^{\rho}\prod_{i=0}^{3}\frac{1}{[(k+r_i)^2-m_i^2]} \tag{B.16}$$

$$D^{\mu\nu\rho\sigma} \equiv \frac{(2\pi\mu)^{\epsilon}}{i\pi^2}\int d^d k k^{\mu}k^{\nu}k^{\rho}k^{\sigma}\prod_{i=0}^{3}\frac{1}{[(k+r_i)^2-m_i^2]}. \tag{B.17}$$

B.2 The tensor integrals decompostion

These integrals can be decomposed in terms of reducible functions as follows:

$$B^{\mu} = r_1^{\mu} B_1 \tag{B.18}$$

$$B^{\mu\nu} = g^{\mu\nu} B_{00} + r_1^{\mu} r_1^{\nu} B_{11} \tag{B.19}$$

$$C^{\mu} = r_1^{\mu} C_1 + r_2^{\mu} C_2 \tag{B.20}$$

$$C^{\mu\nu} = g^{\mu\nu} C_{00} + \sum_{i=1}^{2} r_i^{\mu} r_j^{\nu} C_{ij} \tag{B.21}$$

$$C^{\mu\nu\rho} = \sum_{i=1}^{2} (g^{\mu\nu} r_i^{\rho} + g^{\nu\rho} r_i^{\mu} + g^{\rho\mu} r_i^{\nu}) C_{00i} + \sum_{i,j,k=1}^{2} r_i^{\mu} r_j^{\nu} r_k^{\rho} C_{ijk} \tag{B.22}$$

$$D^{\mu} = \sum_{i=1}^{3} r_i^{\mu} D_i \tag{B.23}$$

$$D^{\mu\nu} = g^{\mu\nu} D_{00} + \sum_{i=1}^{3} r_i^{\mu} r_j^{\nu} D_{ij} \tag{B.24}$$

$$D^{\mu\nu\rho} = \sum_{i=1}^{3} (g^{\mu\nu} r_i^{\rho} + g^{\nu\rho} r_i^{\mu} + g^{\rho\mu} r_i^{\nu}) D_{00i} + \sum_{i,j,k=1}^{2} r_i^{\mu} r_j^{\nu} r_k^{\rho} D_{ijk} \tag{B.25}$$

$$\begin{aligned} D^{\mu\nu\rho\sigma} = {} & (g_{\mu\nu} g_{\rho\sigma} + g_{\mu\rho} g_{\nu\sigma} + g_{\mu\sigma} g_{\nu\rho}) D_{0000} + \sum_{i,j=1}^{3} \Big(g^{\mu\nu} r_i^{\rho} f_j^{\sigma} + g^{\nu\rho} r_i^{\mu} r_j^{\sigma} + g^{\mu\rho} r_i^{\nu} r_j^{\sigma} \\ & + g^{\mu\sigma} r_i^{\nu} r_j^{\rho} + g^{\nu\sigma} r_i^{\mu} r_j^{\rho} + g^{\rho\sigma} r_i^{\mu} r_j^{\nu} \Big) D_{00ij} + \sum_{i,j,k,l=1}^{3} r_i^{\mu} r_j^{\nu} r_k^{\rho} r_l^{\sigma} C_{ijkl}. \end{aligned} \tag{B.26}$$

All correspondig scalar functions such as B_1, C_{ij} , $\cdots$, are totally symmetric in their indices and can be explicilty calculated.

B.3 The reduced relations

The scalar functions, such as B_0, B_1, C_0, C_{00} and C_{12}, can be explicitly calculated, however they satisfy the useful relations. Note also that B_0, B_1, and C_{00} are divergent. By contracting C^{μ} with external momenta p_1^{μ} or p_2^{μ}, we obtain

$$C_{\mu} r_1^{\mu} = \frac{1}{2} B_0(r_2^2, m_0^2, m_2^2) - \frac{1}{2} B_0((r_1 - r_2)^2, m_1^2, m_2^2) - \frac{1}{2} [r_1^2 - m_1^2 + m_0^2] C_0 \tag{B.27}$$

$$C_{\mu} r_2^{\mu} = \frac{1}{2} B_0(r_1^2, m_0^2, m_2^2) - \frac{1}{2} B_0((r_1 - r_2)^2, m_1^2, m_2^2) - \frac{1}{2} [p_2^2 - m_2^2 + m_0^2] C_0 \tag{B.28}$$

Similarly, we obtain addtional relations by contradicting $C^{\mu\nu}$ with two external momenta as follows:

$$
\begin{aligned}
dC_{00} + C_{11}p_1^2 + 2C_{12}(p_1\cdot p_2) + C_{22}p_2^2 &= B_0((r_2-r_2)^2, m_1^2, m_2^2) + m_0^2 C_0 && \text{(B.29)}\\
C_{00} + C_{11}p_1^2 + C_{12}(p_1\cdot p_2) &= \frac{1}{2}B_1((r_2-r_1)^2, m_1^2, m_2^2) + \frac{1}{2}B_0((r_2-r_1)^2, m_1^2, m_2^2)\\
&\quad -\frac{1}{2}[p_1^2 - m_1^2 + m_0^2]C_1 && \text{(B.30)}\\
C_{12}p_1^2 + C_{22}(p_1\cdot p_2) &= \frac{1}{2}B_1(r_2^2, m_0^2, m_2^2) - \frac{1}{2}B_1((r_2-r_1)^2, m_1^2, m_2^2)\\
&\quad -\frac{1}{2}[p_1^2 - m_1^2 + m_0^2]C_2 && \text{(B.31)}\\
C_{11}(p_1\cdot p_2) + C_{12}p_2^2 &= \frac{1}{2}B_1(r_1^2, m_0^2, m_1^2) + \frac{1}{2}B_1((r_2-r_1)^2, m_1^2, m_2^2)\\
&\quad +\frac{1}{2}((r_2-r_1)^2, m_1^2, m_2^2) - \frac{1}{2}[p_2^2 - m_2^2 + m_0^2]C_1 && \text{(B.32)}\\
C_{00} + C_{12}(r_1\cdot r_2) + C_{22}r_2^2 &= -\frac{1}{2}B_1((r_2-r_1)^2, m_1^2, m_2^2) - \frac{1}{2}[p_2^2 - m_2^2 + m_0^2]C_2 && \text{(B.33)}
\end{aligned}
$$

where we can omit the tensor function of C.

B.4 Explicit expression scalar integrals

B.4.1 Explicit expression for A_0

This integral is trivial. There is no Feynman parameter and the integral can be deduced by dimensional regularization scheme. We obtain

$$A_0(m^2) = m^2\left(\Delta_\epsilon + 1 - \ln\frac{m^2}{\mu^2}\right), \tag{B.34}$$

where μ is the mass scale peculiar in the dimensional regualrization and we have introduced the notation

$$\Delta_\epsilon = \frac{2}{\epsilon} - \gamma\ln 4\pi, \tag{B.35}$$

for a combination that will appear in all expressions. This is the divergent part in the integrals.

B.4.2 Explicit expressions for the B functions

The loop function $B_0(p^2, m_1^2, m_2^2)$ can be calculated with Feynman parameters and dimensional regularization scheme as

$$B_0(p^2, m_0^2, m_1^2) = \Delta_\epsilon - \int_0^1 dx \ln\left[\frac{-x(1-x)p^2 + xm_1^2 + (1-x)m_0^2}{\mu^2}\right]. \tag{B.36}$$

In the same way, we obtain the explicit expression of B_1 as

$$B_1(p^2, m_0^2, m_1^2) = -\frac{1}{2}\Delta_\epsilon + \int_0^1 dx x \ln\left[\frac{-x(1-x)p^2 + xm_1^2 + (1-x)m_0^2}{\mu^2}\right]. \tag{B.37}$$

It should be noted that B_1 is not a symmetric function of the masses,

$$B_1(p^2, m_0^2, m_1^2) \neq B_1(p^2, m_1^2, m_0^2). \tag{B.38}$$

B.4.3 Explicit expressions for the C functions

The explicit expressions of C functions are given as follows

$$\begin{aligned}
C_0(r_1^2, r_{12}, r_2^2, m_0^2, m_1^2, m_2^2) &= -\Gamma(3)\frac{1}{2}\int_0^1 dx_1 \int_0^{1-x_1} dx_2 \frac{1}{C} && \text{(B.39)}\\
C_i(r_1^2, r_{12}, r_2^2, m_0^2, m_1^2, m_2^2) &= \Gamma(3)\frac{1}{2}\int_0^1 dx_1 \int_0^{1-x_1} dx_2 \frac{x_i}{C} && \text{(B.40)}\\
C_{12}(r_1^2, r_{12}, r_2^2, m_0^2, m_1^2, m_2^2) &= -\Gamma(3)\frac{2}{4}\int_0^1 dx_1 \int_0^{1-x_1} dx_2 \frac{x_1 x_2}{C}, && \text{(B.41)}
\end{aligned}$$

with

$$\begin{aligned}
C &= x_1^2 r_1^2 + x_2^2 r_2^2 + x_1 x_2^2 (r_1^2 + r_2^2 - r_{12}^2) + x_1 m_1^2 + x_2 m_2^2 \\
&\quad + (1 - x_1 - x_2) m_0^2 - x_1 r_1^2 - x_2 r_2^2. && \text{(B.42)}
\end{aligned}$$

Appendix C

Interactions of exchanged mesons

C.1 Interactions of exchanged mesons

We consider the signs of meson-exchange contributions, π, ρ and ω in NN, $N\bar{N}$ potential.

$P^{(*)}\bar{P}^{(*)}$ and PP states are also discussed, where P stands for heavy mesons, $Q\bar{q}(Q = c, b)$. The potential for each mesons can be classified as three parts, namely spin-dependent part V_C', center force V_C and tensor force V_T, where we use the notation from the previous section.

NN potential

We consider the NN interaction by a nonrelativestic potential [126]. Table C.1 shows the signs of meson exchange contributions for NN potential. In $I = 0$ case, pion is attractive. For the ρ meson interaction, spin-dependent part $V_C^{\rho\prime}$ is attractive, but this contributions is small due to the weak coupling. The center force with the ρ meson, V_C^{ρ} enhances the center force attraction of pion, whereas the ρ meson tensor force V_T^{ρ} depresses the pion tensor force. For the ω meson exchange, spin-dependent part $V_C^{\omega\prime}$ is repulsive, which is stronger than the one of ρ meson, $V_C^{\rho\prime}$, due to the strong coupling. Meanwhile, the coupling for V_C^{ω} and V_T^{ω} is small and their interactions contribute oppositely to the ρ mesons. It is well known that NN with $I = 0$, so called deuteron, is weakly bound state.

In $I = 1$ case, since the ω meson is iso-scalar particle, the interactions are unchanged. In contrast, the pion and ρ mesons are iso-vector states, hence the sign

of interactions in $I = 1$ are opposite to the one in $I = 0$. As a result, most of channels are repulsive. Thus, the NN with $I = 1$ is an unbound state.

$N\bar{N}$ potential

Next, the sign of meson exchange contributions for $N\bar{N}$ potential are considered, which are summarized in Table C.2. The $N\bar{N}$ potential of medium and long range can be deduced from the corresponding NN potential by the G-parity rule, which states that contributions of mesons of odd G-parity change sign.

This modification is essentially important for considering the $N\bar{N}$ interaction. The ω exchange, which is repulsive for the NN state, becomes attractive for $N\bar{N}$. In addition to this, the $V_C^{\rho\prime}$ and V_C^{ρ} for ρ exchange are still repulsive, because of even G-parity for ρ. Thus, the central potential V_C is deeper for $N\bar{N}$ than for NN. In the case of $N\bar{N}$ interaction, all meson exchanges give a contributions of the same sign to the $I = 0$ potential. As a result, tensor force is enhanced compared with the case of NN in $I = 0$, hence we can see that the $N\bar{N}$ $I = 0$ tensor potential is by far the most important.

$P^{(*)}\bar{P}^{(*)}$ potential

Now we consider the potentials for the heavy meson molecules, $P^{(*)}\bar{P}^{(*)}$. It should be noted that the couplings are different to the NN and $N\bar{N}$ potentials. In particular, the coupling constants of ρ and ω are equivalent, hence the difference of their interactions are mainly sign and isospin factor. In the case of $I = 0$, the center and tensor force of pion, V_C^{π} and V_T^{π} are repulsive, whereas ρ and ω mesons enhance each other because of same sign of potential. This implies that the vector meson exchanges sometimes deduce the strong attraction in $P^{(*)}\bar{P}^{(*)}$ $I = 0$, which are ineligible compared with pion exchange.

In the case of $I = 1$, the sign of pion and ρ exchanges become opposite because of the isospin factor. Recall that the couplings of ρ and ω meson interactions are equivalent, we can see that their contributions compensate. Thus, we can expect that pion potential is dominant in the case of $P^{(*)}\bar{P}^{(*)}$ with $I = 1$.

$P^{(*)}P^{(*)}$ potential

The $P^{(*)}P^{(*)}$ potential can be deduced from the corresponding $P^{(*)}\bar{P}^{(*)}$ potential by the G-parity rule in the same way of obtaining the $N\bar{N}$ potential, which states that the sign of potentials of odd G-parity mesons are changed. In the case of $I = 0$, the pion potentials, V_C^{π} and V_T^{π}, are attractive. The center force of ρ exchange, V_C^{ρ} enhances the one of pion exchange, whereas the tensor force of is

weaken the one of pion exchange. The sign of ω potentials are opposite to the one of ρ. These sign relations are equivalent to the NN in $I = 0$ state, however it should be noted that $V_C^{\omega\prime}$ is not stronger than $V_C^{\rho\prime}$ unlike the case of NN potentials. Hence, the vector meson contributions from $V_C^{v\prime}$ and V_C^{v} are still attractive.

The isospin factor changes the sign of contributions of pion and ρ meson exchanges. In this case, most of channels are repulsive.

TABLE C.1: Signs of meson exchange contributions to V_C', V_C and V_T for NN potentials.

	$I=0$			$I=1$		
Meson	V_C'	V_C	V_T	V_C'	V_C	V_T
π	0	$-$	$-$	0	$+$	$+$
ρ	$-$	$-$	$+$	$+$	$+$	$-$
ω	$+$	$+$	$-$	$+$	$+$	$-$

TABLE C.2: Signs of meson exchange contributions to V_C', V_C and V_T for NN potentials.

	$I=0$			$I=1$		
Meson	V_C'	V_C	V_T	V_C'	V_C	V_T
π	0	$+$	$+$	0	$-$	$-$
ρ	$-$	$-$	$+$	$+$	$+$	$-$
ω	$-$	$-$	$+$	$-$	$-$	$+$

TABLE C.3: Signs of meson exchange contributions to V_C', V_C and V_T for $P^{(*)}\bar{P}^{(*)}$ potentials.

	$I=0$			$I=1$		
Meson	V_C'	V_C	V_T	V_C'	V_C	V_T
π	0	$+$	$+$	0	$-$	$-$
ρ	$-$	$-$	$+$	$+$	$+$	$-$
ω	$-$	$-$	$+$	$-$	$-$	$+$

TABLE C.4: Signs of meson exchange contributions to V_C', V_C and V_T for $P^{(\prime)}P^{(*)}$ potentials.

	$I=0$			$I=1$		
Meson	V_C'	V_C	V_T	V_C'	V_C	V_T
π	0	$-$	$-$	0	$+$	$+$
ρ	$-$	$-$	$+$	$+$	$+$	$-$
ω	$+$	$+$	$-$	$+$	$+$	$-$

Appendix D

The properties of heavy meson molecules in heavy quark limit

D.1 The expressions in HQS basis for PP states

Here, we show the expressions in HQS basis for PP states. They are transformed by unitari matrix $U_{I(J^P)}$ from the paritcle basis.

The transformations for the $I(J^P) = 0(0^-)$ state:

$$|\frac{1}{\sqrt{2}}(P\bar{P}^* + P^*\bar{P})(^3P_0)\rangle = U_{0(0^-)}\,|1_H, 1_q, 1_L, 1_l; 0\rangle\ , \tag{D.1}$$

$$U_{0(0^-)} = 1. \tag{D.2}$$

The transformations for the $0(1^+)$ state:

$$\begin{pmatrix} |\frac{1}{\sqrt{2}}(P\bar{P}^* - P^*\bar{P})(^3S_1)\rangle \\ |\frac{1}{\sqrt{2}}(P\bar{P}^* - P^*\bar{P})(^3D_1)\rangle \\ |P^*\bar{P}^*(^3S_1)\rangle \\ |P^*\bar{P}^*(^3D_1)\rangle \end{pmatrix} = U_{0(1^+)} \begin{pmatrix} |0_H, 1_q, 0_L, 1_l; 1\rangle \\ |0_H, 1_q, 2_L, 1_l; 1\rangle \\ |1_H, 0_q, 0_L, 0_l; 1\rangle \\ |1_H, 0_1, 2_L, 2_l; 1\rangle \end{pmatrix} \tag{D.3}$$

$$U_{0(1^+)} = \begin{pmatrix} \frac{1}{\sqrt{2}} & 0 & -\frac{1}{\sqrt{2}} & 0 \\ 0 & \frac{1}{\sqrt{2}} & 0 & -\frac{1}{\sqrt{2}} \\ \frac{1}{\sqrt{2}} & 0 & \frac{1}{\sqrt{2}} & 0 \\ 0 & \frac{1}{\sqrt{2}} & 0 & \frac{1}{\sqrt{2}} \end{pmatrix}. \tag{D.4}$$

The transformations for the $0(1^-)$ state:

$$\begin{pmatrix} |P\bar{P}(^1P_1)\rangle \\ |\frac{1}{\sqrt{2}}(P\bar{P}^* + P^*\bar{P})(^3P_1)\rangle \\ |P^*\bar{P}^*(^1P_1)\rangle \\ |P^*\bar{P}^*(^5P_1)\rangle \\ |P^*\bar{P}^*(^5F_1)\rangle \end{pmatrix} = U_{0(1^-)} \begin{pmatrix} |1_H, 1_q, 1_L, 0_l; 1\rangle \\ |0_H, 0_q, 1_L, 1_l; 1\rangle \\ |1_H, 1_q, 1_L, 1_l; 1\rangle \\ |1_H, 1_q, 1_L, 2_l; 1\rangle \\ |1_H, 1_1, 3_L, 2_l; 1\rangle \end{pmatrix} \tag{D.5}$$

$$U_{0(1^-)} = \begin{pmatrix} \frac{1}{2\sqrt{3}} & \frac{1}{2} & -\frac{1}{2} & \frac{\sqrt{\frac{5}{3}}}{2} & 0 \\ -\frac{1}{\sqrt{3}} & 0 & \frac{1}{2} & \frac{\sqrt{\frac{5}{3}}}{2} & 0 \\ -\frac{1}{6} & \frac{\sqrt{3}}{2} & \frac{1}{2\sqrt{3}} & -\frac{\sqrt{5}}{6} & 0 \\ \frac{\sqrt{5}}{3} & 0 & \frac{\sqrt{\frac{5}{3}}}{2} & \frac{1}{6} & 0 \\ 0 & 0 & 0 & 0 & 1 \end{pmatrix}. \tag{D.6}$$

The transformations for the $0(2^+)$ state:

$$\begin{pmatrix} |\frac{1}{\sqrt{2}}(P\bar{P}^* - P^*\bar{P})(^3D_2)\rangle \\ |P^*\bar{P}^*(^3D_2)\rangle \end{pmatrix} = U_{0(2^+)} \begin{pmatrix} |0_H, 1_q, 2_L, 2_l; 2\rangle \\ |1_H, 0_q, 2_L, 2_l; 2\rangle \end{pmatrix} \tag{D.7}$$

$$U_{0(2^+)} = \begin{pmatrix} \frac{1}{\sqrt{2}} & -\frac{1}{\sqrt{2}} \\ \frac{1}{\sqrt{2}} & \frac{1}{\sqrt{2}} \end{pmatrix}. \tag{D.8}$$

The transformations for the $0(2^-)$ state:

$$\begin{pmatrix} |\frac{1}{\sqrt{2}}(P\bar{P}^* + P^*\bar{P})(^3P_2)\rangle \\ |\frac{1}{\sqrt{2}}(P\bar{P}^* + P^*\bar{P})(^3F_2)\rangle \\ |P^*\bar{P}^*(^5P_2)\rangle \\ |P^*\bar{P}^*(^5F_2)\rangle \end{pmatrix} = U_{0(2^-)} \begin{pmatrix} |1_H, 1_q, 1_L, 1_l; 2\rangle \\ |1_H, 1_q, 1_L, 2_l; 2\rangle \\ |1_H, 1_q, 3_L, 2_l; 2\rangle \\ |1_H, 1_q, 3_L, 3_l; 2\rangle \end{pmatrix}, \tag{D.9}$$

$$U_{0(2^-)} = \begin{pmatrix} -\frac{1}{2} & \frac{\sqrt{3}}{2} & 0 & 0 \\ 0 & 0 & -\frac{1}{\sqrt{3}} & \sqrt{\frac{2}{3}} \\ \frac{\sqrt{3}}{2} & \frac{1}{2} & 0 & 0 \\ 0 & 0 & \sqrt{\frac{2}{3}} & \frac{1}{\sqrt{3}} \end{pmatrix}. \tag{D.10}$$

The transformations for the $1(0^+)$ state:

$$\begin{pmatrix} |P\bar{P}(^1S_0)\rangle \\ |P^*\bar{P}^*(^1S_0)\rangle \\ |P^*\bar{P}^*(^5D_0)\rangle \end{pmatrix} = U_{1(0^+)} \begin{pmatrix} |0_H, 0_q, 0_L, 0_l; 0\rangle \\ |1_H, 1_q, 0_L, 1_l; 0\rangle \\ |1_H, 1_q, 2_L, 1_l; 0\rangle \end{pmatrix}, \tag{D.11}$$

$$U_{1(0^+)} = \begin{pmatrix} \frac{1}{2} & \frac{\sqrt{3}}{2} & 0 \\ \frac{\sqrt{3}}{2} & -\frac{1}{2} & 0 \\ 0 & 0 & 1 \end{pmatrix}. \tag{D.12}$$

The transformations for the $1(0^-)$ state:

$$\begin{pmatrix} |\frac{1}{\sqrt{2}}(P\bar{P}^* - P^*\bar{P})(^3P_0)\rangle \\ |P^*\bar{P}^*(^3P_0)\rangle \end{pmatrix} = U_{1(0^-)} \begin{pmatrix} |0_H, 1_q, 1_L, 0_l; 0\rangle \\ |1_H, 0_q, 1_L, 1_l; 0\rangle \end{pmatrix}, \tag{D.13}$$

$$U_{1(0^-)} = \begin{pmatrix} \frac{1}{\sqrt{2}} & -\frac{1}{\sqrt{2}} \\ \frac{1}{\sqrt{2}} & \frac{1}{\sqrt{2}} \end{pmatrix}. \tag{D.14}$$

The transformations for the $1(1^+)$ state:

$$\begin{pmatrix} |\frac{1}{\sqrt{2}}(P\bar{P}^* + P^*\bar{P})(^3S_1)\rangle \\ |\frac{1}{\sqrt{2}}(P\bar{P}^* + P^*\bar{P})(^3D_1)\rangle \\ |P^*\bar{P}^*(^5D_1)\rangle \end{pmatrix} = U_{1(1^+)} \begin{pmatrix} |1_H, 1_q, 0_L, 1_l; 1\rangle \\ |1_H, 1_q, 2_L, 1_l; 1\rangle \\ |1_H, 1_q, 2_L, 2_l; 1\rangle \end{pmatrix} \tag{D.15}$$

$$U_{1(1^+)} = \begin{pmatrix} 1 & 0 & 0 \\ 0 & -\frac{1}{2} & \frac{\sqrt{3}}{2} \\ 0 & \frac{\sqrt{3}}{2} & \frac{1}{2} \end{pmatrix}. \tag{D.16}$$

The transformations for the $1(1^-)$ state:

$$\begin{pmatrix} |\frac{1}{\sqrt{2}}(P\bar{P}^* - P^*\bar{P})(^3P_1)\rangle \\ |P^*\bar{P}^*(^3P_1)\rangle \end{pmatrix} = U_{1(1^-)} \begin{pmatrix} |0_H, 1_q, 1_L, 1_l; 1\rangle \\ |1_H, 0_q, 1_L, 1_l; 1\rangle \end{pmatrix} \tag{D.17}$$

$$U_{1(1^-)} = \begin{pmatrix} \frac{1}{\sqrt{2}} & -\frac{1}{\sqrt{2}} \\ \frac{1}{\sqrt{2}} & \frac{1}{\sqrt{2}} \end{pmatrix}. \tag{D.18}$$

The transformations for the $1(2^+)$ state:

$$\begin{pmatrix} |P\bar{P}(^1D_2)\rangle \\ |\frac{1}{\sqrt{2}}(P\bar{P}^* + P^*\bar{P})(^3D_2)\rangle \\ |P^*\bar{P}^*(^1D_2)\rangle \\ |P^*\bar{P}^*(^5S_2)\rangle \\ |P^*\bar{P}^*(^5D_2)\rangle \\ |P^*\bar{P}^*(^5G_2)\rangle \end{pmatrix} = U_{1(2^+)} \begin{pmatrix} |1_H, 1_q, 0_L, 1_l; 2\rangle \\ |1_H, 1_q, 2_L, 1_l; 2\rangle \\ |0_H, 0_q, 2_L, 2_l; 2\rangle \\ |1_H, 1_q, 2_L, 2_l; 2\rangle \\ |1_H, 1_q, 2_L, 3_l; 2\rangle \\ |1_H, 1_q, 4_L, 3_l; 2\rangle \end{pmatrix} \tag{D.19}$$

$$U_{1(2^+)} = \begin{pmatrix} 0 & \frac{\sqrt{\frac{3}{5}}}{2} & \frac{1}{2} & -\frac{1}{2} & \frac{\sqrt{\frac{7}{5}}}{2} & 0 \\ 0 & -\frac{3}{2\sqrt{5}} & 0 & \frac{1}{2\sqrt{3}} & \sqrt{\frac{7}{15}} & 0 \\ 0 & -\frac{1}{2\sqrt{5}} & \frac{\sqrt{3}}{2} & \frac{1}{2\sqrt{3}} & -\frac{\sqrt{\frac{7}{15}}}{2} & 0 \\ 1 & 0 & 0 & 0 & 0 & 0 \\ 0 & \frac{\sqrt{\frac{7}{5}}}{2} & 0 & \frac{\sqrt{\frac{7}{3}}}{2} & \frac{1}{\sqrt{15}} & 0 \\ 0 & 0 & 0 & 0 & 0 & 1 \end{pmatrix}. \tag{D.20}$$

The transformations for the $1(2^-)$ state:

$$\begin{pmatrix} |\frac{1}{\sqrt{2}}(P\bar{P}^* - P^*\bar{P})(^3P_2)\rangle \\ |\frac{1}{\sqrt{2}}(P\bar{P}^* - P^*\bar{P})(^3F_2)\rangle \\ |P^*\bar{P}^*(^3P_2)\rangle \\ |P^*\bar{P}^*(^3F_2)\rangle \end{pmatrix} = U_{1(2^-)} \begin{pmatrix} |1_H, 0_q, 1_L, 1_l; 2\rangle \\ |0_H, 1_q, 1_L, 2_l; 2\rangle \\ |0_H, 1_q, 3_L, 2_l; 2\rangle \\ |1_H, 0_q, 3_L, 3_l; 2\rangle \end{pmatrix}, \tag{D.21}$$

$$U_{1(2^-)} = \begin{pmatrix} -\frac{1}{\sqrt{2}} & \frac{1}{\sqrt{2}} & 0 & 0 \\ 0 & 0 & \frac{1}{\sqrt{2}} & -\frac{1}{\sqrt{2}} \\ \frac{1}{\sqrt{2}} & \frac{1}{\sqrt{2}} & 0 & 0 \\ 0 & 0 & \frac{1}{\sqrt{2}} & \frac{1}{\sqrt{2}} \end{pmatrix}. \tag{D.22}$$

D.2 The expressions of Hamiltonians with OPEP in heavy quark limit

Here we consider the Hamiltonians of $P^{(*)}\bar{P}^{(*)}$ states in heavy quark limit. We use the notations, K_l, C and T given in Chapter 7. The hamiltonians in HQS basis, H^{HQ}_{JPC}, are

transformed as,

$$H^{HQ}_{J^{PC}} = U^{-1}_{J^{PC}} H_{J^{PC}} U_{J^{PC}}. \tag{D.23}$$

As a consequence of heavy quark symmetry, we obtain the OPEP's as the block-diagonal forms with the HQS basis. The Hamiltonians with the block-diagonal forms for various quantum numbers are derived as follows:

$$\begin{aligned}
H^{HQ}_{0^{++}} &= U^{-1}_{0^{++}} H_{0^{++}} U_{0^{++}} \\
&= \left(\begin{array}{c|cc} K_0+3C & 0 & 0 \\ \hline 0 & K_0-C & -2\sqrt{2}T \\ 0 & -2\sqrt{2}T & K_2-C+2T \end{array}\right) \vec{\tau_1}\cdot\vec{\tau_2} && \text{(D.24)} \\
&= \left(\begin{array}{c|c} H^{(1,0)}_{0^{++}} & 0 \\ \hline 0 & H^{(1,1)}_{0^{++}} \end{array}\right) \vec{\tau_1}\cdot\vec{\tau_2}, && \text{(D.25)} \\
H^{HQ}_{0^{-+}} &= U^{-1}_{0^{-+}} H_{0^{-+}} U_{0^{-+}} \\
&= \left(\begin{array}{c|c} K_1-C+4T & 0 \\ \hline 0 & K_1+3C \end{array}\right) \vec{\tau_1}\cdot\vec{\tau_2} && \text{(D.26)} \\
&= \left(\begin{array}{c|c} H^{0,0}_{0^{-+}} & 0 \\ \hline 0 & H^{(1,1)}_{0^{-+}} \end{array}\right) \vec{\tau_1}\cdot\vec{\tau_2}, && \text{(D.27)} \\
H^{HQ}_{0^{--}} &= U^{-1}_{0^{--}} H_{0^{--}} U_{0^{--}} \\
&= (K_1-C-2T)\vec{\tau_1}\cdot\vec{\tau_2} && \text{(D.28)} \\
&= H^{(1,1)}_{0^{--}} \vec{\tau_1}\cdot\vec{\tau_2}, && \text{(D.29)} \\
& && \text{(D.30)}
\end{aligned}$$

$$
\begin{aligned}
H^{HQ}_{1^+-} &= U^{-1}_{1^+-} H_{1^+-} U_{1^+-} \\
&= \left(\begin{array}{cc|c|c} K_0 - C & -2\sqrt{2}T & 0 & 0 \\ -2\sqrt{2}T & K_2 - C + 2T & 0 & 0 \\ \hline 0 & 0 & K_0 + 3C & 0 \\ \hline 0 & 0 & 0 & K_2 + 3C \end{array}\right) \vec{\tau_1} \cdot \vec{\tau_2} && \text{(D.31)} \\
&= \left(\begin{array}{c|cc} H^{(0,1)}_{1^+-} & 0 & 0 \\ \hline 0 & H^{(1,0)}_{1^+-} & 0 \\ \hline 0 & 0 & H^{(1,2)}_{1^+-} \end{array}\right) \vec{\tau_1} \cdot \vec{\tau_2}, && \text{(D.32)} \\
H^{HQ}_{1^++} &= U^{-1}_{1^++} H_{1^++} U_{1^++} \\
&= \left(\begin{array}{cc|c} K_0 - C & -2\sqrt{2}T & 0 \\ -2\sqrt{2}T & K_2 - C + 2T & 0 \\ \hline 0 & 0 & K_2 - C - 2T \end{array}\right) \vec{\tau_1} \cdot \vec{\tau_2} && \text{(D.33)} \\
&= \left(\begin{array}{c|c} H^{(1,1)}_{1^++} & 0 \\ \hline 0 & H^{(1,2)}_{1^++} \end{array}\right) \vec{\tau_1} \cdot \vec{\tau_2}, && \text{(D.34)} \\
H^{HQ}_{1^-+} &= U^{-1}_{1^-+} H_{1^-+} U_{1^-+} \\
&= \left(\begin{array}{c|c} K_1 - C - 2T & 0 \\ \hline 0 & K_1 + 3C \end{array}\right) \vec{\tau_1} \cdot \vec{\tau_2} && \text{(D.35)} \\
&= \left(\begin{array}{c|c} H^{(0,1)}_{1^-+} & 0 \\ \hline 0 & H^{(1,1)}_{1^-+} \end{array}\right) \vec{\tau_1} \cdot \vec{\tau_2}, && \text{(D.36)} \\
H^{HQ}_{1^--} &= U^{-1}_{1^--} H_{1^--} U_{1^--} \\
&= \left(\begin{array}{c|c|c|cc} K_1 - C + 4T & 0 & 0 & 0 & 0 \\ \hline 0 & K_1 + 3C & 0 & 0 & 0 \\ \hline 0 & 0 & K_1 - C - 2T & 0 & 0 \\ \hline 0 & 0 & 0 & K_1 - C + \frac{2}{5}T & -\frac{6\sqrt{6}}{5}T \\ 0 & 0 & 0 & -\frac{6\sqrt{6}}{5}T & K_3 - C + \frac{8}{5}T \end{array}\right) \\
&\quad \times \vec{\tau_1} \cdot \vec{\tau_2} && \text{(D.37)} \\
&= \left(\begin{array}{c|c|c|c} H^{(1,0)}_{1^--} & 0 & 0 & 0 \\ \hline 0 & H^{(0,1)}_{1^--} & 0 & 0 \\ \hline 0 & 0 & H^{(1,1)}_{1^--} & 0 \\ \hline 0 & 0 & 0 & H^{(1,2)}_{1^--} \end{array}\right) \vec{\tau_1} \cdot \vec{\tau_2}, && \text{(D.38)}
\end{aligned}
$$

$$
\begin{aligned}
H^{HQ}_{2^{+-}} &= U^{-1}_{2^{+-}} H_{2^{+-}} U_{2^{+-}} \\
&= \left(\begin{array}{c|c} K_2 - C - 2T & 0 \\ \hline 0 & K_2 + 3C \end{array}\right) \vec{\tau_1}\cdot\vec{\tau_2} && \text{(D.39)} \\
&= \left(\begin{array}{c|c} H^{(0,2)}_{2^{+-}} & 0 \\ \hline 0 & H^{(1,2)}_{2^{+-}} \end{array}\right) \vec{\tau_1}\cdot\vec{\tau_2}, && \text{(D.40)} \\
H^{HQ}_{2^{++}} &= U^{-1}_{2^{++}} H_{2^{++}} U_{2^{++}} \\
&= \left(\begin{array}{cc|c|c|cc} K_2 - C & -2\sqrt{2}T & 0 & 0 & 0 & 0 \\ -2\sqrt{2}T & K_2 - C + 2T & 0 & 0 & 0 & 0 \\ \hline 0 & 0 & K_2 + 3C & 0 & 0 & 0 \\ \hline 0 & 0 & 0 & K_0 - C - 2T & 0 & 0 \\ \hline 0 & 0 & 0 & 0 & K_2 - C + \frac{4}{7}T & -\frac{12\sqrt{3}}{7}T \\ 0 & 0 & 0 & 0 & -\frac{12\sqrt{3}}{7}T & K_4 - C + \frac{10}{7}T \end{array}\right) \\
&\quad \times \vec{\tau_1}\cdot\vec{\tau_2} && \text{(D.41)} \\
&= \left(\begin{array}{c|c|c|c} H^{(1,1)}_{2^{++}} & 0 & 0 & 0 \\ \hline 0 & H^{(0,2)}_{2^{++}} & 0 & 0 \\ \hline 0 & 0 & H^{(1,2)}_{2^{++}} & 0 \\ \hline 0 & 0 & 0 & H^{(1,3)}_{2^{++}} \end{array}\right) \vec{\tau_1}\cdot\vec{\tau_2}, && \text{(D.42)} \\
H^{HQ}_{2^{-+}} &= U^{-1}_{2^{-+}} H_{2^{-+}} U_{2^{-+}} \\
&= \left(\begin{array}{c|cc|c} K_1 + 3C & 0 & 0 & 0 \\ \hline 0 & K_3 - C + \frac{2}{5}T & -\frac{6\sqrt{6}}{5}T & 0 \\ 0 & -\frac{6\sqrt{6}}{5}T & K_1 - C + \frac{8}{5}T & 0 \\ \hline 0 & 0 & 0K_3 + 3C & \end{array}\right) \vec{\tau_1}\cdot\vec{\tau_2} && \text{(D.43)} \\
&= \left(\begin{array}{c|c|c} H^{(1,1)}_{2^{-+}} & 0 & 0 \\ \hline 0 & H^{(0,2)}_{2^{-+}} & 0 \\ \hline 0 & 0 & H^{(1,3)}_{2^{-+}} \end{array}\right) \vec{\tau_1}\cdot\vec{\tau_2}, && \text{(D.44)} \\
H^{HQ}_{2^{--}} &= U^{-1}_{2^{--}} H_{2^{--}} U_{2^{--}} \\
&= \left(\begin{array}{c|cc|c} K_1 - C - 2T & 0 & 0 & 0 \\ \hline 0 & K_3 - C + \frac{2}{5}T & -\frac{6\sqrt{6}}{5}T & 0 \\ 0 & -\frac{6\sqrt{6}}{5}T & K_1 - C + \frac{8}{5}T & 0 \\ \hline 0 & 0 & 0 & K_3 - C - 2T \end{array}\right) \vec{\tau_1}\cdot\vec{\tau_2} && \text{(D.45)} \\
&= \left(\begin{array}{c|c|c} H^{(1,1)}_{2^{--}} & 0 & 0 \\ \hline 0 & H^{(1,2)}_{2^{--}} & 0 \\ \hline 0 & 0 & H^{(1,3)}_{2^{--}} \end{array}\right) \vec{\tau_1}\cdot\vec{\tau_2}. && \text{(D.46)}
\end{aligned}
$$

D.3 The wave functions of heavy meson molecules

The wave functions of heavy meson molecules $|P\bar{P}(J^{PC})\rangle$ are expanded by both normalized particle basis ψ^{PB} and HQS basis ψ^{HQ} as

$$\begin{aligned} |P\bar{P}(J^{PC})\rangle &= \sum_{i=1}^{n} c_i \psi_i^{PB} && \text{(D.47)} \\ &= \sum_{i=1}^{n} c'_i \psi_i^{HQ} && \text{(D.48)} \\ &= \sum_{i=1}^{n}\sum_{j=1}^{n} c_i (U_{J^{PC}})_{ij} \psi_j^{HQ}, && \text{(D.49)} \end{aligned}$$

where n is a number of basis and $U_{J^{PC}}$ is a unitary matrix, which relate the two basis.

Here, we show this transormations for each states and discuss the properties of wave functions expected in the heavy quark limit $m_Q \to \infty$.

- $J^{PC} = 0^{++}$; $H^{(0,0)}_{0^{++}}, H^{(1,1)}_{0^{++}}$

In this channel, the wavefunction are expanded as

$$\begin{aligned} |P\bar{P}(0^{++})\rangle &= c_1 \left|P\bar{P}(^1S_0)\right\rangle + c_2 \left|P^*\bar{P}^*(^1S_0)\right\rangle + c_3 \left|P^*P^*(^5D_0)\right\rangle && \text{(D.50)} \\ &= c'_1 \left|0_H, 0_q, 0_L, 0_l; 0\right\rangle + c_2 \left|1_H, 1_q, 0_L, 1_l; 0\right\rangle + c_3 \left|1_H, 1_q, 2_L, 1_l; 0\right\rangle, && \text{(D.51)} \end{aligned}$$

where we use the same notation for the expression of the wave functions for the particle and HQS bases. The cofficients, c_i and c'_i are related as follows:

$$\begin{cases} c'_1 = \frac{1}{2}c_1 + \frac{\sqrt{3}}{2}c_2 \\ c'_2 = \frac{\sqrt{3}}{2}c_1 - \frac{1}{2}c_2 \\ c'_3 = c_3 \end{cases} \qquad \text{(D.52)}$$

The bound states for both $I = 0$ and $I = 1$ of this channel belongs to $H^{(1,1)}_{0^{++}}$, hence the component c'_1, which belongs to $H^{(0,0)}_{0^{++}}$ should take zero in heavy quark limit. Then the

fractions of components in particle basis are expected as

$$\begin{array}{ccc} f(c_1\,|P\bar{P}(^1S_0)\rangle) & : & f(c_2\,|P^*\bar{P}^*(^1S_0)\rangle) \\ \sqrt{3} & : & -1. \end{array} \tag{D.53}$$

- $J^{PC} = 0^{-+}$; $H^{(0,0)}_{0^{-+}}, H^{(1,1)}_{0^{-+}}$

The wave functions are given as

$$|P\bar{P}(0^{-+})\rangle = c_1\,|\frac{1}{\sqrt{2}}(P\bar{P}^* - P^*\bar{P})(^3P_0)\rangle + c_2\,|P^*\bar{P}^*(^3P_0)\rangle \tag{D.54}$$

$$= c_1'\,|0_H, 1_q, 1_L, 0_l; 0\rangle + c_2'\,|1_H, 0, q, 1_L, 1_l; 0\rangle\,, \tag{D.55}$$

The cofficients, c_i and c_i' are related as follows:

$$\begin{cases} c_1' = \frac{1}{\sqrt{2}}c_1 + \frac{1}{\sqrt{2}}c_2 \\ c_2' = -\frac{1}{\sqrt{2}}c_1 + \frac{1}{\sqrt{2}}c_2 \end{cases} \tag{D.56}$$

- $J^{PC} = 0^{--}$; $H^{(1,1)}_{0^{--}}$

The wave functions are given as

$$|P\bar{P}(0^{--})\rangle = c_1\,|\frac{1}{\sqrt{2}}(P\bar{P}^* + P^*\bar{P})(^3P_0)\rangle \tag{D.57}$$

$$= c_1'\,|1_H, 1_q, 1_L, 1_l; 0\rangle\,. \tag{D.58}$$

In this channel, there is only one basis, hence two bases are trivially correspond one-on-one.

- $J^{PC} = 1^{+-}$; $H^{(0,1)}_{1^{+-}}, H^{(1,0)}_{1^{+-}}, H^{(1,2)}_{1^{+-}}$

The wave functions are given as

$$\begin{aligned}|P\bar{P}(1^{+-})\rangle &= c_1\,|\frac{1}{\sqrt{2}}(B\bar{B}^*-B^*\bar{B})(^3S_1)\rangle + c_2\,|\frac{1}{\sqrt{2}}(B\bar{B}^*-B^*\bar{B})(^3D_1)\rangle \\ &\quad +c_3\,|B^*\bar{B}^*(^3S_1)\rangle + c_4\,|B^*\bar{B}^*(^3D_1)\rangle \\ &= c_1'\,|0_H,1_q,0_L,1_l;1\rangle + c_2'\,|0_H,1_q,2_L,1_l;1\rangle + c_3'\,|1_H,0_q,0_L,0_L;1\rangle + c_4'\,|1_H,0_l,2_L,2_l;1\rangle\,,\end{aligned} \tag{D.59}$$

The cofficients, c_i and c_i' are related as follows:

$$\begin{cases} c_1' = \frac{1}{\sqrt{2}}c_1 + \frac{1}{\sqrt{2}}c_3 \\ c_2' = \frac{1}{\sqrt{2}}c_2 + \frac{1}{\sqrt{2}}c_4 \\ c_3' = -\frac{1}{\sqrt{2}}c_1 + \frac{1}{\sqrt{2}}c_3 \\ c_4' = -\frac{1}{\sqrt{2}}c_2 + \frac{1}{\sqrt{2}}c_4. \end{cases} \tag{D.60}$$

- $J^{PC} = 1^{++}$; $H^{(1,1)}_{1^{++}}, H^{(1,2)}_{1^{++}}$

The wave functions are given as

$$|P\bar{P}(1^{++})\rangle = c_1\,|\frac{1}{\sqrt{2}}(P\bar{P}^*+P^*\bar{P})(^3S_1)\rangle + c_2\,|\frac{1}{\sqrt{2}}(P\bar{P}^*+P^*\bar{P})(^3D_1)\rangle + c_3\,|P^*\bar{P}^*(^5D_1)\rangle \tag{D.61}$$

$$= c_1'\,|1_H,1_q,0_L,1_l;1\rangle + c_2'\,|1_H,1_q,2_L,1_l;1\rangle + c_3'\,|1_H,1_q,2_L,2_l;1\rangle\,. \tag{D.62}$$

The cofficients, c_i and c_i' are related as follows:

$$\begin{cases} c_1' = c_1 \\ c_2' = -\frac{1}{2}c_2 + \frac{\sqrt{3}}{2}c_3 \\ c_3' = \frac{\sqrt{3}}{2}c_2 + \frac{1}{2}c_3 \end{cases} \tag{D.63}$$

- $J^{PC} = 1^{-+}$; $H^{(0,1)}_{1^{-+}}, H^{(1,1)}_{1^{-+}}$

The wave functions are given as

$$|P\bar{P}1^{-+}\rangle = c_1\,|\frac{1}{\sqrt{2}}(P\bar{P}^* - P^*\bar{P})(^3P_1)\rangle\, c_2\,|P^*\bar{P}^*(^3P_1)\rangle \quad \text{(D.64)}$$

$$= c_1'\,|0_H, 1_q, 1_L, 1_l; 1\rangle + c_2'\,|1_H, 0_q, 1_L, 1_l; 1\rangle\,. \quad \text{(D.65)}$$

The cofficients, c_i and c_i' are related as follows:

$$\begin{cases} c_1' = \frac{1}{\sqrt{2}}c_1 + \frac{1}{\sqrt{2}}c_2 \\ c_2' = -\frac{1}{\sqrt{2}}c_1 + \frac{1}{\sqrt{2}}c_2 \end{cases} \quad \text{(D.66)}$$

- $J^{PC} = 1^{--}$; $H^{(1,0)}_{1^{--}}, H^{(0,1)}_{1^{--}}, H^{(1,1)}_{1^{--}}, H^{(1,2)}_{1^{--}}$

The wave functions are given as

$$|P\bar{P}(1^{--})\rangle = c_1\,|P\bar{P}(^1P_1)\rangle + c_2\,|\frac{1}{\sqrt{2}}(P\bar{P}^* + P^*\bar{P})(^3P_1)\rangle + c_3\,|P^*\bar{P}^*(^1P_1)\rangle$$
$$+c_4\,|P^*\bar{P}^*(^5P_1)\rangle + c_5\,|P^*\bar{P}^*(^5F_1)\rangle \quad \text{(D.67)}$$

$$= c_1'\,|1_H, 1_q, 1_L, 0_l; 1\rangle + c_2'\,|0_H, 0_q, 1_L, 1_l; 1\rangle + c_3'\,|1_H, 1_q, 1_L, 1_l; 1\rangle$$
$$+c_4'\,|1_H, 1_q, 1_L, 2_l; 1\rangle + c_5'\,|1_H, 1_1, 3_L, 2_l; 1\rangle\,. \quad \text{(D.68)}$$

The cofficients, c_i and c_i' are related as follows:

$$\begin{cases} c_1' = \frac{1}{2\sqrt{3}}c_1 - \frac{1}{\sqrt{3}}c_2 - \frac{1}{6}c_3 + \frac{\sqrt{5}}{3}c_4 \\ c_2' = \frac{1}{2}c_1 + \frac{\sqrt{3}}{2}c_3 \\ c_3' = -\frac{1}{2}c_1\frac{1}{2}c_2 + \frac{1}{2\sqrt{3}}c_3 + \frac{\sqrt{5}}{2\sqrt{3}}c_4 \\ c_4' = \frac{\sqrt{5}}{2\sqrt{3}}c_1 + \frac{\sqrt{5}}{2\sqrt{3}}c_2 - \frac{\sqrt{5}}{6}c_3 + \frac{1}{6} \\ c_5' = c_5 \end{cases} \quad \text{(D.69)}$$

- $J^{PC} = 2^{+-}$; $H^{(0,2)}_{2^{+-}}, H^{(1,2)}_{2^{+-}}$

The wave functions are given as

$$|P\bar{P}(2^{+-})\rangle = c_1\,|\frac{1}{\sqrt{2}}(P\bar{P}^* - P^*\bar{P})(^3D_2)\rangle + c_2\,|P^*\bar{P}^*(^3D_2)\rangle \quad \text{(D.70)}$$

$$= c_1'\,|0_H, 1_q, 2_L, 2_l; 2\rangle + c_2'\,|1_H, 0_q, 2_L, 2_l; 2\rangle\,. \quad \text{(D.71)}$$

The cofficients, c_i and c_i' are related as follows:

$$\begin{cases} c_1' = \frac{1}{\sqrt{2}}c_1 + \frac{1}{\sqrt{2}}c_2 \\ c_2' = -\frac{1}{\sqrt{2}}c_1 + \frac{1}{\sqrt{2}}c_2. \end{cases} \quad \text{(D.72)}$$

- $J^{PC} = 2^{++}$; $H^{(1,1)}_{2^{++}}, H^{(0,2)}_{2^{++}}, H^{(1,2)}_{2^{++}}, H^{(1,3)}_{2^{++}}$

The wave functions are given as

$$|P\bar{P}(2^{++})\rangle = c_1\,|P\bar{P}(^1D_2)\rangle + c_2\,|\frac{1}{\sqrt{2}}(P\bar{P}^* + P^*\bar{P})(^3D_2)\rangle + c_3\,|P^*\bar{P}^*(^1D_2)\rangle$$
$$+c_4\,|P^*\bar{P}^*(^5S_2)\rangle + c_5\,|P^*\bar{P}^*(^5D_2)\rangle + c_6\,|P^*\bar{P}^*(^5G_2)\rangle \quad \text{(D.73)}$$

$$= c_1'\,|1_H, 1_q, 0_L, 1_l; 2\rangle + c_2'\,|1_H, 1_q, 2_L, 1_l; 2\rangle + c_3'\,|0_H, 0_q, 2_L, 2_l; 2\rangle$$
$$+c_4'\,|1_H, 1_q, 2_L, 2_l; 2\rangle + c_5'\,|1_H, 1_q, 2_L, 3_l; 2\rangle + c_6'\,|1_H, 1_q, 4_L, 3_l; 2\rangle\,. \quad \text{(D.74)}$$

The cofficients, c_i and c_i' are related as follows:

$$\begin{cases} c_1' = c_4 \\ c_2' = \frac{\sqrt{3}}{2\sqrt{5}}c_1 - \frac{3}{2\sqrt{5}}c_2 - \frac{1}{2\sqrt{5}}c_3 + \frac{\sqrt{7}}{2\sqrt{5}}c_5 \\ c_3' = \frac{1}{2}c_1 + \frac{\sqrt{3}}{2}c_3 \\ c_4' = -\frac{1}{2}c_1 + \frac{1}{2\sqrt{3}}c_2 + \frac{1}{2\sqrt{3}}c_3 + \frac{\sqrt{7}}{2\sqrt{3}}c_5 \\ c_5' = \frac{\sqrt{7}}{2\sqrt{5}}c_1\sqrt{\frac{7}{15}}c_2 - \frac{\sqrt{7}}{2\sqrt{15}}c_3 + \frac{1}{\sqrt{15}}c_5 \\ c_6' = c_6 \end{cases} \quad \text{(D.75)}$$

- $J^{PC} = 2^{-+}$; $H^{(1,1)}_{2^{-+}}, H^{(0,2)}_{2^{-+}}, H^{(1,3)}_{2^{-+}}$

The wave functions are given as

$$\begin{aligned} |P\bar{P}(2^{-+})\rangle &= c_1\,|\frac{1}{\sqrt{2}}(P\bar{P}^* - P^*\bar{P})(^3P_2)\rangle + c_2\,|\frac{1}{\sqrt{2}}(P\bar{P}^* - P^*\bar{P})(^3F_2)\rangle \\ &\quad + c_3\,|P^*\bar{P}^*(^3P_2)\rangle + c_4\,|P^*\bar{P}^*(^3F_2)\rangle \qquad \text{(D.76)} \\ &= c_1'\,|1_H, 0_q, 1_L, 1_l; 2\rangle + c_2'\,|0_H, 1_q, 1_L, 2_l; 2\rangle \\ &\quad + c_3'\,|0_H, 1_q, 3_L, 2_l; 2\rangle + c_4'\,|1_H, 0_q, 3_L, 3_l; 2\rangle \qquad \text{(D.77)} \end{aligned}$$

The cofficients, c_i and c_i' are related as follows:

$$\begin{cases} c_1' = -\frac{1}{\sqrt{2}}c_1 + \frac{1}{\sqrt{2}}c_3 \\ c_2' = \frac{1}{\sqrt{2}}c_1 + \frac{1}{\sqrt{2}}c_3 \\ c_3' = \frac{1}{\sqrt{2}}c_2 + \frac{1}{\sqrt{2}}c_4 \\ c_4' = -\frac{1}{\sqrt{2}}c_2 + \frac{1}{\sqrt{2}}c_4 \end{cases} \qquad \text{(D.78)}$$

- $J^{PC} = 2^{--}$; $H^{(1,1)}_{2^{--}}, H^{(1,2)}_{2^{--}}, H^{(1,3)}_{2^{--}}$

The wave functions are given as

$$\begin{aligned} |P\bar{P}(2^{--})\rangle &= c_1\,|\frac{1}{\sqrt{2}}(P\bar{P}^* + P^*\bar{P})(^3P_2)\rangle + c_2\,|\frac{1}{\sqrt{2}}(P\bar{P}^* + P^*\bar{P})(^3F_2)\rangle \\ &\quad + c_3\,|P^*\bar{P}^*(^5P_2)\rangle + c_4\,|P^*\bar{P}^*(^5F_2)\rangle \qquad \text{(D.79)} \\ &= c_1'\,|1_H, 1_q, 1_L, 1_l; 2\rangle + c_2'\,|1_H, 1_q, 1_L, 2_l; 2\rangle \\ &\quad + c_3'\,|1_H, 1_q, 3_L, 2_l; 2\rangle + c_4'\,|1_H, 1_q, 3_L, 3_l; 2\rangle \qquad \text{(D.80)} \end{aligned}$$

The cofficients, c_i and c_i' are related as follows:

$$\begin{cases} c_1' = -\frac{1}{2}c_1 + \frac{\sqrt{3}}{2}c_3 \\ c_2' = \frac{\sqrt{3}}{2}c_1 + \frac{1}{2}c_3 \\ c_3' = -\frac{1}{\sqrt{3}}c_2 + \sqrt{\frac{2}{3}}c_4 \\ c_4' = \sqrt{\frac{2}{3}}c_2 + \frac{1}{\sqrt{3}}c_4 \end{cases} \qquad \text{(D.81)}$$

Bibliography

[1] Belle Collaboration, I. Adachi *et al.*, Phys.Rev.Lett. **108**, 032001 (2012), arXiv:1103.3419.

[2] Belle Collaboration, A. Bondar *et al.*, Phys.Rev.Lett. **108**, 122001 (2012), arXiv:1110.2251.

[3] Belle Collaboration, I. Adachi *et al.*, (2012), arXiv:1209.6450.

[4] Belle Collaboration, I. Adachi *et al.*, (2012), arXiv:1207.4345.

[5] S. Ohkoda, Y. Yamaguchi, S. Yasui, K. Sudoh, and A. Hosaka, Phys.Rev. **D86**, 014004 (2012), arXiv:1111.2921.

[6] M. Voloshin, Prog.Part.Nucl.Phys. **61**, 455 (2008), arXiv:0711.4556.

[7] T. Barnes, S. Godfrey, and E. Swanson, Phys.Rev. **D72**, 054026 (2005), arXiv:hep-ph/0505002.

[8] W. Roberts and M. Pervin, Int.J.Mod.Phys. **A23**, 2817 (2008), arXiv:0711.2492.

[9] J. Vijande, F. Fernandez, and A. Valcarce, J.Phys. **G31**, 481 (2005), arXiv:hep-ph/0411299.

[10] J. D. Weinstein and N. Isgur, Phys.Rev. **D41**, 2236 (1990).

[11] J. Oller and E. Oset, Phys.Rev. **D60**, 074023 (1999), arXiv:hep-ph/9809337.

[12] T. Hyodo and D. Jido, Prog.Part.Nucl.Phys. **67**, 55 (2012), arXiv:1104.4474.

[13] Quarkonium Working Group, N. Brambilla *et al.*, (2004), arXiv:hep-ph/0412158.

[14] E. S. Swanson, Phys.Rept. **429**, 243 (2006), arXiv:hep-ph/0601110.

[15] M. Nielsen, F. S. Navarra, and S. H. Lee, Phys.Rept. **497**, 41 (2010), arXiv:0911.1958.

[16] N. Brambilla *et al.*, Eur.Phys.J. **C71**, 1534 (2011), arXiv:1010.5827.

[17] Belle Collaboration, I. Adachi, (2011), arXiv:1105.4583.

[18] A. Bondar, A. Garmash, A. Milstein, R. Mizuk, and M. Voloshin, Phys.Rev. **D84**, 054010 (2011), arXiv:1105.4473.

[19] BESIII Collaboration, M. Ablikim *et al.*, Phys.Rev.Lett. **110**, 252001 (2013), arXiv:1303.5949.

[20] Belle Collaboration, Z. Liu *et al.*, Phys.Rev.Lett. **110**, 252002 (2013), arXiv:1304.0121.

[21] N. Isgur and M. B. Wise, Phys.Lett. **B232**, 113 (1989).

[22] N. Isgur and M. B. Wise, Phys.Lett. **B237**, 527 (1990).

[23] M. Neubert, Phys.Rept. **245**, 259 (1994), arXiv:hep-ph/9306320.

[24] H. Georgi, Phys.Lett. **B240**, 447 (1990).

[25] H. D. Politzer and M. B. Wise, Phys.Lett. **B206**, 681 (1988).

[26] H. D. Politzer and M. B. Wise, Phys.Lett. **B208**, 504 (1988).

[27] A. V. Manohar and M. B. Wise, Camb.Monogr.Part.Phys.Nucl.Phys.Cosmol. **10**, 1 (2000).

[28] Particle Data Group, J. Beringer *et al.*, Phys.Rev. **D86**, 010001 (2012).

[29] E. E. Jenkins, M. E. Luke, A. V. Manohar, and M. J. Savage, Nucl.Phys. **B390**, 463 (1993), arXiv:hep-ph/9204238.

[30] Belle Collaboration, K. Chen *et al.*, Phys.Rev.Lett. **100**, 112001 (2008), arXiv:0710.2577.

[31] S. Ohkoda, Y. Yamaguchi, S. Yasui, and A. Hosaka, Phys.Rev. **D86**, 117502 (2012), arXiv:1210.3170.

[32] N. Isgur and M. B. Wise, Phys.Rev.Lett. **66**, 1130 (1991).

[33] G. Burdman and J. F. Donoghue, Phys.Lett. **B280**, 287 (1992).

[34] M. B. Wise, Phys.Rev. **D45**, 2188 (1992).

[35] T.-M. Yan *et al.*, Phys.Rev. **D46**, 1148 (1992).

[36] M. A. Nowak, M. Rho, and I. Zahed, Phys.Rev. **D48**, 4370 (1993), arXiv:hep-ph/9209272.

[37] A. Badalian, Y. Simonov, and M. Trusov, Phys.Rev. **D77**, 074017 (2008), arXiv:0712.3943.

[38] R. Casalbuoni *et al.*, Phys.Rept. **281**, 145 (1997), arXiv:hep-ph/9605342.

[39] W. A. Bardeen, E. J. Eichten, and C. T. Hill, Phys. Rev. D **68**, 054024 (2003).

[40] T. Matsuki, T. Morii, and K. Sudoh, Prog.Theor.Phys. **117**, 1077 (2007), arXiv:hep-ph/0605019.

[41] S. Dubynskiy and M. Voloshin, Phys.Lett. **B666**, 344 (2008), arXiv:0803.2224.

[42] T. E. O. Ericson and G. Karl, Phys.Lett. **B309**, 426 (1993).

[43] N. A. Tornqvist, Phys.Rev.Lett. **67**, 556 (1991).

[44] N. A. Tornqvist, Z.Phys. **C61**, 525 (1994), arXiv:hep-ph/9310247.

[45] I. W. Lee, A. Faessler, T. Gutsche, and V. E. Lyubovitskij, Phys.Rev. **D80**, 094005 (2009), arXiv:0910.1009.

[46] C. Thomas and F. Close, Phys.Rev. **D78**, 034007 (2008), arXiv:0805.3653.

[47] X. Liu, Z.-G. Luo, Y.-R. Liu, and S.-L. Zhu, Eur.Phys.J. **C61**, 411 (2009), arXiv:0808.0073.

[48] Y.-R. Liu, X. Liu, W.-Z. Deng, and S.-L. Zhu, Eur.Phys.J. **C56**, 63 (2008), arXiv:0801.3540.

[49] M. Suzuki, Phys.Rev. **D72**, 114013 (2005), arXiv:hep-ph/0508258.

[50] J.-R. Zhang, M. Zhong, and M.-Q. Huang, Phys.Lett. **B704**, 312 (2011), arXiv:1105.5472.

[51] D. Bugg, Europhys.Lett. **96**, 11002 (2011), arXiv:1105.5492.

[52] Y. Yang, J. Ping, C. Deng, and H.-S. Zong, J.Phys. **G39**, 105001 (2012), arXiv:1105.5935.

[53] J. Nieves and M. P. Valderrama, Phys.Rev. **D84**, 056015 (2011), arXiv:1106.0600.

[54] Z.-F. Sun, J. He, X. Liu, Z.-G. Luo, and S.-L. Zhu, Phys.Rev. **D84**, 054002 (2011), arXiv:1106.2968.

[55] M. Cleven, F.-K. Guo, C. Hanhart, and U.-G. Meissner, Eur.Phys.J. **A47**, 120 (2011), arXiv:1107.0254.

[56] T. Mehen and J. W. Powell, Phys.Rev. **D84**, 114013 (2011), arXiv:1109.3479.

[57] T. Guo, L. Cao, M.-Z. Zhou, and H. Chen, (2011), arXiv:1106.2284.

[58] C.-Y. Cui, Y.-L. Liu, and M.-Q. Huang, Phys.Rev. **D85**, 074014 (2012), arXiv:1107.1343.

[59] F. S. Navarra, M. Nielsen, and J.-M. Richard, J.Phys.Conf.Ser. **348**, 012007 (2012), arXiv:1108.1230.

[60] A. Ali, PoS **BEAUTY2011**, 002 (2011), arXiv:1108.2197.

[61] M. Karliner, H. J. Lipkin, and N. A. Tornqvist, (2011), arXiv:1109.3472.

[62] A. Ali, C. Hambrock, and W. Wang, Phys.Rev. **D85**, 054011 (2012), arXiv:1110.1333.

[63] D.-Y. Chen, X. Liu, and S.-L. Zhu, Phys.Rev. **D84**, 074016 (2011), arXiv:1105.5193.

[64] D.-Y. Chen and X. Liu, Phys.Rev. **D84**, 094003 (2011), arXiv:1106.3798.

[65] D.-Y. Chen and X. Liu, Phys.Rev. **D84**, 034032 (2011), arXiv:1106.5290.

[66] D.-Y. Chen, X. Liu, and T. Matsuki, Phys.Rev. **D84**, 074032 (2011), arXiv:1108.4458.

[67] M. Voloshin, Phys.Rev. **D84**, 031502 (2011), arXiv:1105.5829.

[68] Particle Data Group, C. Amsler *et al.*, Phys.Lett. **B667**, 1 (2008).

[69] H.-Y. Cheng *et al.*, Phys.Rev. **D49**, 2490 (1994), arXiv:hep-ph/9308283.

[70] H. Ohki, H. Matsufuru, and T. Onogi, Phys.Rev. **D77**, 094509 (2008), arXiv:0802.1563.

[71] C. Isola, M. Ladisa, G. Nardulli, and P. Santorelli, Phys.Rev. **D68**, 114001 (2003), arXiv:hep-ph/0307367.

[72] S. Yasui and K. Sudoh, Phys.Rev. **D80**, 034008 (2009), arXiv:0906.1452.

[73] Y. Yamaguchi, S. Ohkoda, S. Yasui, and A. Hosaka, Phys.Rev. **D84**, 014032 (2011), arXiv:1105.0734.

[74] B. R. Johnson, The Journal of Chemical Physics **69** (1978).

[75] K. Arai and A. Kruppa, Phys.Rev. **C60**, 064315 (1999).

[76] M. Pennington and D. Wilson, Phys.Rev. **D76**, 077502 (2007), arXiv:0704.3384.

[77] ExHIC Collaboration, S. Cho *et al.*, Phys.Rev.Lett. **106**, 212001 (2011), arXiv:1011.0852.

[78] ExHIC Collaboration, S. Cho *et al.*, Phys.Rev. **C84**, 064910 (2011), arXiv:1107.1302.

[79] S. Zouzou, B. Silvestre-Brac, C. Gignoux, and J. Richard, Z.Phys. **C30**, 457 (1986).

[80] H. J. Lipkin, Phys.Lett. **B172**, 242 (1986).

[81] L. Heller and J. Tjon, Phys.Rev. **D35**, 969 (1987).

[82] J. Carlson, L. Heller, and J. Tjon, Phys.Rev. **D37**, 744 (1988).

[83] B. Silvestre-Brac and C. Semay, Z.Phys. **C57**, 273 (1993).

[84] C. Semay and B. Silvestre-Brac, Z.Phys. **C61**, 271 (1994).

[85] S. Pepin, F. Stancu, M. Genovese, and J. Richard, Phys.Lett. **B393**, 119 (1997), arXiv:hep-ph/9609348.

[86] D. Brink and F. Stancu, Phys.Rev. **D57**, 6778 (1998).

[87] B. Silvestre-Brac and C. Semay, Z.Phys. **C59**, 457 (1993).

[88] J. Schaffner-Bielich and A. P. Vischer, Phys.Rev. **D57**, 4142 (1998), arXiv:nucl-th/9710064.

[89] D. Janc and M. Rosina, Few Body Syst. **35**, 175 (2004), arXiv:hep-ph/0405208.

[90] N. Barnea, J. Vijande, and A. Valcarce, Phys.Rev. **D73**, 054004 (2006), arXiv:hep-ph/0604010.

[91] J. Vijande, E. Weissman, N. Barnea, and A. Valcarce, Phys.Rev. **D76**, 094022 (2007), arXiv:0708.3285.

[92] J. Vijande, E. Weissman, A. Valcarce, and N. Barnea, Phys.Rev. **D76**, 094027 (2007), arXiv:0710.2516.

[93] D. Ebert, R. Faustov, V. Galkin, and W. Lucha, Phys.Rev. **D76**, 114015 (2007), arXiv:0706.3853.

[94] F. S. Navarra, M. Nielsen, and S. H. Lee, Phys.Lett. **B649**, 166 (2007), arXiv:hep-ph/0703071.

[95] S. H. Lee, S. Yasui, W. Liu, and C. M. Ko, Eur.Phys.J. **C54**, 259 (2008), arXiv:0707.1747.

[96] S. H. Lee and S. Yasui, Eur.Phys.J. **C64**, 283 (2009), arXiv:0901.2977.

[97] M. Zhang, H. Zhang, and Z. Zhang, Commun.Theor.Phys. **50**, 437 (2008), arXiv:0711.1029.

[98] Y. Yang, C. Deng, J. Ping, and T. Goldman, Phys.Rev. **D80**, 114023 (2009).

[99] J. Vijande, A. Valcarce, and N. Barnea, Phys.Rev. **D79**, 074010 (2009), arXiv:0903.2949.

[100] T. Carames, A. Valcarce, and J. Vijande, Phys.Lett. **B699**, 291 (2011).

[101] J. Vijande, A. Valcarce, and T. Carames, Few Body Syst. **50**, 195 (2011).

[102] J. Ader, J. Richard, and P. Taxil, Phys.Rev. **D25**, 2370 (1982).

[103] J. Vijande, A. Valcarce, and J.-M. Richard, Phys.Rev. **D76**, 114013 (2007), arXiv:0707.3996.

[104] A. V. Manohar and M. B. Wise, Nucl.Phys. **B399**, 17 (1993), arXiv:hep-ph/9212236.

[105] G.-J. Ding, J.-F. Liu, and M.-L. Yan, Phys.Rev. **D79**, 054005 (2009), arXiv:0901.0426.

[106] R. Molina, T. Branz, and E. Oset, Phys.Rev. **D82**, 014010 (2010), arXiv:1005.0335.

[107] R. L. Jaffe, Phys.Rev. **D15**, 267 (1977).

[108] R. Jaffe, Phys.Rev. **D17**, 1444 (1978).

[109] R. L. Jaffe and F. Wilczek, Phys.Rev.Lett. **91**, 232003 (2003), arXiv:hep-ph/0307341.

[110] M. G. Alford, K. Rajagopal, and F. Wilczek, Phys.Lett. **B422**, 247 (1998), arXiv:hep-ph/9711395.

[111] R. Rapp, T. Schäfer, E. V. Shuryak, and M. Velkovsky, Phys.Rev.Lett. **81**, 53 (1998), arXiv:hep-ph/9711396.

[112] M. G. Alford, A. Schmitt, K. Rajagopal, and T. Schäfer, Rev.Mod.Phys. **80**, 1455 (2008), arXiv:0709.4635.

[113] Y. Nambu and G. Jona-Lasinio, Phys.Rev. **122**, 345 (1961).

[114] Y. Yamaguchi, S. Ohkoda, S. Yasui, and A. Hosaka, Phys.Rev. **D85**, 054003 (2012), arXiv:1111.2691.

[115] A. Del Fabbro, D. Janc, M. Rosina, and D. Treleani, Phys.Rev. **D71**, 014008 (2005), arXiv:hep-ph/0408258.

[116] R. Kaiser, A. V. Manohar, and T. Mehen, Phys.Rev.Lett. **90**, 142001 (2003), arXiv:hep-ph/0208194.

[117] M. Voloshin, Phys.Rev. **D85**, 034024 (2012), arXiv:1201.1222.

[118] A. De Rújula, H. Georgi, and S. L. Glashow, Phys. Rev. Lett. **38**, 317 (1977).

[119] M. Cleven *et al.*, Phys.Rev. **D87**, 074006 (2013), arXiv:1301.6461.

[120] G. Li, F.-l. Shao, C.-W. Zhao, and Q. Zhao, Phys.Rev. **D87**, 034020 (2013), arXiv:1212.3784.

[121] P. Colangelo, F. De Fazio, and T. Pham, Phys.Rev. **D69**, 054023 (2004), arXiv:hep-ph/0310084.

[122] Y. Dong, A. Faessler, T. Gutsche, and V. E. Lyubovitskij, J.Phys. **G40**, 015002 (2013), arXiv:1203.1894.

[123] F. Aceti, R. Molina, and E. Oset, Phys.Rev. **D86**, 113007 (2012), arXiv:1207.2832.

[124] S. Yasui *et al.*, Phys.Lett. **B727**, 185 (2013), arXiv:1304.5293.

[125] J. C. Romao, (2004).

[126] R. Machleidt, K. Holinde, and C. Elster, Phys.Rept. **149**, 1 (1987).